

Environmental, Human Health, and Societal Impacts of Nanosilver and Ionic Silver Used
in Industrial and Consumer Products

by

Justin Kidd

A Dissertation Presented in Partial Fulfillment
of the Requirements for the Degree
Doctor of Philosophy

Approved March 2020 by the
Graduate Supervisory Committee:

Paul Westerhoff, Chair
Rosa Krajmalnik-Brown
Andrew Maynard
Francois Perreault

ARIZONA STATE UNIVERSITY

May 2020

ABSTRACT

Engineered nanomaterials (ENMs) are added to numerous consumer products to enhance their effectiveness, whether it be for environmental remediation, mechanical properties, or as dietary supplements. Uses of ENMs include adding to enhance products, carbon for strength or dielectric properties, silver for antimicrobial properties, zinc oxide for UV sun-blocking properties, titanium dioxide for photocatalysis, or silica for desiccant properties. However, concerns arise from ENM functional properties that can impact the environment and a lack of regulation regarding ENMs leads to potential public exposure to ENMs and results in ill-informed public or manufacturer perceptions of ENMs.

My dissertation evaluates the environmental, human health, and societal impacts of using ENMs, with a focus on ionic silver and nanosilver, in consumer and industrial products. Reproducible experiments served as functional assays to assess ENM distributions among various environmental matrices. Functional assay results were visualized using radar plots and aid in a framework to estimate likely ENM disposition in the environment.

To assess beneficial uses of ENMs, bromide ion removal from drinking waters to limit disinfection by-product formation was studied. Silver-enabled graphene oxide materials were capable of removing bromide from water, and exhibited less competition from background solutes (e.g. natural organic matter) when compared against solely ionic silver addition to water for bromide removal.

To assess complex interactions of ENMs with the microbiome, batch experiments were performed using fecal samples spiked with ionic silver or commercial dietary silver nanoparticles. Dietary nanosilver and ionic silver exposures to the fecal microbiome for 24

hours reduce short chain fatty acid (SCFA) production and changes the relative abundance of the microbiota.

To understand the social perceptions of ENMS, statistically rigorous surveys were conducted to assess related perceptions related to the use of ENMs in drinking water treatment devices the general public and, separately, industrial manufacturers. These stakeholders are influenced by costs and efficiency of the technologies, consumer concerns of the safety of technologies, and environmental health and safety of the technologies.

This dissertation represents novel research that took an interdisciplinary approach, spanning from wet-lab engineering bench scale testing to social science survey assessments to better understand the environmental, human health, and societal impacts of using ENMs such as nanosilver and ionic silver in industrial processes and consumer products.

ACKNOWLEDGEMENTS

First and foremost, I would like to thank Dr. Paul Westerhoff, my advisor, for his support and guidance during my PhD. His advice and insight have been instrumental in my development as an environmental engineer. I would also like to thank my committee, Dr. Rosa Krajmalnik-Brown, Dr. Francois Perreault, and Dr. Andrew Maynard. Working on research projects with each of you has provided me with invaluable learning and research experiences and I appreciate all of the support and direction in both my academic and personal life. The research herein has been funded by the Environmental Protection Agency (LCnano) and the Nanosystems Engineering Research Center for Nanotechnology Enabled Water Treatment (NEWTE). I would like to thank my colleagues and mentors who have contributed to my PhD progress as we strived for the same goals in our office cubicles. In no particular order a huge thanks to Heather Tugaoen, Neil Tugaoen, Anjali Mulchandani, Sergi Garcia-Segura, and Abi Garcia. Without your friendship and support, I wouldn't have kept my sanity during the trials and tribulations of this PhD. I would like to thank my family for your enormous amount of support over the last 10 years as I attempted to complete my education at Arizona State University. Lastly, I would like to say thank you to my mother, Pamela Kidd. Words cannot describe how grateful I am to you for your support and encouragement during this time.

TABLE OF CONTENTS

	Page
LIST OF TABLES.....	xiii
LIST OF FIGURES.....	ix
CHAPTER	
1. INTRODUCTION	1
1.1. Dissertation Organization	1
1.2. Research Questions.....	4
2. PHYSICO-CHEMICAL PROPERTIES AND THEIR IMPORTANCE IN THE ENVIRONMENT: CURRENT TRENDS IN NANOMATERIAL EXPOSURES.....	7
2.1. Abstract.....	7
2.2. Introduction.....	7
2.3. The State of Science in Nanomaterial Exposure.....	9
2.4. Tools for Detection and Quantification of Nanomaterial Exposures.....	33
2.5. What the Data Tells Us About Nanomaterial Exposures.....	41
3. DEVELOPING AND INTERPRETING AQUEOUS FUNCTIONAL ASSAYS FOR COMPARATIVE PROPERTY-ACTIVITY RELATIONSHIPS OF DIFFERENT NANOMATERIALS.....	43
3.1. Abstract.....	43
3.2. Introduction.....	44
3.3. Methods and Materials.....	46
3.4. Results and Discussion.....	48

CHAPTER	Page
3.5. Acknowledgements.....	63
3.6. Supporting Information.....	64
4. REMOVAL OF BROMIDE FROM SURFACE WATER: COMPARISON BETWEEN SILVER-IMPREGNATED GRAPHENE OXIDE AND SILVER-IMPREGNATED POWDER ACTIVATED CARBON.....	77
4.1. Abstract.....	77
4.2. Introduction.....	78
4.3. Methods and Materials.....	80
4.4. Results and Discussion.....	84
4.5. Acknowledgements.....	92
4.6. Supporting Information.....	93
5. ANAEROBIC EFFECTS OF COLLOIDAL NANO-SILVER AND IONIC SILVER ON THE GUT MICROBIOME UNDER REALISTIC EXPOSURE CONDITIONS.....	108
5.1. Abstract.....	108
5.2. Introduction.....	109
5.3. Methods and Materials.....	110
5.4. Results and Discussion.....	114
5.5. Acknowledgements.....	118

CHAPTER	Page
6. PUBLIC PERCEPTIONS REGARDING THE USE OF NANOMATERIALS FOR DRINKING WATER TREATMENT	123
6.1. Abstract.....	123
6.2. Introduction.....	124
6.3. Methods and Materials.....	126
6.4. Results and Discussion.....	128
6.5. Acknowledgements.....	137
6.6. Supporting Information.....	145
7. ARE INDUSTRIAL PERCEPTIONS FOR DRINKING WATER TREATMENT NANOTECHNOLOGIES VALIDATED BY PUBLIC PERCEPTIONS?.....	160
7.1. Abstract.....	160
7.2. Introduction.....	161
7.3. Methods and Materials.....	163
7.4. Results and Discussion.....	165
7.5. Acknowledgements.....	172
7.6. Supporting Information.....	178
8. SUMMARY.....	189
8.1. Introduction.....	189
8.2. Identifying Functional Assays to Predict ENM Behavior in the Environment.....	189
8.3. Exploring Environmental Remediation Technologies Using Ionic Silver-Carbon Complexes.....	191

CHAPTER	Page
8.4. Identifying the Effects of Ionic Silver and Nanosilver Exposures on Fecal Microorganism Structure and Function.....	194
8.5. Comparison of Public and Industrial Barriers and Concerns Around the Use of ENMs in Small Scale Drinking Water Purification Devices.....	197
9. CONCLUSIONS AND FURTHER RECOMMENDATIONS.....	198
9.1. Conclusion	198
9.2. Recommendation for Further Research.....	204
REFERENCES	206
APPENDIX.....	234
A. CARBONACEOUS NANO-ADDITIVES AUGMENT MICROWAVE-ENABLED THERMAL REMEDIATION OF SOILS CONTAINING PETROLEUM.....	235
B. YTTRIUM RESIDUES IN MWCNTS ENABLE ASSESSMENT OF MWCNT REMOVAL DURING WASTEWATER TREATMENT....	256
C. DETECTION AND DISSOLUTION OF NEEDLE-LIKE HYDROXYAPATITE NANOMATERIALS IN INFANT FORMULA.....	283

LIST OF TABLES

Table		Page
2-1	Products and Applications Shown to Cause Direct or Indirect Release of ENMs into the Environment	11
2-2	Common Detection Methods and Analytical Tools Used for Engineered Nanomaterials. Detection Limits for each Analytical Tool are Given	15
2-3	Material Properties and Their Subsequent Technological Applications of the Big 10 Nanomaterials.....	21
2-4	Analytical Methods or Analyses for ENMs in Soil, Sediment, and Groundwater for Size Fraction and Distribution, Surface Area, and Phase and Structure.....	34
3-1	Functional Assays and Dimensions Used for Eight Nanoparticles.....	58
3-2	Coefficients of Variation (CV) for the Non-Biological Functional Assays with 8 ENMs.....	59
3-3	Linear Correlation Matrix of the Functional Assays	60
4-1	Characterization of Carbonaceous Adsorbents.....	93
4-2	Quantification of Ag ⁺ Released into Solution from Carbon Adsorbents after 4 Hours of Mixing.....	94
6-1	Comparing Survey Responses of Bottled Water Drinkers and Tap Water Drinkers to Whether they Would use In-home Water Purification Devices that use Nanomaterials to Treat Their Drinking Water.....	144

LIST OF FIGURES

Figure	Page
1-1 Nanomaterial Physico-chemical Properties Influence their Use and Risks.....	2
1-2 Schematic of the Use, Release, Transformations, and Societal Perceptions of ENMs within Society	4
2-1 Big 10 Engineered Nanomaterials in 2010 to the Environment.....	17
2-2 Conceptualization of the Generalizable Relationships for the State of ENMs and their Release Potential Across Product Lines and Commercial Products.....	20
2-3 Van der Waals Force, EDL Force, Total DLVO Forces, and Elastic Force Plotted Together to Find the Total Potential as a Function of Separation Distance.....	24
2-4 Risk-profiling Radar Plot.....	40
3-1 Results for Functional Assays Within Each Activity-profiling Quadrant.....	61
3-2 Activity Profile Radar Plots for the Comparison of Behavioral Trends of Different Engineered Nanomaterials.....	62
4-1 The Removal of Spiked Br ⁻ (200 µg L ⁻¹) in 1mM NaHCO ₃ by 25 mg L ⁻¹ of Adsorbents after Mixing for 4 Hours.....	95
4-2 The Removal of Spiked Br ⁻ (200 µg L ⁻¹) in Four Different Water Matrices by 25 mg L ⁻¹ of Ag ⁺ Impregnated PAC and GO after Mixing for 4 Hours in Polypropylene Batch Bottles.....	96
4-3 Removal of Spiked Br ⁻ (200 µg L ⁻¹) in Natural CAP water by 25 mg L ⁻¹ of Ag ⁺ Impregnated PAC and GO after Jar Tests with 28 mg L ⁻¹ Alum.....	97
4-4 SEM images of PAC-Ag, MH-Ag, and Tour-Ag in 1 mM NaHCO ₃ with 200 µg L ⁻¹ bromide and 20 mg L ⁻¹ chloride.....	98

Figure	Page
5-1	Changes in Gastrointestinal (A) pH and (B) SCFA Production after 24 Hours of Exposure to Three Silver Types and Concentrations.....119
5-2	Ag Distributions in Gastrointestinal Media With and Without Mucin after 24 Hours of Exposure.....120
5-3	Alpha Rarefaction Curves of Fecal Microorganism Communities to Assess Species Richness after Exposure of Microorganisms to Silver121
5-4	Relative Frequencies of Fecal Microorganisms (Phylum Level) in Control and Experimental Samples after 24 Hours of Silver Exposures.....122
6-1	Survey Respondent Perceptions of Fourteen Common Drinking Water Contaminants: A Comparison Between Bottled Water Drinkers and Tap Water Drinkers.....138
6-2	Survey Respondent Drinking Water Source by Average Annual Income.....139
6-3	Percent Response of Respondent Concerns Towards the Use of Nanomaterials in Various Consumer Products.....140
6-4	Respondents' Views on the Importance of Specific Features of In-home Water Purification Devices Using Nanomaterials.....141
6-5	Respondents' Views on the Likelihood They would Purchase each In-home Water Purification Device to Treat their Drinking Water.....142
6-6	Respondents' Answers to (a) Circumstances where They Would Purchase Nanotechnology to Treat Drinking Water and (b) If Their Opinion of Nanotechnology Would Change if Given More Information.....143

Figure	Page
7-1 Industry Concerns that the Following Factors may be Major Barriers to Successful Commercialization of Nanomaterial Enabled POU Devices.....	173
7-2 Industry Rankings of the Importance of Information they Want from Vendors Supplying them with Nanomaterials to Incorporate into POU Devices.....	174
7-3 Industry Beliefs of the Level of Public Concern around Using Nanomaterial-Enabled Devices to Treat Different Source Waters.....	175
7-4 Industry Rankings of the Information they Believe the Public will Want to Know before Purchasing a Nanomaterial Enabled POU Device to Treat Drinking Water.....	176
7-5 Industry Rankings of Ten Commonly Manufactured Nanomaterials and their Potential Impact on Environmental Health and Safety and their Acceptance by the Public if Used in POU Drinking Water Purification Devices.....	177
7-6 Industry Survey Respondents' Response to the Major Barrier to Successfully use Silver Nanomaterials to Treat (A) Drinking Waters and (B) Industrial Waters...	178

CHAPTER 1: INTRODUCTION

The intentional use of engineered nanomaterials (ENMs) in consumer products and industrial processes can improve the quality of human life. However, there have been emerging concerns around the rapid growth of nanotechnologies and deliberate and cautious governmental regulatory bodies. The scientific community has taken proactive approaches to determine if nanomaterials were detrimental to the environment and human health. Initial assessments highlighted to the scientific community that nanomaterials, like many other chemicals/materials, could be hazardous in specific scenarios likely unseen in the natural environment. The effects of ENMs in the environment likely are related to their unique function (e.g. specific surface area, surface reactivity, size distributions). These attributes that arise from ENM function properties have been integrated into technologies like drinking water treatment, remediation of chemical pollutants, and dietary supplements to improve human health. However, most research has focused on the fundamental understanding of ENM properties and ENM use in consumer products and industrial processes and significantly less research has been completed to understand what impact ENMs have from a societal perspective.

While physical scientists and engineers have leveraged ENM properties for industrial-based and consumer technologies, social scientists have studied ENM regulations and public perceptions. I sought to take an interdisciplinary approach to understand how ENM properties can improve the effectiveness of different technologies, what the intended/unintended consequences of these technologies are to the environment and human health, and how these consequences ultimately impact the decision-making of different stakeholders within society (Figure 1.1).

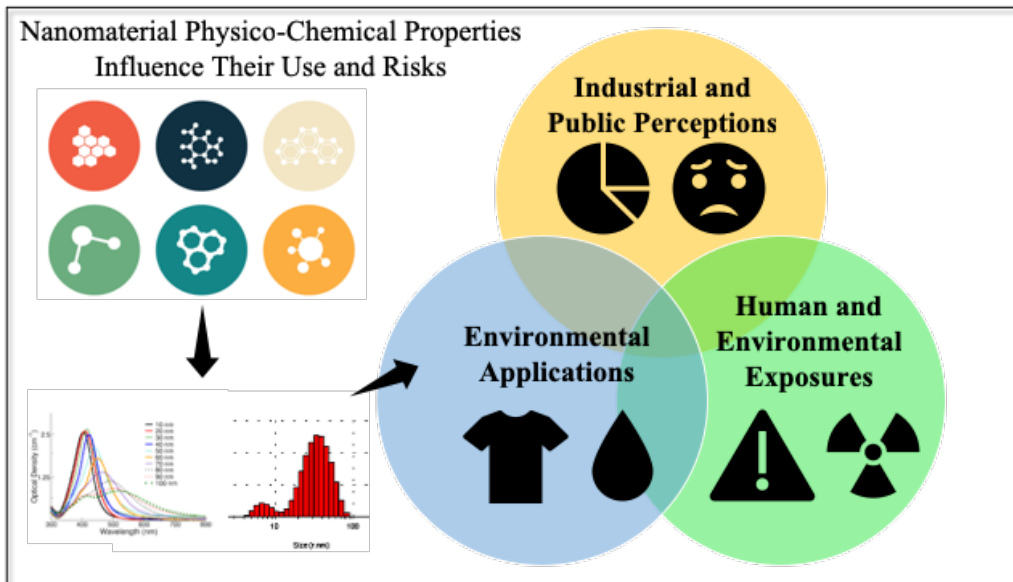


Figure 1.1. Nanomaterial physico-chemical properties influence their use and risks.

There is a growing body of knowledge of the technology-specific release of nanomaterials, of which carbon nanotubes and metal/metal oxide nanomaterials (e.g. Au, TiO₂) are among those nanomaterials with the top ten global releases from technologies¹. The potential for release to the environment and exposure to humans increases the uncertainties and risks surrounding these nanomaterials. Carbon nanotubes have unique functional attributes enabled by their dielectric properties and magnetic properties. Researchers have manipulated these carbon nanotube properties to improve energy storage in batteries, to develop gas sensors (e.g. carbon monoxide, ammonia), and to treat water contaminants through adsorption. Metallic nanomaterials also have unique functional attributes which vary between elemental compositions. Silver nanomaterials (Ag⁰) have anti-microbial properties and are commonly used in the healthcare industry through dressings for burns,

acne and cavity wounds, and hygiene products. Titanium dioxide (TiO_2), cerium oxide (CeO_2), and zinc oxide (ZnO) have photocatalytic properties and are commonly used in sunscreens for UV absorption, as pigments in paint, or as texture additives in food products.

These functional attributes of nanomaterials, while used to enhance technologies, can also lead to unintended releases and risks within society (Figure 1.2). Projections for both the range and the volume of nanomaterial-based technologies show continuous exponential growth. Rapid growth in the manufacturing of nanomaterial-based technologies, combined with their commercial and individual use, is resulting in the release of nanomaterials into the environment from multiple pathways. Point source emissions, such as those from industrial systems or from urban wastewater treatment plants, can release ENMs to air, water, and soil. Diffuse source emissions (throughout the product life cycle) also release ENMs into the environment during synthesis, manufacturing, use, recycling, and end of life. These releases and their dilution in the environment can lead to human and ecosystem exposures.

Rapid screening tools to assess ENM disposition in the environment, additional knowledge of the use of nanomaterials in consumer products and industrial processes, and societal perceptions of ENM use in these products and processes are needed to address missing data gaps around ENMs and provide additional information that can be used to develop regulations and frameworks around ENM use in consumer products and industrial processes. Figure 1.2 serves as the framework for the research within this dissertation which represents the flux of ENMs through urban physical-human systems. Dissertation topics are populated within the schematic.

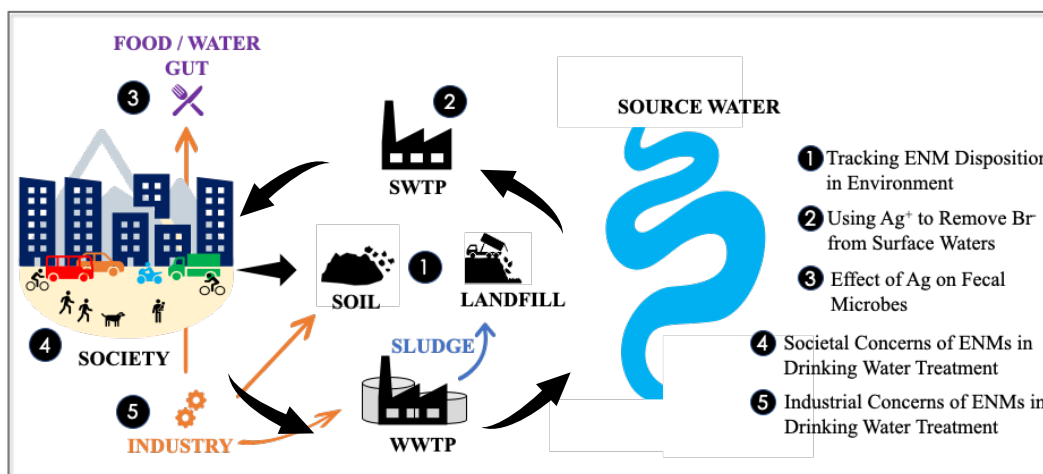


Figure 1.2. Schematic of the use, release, transformations, and societal perceptions of ENMs within society.

Based on a thorough literature review (Chapter 2), a series of research questions are proposed to guide my dissertation. My research focus was on the use of ionic and nanosilver in consumer products and industrial processes. The emergence of novel silver-based technologies and lack of governmental regulation around silver leads to large data gaps around silver distribution into the environment, the use of silver in remediation technologies, the associated effects of silver exposure on fecal microbe structure and function, and social and industrial perceptions of using ENMs (incl. silver) in small scale and point-of-use (POU) drinking water purification technologies. These data gaps lead to the over-arching question: For silver used in consumer products and industrial processes, can we gauge the efficacy of silver for surface water contaminant removal, evaluate societal concerns of its use in consumer products and industrial processes, and accurately predict its environmental disposition in the environment? Specific research questions are related to ENMs (incl. silver) in different fluxes within the urban physical-human system (Figure 1.2).

- Chapter 2 provides a general review of the state of science around nanomaterial physico-chemical attributes and their influence on nanomaterial exposure, specifically on current trends and challenges, nanomaterial releases across their product life cycles, and nanomaterial transformations in the environment.
- Chapter 3 provides insight into the development and interpretation of functional assays to compare and assess physico-chemical properties of ENMs and their impact on environmental activity of said nanomaterials.

Research Question 1: Can nano-specific functional assays be developed to create activity profiles for a range of ENMs in order to provide a framework and estimations of likely nanomaterial disposition in the environment?

- Chapter 4 provides insight into the environmental applications of carbon nanotubes and metallic nanomaterials for remediation purposes, specifically around the removal of bromide from surface waters upstream of drinking water treatment facilities.

Research Question 2: Can silver impregnated graphene oxide remove bromide from surface waters with more efficiency than silver impregnated powder activated carbon in the presence of competing ions and natural organic matter?

- Chapter 5 aims to understand the impact of human exposures to nanomaterials, specifically colloidal nanosilver-based dietary supplements and their effect on different compartments within the gastrointestinal tract.

Research Question 3: Do silver nanomaterials impact the structure and function of fecal microorganisms differently than ionic silver under realistic exposure conditions?

- Chapter 6 aims to understand the societal perceptions of intentionally using nanomaterials, specifically at the barriers around using nanomaterials to treat drinking waters and industrial waters from both an industrial perspective.

Research Question 4: What consumer concerns and barriers arise regarding the use of nanomaterials in point-of-use drinking water purification devices?

- Chapter 7 aims to understand the industrial perceptions of intentionally using nanomaterials, specifically at the barriers around using nanomaterials to treat drinking waters and industrial waters from a consumer perspective.

Research Question 5: What are the overlaps and disconnects between industrial and consumer concerns and barriers regarding the use of nanomaterials in point-of-use drinking water purification devices?

CHAPTER 2: PHYSICO-CHEMICAL PROPERTIES AND THEIR IMPORTANCE IN THE ENVIRONMENT: CURRENT TRENDS IN NANOMATERIAL EXPOSURES

- This chapter has been published as Kidd, J., and Westerhoff, P. (2018). “Chapter 5: Physico-Chemical Properties of Nanomaterials and Their Importance in the Environment: Current Trends in Nanomaterial Exposure.” *Physico-Chemical Properties of Nanomaterials*, by Richard C. Pleus, CRC PRESS, 2018.
- My author contribution: Approximately 90% of the content design, literature review and writing of the manuscript.

2.1. Abstract

The rapid advances in engineered nanomaterial synthesis and manufacturing, combined with their use and eventual disposal, have resulted in the release of nanomaterials into the environment. The objectives of this chapter are to provide a review of the state of science surrounding nanomaterial exposure, explore the methods and data available for nanomaterial releases from products across their life cycle, consider what tools are used to detect and quantify nanomaterial exposure, discuss future steps to understand nanomaterial exposure, and summarize critical data gaps and methods that could advance nanomaterial exposure analysis in the environment.

2.2. Introduction

Engineered nanomaterials (ENMs) are used in a wide range of applications, including healthcare, energy, agriculture, and personal care products. Projections for both the range and the volume of ENM applications show continuous exponential growth. This rapid growth in the manufacturing of nanomaterial-based technologies, combined with their commercial and individual use, has resulted in the release of nanomaterials into the

environment from multiple pathways. Point source emissions, such as those from industrial systems or from urban wastewater treatment plants, emit ENMs to air, water, and soil. Diffuse source emissions (throughout the product life cycle) also release ENMs into the environment during synthesis, manufacturing, use, recycling, and end of life. These releases and their dilution in the environment can lead to human and ecosystem exposures.

There are various ENM physicochemical properties that have implications on these exposure pathways. One particular challenging issue is that multiple forms of the same ENM manufactured, even of the same chemistry, can have different unique properties. For example, quantum dots are semiconducting ENMs commonly used in transistors and light-emitting diodes (LEDs). The alteration in particle diameter by even 1 nm, even with the same metal core, surface chemistry, and shape, can alter its optoelectronic properties such that it emits a unique photoluminescence [1]. This variation creates challenges in regulating nanomaterials. A second challenge is that ENMs undergo biogeochemical transformations and association with surfaces, including sediment and suspended particulate matter [2]. Tracking transformations of ENMs is analytically very difficult in environmental systems. ENM surface properties determine their transformation and aggregation behavior, thus influencing their mobility, interaction with, and bioavailability to organisms.

Models developed for chemical fate and transport (F&T) may not be appropriate for ENMs; however, such models are crucial to develop in order to describe the state of ENMs in the environment. A major obstacle has been uncertainty as to which exposure metric is most suited to ENMs: mass concentration, size distribution, shape, surface versus core composition, etc. The ENM material properties differ to those generated for bulk chemical substances, which have relatively few surface ions relative to its bulk density [3–

5]. Significant advances in how to use exposure data in risk assessment ENM models remain ill-defined.

This chapter first provides a general review of the state of science in nanomaterial exposure, specifically on the current trends in ENM exposure, dosimetry challenges, and concentration levels of concern. Second, we explore the methods and data available for ENM releases from products across their life cycle, explicitly the diversity of ENMs and their transformations in the environment. Third, we consider what tools are used to detect and quantify ENM exposures, while also highlighting ENM sample preparation challenges. Fourth, we discuss data streams and their role in taking future steps to understand ENM exposure. Finally, we summarize critical data gaps and methods that could advance ENM exposure analysis in the environment.

2.3.The State of Science in Nanomaterial Exposure

2.3.1. Nanoparticle Nomenclature

The common definition of “nanomaterial” loosely revolves around structures that are less than 100 nm in at least one of their dimensions, while also exhibiting unique properties. Over the past decade, there have been numerous attempts at developing a universal definition for nanomaterials, but regulatory groups have been giving unique definitions to different entities that manufacture and use nanomaterials in their products [6, 7]. For instance, the European Union (EU) regulations surrounding nano-enhanced products have at least three times given a unique definition for nanomaterials used in three different products. In 2009, the EU’s regulation on cosmetics required nanomaterials to be insoluble or biopersistent and intentionally manufactured. In 2011, its regulation on food labeling

required nanomaterials to be intentionally manufactured but also to be less than 100 nm in one dimension. In 2012, its regulation on biocidal products required nanomaterials to be natural or manufactured and required that at least half of these nanomaterials must have one or more dimensions less than 100 nm. This lack of a sound definition is problematic moving forward, as the majority of the public is unaware of what nanomaterials really are. This uncertainty means that the state of science surrounding nanomaterials is still at an infant phase and will need refinement in order to address the concerns surrounding its further development.

2.3.2. Nanomaterial Manufacturing

There are two approaches for the manufacturing of nanomaterials: the top-down approach and the bottom-up approach [8, 9]. The top-down approach involves the breakdown of bulk materials to generate nanostructures from them. This is a common method when manufacturing interconnected and integrated structures (i.e., electronic circuitry). Synthesis techniques include solid-phase techniques like mechanical attrition through either milling or mechanochemical processing. The bottom-up approach utilizes atoms and molecules to assemble larger nanostructures. This method allows for precise reproducibility of simple, identical nanostructures. Synthesis techniques include vapor-phase techniques like flame pyrolysis, molecular condensation, arc discharge generation, laser ablation, plasma, and chemical vapor deposition. Liquid-phase techniques include sol-gel, solvothermal methods, and sonochemical methods.

2.3.3. Nanomaterial Release from Industry

The physicochemical properties of nanomaterials allow for them to have transformative benefits to individuals and society through applications including but not limited to

enhanced food products, improved energy storage, antimicrobial fabrics, and water purification. Estimations for the value of the engineered nanotechnology sector range in the hundreds of billions of dollars [10–12]. As nanomaterial manufacturing continues to rise, it is imperative to understand how nanomaterial properties can enhance release potential. The presence of ENMs in the environment is thought to occur from the increase in production of nanomaterials of all natures, thus increasing the potential for their release and subsequent effects on ecosystem health [13]. Potential releases of ENMs, shown in Table 2-1, can come from a variety of release scenarios, including release during production, manufacturing, and use of products.

Table 2-1. Products and applications shown to cause direct or indirect release of ENMs into the environment

Type of release	Example products/applications	Likely mode of release	Ref.
Direct	Nano-aerosols	Inhalation	[14]
	Food additives	Digestion	[15]
	Nanopaint	Weathering	[16]
Indirect	Nanosunscreens	Application to skin	[17]
	Automotive fuel	Combustion	[18]
	Nanotextiles	Abrasion/washing	[19]

2.3.4. Natural Sources of Nanomaterials

There are many physical, chemical, and biological processes that occur naturally and form nanomaterial byproducts. These can include volcanic ash, ocean spray, fine dust and sand, erosion, and biological matter. These are diverse nanomaterials that can rival their synthetically engineered counterparts and are found in soil, aquatic, and atmospheric systems. The most abundant nanomaterials in soil systems are layer silicate nanoclays, metals, and metal hydroxides [20]. Nanoclays are formed by three unique abiotic weathering processes. Microorganisms can form metal nanostructures due to their negatively charged peptidoglycan cell wall and their high surface-area-to-volume ratio. Cationic metals accumulate along their surface and combine with anions in the surrounding media, resulting in nanoscale mineral formations [21].

Nanomaterial distribution in various aquatic environments is influenced by the hydrodynamic and morphological characteristics of rivers and coastal zones [22]. A common occurrence of nanomaterials in aquatic systems results from the increase in temperature and evaporation over water bodies. Increases in water temperature reduce the solubility of mineral basins, causing the formation and precipitation of nanomaterials and their eventual release as sea salt aerosols [23]. Natural organic matter (NOM) in surface waters can interact with metal salts or ions via photochemical-generated reactive oxygen species (ROS), causing the formation of metal-based nanomaterials [24–26]. Metal ions and sulfur in the ocean can be emitted by hydrothermal vents on the ocean floor, where they react with each other and form metal-bearing sulfide nanomaterials [25].

Nanomaterials in the atmosphere may be present by either primary emission (direct release from source) or secondary emission (atmospheric reactions). Over half of

atmosphere-produced nanomaterials come from terrestrial dust storms [27–29]. These nanomaterials are lifted into the atmosphere via air currents and distributed globally through dust migration across the continents, demonstrating the reach and influence of environmental nanomaterials. Forest fires can also spread ash and smoke over thousands of miles, increasing nanoparticulate matter in the atmosphere. Volcanoes are another source for naturally occurring atmospheric nanoparticles. Volcanic eruptions throw basaltic lava into the atmosphere, which is rich in magnesium and iron nanoparticles. As the ash spreads into the atmosphere, the gas temperature lowers, leading to the accumulation and deposition of nanoparticles into clusters due to electrostatic forces of attraction [30]. Nanoparticles in the atmosphere may linger there for years or accumulate, decompose, or react to enter food chains. A major challenge is detecting the amount and characteristics of what may be relatively small amounts of engineered ENMs within this group of natural ENMs.

2.3.5. The methods and data available for releases from products across the life cycle

2.3.5.1. Nanomaterial concentration levels of concern in the environment

Identification of nanomaterial waste streams often relies on use patterns, estimates of manufacturing volumes, and laboratory models. Measurement methods and instrumentation are nonspecific, making it difficult to differentiate between naturally occurring and engineered particles. Detecting nanoparticles is complex, both in gases and in liquids. Nanomaterials are so small that they cannot be detected by optical microscopes. Chemical analysis of individual nanomaterials in gases and liquids has been limited because of their low mass. Only recently have analytical instruments and methods become

available for this purpose, and as a result, nanomaterials as small as 1 nm can be detected [31, 32]. While the instruments used are not themselves size selective, they can be coupled with other instruments covering specific size ranges. Table 2 highlights the current methods and their subsequent generalized detection limits for an array of different nanomaterial natures.

Table 2-2 Common detection methods and analytical tools used for engineered nanomaterials. Detection limits for each analytical tool are given.

Method	Nanomaterial type	Generalized detection limit comments
Light scattering (UV/Vis)	Any	>1 mg/L in water 0.05 mg/L with HPLC of nanomaterial extract
ICP-MS TOF-MS (emerging)	Metals	>10 ppt in water (total metal concentration)
LC-MS	C ₆₀	~1 ppt
Thermal combustion or Microwave thermal analysis	MWCNT and SWCNT	~1 ppb
Isotopes	¹³ C metal isotopes	<1 ppb by scintillation counting isotopic ratios

UV/Vis, ultraviolet-visible; ICP-MS, inductively coupled plasma mass spectrometry; TOF-MS, time-of-flight mass spectrometry; LC-MS, liquid chromatography–mass spectrometry; MWCNT, multiwalled carbon nanotube; SWCNT, single-walled carbon nanotube.

2.3.6. The big 10 nanomaterials

In 2013, Keller et al. published on the global life cycle releases of ENMs (metric tons/year) from manufacturing, applications, disposal, and release into the environment, with some consideration of the high range of production estimates and releases [33]. From this analysis we term the “big 10 nanomaterials” as the top 10 ENMs that are currently being released into the environment: (i) titanium dioxide, (ii) silver, (iii) iron oxides, (iv) zinc oxide, (v) copper oxides, (vi) aluminum oxide, (vii) cerium oxide, (viii) nanoclays, (ix) carbon nanotubes (CNTs), and (x) silicon dioxide. They are used in a variety of manufactured applications (i.e., cosmetics, paints, electronics, food, etc.). The majority of these ENMs end up disposed in landfills (up to 90%), soil (up to 28%), water (up to 7%), or the atmosphere (up to 1.5%). In specific cases, the ENMs are released and flow through wastewater treatment plants (WWTPs) or waste incineration plants (WIPs) before they reach their eventual environmental endpoint. Figure 2-1 shows the global material emission distributions for the big 10 nanomaterials in 2010 to the environment.

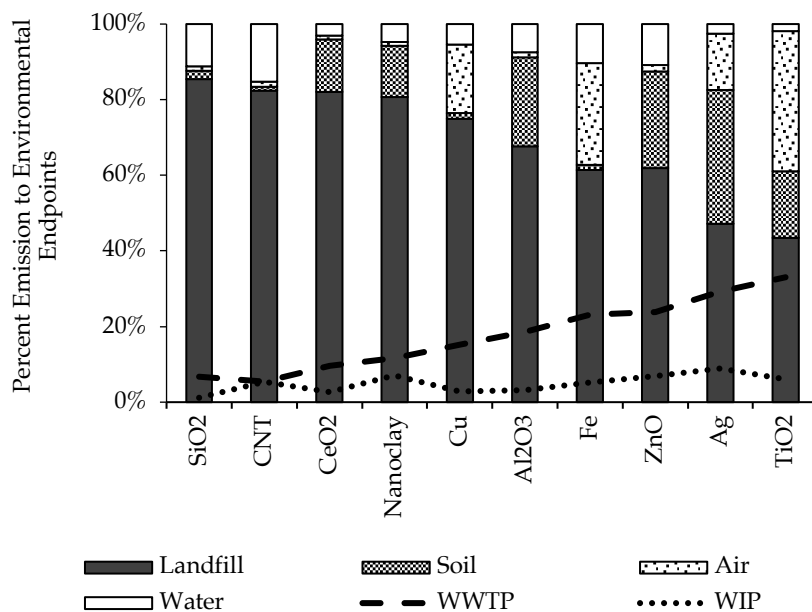


Figure 2-1 Big 10 engineered nanomaterials in 2010 to the environment. The majority of these ENMs are released to landfills before or after flow through wastewater treatment plants (WWTPs) or waste incineration plants (WIPs), which are not considered endpoints. The dashed lines depict the percentage of total nanoparticle emissions through each plant before translocation to one of the four environmental compartments. Data reconstructed from Keller et al. 2013.

2.3.7. The impact of ENM properties on their environmental release

ENMs that release into the environment are guided by their material properties, but isolating and determining the specific material property responsible for the release is a complex task because nanomaterials fall into a “gray area,” where they can behave either like small particles or like large solutes. To complicate it further, currently there are no techniques able to distinguish ENMs from naturally formed nanomaterials in the environment. In this section we will examine different nanomaterial properties to determine whether they influence the release of ENMs into the environment.

Even though studies have shown a release of ENMs from an anthropogenic product (i.e., Ag ENMs on textiles released during washing), very few of these studies have explored further to determine the relationship between nanomaterial properties and release potential.

The most common material properties found to influence ENM release are dissolution and aggregation. However, these are chemical and physical transformation processes, which we will discuss later in the chapter. While dissolution will release metal oxide ENMs into the external environment, they end up as cationic ions and can no longer be called nanomaterials. Abrasion of textiles can lead to aggregation of ENMs, but this physical transformation converts the once nanomaterials into the microscale. Nanomaterial properties studied that show release potential, while keeping the ENM intact are few and far between. One study found that size can potentially play a role as smaller quantum dots (<10 nm) were released in greater amounts than those with 30 nm diameter from hydrogels [34]; however, hydrogel mesh size variability could influence these results. Another study found that the aspect ratio of ENMs plays a role in colloid transport, where nanomaterials with higher aspect ratios show a decrease in electric double-layer (EDL) thickness and display greater biological cell retention [35]. This has been commonly observed in studies that focus on ENM translocation through biological matrices, where smaller, spherical ENMs have greater translocation through cell membranes and more release into interstitial regions than larger, rod-shaped ENMs [35]. This is a relatively untouched area of nanoscience, and the uncertainty surrounding the influence of ENM properties on environmental release potential is a major challenge moving forward. It should be a priority to reduce the knowledge gaps in this area.

2.3.8. The Diversity of Nanotechnology Products

ENM applications are very diverse. Figure 2-2 highlights the technological applications of the big 10 nanomaterials and the unique material properties that make them an effective technology. Current application product lines involving ENMs can be broken down into four product lines: (i) the dispersion of ENMs into liquids that are used in industrial manufacturing (i.e., polishing agents), (ii) the dispersion of ENMs into products (i.e., foods), (iii) the embedding of ENMs into composite polymers (i.e., thermoplastics, membranes for water filtration), and (iv) the coating of ENMs on the surfaces of flexible polymeric materials (i.e., textiles). These product lines utilize nanomaterial functionality to optimize their application, as seen in Fig. 6.2. The *y* axis in the figure corresponds to the reactivity of ENMs in the four product lines. Product lines A and D utilize the reactive properties of ENMs during product design and synthesis (i.e., redox activity, hydrophilicity), while product lines B and C utilize ENMs for structural support and product stability (i.e., mechanical strength). The *x* axis in the figure corresponds to the physical relationship of the ENMs and the products. Product lines A and B contain ENMs that either do not reside in the final consumer product or are loosely bound to the surface of the product (i.e., food coating). Product lines C and D contain ENMs that are embedded within the product and are unlikely to be released during their use or disposal. These can include ENMs in polymers or floor coating.

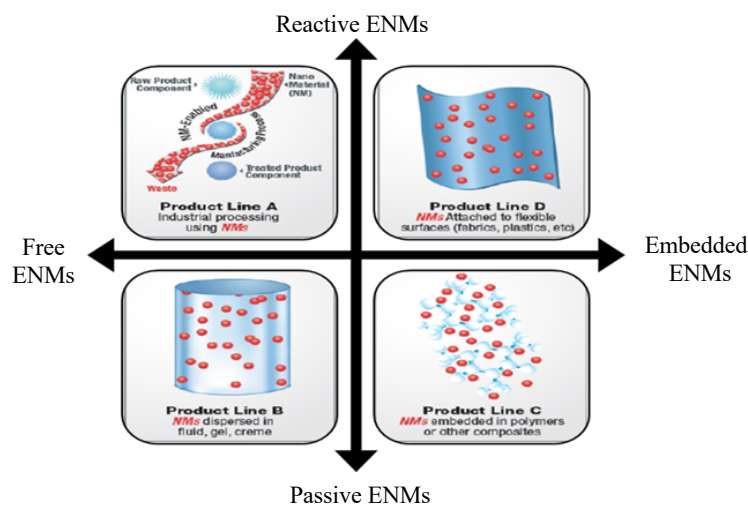


Figure 2-2 Conceptualization of the generalizable relationships for the state of ENMs and their release potential across product lines and commercial products.

Product line A includes polishing agents like chemical-mechanical polishing (CMP) fluids. Over 5500 tons per year of CMPs are used [36]. We can realistically estimate that in urban locations, there is between 0.1 and 1.0 mg ENMs/L that flow through a WWTP at any given time that originate from CMP fluids [36]. In the semiconductor industry there are concerns surrounding workplace exposure and monitoring and the lack of on-site CMP industrial treatment. Product line B includes nanomaterials in foods. ENMs are added to food for a variety of reasons, including texture, anticaking, color, oxygen barrier, abrasives, and antimicrobial properties [11]. Unfortunately, there is little confirmed occurrence and exposure data available. Product line C includes embedded nanomaterials throughout polymers. This includes formed plastics, where ENMs are added for strength [37]. Product line D includes nano-enabled textiles, which are used because of their “self-cleaning,”

flame retardancy, and antimicrobial properties [38]. Table 2-3 highlights the variety of technological applications that utilize ENMs for their unique material properties.

Table 2-3 Material properties and their subsequent technological applications of the big 10 nanomaterials

ENM	Material property	Technological applications	Ref.
TiO₂	Photocatalysis	Sunscreen, pigments	[39]
	Texture	Food, toothpaste	[40]
Ag	Antimicrobial	Healthcare, textiles	[41]
Fe	Magnetism	Groundwater treatment	[42]
ZnO	Photocatalysis	Sunscreen, pigments	[43]
	Luminescence	Electronics, displays	[44]
CuO	Catalysis	Gas sensors, lithium cells	[45]
Al₂O₃	Strength	Filler for rubber	[46]
CeO₂	UV absorption	Sunscreen	[47]
Nanoclay	Strength	Reinforced plastics	[48]
CNT	Antimicrobial	Antifouling membranes	[49]
	Strength	Sporting equipment	[50]
SiO₂	Resistance	Glass, optics	[51]
	Texture	Food	[52]

2.3.9. Transformations of ENMs Have an Impact on Exposures

Current research efforts toward understanding nanomaterial fate, transport, and reactivity in the environment have focused on testing pristine ENMs that have had no prior contact

with the environment. The truth is that the physicochemical properties of ENMs make them highly reactive in environmental systems, resulting in transformations that will greatly influence their behavior. These properties, coupled with the complex and random nature of environmental systems, greatly complicate our understanding of risks associated with the release of ENMs in the environment. Oxidation and reduction reactions, dissolution, aggregation, and adsorption of macromolecules all readily occur in the environment [53], but there is still uncertainty surrounding the role these transformations play on both exposure and impacts across the whole life cycle of ENMs. In this section, we will discuss chemical, physical, and macromolecule-influenced transformations of ENMs in the environment and the hazards associated with ENM release.

2.3.10. Chemical transformations

Reduction and oxidation (redox) reactions are coupled processes that involve the transfer of electrons between two entities. Redox processes are also the basis of various precipitation and dissolution reactions that influence the sequestration and mobility of inorganic metals. Thus, redox reactions might be important for the transformation and fate of ENMs. ENMs can contain material properties that will undergo reduction, oxidation, or both in the environment [54]. Aquatic conditions with high dissolved oxygen exist in many well-mixed surface waters. Low-oxygen-containing environments exist in carbon-rich sediments and groundwater, hypolimnionic reservoirs, WWTPs that implement denitrification, etc. Tidal zones can have cycling between redox states. Sunlight can induce catalyzed redox reactions (photo-oxidation and photoreduction), which can affect ENM coatings, oxidation states, generation of ROS, and ENM persistence in the environment [25].

Dissolution occurs when molecules of the dissolving ENM migrate from the ENM surface to the bulk solution through a diffusion layer, where the concentration gradient between the ENM surface and the bulk solution acts as the driving force. The rate of dissolution depends on ENM properties (i.e., size, surface coating, aggregation potential), combined with the mass/molar concentration, which determines the concentration of ENM surface area available for dissolution reactions and water quality [55, 56]. For example, nanosilver (Ag^0) equilibrium with dissolved silver ions behaves more like a redox equilibrium than a solubility equilibrium because oxidation proceeds Ag^+ release. As Ag^+ is released in a closed system, the equilibrium changes [57, 58].

Metal oxide nanomaterials can undergo proton-promoted dissolution in aqueous matrices. In this mechanism, protons are bound to oxide ions closest to the surface of the nanoparticle [59]. The protons polarize the bonds between the oxide and metal ions. Because sorption of protons to the ENM surface is fast, the rate of dissolution is proportional to the concentration of the nanomaterial. However, if there is a ligand attachment on the ENM surface, the reaction can be inhibited [60]. This occurs because ligands form surface complexes with metal oxide ENMs. More importantly, the dissolution kinetics of ENMs are strongly influenced by the water chemistry of the aqueous media, such as pH, redox potential, and the type of concentration of inorganic and organic ligands [61]. The presence of some inorganic ligands (i.e., phosphate, sulfide, carbonate) can induce the transformation of soluble ENMs to less soluble minerals (ZnO ENMs to zinc sulfides), thus decreasing dissolved metal concentrations [62]. Like redox reactions, dissolution of ENMs varies significantly with environmental matrices. While it is still relatively uncertain, we can begin to conclude that the environment to which ENMs are

released may be just as important in their release as the intrinsic physicochemical properties of the ENMs.

2.3.11. Physical transformations

The aggregation of ENMs occurs when their surfaces come in contact with each other and close-range thermodynamic interactions drive particle–particle attachment. For ENMs <100 nm in size, Brownian diffusion controls the forces between individual particles, causing random collisions, resulting in their attachment or repulsion. The thermodynamic interactions that control this can be understood through Derjaguin–Landau–Verwey–Overbeek (DLVO) theory. This theory predicts the probability of two particles sticking together by the summation of van der Waals (vdW) and EDL potentials to determine whether forces are net attractive or net repulsive. For example, in Figure 2-3, vdW and EDL potentials are plotted as a function of separation distance between the particles. Summation of these curves demonstrates that particles can have a net attraction in a primary or a secondary well. Primary well particles are irreversibly aggregated, whereas secondary well particles are reversibly aggregated.

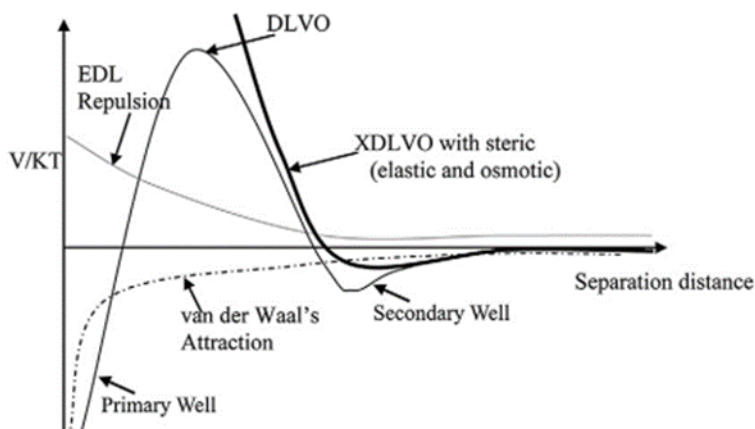


Figure 2-3 Van der Waals force, EDL force, total DLVO forces, and elastic force plotted together to find the total potential as a function of separation distance. XDLVO is extended DLVO. V/KT is the potential energy divided by Boltzmann's constant and absolute temperature [63].

DLVO forces alone are not sufficient to accurately predict ENM aggregation behavior. Steric repulsion forces occurring from ENM coatings or NOM makes it so these particles might only have a net attraction in the secondary well [64]. This means that coated ENMs can aggregate reversibly, which plays a major role in the release, fate, transport, and bioavailability of ENMs in the environment. These additional forces are summed with DLVO, resulting in extended DLVO (XDLVO).

If we apply these concepts to aggregation in the environment, it becomes clear that there are two types of aggregation that are important: homoaggregation and heteroaggregation. Homoaggregation refers to the aggregation of two similar particles. This is observed in homogenous suspensions of particles that are typically studied in the lab to correlate research with DLVO theory. Homoaggregation is primarily influenced by diffusion potential at the colloidal scale, the radius of particle collisions, mixing conditions, and properties of ENMs (i.e., zeta potential, Hamaker constants). Experimental studies have a vast knowledge of the fundamentals of homoaggregation theory and its mechanisms [65]; however, environmental systems contain natural particles in numbers far greater than the number of manufactured ENMs, so we assume that homoaggregation has a minimal impact on ENMs in the environment. Heteroaggregation refers to aggregation of dissimilar particles in terms of their chemical composition, electrical charge, size, or shape. Nanomaterial interaction in complex environmental systems is likely to be influenced by

physicochemical properties and background chemical conditions [63]. Heteroaggregation of ENMs with low-density natural colloids may facilitate the stabilization or disaggregation of ENMs, which would increase their residence times in water bodies, making the aggregation state of ENMs more difficult to predict. Heteroaggregation with bacteria, NOM, or mobile colloids could enhance ENM stability, but heteroaggregation to large enough particles could also destabilize ENM dispersions [66].

Recently there have been a handful of new studies that have tried to create a framework to determine the heteroaggregation rates for collisions between ENMs and NOM, as well as ENMs and natural nanomaterials (NNMs). While not validated, a working theory suggests that we can develop aggregation rate constants for heteroaggregation using Equation 1 [67]:

$$k_{\text{het}} = K \times \alpha, \quad (1)$$

where k_{het} is the aggregation rate constant for heteroaggregation, K is the product of collision frequency, and α is the attachment efficiency (stickiness factor). However, it is important to note that this rate constant provides estimates for the average behavior of ENMs and is not indicative of all potential release and transformation scenarios. This is further complicated when investigating ENMs with structural deformations or complex matrices, as this theory has only been utilized in ideal systems with spherical ENMs. The complexities of natural systems and uncertainties surrounding ENM release and subsequent transformation by aggregation need further refinement, and it may be necessary

to develop unique aggregation constants for specific ENMs and specific natural systems, as a universal constant applicable to all aggregation scenarios is highly unlikely.

2.3.12. Macromolecule-induced transformations

The adsorption of macromolecules (i.e., NOM) on ENMs can occur in all environments. Once released into the environment, both uncoated and coated ENMs can become transformed through interactions with NOM, whose concentrations are typically orders of magnitude higher in concentration than manufactured ENMs, resulting in the significant modification of ENM properties and behaviors. Most ENM–NOM interactions will involve the displacement of weakly bound coatings on the particle surface to form thin monolayer, thick monolayer, or multilayer surface coatings of NOM with varying coherence. The consistency and thickness of the ENM–NOM interactions depends on the ENM properties, and the matrix conditions (e.g., pH and ionic strength) during interaction negatively affect homoaggregation and heteroaggregation. In addition to changes in aggregation, ENM–NOM complexes have been shown to reduce short-term bacterial toxicity for metal-based nanomaterials [68]. It is thought that NOM prohibited the effect of the ENMs, either by directly coating the surface or by minimizing dissolution.

2.3.13. Hazards of Nanomaterial Release

There is potential for nanomaterials to be toxic in the environment. However, despite over a decade of findings surrounding ENM physicochemical properties and their associated biological health effects, uncertainties remain on universal frameworks, such as those that exist for traditional chemicals to a priori predict ENM toxicity. As the number of ENM-

enhanced technologies increases, release and exposure of ENMs into soil, water, and atmospheric systems can lead to hazardous conditions. Nanotoxicity is complicated further by the number of ENM transformations that occur in the environment. Alterations in ionic strength, the ENM surface chemistry, or contact with NOM can change the aggregation potential and size of the nanoparticles, leading to bioaccumulation within organisms, thus increasing body burdens and stress [69–71]. For some ENMs with smaller diameters, their chemical reactivity is high, which, in turn, can result in the increased production of ROS, causing toxicity in biological organisms [72]. Some nanoparticles, like silver (Ag), are susceptible to surface reactions with oxygen and sulfur atoms, while other nanomaterials can experience dissolution to ions or chemical reactions [58], which can be more toxic than the nanomaterial itself (i.e., cadmium quantum dots to cadmium ions). All of these scenarios impact ENM physicochemical properties that can ultimately drive the toxicity, bioavailability, and even bioaccumulation of nanoparticles within the environment.

In the environment, bacteria play an integral role in nutrient cycling, in photosynthesis, and as a food source. While it has been shown that some ENMs are toxic to bacteria, the exact toxic pathway is somewhat controversial. Current research indicates that both ROS production and metal ion dissolution are potential causes of bacterial nanotoxicity [73], but more research needs to be conducted to verify working theories. In some cases, photocatalytic ROS production under ultraviolet (UV) light has been shown to produce electron–hole pairs that cause reduction/oxidation of nearby biological species [57]. In other cases, increases in metal ion concentrations intensify nanotoxicity toward bacterial species by causing the formation of oxidative radicals [74]. At this time, there have not been enough studies to correlate nanoparticle physicochemical properties to

specific bacterial nanotoxicity, leaving much to be desired in this field of research. Advances in real-time biological assays and linkage of nanotoxicity/gene expression will contribute to reducing these knowledge gaps.

There is some evidence for plant toxicity due to nanoparticles. Studies have shown that plants facilitate translocation of nanoparticles from their roots to their leaves via the upward transport water system [75], but there is a lack of analytical tools to allow visualization of nanoparticle–plant interactions (i.e., super-resolution microscopy), creating an expansive knowledge gap. Right now we rely on phenotypic assessments and standard assay kits, which are incapable of such detection. Some studies have shown that introduction of nanomaterials during plant germination have resulted in the impediment of plant growth [76]. However, these results are often contradictory, as nanoparticle type and plant type appear to play a significant impact in toxicity, with even some studies showing increases in plant and crop yields when introduced to nanoparticles [78].

Multicellular organisms have been used most to examine nanotoxicity. Common model aquatic organisms are the medaka (*Oryzias latipes*) and zebrafish (*Danio rerio*). The nanotoxic effects on the medaka are influenced by the nanomaterial nature and surface coating, where nanotoxicity is a function of concentration, not mass [79]. Specific mechanisms of toxicity involve increased oxidative stress and the down-regulation of genes coding for growth, cell proliferation, and differentiation. The nanotoxic effects on zebrafish can be related to the shape of the nanomaterial, as sharp-edged nanomaterials can lyse cell membranes [79]. A common model terrestrial organism is the earthworm (*Lumbricus terrestris*). The nanotoxicity impact for these organisms varies by the nature of the nanomaterial [80]. Inorganic nanoparticles each cause growth and reproductive damage at

different concentrations, while carbon nanoparticles are likely to become sequestered in soil systems, reducing their bioavailability and toxicity to earthworms.

Species sensitivity distributions (SSDs) can be used to predict the potential impacts of ENMs on biological organisms when exposed to ENMs in natural environmental conditions by modeling the affected fraction of species that would be harmed when exposed to ENMs. Unfortunately, there are few exposure limits put into place for specific ENMs, and what currently exists may not be sufficient to effectively reduce the risks associated with ENM exposure. One research area currently working to better understand ENM exposures is the field of modeling, where the collection of data may lead to breakthroughs in identifying the driving parameters for ENM exposure and subsequent toxicity.

2.3.14. The Current State of Modeling Efforts on Nanomaterial Exposure in the Environment

Models are powerful tools for describing the behavior of contaminants in complex environmental systems. The aim of investigating the fate and behavior of nanomaterials is to determine whether they pose a risk to environmental and human health and to guide management strategies; however, the current detection of ENMs in environmental systems is very challenging and suitable analytical methods are still under development. Most ENM models have also been used for the identification of important fate processes or parameters via parametric analysis or sensitivity analysis, the estimation of potential for long-range transport, and the estimation of overall residence times. Two general modeling approaches for ENMs in the environment are material flow analysis (MFA) and process-based F&T.

2.3.14.1. Material flow analysis

The earliest approaches to ENM fate modeling relied on MFA, which is a specific assessment methodology used to track the amount and flow of substances into and between technological “compartments” and environmental “compartments” (i.e., air, water, soil, landfills, etc.). These models are not spatially explicit, but they do help conceptualize a material’s life cycle. ENM size, shape, aggregation state, surface coatings, particle chemistry, and phase changes are not explicitly considered in this model framework [81]. Instead, they are implied factors. MFAs are not the most appropriate tool for predicting environmental concentrations or specific locations (i.e., downstream of WWTPs) but are helpful in understanding general use and fate patterns. Experimental research and heteroaggregation models show that ENMs typically associate strongly with solid phases, leading to sedimentation and the accumulation of ENMs in sediments at “hot spots” near points of release and exposure [82].

2.3.14.2. Process-based fate and transport analysis

Even though ENMs behave differently than larger particles and solutes in the environment, they are largely subject to the same F&T processes that have been modeled successfully for organic and ionic contaminants. Existing chemical F&T modeling frameworks are capable, with some adaptation, of describing all major ENM fate processes, but major assumptions are made with respect to model scale and spatial resolution, steady state or time variable, and whether transformations and heteroaggregation are expressed as dependent on ENM properties, environmental conditions, or both [81]. Some models conserve mass, while others conserve particle number. For example, some models compare

the sizes of ENMs and use time-independent partitioning ratios for heteroaggregation and attachment of ENMs in different environmental compartments, using only one transformation parameter (i.e., dissolution), while neglecting the rest [83]. Other modeling efforts include colloidal science instead of partitioning to determine the fate of ENMs [84]. Such radically different assumptions can completely change predicted results. If we compare the two modeling analyses, process-based models can provide better estimates of ENM environmental concentrations than MFAs because they model relevant environmental processes at a higher spatial resolution than MFAs. However, there is a need to validate these models using field exposure measurements of predicted hotspots.

2.4.The Tools for Detection and Quantification of Nanomaterial Exposures

2.4.1. Measurement Exposures

Measurement methods and instrumentation are nonspecific, making it difficult to differentiate between naturally occurring and engineered nanoparticles. Furthermore, the background levels of naturally occurring nanomaterials are unknown. Due to the complexity surrounding the potential transformations of ENMs in the environment, it is important to determine the most appropriate metrics for detection and quantification of ENMs in environmental matrices. For instance, particle size is ambiguous but has multiple parameters that play a large role in ENM release and F&T. These parameters that need to be evaluated are particle diameter (electron microscopy), hydrodynamic diameter (dynamic light scattering), and radius (static light scattering). Each parameter is as equally important as the others, but we can only obtain each parameter with a unique analytical tool. Only determining one parameter may not be sufficient. Table 4 highlights different nanomaterial properties and the corresponding analytical methods or analysis required to fully characterize them.

Table 2-4 Analytical methods or analyses for ENMs in soil, sediment, and groundwater for size fraction and distribution, surface area, and phase and structure. Reconstructed from U.S. EPA (600/R-14/244, 2014) [85]

Metric	Analytical method or analysis
Size fractionation	Centrifugation
	Ultrafiltration: direct flow or tangential flow (TFF)
	Field flow fractionation (FFF)
	Capillary electrophoresis (CE)
	Size-exclusion chromatography (SEC)
Size distribution	Transmission electron microscopy (TEM)
	Scanning electron microscopy (SEM)
	Scanning probe microscopy (SPM)
	Dynamic light scattering (DLS)
	Laser-induced breakdown detection (LIBD)
	Small-/wide-angle X-ray scattering (SAXS/WAXS)
Surface area	Brunauer–Emmett–Teller (BET) method
	Calculation from TEM, atomic force microscopy (AFM)
Phase and crystalline structure	Electron diffraction
	X-ray diffraction (XRD)
	X-ray absorption spectroscopy (XAS)
	Raman spectroscopy

2.4.2. Mass concentration–based approach

The method for expressing concentration of ENMs is influenced by the research question at hand and by the anticipated analytical methods. Mass concentrations (mass/vol) are generally used for nonparticulate contaminants and may also be appropriate metrics for

some ENMs. For readily soluble ENMs, mass concentration may be the most important metric, because exposure is based on the soluble metal and uptake is based on the particle mass. Some analytical methods, such as transmission electron microscopy (TEM) and nanotracking analysis (NTA), rely on detecting and quantifying individual particles. Other methods such as field flow fractionation–inductively coupled plasma mass spectrometry (FFF-ICP-MS) determine the mass-to-size ratio using the integrated signal of the many thousands of particles present in any given elution volume. Information on ENP size, shape, and density allows conversion between mass- and number-based concentrations, at least for simple ENMs.

2.4.3. Surface area–based approach

Traditional measurements of surface area (i.e., N₂ deposition using Brunauer–Emmett–Teller [BET] analysis) cannot be performed for ENM solutions because these measurements must be conducted in nonaqueous environments. Nuclear magnetic resonance (NMR) spectroscopy techniques can provide surface area information in aqueous media, but the required concentration range (on the order of a few weight percent) makes it impractical for application to natural samples. Rather, surface area must generally be inferred indirectly from both geometric characterization (size, shape, porosity) and mass or number concentration. It can also be calculated from FFF or single-particle inductively coupled plasma mass spectrometry (spICP-MS) with assumptions of ENM density.

2.4.4. ICP-MS analytical approach

The fastest expanding technique is most likely ICP-MS, which, within a few years, had its status changed from an advanced technique to a routine analytical method, although ICP-MS and laser ablation ICP-MS are capable only of determining total elemental

concentrations on a bulk or spatially resolved basis. ICP-MS techniques have microgram-per-kilogram sensitivity and can discriminate between different isotopes of the same element. This includes metallic ENMs and CNTs (using metal catalysts).

2.4.5. Thermal method analytical approach

Thermal methods can be used to quantify CNTs. One method is through microwave-induced heating, where rapid heating of CNTs from microwave absorption can be used to create a CNT mass-to-temperature relationship used in quantifying the amount of CNTs in biological samples [86]. Another method is through programmed thermal analysis (PTA), which relies on the thermal stability of CNTs. Organic carbon and CNTs have different thermal stability and as such will have a different analytical footprint [87]. This technique can also be used to determine whether changes in the thermal stability of CNTs occur if extracted from environmental or complex matrices.

2.4.6. X-ray analytical approach

A number of X-ray-based techniques, such as X-ray absorption and fluorescence, as well as their microfocused declinations, are applicable, in theory, to the entire periodic table [88]. Synchrotron-based X-ray absorption techniques also are able to probe chemical speciation and the local electronic structure of elements. Determining the local electronic structure of metal atoms can be used to identify ENMs in a sample [80]. Conversely, although X-ray-based techniques have milligram-per-kilogram sensitivity, sensitivity of X-ray-based techniques can be enhanced by using spatially resolved analysis, which exploits the occurrence of foci of elevated concentrations relative to the bulk sample that can correspond to isolated or aggregated nanoparticles [80]. X-ray photoelectron

spectroscopy and related techniques are attractive in the sense that they provide element-specific information while probing the surface of nanoparticles or their aggregates.

2.4.7. Environmental Sample Preparation Challenges

Presently, there is a lack of techniques for collecting, preserving, and storing samples containing ENMs. Which techniques are appropriate will depend on the sample type, ENM property of interest, and analytical method to be used. ENM systems are extremely sensitive to agitation from factors such as pH, ionic strength, sunlight, bacterial growth, and temperature. Processes such as aggregation, dispersion, and dissolution may affect the environmental state of ENMs. It is therefore important to determine the most appropriate metrics for detection, quantification, and characterization of ENMs in environmental and biological media. In some cases, sample preservation may not be possible for a given property of interest that must be analyzed, such as aggregation state. In other cases, sample preparation steps may be taken to preserve sample fractions for subsequently measuring properties of interest, such as particle concentrations. For example, some ENMs are extremely redox active (i.e., Ag ENMs). Quantification of dissolved ions in liquid media does not allow for proper storage, because dissolution may not be at equilibrium [53]. Dissolved ions first must be separated from the system using techniques such as ultracentrifugation or ultrafiltration and then preserved for analysis. Ultrafiltration is a type of filtration where pressure or concentration gradients can lead to the size separation of ENMs. Large ENMs are retained by the filter, while smaller ENMs and potentially dissolved metal ions pass through the filter [90]. This technique can be used to separate nanomaterials from their complex environmental matrices. Another technique is through

cloud point extraction (CPE) [91]. CPE utilizes nonionic surfactants to capture ENMs out of liquid phases by heating. As the temperature of the solution rises, the surfactants form micelles that surround ENMs. As the temperature increases above the cloud point, the micelles become dehydrated and aggregate. This leads to phase separation of the matrix and the surfactant, resulting in the extraction of ENMs from their complex matrix.

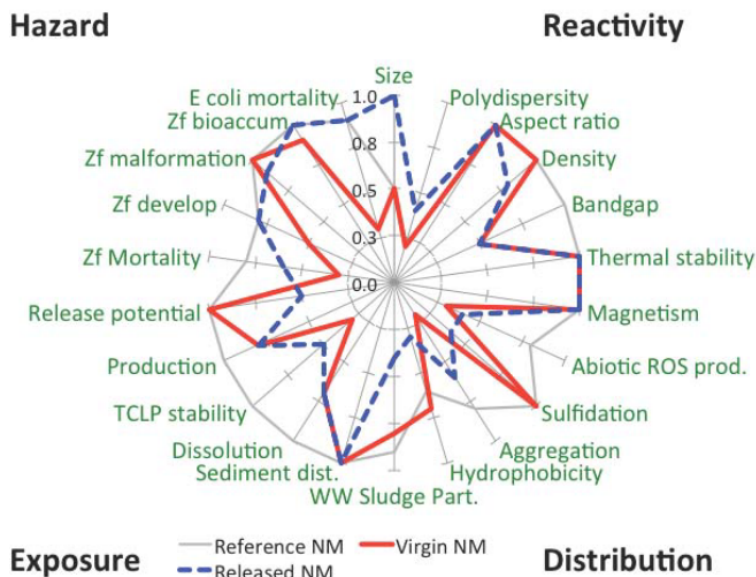
2.4.8. The Need for Multiple Lines of Evidence for Nanomaterial Detection

ENM systems are complex; thus, multiple orthogonal lines of evidence are needed to detect and physicochemically characterize nanoparticles in complex media. In traditional chemical analytical techniques, one must identify chemical species in at least two independent ways. ENM systems may have even more rigorous requirements for identification and quantification, relying on numerous techniques because they are not discrete molecular species. For example, identification of CeO₂ nanoparticles in a soil solution may require separation based on particle size, verification of separation using light-scattering techniques, chemical identification using ICP-MS, examination of particle size distribution, crystal structure, and chemical composition using TEM. Each ENM's nature must be taken into account, and independent measures of each physicochemical property of interest are needed for validation. Each analytical technique must be validated using standards, quality control procedures, and standard reference materials. However, for ENMs, very little standard reference materials are available for nanomaterials. To make things more challenging, current standards for ENMs in complex matrices are not available for ENMs because of the inherent instability of ENMs.

2.4.9. Functional Assays and Radar Plots

The physicochemical properties associated with a unique ENM functionality can also influence inherent hazard and potential exposure routes of an ENM. For example, a material whose beneficial function is to generate ROS may be inherently more toxic than a material that does not. Further, the ability to generate ROS may promote the ENM's release from the matrix in which it is encapsulated. Elucidating these parametric relationships through functional assays allows for the prediction of the efficacy and unintended consequences in a desired application. Functional assays are high-throughput screening tools designed to elucidate ENM property–exposure relationships from a life cycle perspective by parameterizing exposure models and by comparing ENMs or transformations of ENMs [92]. Although functional assays (i.e., octanol–water partitioning) for longevity and mobility have been developed for organic compounds, this is a relatively new concept for ENMs. These functional assays are developed to quantify the basic material properties of ENMs that are consistent with proxies for the risks of ENMs in the environment (i.e., exposure, hazard, reactivity, and distribution). These risk parameters can be summarized as mean values on a radar plot where data for a given ENM, or release of ENMs along a product value chain, are grouped together. Large scores in these parameters signal a higher potential risk. This can be observed in Figure 2-4.

Figure 2-4 Risk-profiling radar plot. (Zf is the response to a high-throughput zebrafish embryo assay.)



Functional assays can also be used to quantify parameters that describe a specific process within a complex matrix. They can be used as predictors of ENM behaviors in the environment that will help determine the release, fate, and effects of ENMs [92]. There are three components to functional assays: The first component is that they can be used as standard protocols to determine ENM property parameter by differentiating between intrinsic physicochemical properties of ENMs and extrinsic, system-dependent properties. The second component is that they are reference systems for reporting ENM exposure data. Using functional assays and radar plots to compare different combinations of ENMs and environmental systems provides a backbone for the future standardization of ENMs. The third component is that they are key for predicting exposures. All of the potential transformations that can occur in an environment can be evaluated with functional assays. For instance, measuring the dissolution rate of an ENM in an environmental matrix can be

compared with ENM bioavailability, toxicity, and persistence in the environment. Overall, functional assays provide a systematic path that will allow for more sustainable and rationale research, as well as aligning modeling efforts with lab-generated data.

2.5.What Does the Data Tell Us about Nanomaterial Exposure?

2.5.1. What Do We Know?

Current exposure measurements and models, while not perfect, have given insight into ENM exposure in the environment. The state of science pertaining to ENM exposure is still in the infant stage but is quickly developing. Intrinsic ENM properties and extrinsic, matrix-sensitive properties can create unique exposure scenarios that are currently too complex for available methodologies.

Currently, we are unable to determine whether specific ENM properties, or a combination of ENM properties, are responsible for ENM release and exposure in the environment. Quantification of ENMs and ENM material properties requires a number of different analytical tools because of a lack of analytical tools capable of conducting analysis on more than one specific parameter. ENM transformations in the environment (i.e., dissolution, aggregation) are key components in altering the release potential of ENMs in products. We can characterize feedstocks and pristine ENMs. Analysis of ENMs in complex matrices remains largely a purview of research labs. ENM manufacturers use both dry and wet ENM feedstocks, so it is difficult to distinguish between ENMs and NNMs. Few human studies track ENM distribution, availability, accumulation, or adverse outcomes released from consumer products.

2.5.2. What Should We Be Doing?

First, we should assess uncertainties surrounding common ENMs, like titanium dioxide and silicon dioxide. Some areas to address would involve answering the following questions:

- Should we remove these ENMs from concern?
- Do we really understand their consumer exposures?
- Are there sensitive consumer population or nano-specific adverse outcomes?

Second, we should apply functional assays to reduce uncertainties surrounding ENM use in products, as well as a guiding tool for life cycle exposures. We can utilize high-throughput screening assays to measure unique properties (optical, thermal, magnetic, etc.) and group products and exposure scenarios around ENM functional uses. Third, we should design studies across the life cycle of ENMs to validate models. In this way we can validate assumptions that pristine ENMs can be seen as precursors. Fourth, we can assess human exposures (workers, consumers) to measured ENM exposure levels (inhalation, oral, dermal), within biological fluids (nasal, urine, blood) and health outcomes. Finally, we should continue life cycle studies but compare efficacy versus exposure and toxicity risk and compare the risks of ENMs relative to use of other anthropogenic chemicals.

2.6. Acknowledgments

I would like to acknowledge the LCnano community, which is funded by the Environmental Protection Agency (EPA grant number RD835558001).

CHAPTER 3: DEVELOPING AND INTERPRETING AQUEOUS FUNCTIONAL ASSAYS FOR COMPARATIVE PROPERTY-ACTIVITY RELATIONSHIPS OF DIFFERENT NANOMATERIALS

- This chapter has been published as **Kidd, J.**, Truong, L., Hristovski, K., Tanguay, R., Westerhoff, P. (2018). Developing and Interpreting Aqueous Functional Assays for Comparative Property-Risk Relationships of Different Nanoparticles. *Science of the Total Environment*, 628-629, pp. 1609-1616
- My author contribution: Approximately 75% of the research and 80% of the text

3.1. Abstract

It is difficult to relate intrinsic nanomaterial properties to their functional behavior in the environment. Unlike frameworks for dissolved organic chemicals, there are few frameworks comparing multiple and inter-related properties of engineered nanomaterials (ENMs) to their fate, exposure, and hazard in environmental systems. We developed and evaluated reproducibility and inter-correlation of 12 physical, chemical, and biological functional assays in water for eight different engineered nanomaterials (ENMs) and interpreted results using activity- profiling radar plots. The functional assays were highly reproducible when run in triplicate (average coefficient of variation [CV] = 6.6%). Radar plots showed that each nanomaterial exhibited unique activity profiles. Reactivity assays showed dissolution or aggregation potential for some ENMs. Surprisingly, multi-walled carbon nanotubes (MWCNTs) exhibited movement in a magnetic field. We found high inter-correlations between cloud point extraction (CPE) and distribution to sewage sludge ($R^2 = 0.99$), dissolution at pH 8 and pH 4.9 ($R^2 = 0.98$), and dissolution at pH 8 and zebrafish mortality at 24 hpf ($R^2 = 0.94$). Additionally, most ENMs tend to distribute out of water and into other phases (i.e., soil surfaces, surfactant micelles, and sewage sludge).

The activity-profiling radar plots provide a framework and estimations of likely ENM disposition in the environment.

3.2.Introduction

Relative to work with dissolved organic chemicals, there are few strategies to compare the multiple and inter-related properties of engineered nanomaterials (ENMs) to their fate, exposure, and hazard in environmental systems (Westerhoff & Nowack, 2013; Yokel & MacPhail, 2011). Frameworks exist that relate intrinsic properties (e.g. crystal lattice structure) to negative environmental impacts (e.g. redox potential, band gap, cellular dysfunction) (Naldoni et al., 2012; Zhang et al., 2012; George et al., 2011), but such mechanistic models have not yet been integrated into predictive mechanistic fate and transport models for ENMs in water or soils (Gottschalk et al., 2009; Darlington et al., 2009; Praetorius et al., 2012) or absorption, distribution, metabolism, and excretion (ADME) models for whole organism exposures (Selick et al., 2002; Yu & Adedoyin, 2003). High-throughput testing platforms for hazards or toxicity have been developed to assess ENM functional behavior in complex systems (Mandrell et al., 2012; Truong et al., 2013; Cassano et al., 2016; Goldberg et al., 2015; Winkler, 2016; Silva et al., 2014; Vazquez-Munoz et al., 2017). For example, zebrafish are used as a sensitive, relevant whole-animal system to define the inherent toxicity of ENMs, chemicals, and complex mixtures (Allan et al., 2012; Kim et al., 2013; Chen et al., 2013; Corvi et al., 2012; Kim et al., 2012; Liu et al., 2012; Lin et al., 2013). Other emerging testing platforms for ENMs include surface photocatalytic reactivity using a methylene blue dye redox system (Corredor et al., 2015; Khaksar et al., 2015; Sabry et al., 2016), hydrophobicity using an

octanol-water partitioning system (Nel et al., 2009; Xiao & Wiesner, 2012; Hristovski et al., 2011), and magnetization using external magnets (Shahbazi-Gahrouei et al., 2013; Park et al., 2013). Assays for ENM attachment behavior in different aqueous solutions onto different substrates (e.g., suspended lipid bi-layers) have also been developed (Liu & Chen, 2015; Pokhrel et al., 2013a; Pokhrel et al., 2013b). Nevertheless, we still lack frameworks or assays to assess and interpret how the unique properties that arise at the nanoscale (e.g., magnetisms, plasmonic resonance) impact ENM environmental fate and ecotoxicity. Furthermore, while many studies include a single or few assays on a specific ENM, current literature lacks studies including multiple assays on the same ENM.

At least two approaches exist for utilizing functional assays as a tool to assess the relationships between ENM properties and environmental outcomes. First, functional assays can obtain rate or aggregation parameters for mechanistic fate modelling. Hendren et al. (2015) applied separate functional assays for dissolution rates and aggregation rates and developed a protocol to collect data suitable to parameterize nanomaterial fate and transport models. Second, functional assays can compare the relative activity of pollutants across multiple quadrants of activity-profiling plots. Crittenden et al. (2014) applied this method to compare the relative safety and sustainability of different chemicals by graphing numerous factors on a radar plot. Prior work on organic chemicals estimates activity using fugacity-based parameters and experimental functional assays (e.g., octanol-water partitioning coefficients). In this paper, we evaluated the applicability of nano-specific functional assays to develop activity profiles (i.e. radar plots for several ENMs).

This study's goal was to evaluate the suitability and reproducibility of functional assays that cover a wide range of behaviors exhibited by various ENMs. Our objective was

to develop relationships between an ENM's physico-chemical properties and functionality and use those relationships to predict their fate and transport in the environment, not to obtain parameters for fate and transport modelling. Eight ENMs that exhibit unique properties (plasmon resonance, magnetism, dissolved ion delivery, etc.) and are used in commercial products were selected for evaluation in this study. First, we designed functional assays to measure reactivity, distribution, physical and hazard behavioral outcomes of ENMs. Desirable features of the assays were that they took < 24 hours and utilized small masses of ENMs. Second, the assay reproducibility was evaluated. Third, the inter-correlated relationships were determined among different functional assay results. Finally, a strategy was developed to plot and interpret the assay outcomes.

3.3. Methods and Materials

3.3.1. Nanoparticle selection and quantification

Eight commercially relevant ENMs were used in this study: (1) Citrate-coated silver, (2) polyvinyl pyrrolidone-coated magnetite Fe_3O_4 , (3) tannic acid-capped gold, (4) fluorescein-capped SiO_2 , (5) colloidal SiO_2 , (6) ZnO , (7) CeO_2 , and (8) dispersed MWCNTs. (See Table S1 and Fig. S1 for manufacturer information). For non-biological functional assays, ENMs were purchased and received already dispersed in solution at concentrations between 20 mg/L and 200 mg/L. For non- biological functional assays, the ENM stock solutions were dispersed in 1 mM NaHCO_3 buffer at $\text{pH } 7.4 \pm 0.2$ at a concentration of 5 mg/L. For biological functional assays, the ENM stock solutions were dispersed at 6 different concentrations in ultrapure water, and then diluted as described below. Triplicate samples were prepared for each nanoparticle dispersion used in the

functional assays. Metal-based nanoparticles were quantified using inductively coupled plasma mass spectroscopy (ICP-MS) after digestion in 2% nitric acid (Speed et al., 2015; Lee et al., 2014; Bi et al., 2014; Mitrano et al., 2013; Reed et al., 2012) and MWCNTs were quantified using programmed thermal analysis (PTA) or UV/Vis light scattering (Doudrick et al., 2012). Additional nanoparticle analysis details are provided in the supporting information (SI).

3.3.2. Functional assays

Table 3-1 places the functional assays into activity-profiling quadrants (hazard, physical, reactivity, and distribution) and summarizes the functional assay methods, analytical tools, and quantitative output parameters. Although not inclusive of all possible activity endpoints, the table provides several possible assays that can be used to evaluate, plot, and interpret nanomaterial activity in the environment. Detailed descriptions of the functional assays are provided in the SI and briefly outlined here.

Unless otherwise stated, functional assays were conducted in either 40 mL glass vials with Teflon™ septa screw caps or 50 mL polypropylene centrifuge vials to minimize ENM losses onto the vessels. Assays involving agitation were conducted in a 45-rpm rotator table. ENMs were separated from ionic forms using 30 kDa centrifugal ultrafilters (Millipore, Ultracel Regenerated Cellulose Membrane, >90% Recovery). Samples were prepared for analysis within 1 h of completing the assay to prevent adsorption to vials and analyzed within 24 h. Individual ENMs were analyzed in triplicate for each functional assay to determine assay reproducibility. For the toxicity characteristic leaching procedure (TCLP) functional assay, the solution was adjusted to pH 4.9 to reflect the acidic conditions of a landfill and was conducted following the U.S. Environmental Protection Agency

(EPA) standard method (USEPA, 1992). The TCLP assay was conducted to assess dissolution potential of the nanoparticles in landfill leachate solutions and is not indicative of a toxicity assay.

The zebrafish ecotoxicity assay was conducted using a separate methodology than the other assays (Details in SI). Tropical 5D wild- type adult zebrafish embryos were collected, and the chorion was enzymatically removed using pronase to increase bioavailability. To track exposures, six concentrations were tested for each ENM using one animal per well in a 96-well plate. Each condition used 32 replicates. The 96-well plates (with embryos) were agitated overnight at 230 rpm on an orbital shaker. To track mortality and morphology responses, the zebrafish embryos were statically exposed until 120 h post fertilization (hpf). At 24 hpf, four developmental toxicity endpoints were assessed in each embryo: mortality at 24 hpf (MO24), developmental progression (DP), spontaneous movement (SM), and notochord distortion (NC). At 120 hpf, 18 developmental endpoints were assessed. The zebrafish acquisition and analysis program (ZAAP), a custom program designed to inventory, acquire, and manage zebrafish data, was used to collect developmental endpoints as either present or absent. For the zebrafish toxicity and behavioral biological assays, we assigned a “1” to values that were absent and “2” to values that were present.

3.4. Results and Discussion

3.4.1. Reproducibility of functional assays

Table 3-2 summarizes functional assay reproducibility for each ENM with the coefficient of variation (CV), calculated using the following equation:

$$CV = \frac{\sigma}{|\mu|}$$

where σ is the standard deviation and $|\mu|$ is the absolute value of the mean.

For the nanoparticles and functional assays evaluated, approximately one quarter of the data sets had CV >10%, and only about 5% of the data sets had CV >30% (Table 3-2), indicating that these functional assays are highly reproducible. The zebrafish assays are evaluated on absence/presence of biological behavior or toxicity. The nominal values collected for those assays are unable to be analyzed by CV. Although not considered here, previous studies have evaluated the reproducibility of ENM toxicity on Zebrafish systems (Liu et al., 2017; Busquet et al., 2014).

3.4.2. ENM comparisons for functional assay groupings

The functional assays are grouped into four environmental outcome quadrants: reactivity, distribution, physical, and hazard. The reactivity quadrant has measured outcomes that indicate ENM interactions with light (optical resonance), magnetic fields, or undergo dissolution. The distribution quadrant has measured outcomes that indicate potential ENM preference for non-aqueous phases (e.g. solids, solvents, micelles, sludge). The physical quadrant has measured outcomes that indicate ENM properties related to the system (1 mM NaHCO₃ water). The hazard quadrant has measured outcomes that indicate potential ENM interactions and hazards to Zebrafish development and Zebrafish toxicity. Results from each quadrant highlight the activity outcomes we observed experimentally. Additional assay outcomes can be found in the SI.

3.4.2.1. Nanomaterial property-reactivity relationships

Figure 3-1A compares the fraction of ENMs that dissolved for the eight different nanoparticles in two environmental matrices (1 mM NaHCO₃ buffer [pH 8.0] or TCLP landfill leachate [pH 4.9]). Triplicate experiments showed highly reproducible results

(Average SD = $\pm 1.5\%$ dissolution). ZnO was the only nanoparticle from the group of eight exhibiting N50% dissolution. The remaining seven nanoparticles had $\leq 20\%$ dissolution. Given that literature (Telgmann et al., 2016; Liu & Hurt, 2010) show nano-Ag dissolution increases in low pH conditions, it was surprising that $\leq 20\%$ of the silver dissolved in the functional assays under neutral or acidic pH. While the TCLP solution has a pH of 4.9, it also contains high acetate levels, which can influence the formation of $\text{AgC}_2\text{H}_3\text{O}_2$ particulates ($K_{sp} = 2.0 \times 10^{-3}$). Consequently, a lower amount of silver dissolution relative to the larger amount of zinc dissolution is reasonable.

3.4.2.2. Nanomaterial property-distribution relationships

Figure 3-1B compares hetero-aggregation potential for the eight ENMs by quantifying their distribution to wastewater biomass in 1 mM NaHCO_3 buffer (pH 8.0). Over 90% of Ag, Au, CeO_2 , and MWCNT ENMs associated with biomass. In contrast, $< 30\%$ of the mass of Fe_3O_4 , SiO_2 -colloidal, and SiO_2 -Fluorescein associated with biomass. This information is useful when we begin exploring potential ENM environmental implications. ENMs with high distribution to sludge will likely be removed within wastewater treatment plants (WWTP). ENMs with a low distribution to sludge have a higher likelihood of passing through a WWTP and ending up in downstream waters.

3.4.2.3. Nanomaterial property-physical relationships

Figure 3-1C shows the change in ENM size due to homo-aggregation before and after mixing in 1 mM NaHCO_3 buffer aqueous matrix for 24 h. MWCNTs, SiO_2 -F and SiO_2 -C had significantly increased changes in size during mixing. After 24 h of mixing, mean hydrodynamic diameters of Au, Ag, CeO_2 , and ZnO ENMs remained similar to their initial dynamic light scattering (DLS) diameters, while SiO_2 -colloidal, SiO_2 -Fluorescein,

MWCNTs, and Fe₃O₄ ENMs all showed significantly greater mean diameters. The high-aspect ratio of MWCNTs and their change in displacement during the assay could interfere with the DLS measurements, resulting in their variability in particle size, rather than homo-aggregation. After 24 h of mixing, polydispersity (Fig. S3.2) was below 0.35 for all ENMs, indicating that any homo-aggregation of ENMs during the assay allowed the ENMs to retain a relatively uniform size.

3.4.2.4. Nanomaterial property-hazard relationships

After 24 and 120 h of non-chorion embryonic exposure to each ENM, mortality from toxic effects was determined by counting number of dead zebrafish embryos after exposure. Mortality at applied ENM doses of 0.6 and 50 mg/L are shown in figure 3-1D. Percent mortality for all 8 ENMs at different dosing concentrations is shown in the SI. Au nanoparticles induced significant mortality at 30 mg/L or higher (38–81%), while MWCNTs showed induced mortality (60%) at 50 mg/L. ZnO was the most toxic because it induced significant mortality (N87%) at 10 mg/L or higher. The other five nanoparticles caused insignificant or low mortality (<15%) to the zebrafish.

In addition to using mortality, we also evaluated presence/absence of morphological and biological traits as a measure of ENM toxicity and indicator of zebrafish survival in the environment. A set of 21 of the 32 functional assays used here can also assess zebrafish phenotype and morphological traits upon ENM exposure. Here we only highlight endpoints that are statistically relevant for living embryos. Ag nanoparticles, while not eliciting a high percent mortality value, had an impact on zebrafish phenotype and morphology. At 5 mg/L Ag, 25% of the zebrafish exhibited developmental progress delays at 24 hpf and 25% exhibited excessive fluid accumulation around their yolk sac after

120 hpf. Exposure to CeO₂ at 50 mg/L resulted in 34% of zebrafish exhibiting developmental progress delays at 24 hpf. Exposure to ZnO at 3.3 mg/L, which is slightly lower than the toxicity threshold for ZnO, resulted in 10% of the zebrafish having their brain absent or malformed. High mortality can mask the impact of ENMs on zebrafish phenotype and morphology because once a zebrafish embryo is dead, we no longer monitored its phenotype or morphological traits. In presence of ZnO at 24 hpf at a concentration of 10 mg/L, only 12.5% of the zebrafish population remained, and any phenotype or morphological responses observed of the zebrafish to the ZnO are insignificant when compared to the original population size. Additional information for the zebrafish mortality and phenotype assays is presented in the SI.

3.4.3. Inter-correlations of functional assays

Table 3-3 presents a correlation matrix for the functional assays and shows statistical parameters (P and R² values) based on linear relationships. No Zebrafish phenotype assays were shown because no correlations were found due to either (Westerhoff & Nowack, 2013) the significant mortality of Zebrafish, which prevents phenotypes from being observed, or (Yokel & MacPhail, 2011) no effect of ENMs on Zebrafish phenotype.

Four parameters showed high correlations with an R² > 0.9. Cloud point extraction (CPE) and wastewater sludge partitioning had an R² of 0.99. Both dissolution assays (pH 4.9 and 8.0) had an R² of 0.98. Zebrafish mortality (24 hpf) and the TCLP dissolution assay (pH 4.9) had an R² of 0.92. Zebrafish mortality (24 hpf) and the dissolution assay (pH 8.0) had an R² of 0.94. Plots of these four correlations are available in the SI.

These correlations lead to three basic inferences. First, most of the functional assays are independent from each other and thus represent different phenomena. Second, CPE appears to be a reasonable surrogate for measuring ENM partitioning to wastewater sludge. CPE chemistry is based on surfactants first attaching to the ENM, and then this newly functionalized surfactant-ENM becoming enmeshed within a surfactant miscelle that can be separated from liquid above its cloud point temperature (Duester et al., 2016). ENM attachment to and removal with wastewater biomass appears to involve interactions with biosurfactants and depends on ENM incorporation into physical structures (e.g., liposomes), and the heat treatment of biomass denatures such proteins and liposome structures (Kiser et al., 2012; Kiser et al., 2010). Thus, some similarity emerges in terms of ENM interaction with surfactants and enmeshment into physical structures (miscelles or cell wall biological structures) as a common mechanism in these two functional assays. It may be possible to use CPE to screen the potential for ENM removal at wastewater treatment plants, but more work to validate this hypothesis would be required where ENMs are added to a variety of sewage water matrices at different concentrations. Third, ENMs with higher dissolution potential correlate well in functional assays at pH 4.9 or 8.0 because both essentially are based on the potential of an ENM to undergo redox reactions that evolve to soluble ions. The presence of toxic metal ions in solution is recognized as source for adverse biological outcomes (Garner et al., 2015), but uncertainty exists about the mechanisms leading to adverse outcomes on zebrafish toxicity mechanisms for ENMs and their ionic counterparts (Bai et al., 2010; Shaw & Handy, 2011). However, it is reasonable that an adverse biological outcome (i.e., zebrafish mortality at 24 hpf) correlates with functional assays that indicate higher potential for release of soluble toxic metal ions.

Overall, the correlation analysis is an important tool in understanding differences between ENMs and responses from the different functional assays and should not be misinterpreted as causal inference.

3.4.4. Developing activity-profiling radar plots

Activity-profiling radar plots (e.g., Fig. 3-2) show results of several ENM functional assays to give insight on nanoparticle behavior trends. For this work, we followed an approach used by Crittenden et al. (Crittenden et al., 2014) for developing chemical comparisons where the radar plot maps out all the functional assay responses to a specific chemical or, in this case, ENM.

There are different ways to normalize divisions on each spoke of the radar plot, but here the spokes on each dimension of the radar plots were given a ranking between 0 and 10, where each ranking number is associated with a corresponding range of outcomes. These outcome ranges typically fall under one of the following categories: (Westerhoff & Nowack, 2013) percent removals from different environmental phases (e.g., removal from water by magnet), (Yokel & MacPhail, 2011) percent distributions to different environmental phases (e.g., water to soil), (Naldoni et al., 2012) change in size (e.g., aggregation potential), and (Zhang et al., 2012) percent biological response (e.g., zebrafish percent mortality). The radar plots are a unique tool to allow for the audience to visualize the grouping of nanomaterial physico-chemical property parameters together. Large scores in these parameters signals higher potential environmental activity. Radar plots allow for a comparison of the environmental activity of these different nanomaterials. Radar plots can be used as reference systems for reporting ENM exposure data, and thus can be used in

standard protocols to determine nanomaterial property parameters. This provides a backbone for the future standardization of nanomaterials.

3.4.5. Radar plot comparisons for different nanoparticles

Fig. 3-2 contains activity profile radar plots to compare the behavioral trends of different engineered nanomaterials used in three different industrial applications. Figure 3-2A compares three ENMs (Au, Ag, and ZnO), all which are used for their antimicrobial properties. Au and Ag have almost identical behavioral profiles with similar activity profiles for size distribution, resonance wavelength, low dissolution potential, etc. The major differences between the two ENMs is that Au ENMs were found to distribute to biomass and soil to a greater extent than Ag ENMs, while Ag ENMs were found to impact Zebrafish behavior more significantly than Au ENMs. ZnO was also similar to Au and Ag ENMs; however, it was found to have high dissolution potential and had high Zebrafish mortality (>90%). This result agrees with the current thought that ions that dissolve from metallic ENMs are largely responsible for the ecotoxic properties of ENMs. Figure 3-2B compares two ENMs (CeO_2 and $\text{SiO}_2\text{-C}$), both of which are used in the semiconductor industry for chemical mechanical polishing. Both ENMs show a tendency to aggregate after 24 h. CeO_2 shows an affinity to adsorb to micelles or cell wall biological structures. Figure 3-2C compares two of the ENMs (Fe_3O_4 and MWCNTs), both of which are used for chemical pollutant adsorption in water treatment. Both ENMs show potential for magnetic separation. The Fe_3O_4 is intrinsically magnetic, whereas iron residuals in MWCNTs appear to give them their magnetic properties. While no reported toxicity mechanisms are associated with magnetism, literature suggests some ferrobacteria can align cells in a magnetic field (Uebe & Schuler, 2016). Emerging water treatment practices

are attempting to reduce the effects of hard water by passing it through a magnetic field, as a non-chemical alternative to water softening. MWCNTs tend to distribute to non-aqueous phases, which is probably associated with their hydrophobicity, while Fe_3O_4 nanoparticles remain in aqueous solutions. Thus, Fe_3O_4 may have a higher tendency to remain in effluent streams out of a wastewater treatment facility than MWCNTs. These observations give insight into the activity of these nanoparticles so that researchers and manufacturers can make more informed decisions when manufacturing ENMs and ENM-enabled products for consumer use. Additional radar plot comparisons were made and are available in the SI.

3.5. Conclusions

The development ENM activity profiles across a suite of different assays in these four activity quadrants provides valuable insight into how the physicochemical properties associated with ENMs can influence their inherent hazard and potential exposure routes. Elucidating these relationships via ENM activity-profiling radar plots should allow us to predict the efficacy and unintended consequences of ENMs in desired applications and would represent a unique strategy to efficiently and effectively anticipate potential environmental impacts. Overall, we demonstrated the reproducibility of functional assays for ENMs suspended in a standard 1 mM NaHCO_3 buffer, and we developed a strategy to plot and interpret the outcomes of the functional assays by using activity-profiling radar plots. Conducting functional assays and preparing activity-profiling radar plots for ENMs used in common products is an emerging way of visualizing potential environmental activity and impacts of ENMs, and these experiments allowed us to compare a

multifunctional array of nanomaterial attributes to assess factors that may be important for both nanomaterial benefits and risks. Few correlations emerged between assays for a single ENM or among different ENM, potentially it difficult to group or read-across difficult among ENM classes.

Future work in this area would be to expand upon these functional assays and create new assays for different situations, including biological systems, chemical systems, and physical systems. It is also important for future work to streamline functional assays and make them higher throughput, allowing for a more rapid diagnosis of ENM material properties. If multiple assays continue to provide results similar to each other (e.g. CPE and distribution to WW Biomass), it may be feasible to use a specific functional assay as a surrogate for additional ones, which would reduce experimental time and costs. It would be of interest to harmonize a single test solution matrix (pH buffering capacity, ionic strength and composition, NP mass concentration ranges) across all assays, and such efforts could improve the ability to cross-correlate causal factors in observed trends (e.g., correlation between biomass sorption and zebrafish toxicity). Additionally, it would be beneficial to understand the dynamics between surface coatings and environmental composition on ENM behavior. Prior studies have shown that the coating of nanoparticles with surfactants (i.e. sodium dodecyl sulfate, SDS) increases ENM stability in solution (Gimbert et al., 2007) and mobility in porous media (Lecoanet et al., 2004). Environmental composition has also been shown to play a role in ENM behavior. Organic acids (i.e. humic and fulvic acids) have shown to inhibit aggregation of CNTs (Hyung et al., 2007), while proteins in biological fluids stabilize metallic ENMs regardless of their chemical composition, surface structure, and surface charge (Jurasin et al., 2016).

Table 3-1. Functional Assays and dimensions used for eight nanoparticles. Size and polydispersity can be considered for both reactivity and physical activity profiling quadrants

Activity Profiling Quadrant	Functional Assay	# of Assays	Method Description	Analytical Tool	Functional Assay Outcome Parameter	Assay Outcome Mechanism
Reactivity	Magnetism	1	Removal of ENM from solution using magnet	ICP-MS / PTA	% Removed from Solution	Ferro-magnetism
	Resonance Wavelength	1	Wavelength scan from 200-800nm to find wavelength and absorbance of optimal peak	UV-Vis Spectroscopy	Wavelength (λ)	Resonance
	Dissolution (pH 8.0)	1	Dissolution potential of ENMs in a basic aqueous matrix	ICP-MS / PTA	% Dissolution	Dissolution
	TCLP Dissolution (pH 4.9)	1	Dissolution potential of ENMs in an acidic aqueous matrix	ICP-MS / PTA	% Dissolution	
Distribution	Cloud Point Extraction	1	Removal of ENM from solution using surfactant	ICP-MS / PTA	% ENM extraction from media	Hetero-Aggregation
	Hydrophobicity	1	Octanol-Water partitioning test	ICP-MS / PTA	% Distribution	
	Wastewater Sludge Partitioning	1	Partitioning of ENM to biomass collected from a local wastewater treatment facility	ICP-MS / PTA	% Distribution	
	Partitioning to Sediment	1	Partitioning of ENM to IHSS sandy loam soil	ICP-MS / PTA	% Distribution	
Physical	Size	1	Light scattering method using 1cm ³ quartz cuvettes	Dynamic Light Scattering (DLS)	Mean hydrodynamic diameter (nm)	Homo-Aggregation
	Polydispersity	1	Light scattering method using 1cm ³ quartz cuvettes	Dynamic Light Scattering (DLS)	polydispersity	
Hazard	Zebrafish Phenotype	21	Behavioral impact of ENM on tropical 5D wild-type zebrafish embryos	Zebrafish acquisition and analysis program (ZAAP)	Zebrafish developmental outcomes (Absent v. Present)	Biological Development
	Zebrafish Toxicity	1	Toxicity impact of ENM on tropical 5D wild-type zebrafish embryos	Zebrafish acquisition and analysis program (ZAAP)	% Mortality	Biological Toxicity

Table 3-1. Coefficients of variation (CV) for the non-biological functional assays with 8 ENMs. Data are presented as percentages. Black-highlighted CVs are greater than 30%. Grey-highlighted CVs are greater than 10% (and less than 30%). The zebrafish assay data was collected as presence/absence, so a CV was not obtainable.

Functional Assays	Ag	Au	CeO ₂	Fe ₃ O ₄	MWCNT	SiO ₂ - C	SiO ₂ - F	ZnO
Size	20	5.9	0.4	9.8	4.8	0.6	4.3	0.3
Polydispersity	16	41	6.2	18	14	2.6	6.8	4.3
Magnetism	2.9	1.0	7.0	5.3	7.5	3.1	3.3	0.5
Resonance Wavelength	0.2	0.1	0.5	0.3	0.2	0.0	0.3	0.2
Dissolution (pH 8)	9.8	9.3	34	17	0.0	14	11	7.1
Dissolution (pH 4.9)	4.0	5.7	6.1	15	0.0	24	25	4.5
Cloud Point Extraction	1.3	13	3.9	1.5	15	4.3	1.7	0.6
Hydrophobicity	1.3	4.1	1.4	3.3	39.7	4.2	3.7	3.0
WW Sludge Partitioning	1.1	1.0	15.6	3.4	5.7	3.3	2.1	1.7
Distribution to Sediment	1.8	0.8	12.5	3.6	5.5	3.8	2.0	1.8

Table 3-3. Linear correlation matrix of the functional assays. Zebrafish phenotype assays were omitted because no correlation could be found. Results to the left of the correlation values of 1.00 are R² values. Zebrafish mortality (24hpf) was analyzed for the ENM exposure concentration of 10mg/L. Grey-shaded regions are functional assays with high correlations.

	Size	Polydispersity	Magnetism	Resonance Wavelength	Dissolution (pH 8.0)	TCLP Dissolution (pH 4.9)	Cloud Point Extraction	Hydrophobicity	WW Sludge Partitioning	Partitioning to Sediment	Zebrafish Mort @ 24 hpf
Size	1.00										
Polydispersity	0.02	1.00									
Magnetism	0.02	0.18	1.00								
Resonance Wavelength	0.37	0.05	0.01	1.00							
Dissolution (pH 8.0)	0.04	0.00	0.17	0.00	1.00						
TCLP Dissolution (pH 4.9)	0.04	0.00	0.18	0.00	0.98	1.00					
Cloud Point Extraction	0.00	0.12	0.05	0.13	0.00	0.01	1.00				
Hydrophobicity	0.23	0.12	0.15	0.06	0.08	0.10	0.11	1.00			
WW Sludge Partitioning	0.00	0.13	0.07	0.10	0.00	0.01	0.99	0.08	1.00		
Partitioning to Sediment	0.04	0.03	0.04	0.05	0.26	0.26	0.18	0.21	0.19	1.00	
Zebrafish Mort @ 24hpf	0.06	0.01	0.06	0.00	0.94	0.92	0.01	0.02	0.02	0.43	1.00

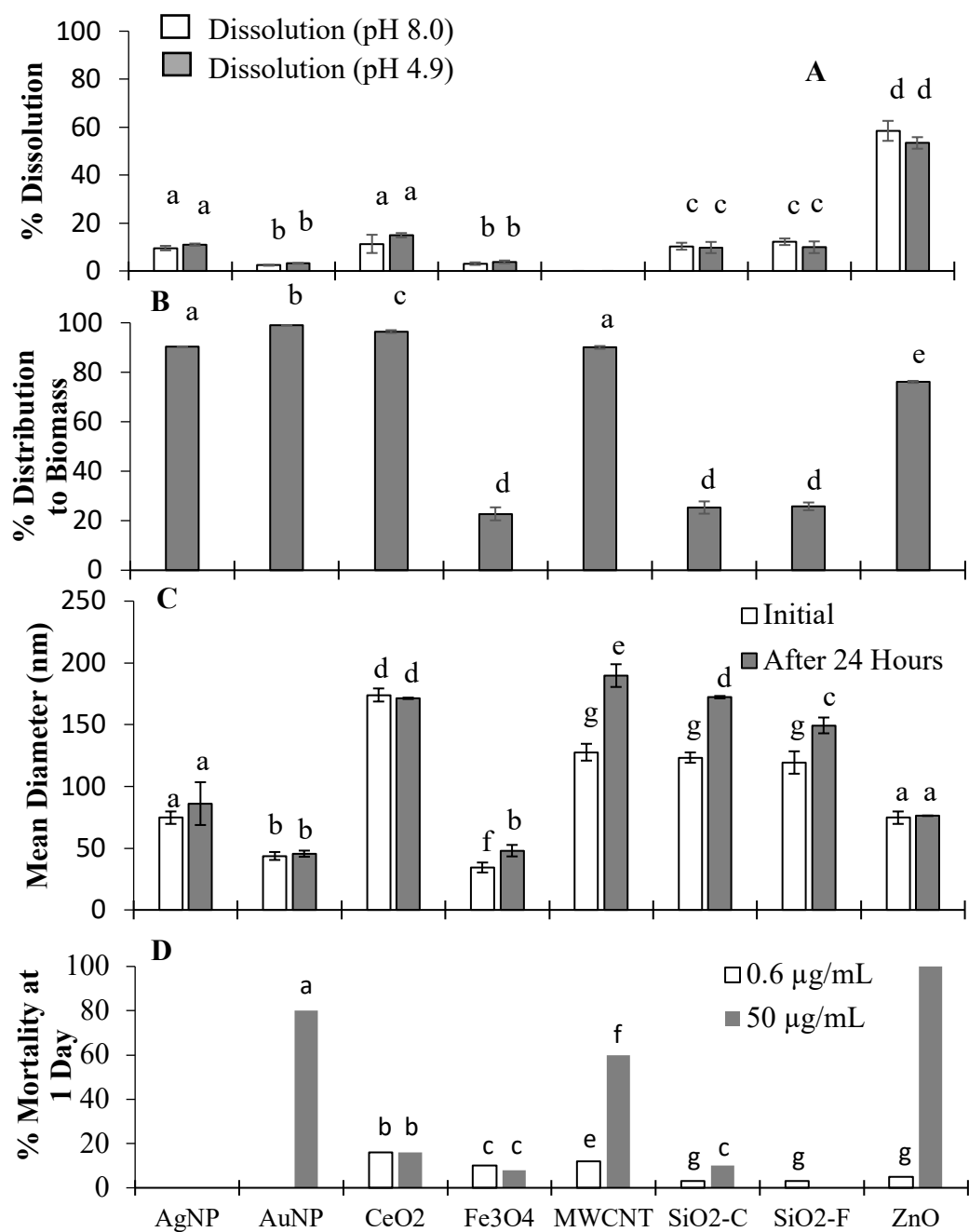


Figure 3-1. Results for functional assays within each activity-profiling quadrant. A) % Dissolution of the 8 ENMs within the reactivity-risk quadrant. B) % Sorption to WW Biomass of the 8 ENMs within the distribution-risk quadrant. C) Mean diameters of the 8 ENMs within the physical-risk quadrant. D) % Mortality Values for the 8 ENMs within the hazard-risk quadrant (Other functional assay outcomes available in SI). Error bars represent 1 standard deviation based upon triplicate assays. Letters above bars denote statistically significant results at a 95% confidence level (ANOVA).

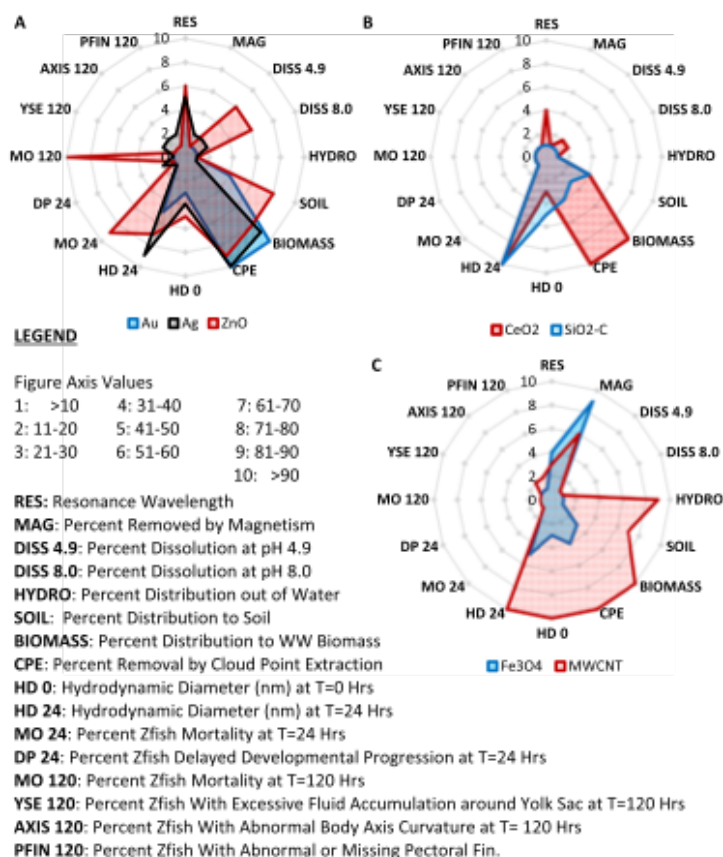


Figure 3-2. Activity profile radar plots for the comparison of behavioral trends of different engineered nanomaterials. (A) comparison of Au, Ag, and ZnO ENMs used as antimicrobials, (B) comparison of CeO₂ and SiO₂-C ENMs used as chemical mechanical polishers, and (C) comparison of Fe₃O₄ and MWCNT ENMs used as adsorbents for water treatment

3.5. Acknowledgements

This research was partially funded by the U.S. Environmental Protection Agency (RD 83558001) and the National Science Foundation through the Nanosystems Engineering Research Center for Nano- Enabled Water Treatment (EEC 1449500).

3.6. Supplemental Information

Functional Assay Methods

Resonance wavelength assay

A 1 mL aliquot of a nanoparticle sample was taken and dispensed into a 1 cm quartz cuvette. The cuvette was placed in a UV-Vis spectrophotometer, and a wavelength scan from 200 nm to 800 nm was conducted to obtain a unique spectra footprint for each nanoparticle. Concentrations were varied to allow for the highest wavelength peak to be below an absorbance of 1 cm^{-1} . Final nanoparticle concentrations of 5 mg L^{-1} were used to obtain desired absorbance. The wavelength of at the top of the main absorbance peak was recorded for each nanoparticle.

Size and polydispersity assays

Particle sizing was conducted using a Brookhaven ZetaPALS instrument. The nanoparticle solutions were aliquoted into 1 cm quartz cuvettes at least 2 mm above the entrance height of the laser beam of the dynamic light scattering (DLS) machine to ensure measurement accuracy. The sample was capped and observed to make sure no air bubbles were present. The internal DLS program was run, and three independent measurements per sample were made at run times of 2 minutes to establish measurement repeatability. Nanoparticle hydrodynamic diameter and polydispersity were measured after run time.

Cloud point extraction assay

Experiments were conducted in 40 mL glass vials with septa screw caps. Triplicate samples with 40 mL of desired nanoparticle solution in 1mM NaHCO_3 buffer were added to the

vials. 200 μL of 1.25 M sodium acetate, 50 μL of 1 M acetic acid, 500 μL of saturated Ethylenediaminetetraacetic acid (EDTA), and 500 μL of 10% TX-114 were then added to the vial. The vial was vortexed for 2 minutes and then placed in a 40°C water bath for 30 minutes. The sample was then transferred to a plastic centrifuge vial and centrifuged for 12 minutes at 5,000 revolutions per minute (rpm). The sample was then cooled down to room temperature in a zero-degree ice bath before taking a 10 mL aliquot from the supernatant for analysis. Triplicate controls with nanoparticle only and buffer only were also created.

Hydrophobicity assay

Experiments were conducted in 40 mL glass vials with septa screw caps. Triplicate samples with 20 mL of octanol and 20 mL of desired nanoparticle solution in 1 mM NaHCO_3 buffer were added to the vials. Triplicate controls with 20 mL octanol and 20 mL buffer only were also created. The vials were tightly sealed and rotated on a rotator table for 3 hours at 45 rpm. After rotation, the samples were given 30 minutes to equilibrate and, using a pipette, the octanol phase was vacuumed off. 10 mL aliquots were saved for analysis. 10 mL of the aqueous phase was then extracted for nanoparticle concentration analysis.

Wastewater partitioning assay

Wastewater biomass was collected from a local wastewater facility with a 1 L Nalgene bottle. The biomass was stored at 4°C prior to use. To determine the starting concentration of biomass (grams total suspended solids per liter [g TSS/L]), the collected biomass was stirred with a stir bar to shear larger particles and obtain more uniform particle size. 10 mL

of biomass sample was vacuum filtered with a 0.45-micron glass fiber filter, followed by three 10 mL rinses of nanopure water. The filter with biomass was then carefully removed and placed into an aluminum weighing dish and dried at 105°C until the change in biomass weight between sampling periods was less than 4% of total sample weight. The recorded weight was then calculated to g TSS/L. During experimental use, the remaining biomass was rinsed three times with carbonate buffer (10 mM NaCl + 4 mM NaHCO₃) solution and centrifuged at 350 g for 15 minutes. The supernatant was discarded, and the de-watered biomass was re-suspended with 1 mM NaHCO₃ buffer solution at an experimental concentration of 1g TSS/L. Experiments were conducted in 40mL glass vials with septa screw caps. Triplicate samples with 35 mL of wastewater biomass and 5 mL of nanoparticle solution were added in desired concentrations. Triplicate controls with wastewater biomass only and nanoparticle solution only were also created. Vials were sealed and secured on a rotator table for 3 hours at 45 rpm. After rotating, the samples were allowed to equilibrate in the lab for 1 hour to allow for biomass settling, and a 10 mL aliquot was taken from the middle of the supernatant for further analysis.

Distribution to sediment assay

Experiments were conducted in 40 mL glass vials with septa screw caps. Triplicate samples with 40 mg of soil from the international humic substances society (IHSS) and 40 mL of nanoparticle solution in 1mM NaHCO₃ buffer were added to each vial. Triplicate controls with soil and buffer only and nanoparticle solution only were also created. The vials were sealed tightly and rotated on a rotator table for 3 hours at 45 rpm. After rotation, the samples

were allowed to equilibrate for 2 hours and a 10 mL aliquot was taken of the supernatant for analysis.

Dissolution assay

Nanoparticle solutions in 40 mL of 1mM NaHCO₃ buffer were rotated in 40 mL glass vials with septa screw caps for 24 hours at 45 rpm. Triplicate controls with no nanoparticles and nanoparticle dispersion in 1 mM NaHCO₃ buffer solution only were also created. After rotation, 15 mL aliquots were extracted and placed in a 30-kDa ultrafilter. The filters were placed in centrifuge vials, and the samples were centrifuged for 12 minutes at 1500 rpm. The ultrafilters were discarded, and the solution collected in the centrifuge vial was extracted for analysis

Magnetism assay

Nanoparticle solutions in 40 mL of 1 mM NaHCO₃ buffer were placed in 40 mL glass vials with septa screw caps. Triplicate controls with no nanoparticles and no magnet were also created. A 1550 G magnet was placed next to the glass vial for 10 minutes for solid phase extraction of the nanoparticles out of solution. After 10 minutes, a 10 mL aliquot was taken from the middle of the vial for analysis.

Landfill dissolution assay

5.7 mL of glacial acetic acid was diluted into 1 L of nanopure water to a pH of 4.9. The nanoparticle solution was diluted to desired concentration in glacial acetic acid up to 40 mL in a 40 mL glass vial with septa screw caps and rotated for 24 hours at 45 rpm. Triplicate controls with no nanoparticles and nanoparticle in 1 mM NaHCO₃ buffer

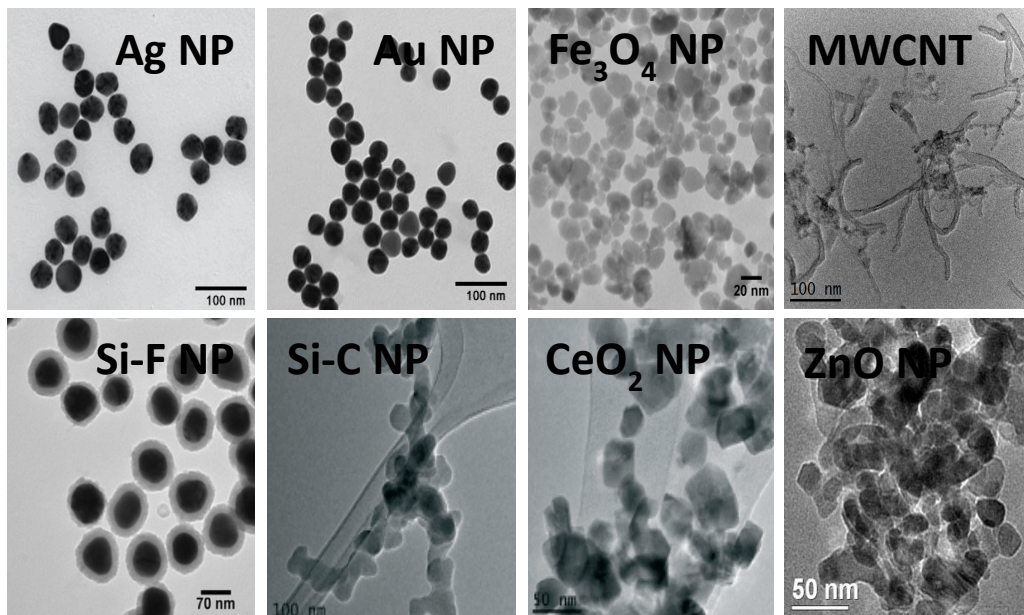
solution only were also created. After rotation, 15 mL aliquots were extracted and placed in a 30-kDa ultrafilter. The filters were placed in centrifuge vials, and the samples were centrifuged for 12 minutes at 1500 rpm. The ultrafilters were discarded and the solution collected in the centrifuge vial was extracted for analysis.

Zebrafish Toxicity assays

Tropical 5D wild-type adult zebrafish were housed at an approximate density of 1000 fish per 100 gallons of water. Spawning funnels were placed into the tanks the night prior, and embryos were collected and staged. To increase bioavailability, the chorion was enzymatically removed using pronase (63.6 mg/mL, ≥ 3.5 U/mg) at 4 hours post fertilization (hpf) using a custom automated dechorionator. To track exposures, each nanoparticle sample was tested in 6 concentrations using one animal per well in a 96-well plate. The chemical plate was run in duplicate so that $n=32$ animals per concentration. Zebrafish embryos without the chorion were loaded 1 per well at 6 hpf with chemical solution preloaded. The 96-well plates (with embryos) were lightly agitated overnight at 230 rpm on an orbital shaker. To track mortality and morphology responses, the zebrafish embryos were statically exposed until 120 hpf. At 24 hpf, embryos were assessed for four developmental toxicity endpoints: mortality at 24 hpf (MO24), developmental progression (DP), spontaneous movement (SM), and notochord distortion (NC). At 120 hpf, 18 developmental endpoints were assessed. The zebrafish acquisition and analysis program (ZAAP), a custom program designed to inventory, acquire, and manage zebrafish data, was used to collect developmental endpoints as either present or absent (i.e., binary responses were recorded). An internal QAQC plate consisting of 48 control animals and 48 animals exposed to 0.2 μ M Ziram was also run each day as an internal check for response consistency in the animals from different hatches. For quality assurance, negative controls

must exhibit less than 20% cumulative mortality and morbidity, and for the positive (Ziram) control, at least 80% of the exposed animals must display adverse effects.

1. TEM Characterization and Zeta Potential of Nanoparticles



Nanoparticle	AgNP	AuNP	Fe ₃ O ₄	MWCNT	Si-F	Si-C	CeO ₂	ZnO
Zeta Potential (mV)	-44	-53	-61	-24	-6	-21	43	22

Figure S1. TEM images and Zeta Potential Values of 8 nanoparticles used in functional assay study

2. Additional Functional Assay Data

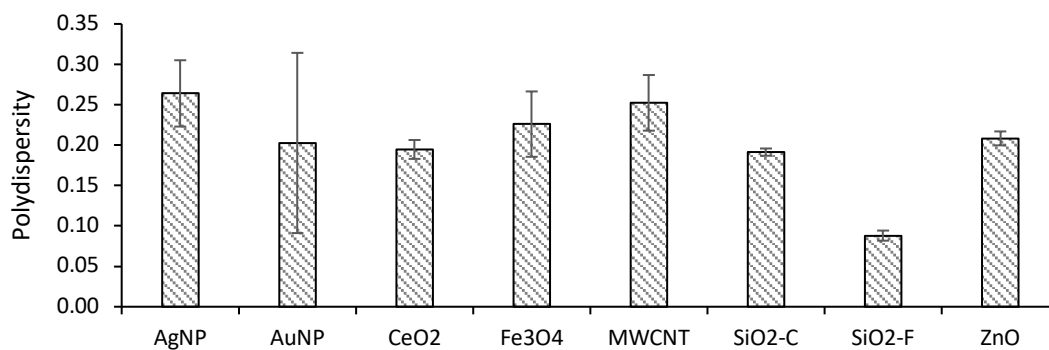


Figure S2. Polydispersity of NPs in 1 mM NaHCO₃ buffer solution. Measurements were collected in triplicates and analyzed using DLS.

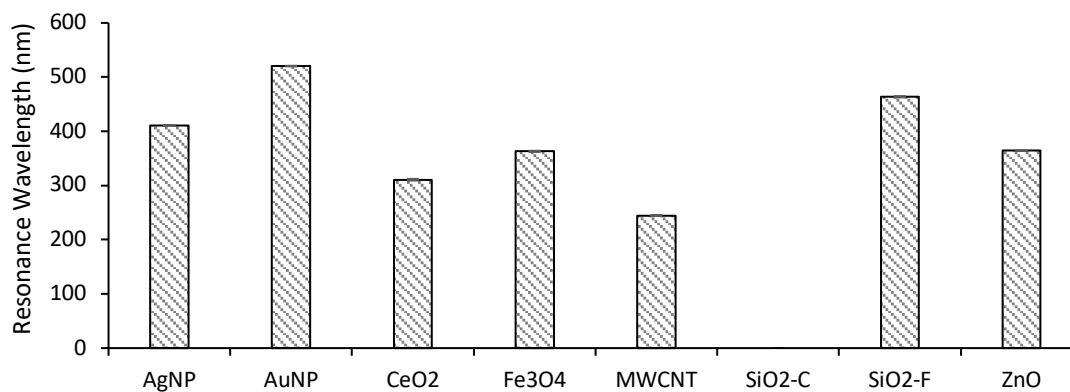


Figure S3. Resonance wavelength of NPs in 1 mM NaHCO₃ buffer solution. Measurements were collected in triplicate and analyzed using UV-Vis Spectrophotometer with a 200–800 nm wavelength scan.

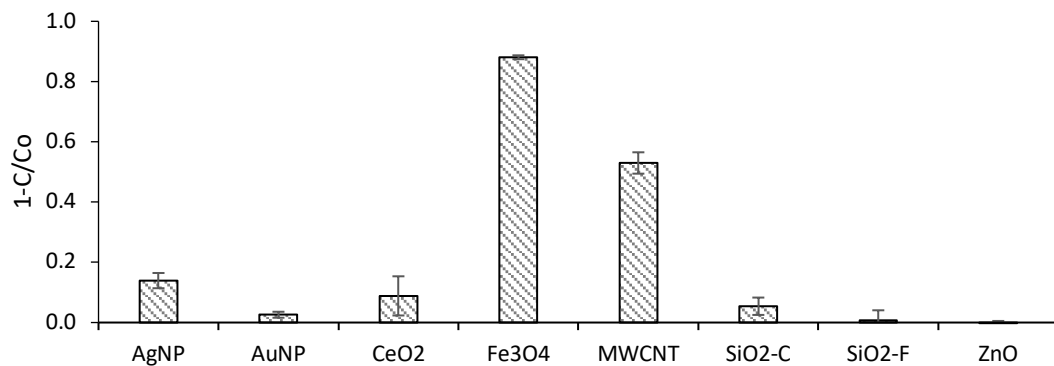


Figure S4. Magnetic removal of nanoparticles from a 1 mM NaHCO₃ buffer solution. Measurements were collected in triplicate and analyzed using ICP-MS

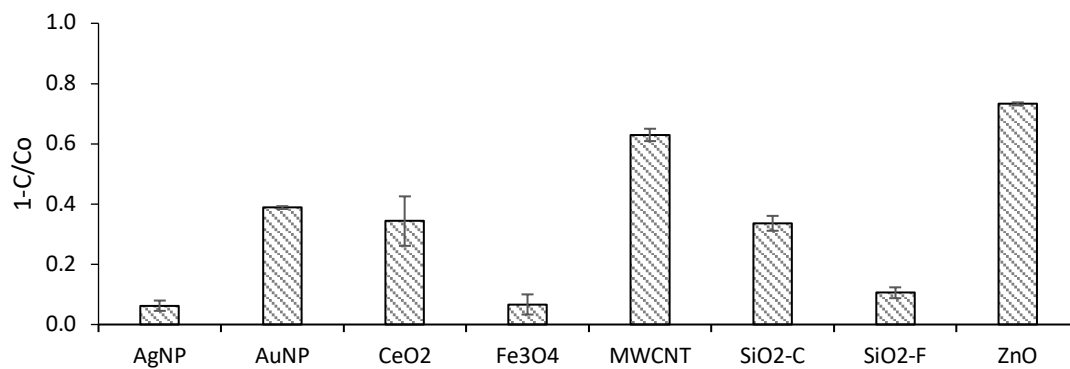


Figure S5. Partitioning of nanoparticles to soil from 1 mM NaHCO₃ buffer solution, Measurements were collected in triplicate and analyzed using ICP-MS

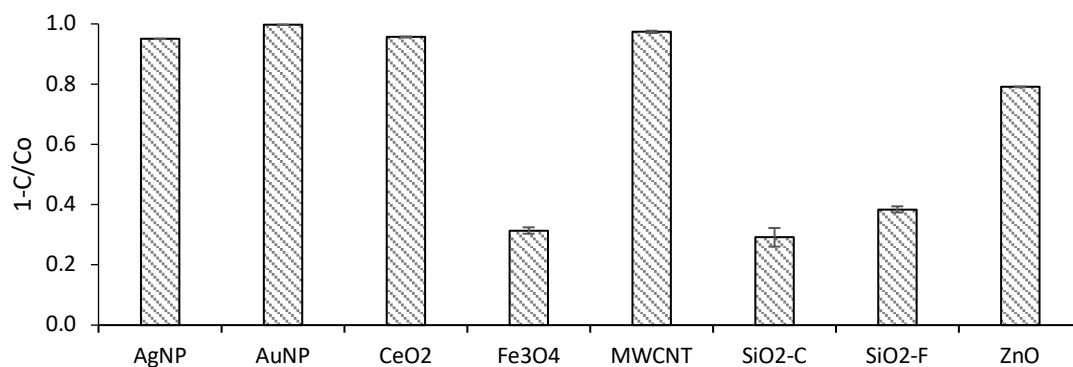


Figure S6. Cloud point extraction of nanoparticles from 1 mM NaHCO₃ buffer solution.

Measurements were collected in triplicate and analyzed using ICP-MS

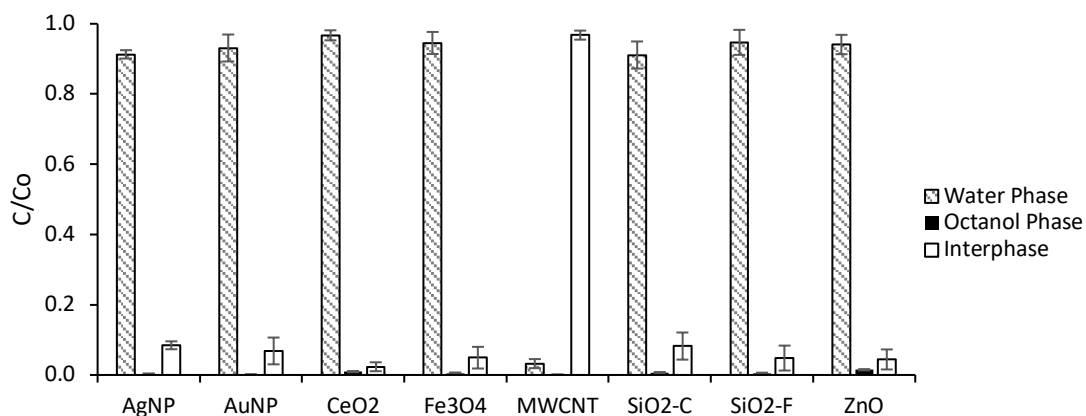


Figure S7. Hydrophobicity of nanoparticles using an octanol:1 mM NaHCO₃ buffer matrix.

The 1 mM NaHCO₃ buffer phase was measured in triplicates and analyzed using ICP-MS.

The octanol phase was measured in triplicates and analyzed using UV-Vis spectroscopy.

The interphase was calculated as the difference between starting nanoparticle concentrations and the sum of nanoparticle concentrations remaining in the octanol and water phases.

Nanoparticle Sources

Table S2. Sources of the nanoparticles used in this study

Nanoparticle	Source
Citrate-coated Ag	NanoComposix (San Diego, CA)
PVP-coated Magnetite Fe ₃ O ₄	NanoComposix (San Diego, CA)
Tannic acid-coated Au	NanoComposix (San Diego, CA)
Fluorescein-capped SiO ₂	NanoComposix (San Diego, CA)
Colloidal SiO ₂	Speed et al. 2015
ZnO	Sigma Aldrich
CeO ₂	Speed et al. 2015
MWCNT	Undisclosed Industrial Company

Concentration (mg/L)	M O2	D P2	S M C2	N C2	MO RT	Y S E	A XI	E Y	SN OU	JA W	O TI	P E	BR AI	SO MIT	PF IN	CF IN	PIG MEN	CI R	TR UN	SW IM	N C	T R	ANY Except MORT	ANY EFPEC T
0	0	0	0	0	0	0	0	0	0	0	0	0	0	0	0	0	0	0	0	0	0	0	0	0
0.3125	0	0	0	0	0	0	0	0	0	0	0	0	0	0	0	0	0	0	0	0	0	0	0	0
0.625	0	1	0	0	1	1	0	0	0	0	0	0	0	0	0	0	0	0	0	0	0	0	0	0
1.25	1	1	0	0	2	1	1	1	1	1	1	1	1	1	1	1	1	1	1	1	1	1	2	3
2.5	0	0	0	0	0	1	0	1	1	0	0	1	1	1	0	0	0	0	0	0	0	0	1	1
5	1	8	0	0	2	8	5	5	4	4	5	4	5	4	5	5	4	5	4	5	4	5	14	16
Concentration (mg/L)	M O2	D P2	S M C2	N C2	MO RT	Y S E	A XI	E Y	SN OU	JA W	O TI	P E	BR AI	SO MIT	PF IN	CF IN	PIG MEN	CI R	TR UN	SW IM	N C	T R	ANY Except MORT	ANY EFPEC T
0	0	1	0	0	0	2	1	1	1	1	1	1	1	1	1	1	1	1	1	1	1	1	2	2
0.34	0	0	0	0	0	2	0	1	2	0	0	2	0	0	0	1	0	0	0	0	0	0	1	2
1.67	1	0	0	0	2	0	0	0	0	0	0	0	0	0	0	0	0	0	0	0	0	0	1	2
5	0	2	0	0	1	1	1	0	1	0	0	0	0	0	0	0	0	0	0	0	0	0	1	3
30	12	2	0	0	14	1	3	1	1	0	0	1	1	0	1	1	0	0	5	0	0	1	6	20
50	26	1	0	0	26	0	0	0	0	1	0	0	0	0	0	1	0	0	1	0	0	0	1	28
Concentration (mg/L)	M O2	D P2	S M C2	N C2	MO RT	Y S E	A XI	E Y	SN OU	JA W	O TI	P E	BR AI	SO MIT	PF IN	CF IN	PIG MEN	CI R	TR UN	SW IM	N C	T R	ANY Except MORT	ANY EFPEC T
0	3	0	0	0	3	1	0	1	1	1	0	0	0	0	1	1	0	0	0	0	0	0	1	4
0.67	5	2	0	0	5	2	0	0	0	0	0	0	0	0	3	0	0	0	0	0	0	0	7	12
3.33	5	1	0	0	5	2	0	0	0	0	0	0	0	0	2	2	0	0	0	0	0	1	0	5
5	2	0	0	0	2	1	1	1	1	1	0	1	0	1	1	6	0	0	0	0	0	0	0	6
30	5	1	0	0	5	3	0	0	0	1	0	0	0	0	4	4	0	0	0	0	0	0	8	13
50	5	11	0	0	7	3	0	0	0	2	0	1	0	0	4	3	0	0	0	0	0	0	15	22
Concentration (mg/L)	M O2	D P2	S M C2	N C2	MO RT	Y S E	A XI	E Y	SN OU	JA W	O TI	P E	BR AI	SO MIT	PF IN	CF IN	PIG MEN	CI R	TR UN	SW IM	N C	T R	ANY Except MORT	ANY EFPEC T
0	2	1	0	0	2	0	0	0	0	0	0	0	0	0	0	0	0	0	0	0	0	0	1	3
0.67	2	0	0	0	3	2	0	1	1	1	0	1	0	1	3	0	0	0	0	0	0	0	3	6
3.33	3	0	0	0	3	0	0	0	0	0	0	0	0	0	0	0	0	0	0	0	0	1	0	3
5	1	0	0	0	1	1	1	1	1	1	0	1	0	0	1	0	0	0	0	0	0	0	1	2
30	2	0	0	0	2	1	0	1	0	1	0	1	0	0	0	0	0	0	0	0	0	0	2	4
50	2	0	0	0	2	0	0	0	0	0	0	0	0	0	5	0	0	0	0	0	0	0	5	7

Table S2. Zebrafish Mortality, Behavior, and Morphology Data. Number of zebrafish affected by each assay at each ENM dose. Number corresponds to the response found in zebrafish (n=32). Red values were found to be significant results outside background responses. Key to endpoints: [24 hpf endpoints] MO24, mortality at 24 hpf; DP24, developmental progress delayed at 24 hpf; SM24, absent tail flexions by visual check; NC24, notochord abnormal at 24 hpf. [120 hpf endpoints] MORT, mortality at 120 hpf; YSE, excessive fluid accumulation around yolk sac, AXIS, body axis curvature; EYE, edema, size, location or number abnormal; SNOUT and JAW, visibly malformed; PE, excessive fluid accumulation around heart; OTIC, ear malformed; BRAIN, brain absent or malformed; SOMITE, somite trunk muscle organization abnormal; PFIN, pectoral fins absent or abnormal; CFIN, caudal fin underdeveloped or malformed; PIGMENT, pigmentation hyper- or hypo-development of melanocytes; CIRC circulation visibly slower/faster or less developed; TRUNK, trunk body length shorter than normal; SWIM, swim bladder not present or not inflated; NC, notochord curvy or otherwise abnormal; TR, touch response, gentle touch of head or tail region fails to elicit an escape response; Any except mortality, summation of all non-mortality endpoint incidences; Any effect, summation of all endpoint incidences.

MW CNT	Concen- tration (mg/L)	M O2	D P2	S M	N C2	MO RT	Y S	A XI	E Y	SN OU	JA W	O TI	P E	BR AI	SO MIT	PF IN	CF IN	PIG MEN	CI R	TR UN	SW IM	N C	T R	ANY Except MORT	ANY EFFEC T
	0	1	3	0	0	4	1	0	0	0	0	0	1	0	0	0	0	0	0	1	0	0	0	4	5
	0.67	4	1	0	0	4	0	5	0	0	0	0	0	0	0	2	0	0	0	0	0	0	2	9	13
	3.33	1	1	0	0	1	1	4	0	0	0	0	0	0	0	2	0	0	0	0	0	0	1	8	9
	5	1	2	0	0	1	0	8	0	0	0	0	0	0	0	4	0	0	0	0	0	0	1	15	16
	30	5	21	0	0	9	6	4	0	0	0	0	2	0	0	5	0	0	1	0	0	0	1	27	31
	50	19	12	0	0	30	3	1	1	0	0	0	1	0	0	3	1	0	0	0	0	0	1	12	32
		M	D	S	N	MO	Y	A	E	SN	JA	O	P	BR	SO	PF	CF	PIG	CI	TR	SW	N	T	ANY	ANY
		O2	P2	M	C2	RT	S	XI	Y	OU	W	TI	E	AI	MIT	IN	IN	MEN	R	UN	IM	C	R	Except	EFFEC
		4	4	24	4	4	E	S	E	T	C	C	N	N	E	IN	IN	T	C	K	IM	C	R	MORT	T
		4	4	24	4	4	0	0	0	0	0	0	0	0	0	0	0	0	0	0	0	0	0	0	0
	0	1	2	0	0	1	0	0	0	0	0	0	0	0	0	0	0	0	0	0	0	0	0	0	1
	0.67	3	1	0	0	3	1	0	1	0	0	0	0	0	0	0	0	0	0	0	0	0	1	3	6
	3.33	3	1	0	0	4	0	0	0	0	0	0	0	0	0	0	0	0	0	0	0	0	1	4	
	5	1	0	0	0	2	0	0	0	0	0	0	0	0	0	0	0	0	0	0	0	0	0	2	
	30	0	0	0	0	0	0	0	0	0	0	0	0	0	0	0	0	0	0	0	0	0	0	0	
	50	3	1	0	0	4	0	0	0	0	0	0	0	0	0	0	0	0	0	0	0	0	0	1	4
		M	D	S	N	MO	Y	A	E	SN	JA	O	P	BR	SO	PF	CF	PIG	CI	TR	SW	N	T	ANY	ANY
		O2	P2	M	C2	RT	S	XI	Y	OU	W	TI	E	AI	MIT	IN	IN	MEN	R	UN	IM	C	R	Except	EFFEC
		4	4	24	4	4	E	S	E	T	C	C	N	N	E	IN	IN	T	C	K	IM	C	R	MORT	T
		4	4	24	4	4	0	0	0	0	0	0	0	0	0	0	0	0	0	0	0	0	0	0	0
	0	3	0	0	0	4	0	0	0	0	0	0	0	0	0	0	0	0	0	0	0	0	0	0	4
	0.16	4	1	0	0	5	1	0	1	1	1	0	2	1	2	0	2	0	0	0	0	0	0	4	8
	0.31	5	0	0	0	5	0	0	0	0	0	0	0	0	0	0	1	0	0	0	0	0	0	1	6
	0.63	1	0	0	0	1	1	0	0	0	1	0	0	0	0	0	0	0	0	0	0	0	0	2	3
	1.25	5	0	0	0	5	1	0	0	0	0	0	0	0	0	0	0	0	0	0	0	0	0	1	6
	2.5	3	0	0	0	3	0	0	0	0	0	0	0	0	0	0	0	0	0	0	0	0	0	0	3
		M	D	S	N	MO	Y	A	E	SN	JA	O	P	BR	SO	PF	CF	PIG	CI	TR	SW	N	T	ANY	ANY
		O2	P2	M	C2	RT	S	XI	Y	OU	W	TI	E	AI	MIT	IN	IN	MEN	R	UN	IM	C	R	Except	EFFEC
		4	4	24	4	4	E	S	E	T	C	C	N	N	E	IN	IN	T	C	K	IM	C	R	MORT	T
		4	4	24	4	4	0	0	0	0	0	0	0	0	0	0	0	0	0	0	0	0	0	0	0
	0	1	0	0	0	1	0	1	0	0	0	0	0	0	0	0	0	0	0	0	0	0	0	1	2
	0.67	2	4	0	0	6	4	4	0	0	1	0	0	0	0	1	0	0	1	0	0	0	2	13	18
	3.33	3	1	0	0	26	2	1	0	0	0	0	1	3	0	0	2	0	0	0	0	1	0	5	29
	5	5	28	2	0	30	1	0	0	0	0	0	0	0	0	1	1	0	1	1	0	0	1	2	32
	30	32	0	0	0	32	0	0	0	0	0	0	0	0	0	0	0	0	0	0	0	0	0	0	32
	50	32	0	0	0	32	0	0	0	0	0	0	0	0	0	0	0	0	0	0	0	0	0	0	32

Table S3. Zebrafish mortality (%) at 24hpf from the 8 ENMs at different doses. ZnO showed the highest toxicity potential. Percent mortalities are based on counting live and dead zebrafish embryos (n=32 per ENM and dose). Grey-shaded regions are doses where a significant zebrafish mortality occurred.

ENMs	ENM Dosing (mg/L)										
	0	0.1	0.3	0.6	1.3	1.6	2.5	3.3	5	30	50
Ag-Citrate	0	-	0	0	3.1	-	0	-	3.1	-	-
Au	0	-	-	0	-	3.1	-	-	0	37.5	81.3
CeO ₂	9.4	-	-	15.6	-	-	-	15.6	6.2	15.6	15.6
Fe ₃ O ₄	6.3	-	-	9.4	-	-	-	9.4	3.1	6.2	6.2
MWCNT	3.1	-	-	12.5	-	-	-	3.1	3.1	15.6	59.4
SiO ₂ -Colloid	3.1	-	-	3.1	-	-	-	9.4	3.1	0	9.4
SiO ₂ -Fluorescein	9.4	12.5	15.6	3.1	15.6	-	9.38	-	-	-	-
ZnO	3.1	-	-	6.2	-	-	-	9.4	87.5	100	100

CHAPTER 4: ENVIRONMENTAL APPLICATIONS USING NANO: REMOVAL OF BROMIDE FROM SURFACE WATER: COMPARISON BETWEEN SILVER-IMPREGNATED GRAPHENE OXIDE AND SILVER-IMPREGNATED POWDER ACTIVATED CARBON

- This chapter has been published as **Kidd, J.**, Barrios, A., Apul, O., Perrault, F., Westerhoff, P. (2018). Removal of Bromide from Surface Water: A Comparison between Silver-Impregnated Graphene Oxide and Silver-Impregnated Powdered Activated Carbon. *Environmental Engineering Science*, 35 (9)
- My author contribution: Approximately 70% of the research and 80% of the text

4.1. Abstract

This study demonstrates that silver (Ag^+) impregnated graphene oxide (GO) reduces anion and natural organic matter (NOM) competition for bromide (Br^-) adsorption sites compared with Ag^+ impregnated powdered activated carbon (PAC). We impregnated two GO (Tour and Modifier Hummers [MH] method) and one PAC with silver ions. Batch studies were conducted to assess Br^- removal in model waters with Br^- , chloride (Cl^-), bicarbonate (HCO_3^-), and/or NOM and natural surface waters. In buffered ultrapure water, Tour-Ag, MH-Ag, and PAC-Ag all removed $>85\%$ of Br^- , while sorbents without Ag^+ removed $<3\%$ of Br^- . In all water matrices, Tour-Ag removed $>75\%$ of Br^- , MH-Ag removed $>50\%$, and PAC-Ag removed $>30\%$, highlighting that GO-Ag is more effective at removing Br^- from water than PAC-Ag ($p < 0.05$). Scanning electron microscopy and energy dispersive X-ray spectroscopy analysis show that Br^- is evenly dispersed on the surface of GO-Ag, indicating possible attachment to oxygen groups and silver on the GO

surface. A leaching test of GO-Ag in buffered water showed that *20% of Ag^+ loaded onto GO leaches into solution, of which only 1–3% remains when Br^- is spiked into solution, indicating possible complexation and precipitation as AgBr. GO-Ag and PAC-Ag were introduced separately in combination with alum during coagulation and flocculation operations. Both MH-Ag and Tour-Ag showed high removal of Br^- , demonstrating that GO-Ag could supplement current technologies used in water treatment facilities when Br^- removal is needed.

4.2. Introduction

Bromide (Br^-) is commonly found at concentrations between 0.01 and 0.2 mg/L in ground and surface waters used for potable water and up to 65 mg/L in seawater (Minear and Amy, 1995; Fehn et al., 2000). Industrial operations like coal-fired power plants and hydraulic fracturing (Davis et al., 1998; Wilson and VanBriesen, 2012, 2013) contribute to Br in surface water. Coal-fired power plants add Br^- in their wet scrubbers to reduce mercury in air emissions. This process results in Br^- at up to 50 mg/L in the waste streams discharged to surface waters (Kolker et al., 2012). In hydraulic fracturing Br^- , as well as chloride and iodide, is naturally enriched in subsurface brine, and the wastewater produced typically contains Br^- up to 60 mg/L. This wastewater returns to surface water and is processed through surface water treatment plants (SWTPs) (Norman et al., 1996; Harkness et al., 2015). Br^- increases at SWTPs downstream of such operations are now being reported in the United States (Amy et al., 1994; Richardson et al., 2008; Ferrar et al., 2013; Sawade et al., 2016). Efforts in Switzerland to reduce Br^- discharges from large industries

are also being pursued (Soltermann et al., 2016). There is currently no common practice in SWTPs that can remove Br⁻. Electrolysis can remove Br⁻ by selective ion exchange resins but can be difficult to deploy at SWTPs.

SWTPs typically use chemical oxidation such as chlorination to achieve disinfection before distributing to consumers because of its low costs and broad-spectrum biocidal potency. However, oxidants can form disinfection by-products (DBPs). Bromide can react with ozone (O₃) or hypochlorous acid (HOCl) to form hypobromous acid (HOBr), which reacts with organic matter to form Br-DBPs (e.g., brominated trihalomethanes or haloacetic acids) (Kampioti and Stephanou, 2002; McTigue et al., 2014; Zhai et al., 2014; Winid, 2015). Br-DBPs are more cyto- and genotoxic than their chlorinated analogs (Plewa et al., 2008; Richardson et al., 2008; Yang et al., 2014). As water regulation becomes increasingly stringent, reducing and controlling the formation of emerging Br-DBPs is becoming more important, raising the requirement for novel technologies to effectively remove Br⁻ before disinfection in water treatment facilities (Richardson and Postigo, 2017).

Bromide in surface waters can be removed using granulated activated carbon (GAC) (Frommer and Dalven, 2000) or powdered activated carbon (PAC) (Chen et al., 2016) impregnated with silver ions. Silver ions adsorbed onto the carbon surface can form insoluble precipitates with Br⁻ ($\text{Ag}^+ + \text{Br}^- \rightarrow \text{AgBr(s)}$, $K_{\text{sp}} = 5.2 \cdot 10^{-13}$). However, Br⁻ removal by silver impregnated activated carbon in complex aqueous matrices may be challenging because of competing components and low intraparticle diffusion rates. For example, the molar ratio of chloride (Cl⁻) to Br⁻ in seawater and many drinking waters is

between 300:1 and 1,000:1, although competing precipitation reactions with chloride ($\text{Ag}^+ + \text{Cl}^- / \text{AgCl(s)}$, $K_{\text{sp}} = 2.8 \cdot 10^{-10}$) are less favorable than Br^- (Davis et al., 1998; Mullaney et al., 2009; Katz et al., 2011). There are other ions that may compete with Br^- for Ag^+ on the carbon surface such as iodide (I^-). In addition, natural organic matter (NOM) can block activated carbon pores or occupy sites that contain silver, likely reducing the ability of activated carbon to remove Br^- from natural waters proficiently (Li et al., 2003; Chen et al., 2016). Graphene oxide (GO), a sp^2 -bonded two-dimensional (2D) carbonaceous material with a sheet-like structure, can overcome such practical limitations by accommodating competing ions, NOM, and Br^- concurrently and decreasing the time required for intraparticle diffusion (Apul et al., 2013; Ersan et al., 2016). Theoretically, GO has a high surface area like other carbonaceous materials, which allows for a high number of sorption sites. When in an aqueous suspension, however, the surface area of GO is slightly diminished due to aggregation. In addition, the high oxygen content of GO provides an abundance of functional groups that can be used for the impregnation of GO with silver ions. The GO functional groups have been previously used to synthesize a variety of graphene-based sorbents for cationic contaminant removal (Zhao et al., 2011; Perreault et al., 2015). We hypothesize that the 2D open nature of GO, compared with the intrapore surface area of activated carbon, will improve Br^- removal when impregnated with Ag^+ ions.

The goal of this study was to evaluate the potential of silver impregnated GO nanomaterials (GO-Ag) as a new sorbent material for removing Br^- from surface water.

The objectives of our study were to (1) determine the ability of attaching Ag^+ onto functionalized GO surfaces, (2) evaluate the ability of silver impregnated GO-Ag to precipitate Br^- from aqueous media, (3) compare Br^- removal efficiency of GO-Ag versus PAC-Ag, (4) investigate the impact of surface water chemistry on Br^- removal by GO-Ag, and (5) understand the mechanism for Br^- removal by GO-Ag.

4.3. Materials and Methods

4.3.1. Solution Preparation

The Br^- and Cl^- stock solutions (20 mg L^{-1}) were prepared by dissolving sodium bromide (EM Science, CAS# 7647-15-6, > 99% purity) or sodium chloride (Sigma Aldrich, CAS# 7647-14-5, > 99.5% purity) in ultrapure water ($18.2 \text{ M}\Omega\cdot\text{cm}$, Thermo Fisher Barnstead GenPure xCAD Plus Water Purification System, Art no. 50136170). Because Br^- adheres to glass, all stock solutions were prepared in plastic bottles to avoid adhesion losses. The buffered water solution (1 mM NaHCO_3 , pH ~ 8) was prepared by dissolving sodium bicarbonate (Amresco, CAS# 144-55-8) in ultrapure water.

NOM isolate was purchased from International Humic Substances Society (IHSS, CAT # 2R101N, Suwannee River NOM RO Isolation). The NOM stock solution (50 mg NOM L^{-1}) was prepared in ultrapure water. The SUVA_{254} value of the NOM isolate solution was $4.19 \text{ L/mg}\cdot\text{m}$. The natural river water was sampled from the Colorado River at the Central Arizona Project (CAP) canal at the City of Scottsdale Water Campus (Average DOC of 3.0 mg L^{-1}). The CAP water characteristics are summarized in Table S1.

4.3.2. Carbonaceous Adsorbent Synthesis and Characterization

Graphite used to synthesize GO was purchased from Bay Carbon (CAS# 7782-42-5, > 99.5% purity). Two different GO materials were produced from the Bay Carbon graphite using the Modifier Hummers (MH) and the Tour (Tour) chemical oxidation protocols (Tung et al., 2008; Marcano et al., 2010). GO syntheses details can be found in the SI. As-purchased PAC (Norit 20B M-1789) was oxidized in concentrated nitric acid at ~90 °C for 1 hour to produce oxidized PAC. The complete oxidation procedure is described in the SI.

Silver nitrate (Sigma Aldrich, CAS# 7761-88-8) was used to impregnate GOs and PAC. Silver impregnation of the different carbonaceous materials was done by dispersing 200 mg of oxidized PAC, MH, or Tour in 0.5 M AgNO₃ for 2 days and then collecting the material by centrifugation and vacuum drying. Complete material preparation procedure is described in the SI.

The carbonaceous nature of the different materials and the abundance of defects introduced by the oxidation procedure were characterized by Raman spectroscopy (full spectra in Figure S1). The silver content of the carbonaceous material before and after silver impregnation was determined by acidifying samples in 2% HNO₃ for 24 hours and quantifying total silver with inductively coupled plasma mass spectroscopy (ICP-MS, Thermo Scientific X Series II). Some silver ions may be impregnated into pores of the carbonaceous materials and may not be dissolved in 2% HNO₃. There was not enough sample size to run a microwave digestion, which would have been the alternative method for silver ion quantification. The size and morphology of the carbonaceous material and silver precipitates before and after the experiments were conducted by scanning electron microscopy (SEM). Energy dispersive X-ray spectroscopy (EDAX) was coupled with

SEM to identify elements in the SEM micrographs. SEM/EDAX was used to characterize the Ag^+ adsorbate distribution on the carbon surface. The samples were filtered through 0.2-micron nylon syringe filters (Thermo Scientific F2500-2) to remove excess organics and carbon sorbents. The filters were air-dried, and the carbon sorbents trapped in the filters were imaged with SEM/EDAX (FE-SEM, Amray 1910). The specific surface area of the materials was quantified by nitrogen gas adsorption at 77 K with a physio-sorption analyzer (Micromeritics TriStar II 3020). The Brunauer-Emmett-Teller (BET) equation was used to calculate surface areas from adsorption isotherms.

4.3.3. Bromide Removal Experiments

Bromide removal experiments were conducted in 125 mL plastic vials that were shaken using an in-house end-over-end rotational mixer (45 rpm). Bottle-point experiments used a 4-hour contact time, which represented the hydraulic residence time (HRT) for PAC treatment at water treatment plants (Westerhoff et al., 2005). Four water samples that were spiked with $200 \mu\text{g L}^{-1} \text{Br}^-$ were used: (1) 1 mM NaHCO_3 buffered ultrapure water, (2) 1 mM NaHCO_3 buffered ultrapure water spiked with 20 mg L^{-1} chloride, (3) 1 mM NaHCO_3 buffered ultrapure water spiked with 20 mg L^{-1} chloride and 10 mg L^{-1} NOM, and (4) natural Central Arizona Project (CAP) surface water. Each carbon adsorbent was added as a powder to a concentration of 25 mg L^{-1} . Details are in SI Table S2. To simulate water treatment processes, bromide removal experiments using CAP water as the background matrix were conducted in 2-L jar testers (Phipps and Bird). All acrylic jars were filled with 1 L of source water and initially mixed for 6 minutes at 200 rpm, simulating coagulation (i.e., rapid mixing). During the rapid mixing step, 28 mg L^{-1} of alum (provided by the

Scottsdale Water Campus) and each carbon adsorbent was added as a powder to a concentration of 25 mg L^{-1} . The mixing speed was later decreased to 25 rpm for 30 minutes, simulating flocculation (i.e., slow mixing). Mixing was ceased and the flocs settled for 1 hour (i.e., sedimentation). No additives were used during the slow mixing and sedimentation steps. After sedimentation, an aliquot for analysis was withdrawn from the middle of the jar using a 50-mL plastic syringe. Careful consideration was taken to obtain the aliquot without upsetting the sediment.

4.3.4. Silver Leaching Experiments

Silver leaching experiments were conducted in 125 mL plastic vials that were shaken using an in-house end-over-end rotational mixer (45 rpm) to determine the amount of Ag^+ leached into solution during mixing. Each carbon adsorbent was added to a concentration of 25 mg L^{-1} in four different water matrices: (1) 1 mM NaHCO_3 , (2) 1 mM NaHCO_3 with $200 \text{ } \mu\text{g L}^{-1} \text{ Br}^-$, (3) Natural CAP water, and (4) Natural CAP water with $200 \text{ } \mu\text{g L}^{-1} \text{ Br}^-$. The vials were shaken for 4 hours.

4.3.5. Measurements of Dissolved Species

UV_{254} (UV-Vis Spectroscopy, Horiba Scientific Aqualog) and dissolved organic carbon (DOC; SEC-DOC, Shimadzu ASI-V) were measured on filtered (0.2-micron nylon) samples. Filtered samples were analyzed for Br^- and Cl^- using ion chromatography (IC, Thermo Scientific Dionex ICS-5000) to measure anions remaining in solution (IonPac™ AS18 Column, 30 mM KOH Eluent, 25 μL injection volume) following the EPA 300.1 method. Select experiments were also analyzed for Br^- in solution by acidifying filtered

solutions in 2% HNO₃ for 24 hours and quantifying total Br⁻ using ICP-MS (Thermo Scientific X Series II).

4.4. Results and Discussion

4.4.1. Characterization of the Silver Impregnated Carbon Sorbents

Table 4-1 summarizes characterization data for the PAC and GO adsorbents before and after silver impregnation and shows how their physicochemical properties are altered by the silver-adsorbent interaction. Raman spectroscopy detected G and D bands, which are characteristic of oxidized carbon materials (Figure S1). The G band is related to the sp²-bonded carbon lattice, and the D band is related to carbon structure disorder, which may be caused by structural defects, the introduction of new functional groups, or decreasing crystallite size (Ferrari, 2007; Ferrari and Basko, 2013). The D:G ratios of the oxidized PAC, MH, and Tour were 1.023, 0.882, and 0.834, respectively, indicating high disorder in the oxidized carbon structure (Table 4-1). All three carbonaceous materials had high oxygen content, with Tour having the highest oxygen content (C:O ratio of 1.787) and oxidized PAC having the lowest oxygen content (C:O ratio of 7.310) (Table 5-1). The differences in C:O ratios result from different oxidation conditions present during material synthesis, which is known to influence carbon material functionalization (Dreyer et al., 2014). The specific surface area of the three materials were 716 m² g⁻¹ for oxidized PAC, 9.38 m² g⁻¹ for Tour, and 0.55 m² g⁻¹ for MH (Table 5-1). The specific surface area of the GO materials was noticeably lower than the theoretical value of 2,632 m² g⁻¹ for graphene. This lower value for GO has been observed multiple times for different GO materials and

can be attributed to the tight restacking and aggregation of GO sheets (Perreault et al., 2015; Guo et al., 2014).

4.4.2. Effects of Silver Impregnation on Bromide Removal

The capacity of parent and Ag^+ impregnated carbon adsorbents to remove Br^- from water was evaluated in 100 mL batch bottle studies (25 mg L^{-1} adsorbents, $200 \mu\text{g L}^{-1} \text{ Br}^-$). Figure 4-1 compares the percent removal of Br^- and the Br^- removal capacity of each adsorbent after 4 hours of mixing. A control sample with no carbon recovered $> 99\%$ of spiked Br^- , which equates to $< 1\%$ Br^- removal in control experiments. The non-impregnated adsorbents had minimal Br^- removal ($< 3\%$). PAC-Ag, MH-Ag, and Tour-Ag removed 86%, 82%, and 91% of Br^- , respectively.

4.4.3. Effects of Background Water Characteristics on Bromide Removal

Figure 4-2 compares Br^- removal by Ag^+ impregnated carbon adsorbents for four different water matrices with controlled complexities. Tour-Ag removed $>90\%$ of Br^- in all water matrices except natural CAP water, where it removed $\sim 75\%$ of Br^- . MH-Ag removed $\sim 70\%$ of Br^- when Cl^- was introduced, $\sim 70\%$ of Br^- when Cl^- and NOM were introduced, and it removed $\sim 50\%$ of Br^- in natural CAP water. PAC-Ag removed $\sim 60\%$ of Br^- when Cl^- was introduced, $\sim 50\%$ of Br^- when Cl^- and NOM were introduced, and only $\sim 30\%$ of Br^- in natural CAP water. We attributed the lack of Br^- removal by PAC-Ag to its porous nature, where complex organics and competing ions can block pore channels or compete for sorption sites on the carbon, thereby rendering Ag^+ not on the PAC-Ag surface unavailable for interactions with Br^- in solution.

4.4.4. Jar Testing Experiments to Simulate Bromide Removal at a Water Treatment Facility

Figure 4-3 shows Br⁻ removal for PAC-Ag, MH-Ag, and Tour-Ag in natural CAP water in jar tests simulating coagulation and flocculation in a water treatment facility. In each of the jar test experiments, the coagulant formed settleable flocs. Adding any form of silver achieved turbidity removal equal to the alum alone. Alum by itself did not remove Br⁻. In combination with alum, both MH-Ag and Tour-Ag removed approximately 70% of Br⁻, while PAC-Ag with alum removed approximately 40% of Br⁻, which was statistically worse than MH-Ag and Tour-Ag. MH-Ag with alum had the greatest Br⁻ removal capacity per mol of Ag⁺ of the adsorbents.

4.4.5. Characterization of the Silver Impregnated Carbon Sorbents

The silver impregnated adsorbent made with Tour-Ag had the highest Ag⁺ content by mass (12.6%) followed by PAC-Ag (5.8%) and MH-Ag (4.9%). This means Ag⁺ loading is not determined by the surface area of the material, as the lower surface area GOs had equivalent to higher silver content than PAC-Ag. Rather, the high Ag⁺ loading of the Tour indicates that Ag⁺ attaches to the oxygen groups found on the oxidized material. As GO oxygen content increased, more Ag⁺ was attached. Raman spectroscopy further confirmed the attachment of Ag⁺ to the carbon structure. The Raman spectra of the different materials after silver impregnation showed a consistent increase in the D band intensities (Figure S1). This increase is due to the adsorption of silver ions to the carbon lattice, thus disturbing the electron distribution of the material, as previously observed for silver nanoparticles or thiolated functionalized GO sheets (Das et al., 2011; Pham et al., 2013). This is not the case for PAC-Ag, which had less oxygen than the GO materials but slightly more Ag⁺ attached than MH-Ag. We believe Ag⁺ attachment on PAC-Ag may be related to the specific surface

area (SSA) of PAC. To test this, the BET equation was used to calculate SSA before and after Ag^+ impregnation. Ag^+ surface attachment decreased the SSA of the adsorbents, with PAC-Ag having a significantly larger SSA than the GO, as expected. These findings align with previous findings, which were attributed to silver ions occupying sorption sites (Chen et al., 2016). Our work differs from prior work with silver impregnated PAC/GAC because we do not heat treat the material, which could form silver oxides (Chen et al., 2016). It is also different from the formation of zero valent silver, which requires H_2O_2 addition to produce Ag^+ (He et al., 2012; Polo et al., 2016).

4.4.6. Effects of Silver Impregnation on Bromide Removal

Stoichiometrically, to remove 100% of the $200 \mu\text{g L}^{-1} \text{Br}^-$, there only needs to be $2.5\text{E-}06$ moles of Ag^+ , which equates to 1.08% dry mass of Ag^+ loaded on the tested carbon adsorbent dose of 25 mg L^{-1} ; however, even with silver loadings of 4.9% (MH-Ag), 5.8% (PAC-Ag), and 12.6% (Tour-Ag), the maximum removal capacity of Ag^+ for Br^- is no higher than 0.13 mol Br^- per mol Ag^+ . One explanation is that the high Ag^+ loading on the carbon and the low Br^- present in solution results in a high fraction of Ag^+ unavailable to complex with Br^- . In Figure S2, we compare Br^- removal versus the initial Ag^+ loaded onto the carbon adsorbents. Compared to the control (i.e., without Ag^+), adding Ag^+ increased Br^- removal in all samples, but there was little difference in Br^- removal with different Ag^+ loadings, further validating that excess Ag^+ to remove Br^- is only beneficial to an extent. We attribute this to excess Ag^+ in solution that may not come in contact with the small concentration of Br^- available. These results indicated that (1) the impregnation of silver ions on the carbon adsorbents was required for Br^- removal and (2) Br^- removal capacity

may not be influenced only by Ag^+ loading onto carbon, but also the availability of silver for interactions with Br^- .

4.4.7. Effects of Background Water Characteristics on Bromide Removal

The Br^- removal capacity per mol of silver remained low for all three adsorbents across the four water matrices (< 0.13 mol of Br^- per mol Ag^+). For both PAC-Ag and MH-Ag, their Br^- removal capacity and percent Br^- removal both decreased as chloride and NOM were added and as natural CAP surface water was used. We believe this was a result of competing ions and organic matter complexing with the Ag^+ , rendering much of it unavailable to react with Br^- in solution. For Tour-Ag, the amount of Br^- removed per mol of Ag^+ and the percent Br^- removal both increased as chloride and NOM were added. In CAP surface water, the amount of Br^- removed per mol of Ag^+ was similar to the model water with Cl^- and NOM; however, the percent Br^- removal decreased. We attributed these results to the high silver loading on Tour-Ag (12.6%) relative to MH-Ag (4.8%) and PAC-Ag (5.9%). The high loading of Ag^+ on Tour-Ag means that the Br^- removal capacity per mol of Ag^+ is relatively low in comparison to PAC-Ag and MH-Ag, both which have half the amount of Ag^+ present, when tested in model waters with limited competing elements. However, this high Ag^+ loading on Tour-Ag means that more Ag^+ is available to interact with Br^- and competing ions present in more complex waters. This allows Tour-Ag to achieve greater Br^- removal per mol of Ag^+ and percent Br^- removal than PAC-Ag and MH-Ag in CAP water. It is important to note that the increase in Ag^+ present in Tour-Ag increases the potential for Ag^+ and Br^- interactions; however, competing ions will still have an effect on Br^- removal.

4.4.8. Jar Testing Experiments to Simulate Bromide Removal at a Water Treatment Facility

Even though PAC-Ag had a similar Ag^+ content to MH-Ag and it performed well when removing Br^- from ultrapure water, intraparticle diffusion and kinetic challenges present in the complex natural water limits the ability of PAC-Ag to remove Br^- in the natural CAP surface water. Instead, both MH-Ag and Tour-Ag showed greater promise for Br^- removal in complex surface waters such as the natural CAP water tested. An additional test was done where we spiked AgNO_3 salt at five times the stoichiometric ratio of Ag:Br into jar testers to determine if a carbon adsorbent was necessary for Br^- removal. This test removed ~50% of Br^- and had a bromide removal capacity per mol of silver of < 0.07 mol Br^- per mol of Ag^+ demonstrating that AgNO_3 was less effective than silver impregnated carbon adsorbents at removing Br^- from natural CAP water; however, this may be a result of the background characteristics of the natural CAP water, and results may vary with other surface waters.

4.4.9. Consideration of Bromide Removal Mechanisms by Ag-Impregnated Graphene Oxide

There are two potential mechanisms for Br^- removal by Ag^+ impregnated GO adsorbents: (1) Br^- ions diffuse from the bulk water onto the sorbent surfaces where they complex with the Ag^+ (Ag-Br); (2) Ag^+ releases from the adsorbents into water and interacts with Br^- ions, forming sparingly soluble $\text{AgBr}_{(s)}$ crystals.

To determine if Br^- complexes with Ag^+ on the adsorbent surface, we captured PAC-Ag, MH-Ag, and Tour-Ag on 0.2-micron filters after Br^- interactions and imaged them with SEM and EDAX. Figure 4-4 shows SEM images with and without EDAX

elemental mapping of bromide, silver, chloride, and oxygen. Since EDAX provides information about the adsorbent surface, the silver that was not detected by EDAX should not be present on the adsorbent surface. For each of the adsorbents, most silver is in clusters on the adsorbent surface. Bromide was found on the filter surface and on the adsorbent surface and did not appear to cluster around silver or oxygen groups on the adsorbents. A control with Br⁻ only (no adsorbents) showed that free Br⁻ is retained by the filters, indicating that Br⁻ found in the SEM/EDAX images not attached to carbon adsorbents is likely not free AgBr complexations. Chloride appears to be in clusters similar to silver clusters on the adsorbent surface, indicating that there may be complexation of AgCl on the carbon adsorbent surfaces. EDAX mapping has a detection limit of < 0.1%, so more silver that is not detectable is likely present on the adsorbent surface. There was also some silver present on the filters, which may indicate free Ag⁺ in solution. ICP-MS data was collected for Ag⁺ in solution and verified that Ag⁺ leached off the adsorbents.

To determine if Ag⁺ leaches into solution and forms AgBr complexations, we conducted a Ag⁺ leaching test for 1mM NaHCO₃ and Natural CAP water with and without Br⁻ present. In Table 4-2, we explored the potential leaching of Ag⁺ into solution. When we compare the leaching of Ag⁺ in 1mM NaHCO₃ and CAP Water. In 1mM NaHCO₃ water, PAC-Ag and MH-Ag release 12.7 mg/g carbon and 9.9 mg/g carbon, respectively. In CAP water, PAC-Ag releases 3.6 mg/g carbon and MH-Ag releases 7.5 mg/g carbon. We observe that the amount of Ag⁺ leached into solution from PAC-Ag is more hindered by CAP water than MH-Ag. This demonstrates that the competing ions and NOM in CAP

water prohibit the release of Ag^+ into solution and is likely the reason why PAC-Ag performs worse than MH-Ag in complex waters.

When we compare the leaching of Ag^+ in 1mM NaHCO_3 with and without Br^- present, the amount of Ag^+ present for all three adsorbents decreases significantly, indicating that the Ag^+ that leaches into solution likely complexes with Br^- , forming AgBr complexes and precipitating out of solution. This is also observed in Natural CAP water with and without Br^- present. Lower amounts of Ag^+ remain in CAP water than in 1mM NaHCO_3 water, indicating that Ag^+ is also likely complexing with Cl^- in solution, forming both AgBr and AgCl precipitates.

The SEM/EDAX and silver leaching results illustrate that the likely potential mechanism for bromide removal by PAC-Ag, MH-Ag, and Tour-Ag is the leaching of Ag^+ into solution and the complexation of AgBr precipitates. Additional future research is needed to determine the exact mechanisms at play for bromide removal by silver impregnated carbon adsorbents

4.4.10. Environmental Implications and Research Needs

Carbon adsorbents without silver impregnation were unable to remove Br^- from surface water. In buffered ultrapure waters spiked with Br^- , all Ag^+ impregnated carbon adsorbents performed well; however, the introduction of competing ions (Cl^-) and organics (NOM) and the use of natural CAP water significantly reduced the ability of PAC-Ag to remove Br^- from surface waters, which we attributed to its porous nature. The sheet-like structure of MH-Ag and Tour-Ag provided the advantage of reducing the competition for adsorption sites compared to PAC-Ag. They performed as superior adsorbents for Ag^+ based Br^-

removal. Both MH-Ag and Tour-Ag showed the ability to remove more Br^- than PAC-Ag when competing ions and organics were present. All three silver impregnated adsorbents reduced Br^- in surface water when used in conjunction with alum during coagulation and flocculation, making silver impregnated GO a viable technology to be introduced into the current treatment processes framework of water treatment facilities. The mechanism for Br^- removal by silver impregnated GO appears to be initiated by Ag^+ leaching into solution, complexing with Br^- , and forming and precipitating AgBr salts. In complex waters with chloride and/or NOM present, $\text{AgCl}_{(s)}$ or Ag-NOM complexes likely compete with AgBr reactions. The likely minor pathways for Br^- removal are by Br^- complexing with Ag^+ on the adsorbent surface, which are shown in the SEM/EDAX images (Figure 4-4).

Future research should address the need to improve the Br^- removal capacity of Ag^+ impregnated GO. Despite the improved performance of GO-Ag, Br^- removal efficiency is still far from the theoretical molar ratio of Ag:Br of 1:1. To improve the economic viability of this new Br^- removal process, future research should examine new materials and process designs that improve the Br^- removal per amount of Ag^+ added as well as the recovery and regeneration of silver on these adsorbents. Changes in the material design, by changing the support structure or the silver impregnation process, are one possible development avenue.

4.5. Acknowledgements

This work was partially funded through the Nanotechnology- Enabled Water Treatment Nanosystems Engineering Research Center by the National Science Foundation (EEC-1449500).

Table 4-1. Characterization of Carbonaceous Adsorbents. XPS refers to X-ray Photoelectron Spectroscopy. BDL refers to below instrument detection limit. *Images are in the supplemental information.

Adsorbents	Raman Defects* (D:G Ratio)	XPS* (C:O Ratio)	Silver Content (Dry Mass %)	BET Surface Area (m² g⁻¹)
PAC (Oxidized)	1.023	7.310	0.4 ± 0.1	716
PAC-Ag	1.037	-	5.8 ± 1.2	344
MH	0.982	1.932	0.0 ± 0.0	0.55
MH-Ag	1.038	-	4.9 ± 0.6	BDL
Tour	0.823	1.787	0.0 ± 0.0	9.38
Tour-Ag	0.939	-	12.6 ± 3.3	BDL

Table 4-2. Quantification of Ag⁺ Released into Solution from Carbon Adsorbents after 4 Hours of Mixing. 24 Hour acid digestion with nitric acid was conducted to approximate total silver content. Natural CAP water refers to natural river water managed by the Central Arizona Project.

Batch Bottle Leaching Test	Ag ⁺ Concentration (mg Ag ⁺ / g Adsorbent)		
	PAC-Ag	MH-Ag	Tour-Ag
2% HNO ₃ Digestion (T=24Hrs)	55.6 ± 11.7	49.2 ± 5.8	126.2 ± 32.7
1 mM NaHCO ₃ (T=4Hrs)	12.7 ± 1.6	9.9 ± 1.2	25.6 ± 2.1
1 mM NaHCO ₃ + 200 µg L ⁻¹ Br ⁻ (T=4Hrs)	2.2 ± 0.0	1.8 ± 0.0	1.9 ± 0.1
Natural CAP Water + 200 µg L ⁻¹ Br ⁻ (T=4Hrs)	0.3 ± 0.0	0.4 ± 0.1	0.8 ± 0.2

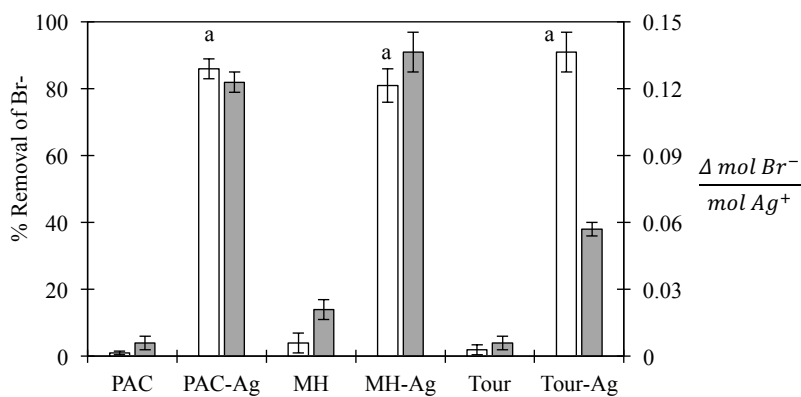


Figure 4-1. The removal of spiked Br⁻ (200 µg L⁻¹) in 1mM NaHCO₃ by 25 mg L⁻¹ of adsorbents after mixing for 4 hours. The white bars correspond to the left axis (% removal of Br⁻), and the grey bars correspond to the right axis (Br⁻ removal capacity per mol of silver). The data represent average of experiment triplicates with error bars (total 1 standard deviation). Letters above bars indicate no statistical significance between data sets (one-way analysis of variance, 95% CI, ANOVA).

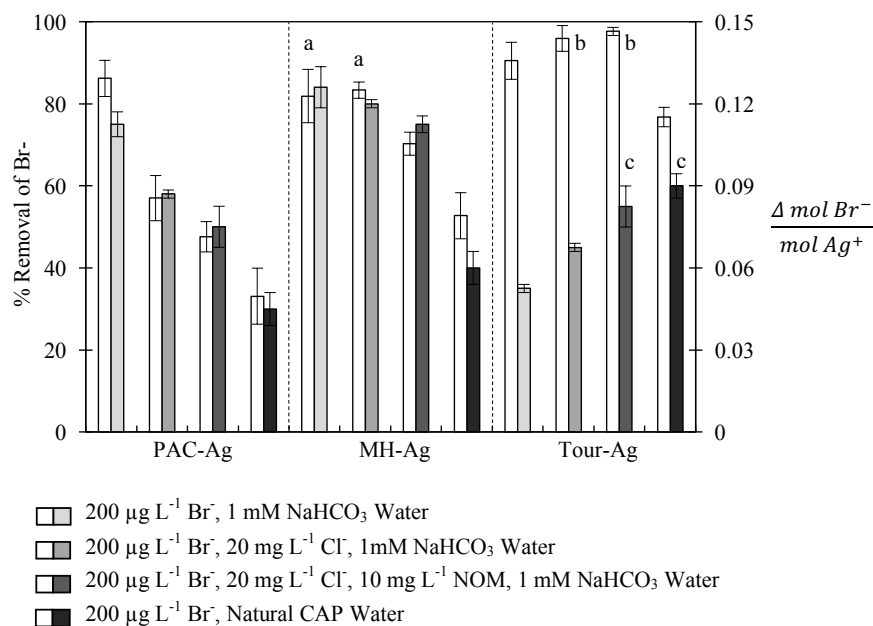


Figure 4-2. The removal of spiked Br⁻ (200 µg L⁻¹) in four different water matrices by 25 mg L⁻¹ of Ag⁺ impregnated PAC and GO after mixing for 4 hours in polypropylene batch bottles. The water matrix chemistry is provided in the legend. The white bars correspond to the left axis (% removal of Br⁻), and the grey bars correspond to the right axis (Br⁻ removal capacity per mol of silver). The data represent average of experiment triplicates with error bars (total 1 standard deviation). Letters above bars indicate no statistical significance between data sets (one-way analysis of variance, 95% CI, ANOVA).

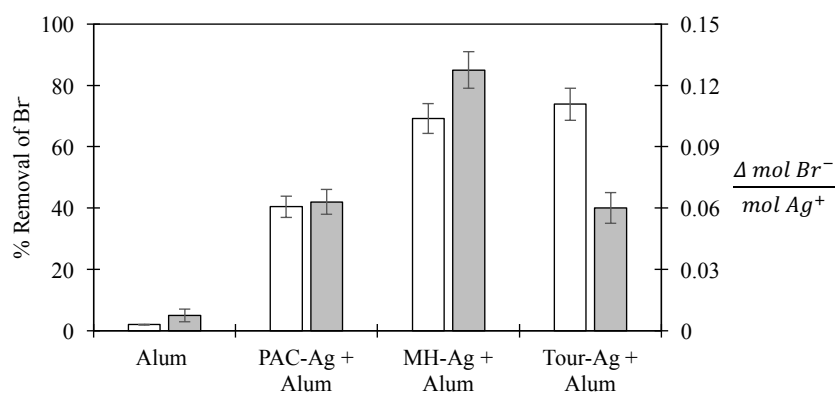


Figure 4-3. Removal of spiked Br⁻ (200 µg L⁻¹) in natural CAP water by 25 mg L⁻¹ of Ag⁺ impregnated PAC and GO after jar tests with 28 mg L⁻¹ alum. The white bars correspond to the left axis (% removal of Br⁻), and the grey bars correspond to the right axis (Br⁻ removal capacity per mol of silver). The data represent average of experiment triplicates with error bars (total 1 standard deviation). Letters above bars indicate no statistical significance between data sets (one-way analysis of variance, %95 CI, ANOVA).

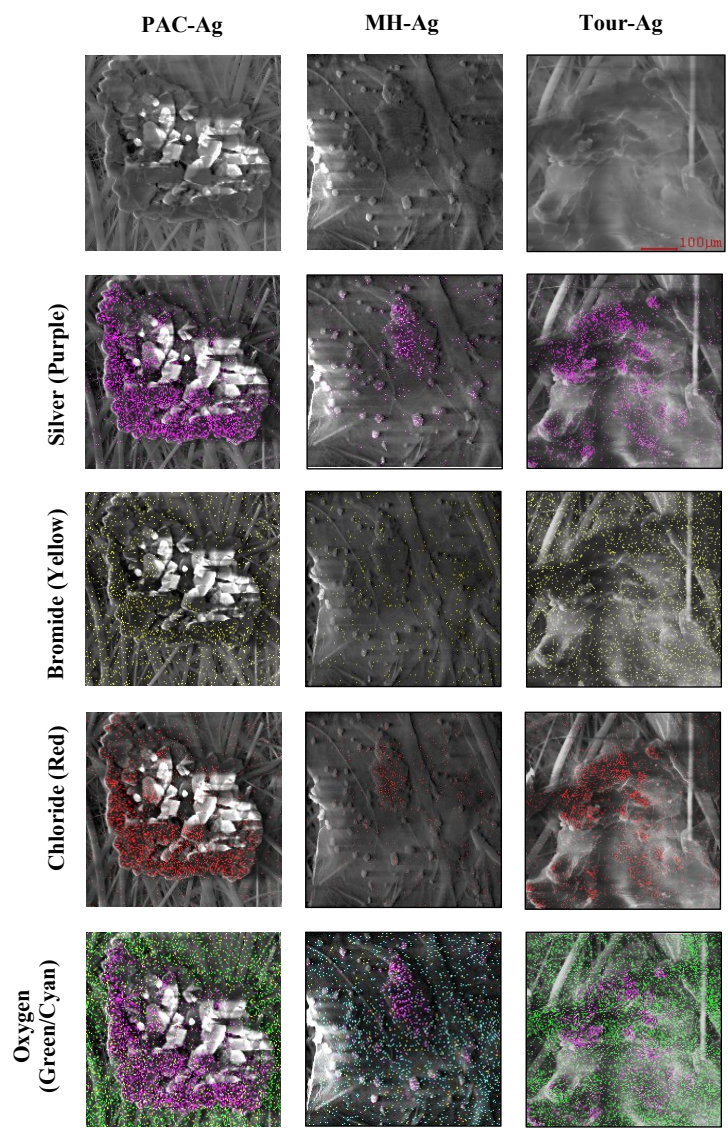


Figure 4-4. SEM images of PAC-Ag, MH-Ag, and Tour-Ag in 1 mM NaHCO₃ with 200 ug L⁻¹ bromide and 20 mg L⁻¹ chloride. Each figure is on the same scale (top right figure). Each column corresponds to an individual adsorbent. The first row is of SEM images with no EDAX elemental scanning, and the other rows show silver, bromide, chloride, or oxygen from EDAX elemental scanning. The EDAX scans can be found in Figure S3.

4.6. Supplemental Information

Synthesis of Graphene Oxide from Graphite

Graphene oxide was synthesized from graphite using the MH (modified Hummer's method)³⁰ and the Tour methods³¹. For the MH method, SP-1 graphite powder (1.0 g) was dispersed in concentrated sulfuric acid (5 mL) and pre-oxidized using $K_2S_2O_8$ (1.0 g) and P_2O_5 (1.0 g). This suspension was maintained at 80 °C for 4.5 h, poured into 160 mL of DI water, and allowed to rest and cool to room temperature overnight. The pre-oxidized graphite powder was collected by vacuum filtration on a 0.45 μ m Polytetrafluoroethylene (PTFE) membrane (Millipore), washed extensively with deionized (DI) water, and dried overnight at room temperature. The pre-oxidized graphite was then placed in concentrated sulfuric acid (40 mL), and $KMnO_4$ (5.0 g) was slowly added to the graphite suspension, with the temperature closely monitored to avoid an increase above 10 °C by using an ice bath. After the $KMnO_4$ addition, the mixture was slowly heated to 35 °C and left to react for 2.5 h. DI water (77.0 mL) was then slowly added into the suspension, not allowing the temperature to exceed 50 °C. After water addition, the mixture was left to react for an additional 2 h at room temperature. The solution was then poured into 240 mL of DI water, and 4.2 mL of H_2O_2 (30%) were added, which turned the solution a bright yellow color. The solution was kept at room temperature for 2 days, and the precipitate was recovered by centrifugation (12,000 x g, 30 min) and washed with 100 mL of a 1:10 HCl solution (2x) and DI water to remove residual chemicals. The resulting material was re-suspended in DI water and dialyzed with Fisherbrand[®] dialysis tubing (molecular weight cut-off 3,500

Da) for 3 days for additional purification. The final dark brown graphite oxide suspension was dried by lyophilization (5 days) and stored at room temperature until use.

For the Tour method, graphite (1.0 g) was added to 200 mL of a 9:1 mixture of H_2SO_4 : H_3PO_4 and bath sonicated (M3800 Branson Ultrasonic Bath, Emerson, Danbury, CT) for 5 min. The reaction vessel was placed in an ice bath, and KMnO_4 (6.0 g) was added to the mixture under constant stirring. The solution was then slowly heated to 50 °C and stirred for 12 h. The temperature was strictly kept at 50 °C because Mn_2O_7 , formed by adding KMnO_4 to a concentrated sulfuric acid, can detonate at temperatures higher than 55 °C. Next, the solution was cooled to room temperature overnight and poured into iced DI water (~400 mL) with 3 mL of H_2O_2 . The precipitate was then washed in succession with 100 mL of DI water (2x), 100 mL of 1:10 HCl (2x), and 100 mL of DI water. After each washing step, the mixture was centrifuged (12,000 x g, 30 min) and the supernatant decanted until the pH was equivalent to that of the DI water (~4.0). Next, the material was purified by dialysis (3,500 Da membranes) for 72 h. Finally, the dark brown product was dried by lyophilization (5 days) and stored in a sealed Falcon tube at room temperature until use.

Oxidation of Powder Activated Carbon

A suspension was made by combining six grams of powdered activated carbon (20B, Norit Americas Inc., Atlanta, GA, USA) and 150 mL of 15.7 N HNO_3 solution in an Erlenmeyer flask. This suspension was then heated and stirred on a magnetic stirrer with hot plate at ~90 °C for 1 h. The flask was removed from the hot plate and cooled down to room temperature. The suspension was then vacuum filtered to remove the PAC from the

solution through 0.7 μm GF/F grade filter paper. The oxidized PAC accrued on the filter paper was rinsed with 500 mL of nanopure water several times until the pH of the rinse solution remained constant to ensure excess acid was removed. The oxidized and rinsed PAC was dried at 90 °C under vacuum and stored in a sealed container at room temperature.

Silver Impregnation of Carbon Materials

To impregnate the carbon materials with silver, each carbon (200 mg) was soaked in 10 mL of 0.5 M AgNO_3 solution. The carbon-silver slurries were stirred for two days at 150 rpm at room temperature. Then they were centrifuged for 30 minutes at 12,000 G. The supernatants were removed from the centrifuge tubes by Pasteur pipettes and replaced with 50 mL of nanopure water for rinsing. The carbon slurries with nanopure water were re-suspended with vortex mixer and separated by repeating the centrifuge step. To ensure removal of excess silver, each rinse was repeated three times. The silver impregnated carbons were dried at 90 °C under vacuum and stored in a sealed container at room temperature.

Table S1. Colorado River (Central Arizona Project (CAP)) Surface Water Background Chemistry* ND is non-detect in sample. Detection limits are provided next to non-detect samples.

General Chemistry Analytes	Units	Concentration (January 2017)
Alkalinity as CaCO ₃	mg/L	125
Ammonia Nitrogen	mg/L	ND (DL 0.05)
Barium, Total, ICAP/MS	µg/L	140
Bromide	µg/L	85
Calcium, Total, ICAP	mg/L	76
Chloride	mg/L	93
Copper, Total, ICAP/MS	µg/L	ND (DL 2.0)
Iron, Dissolved, ICAP	mg/L	ND (DL 0.02)
Iron, Total, ICAP	mg/L	0.16
Magnesium, Total, ICAP	mg/L	27
Manganese, Total, ICAP/MS	µg/L	6.1
Nitrate as Nitrogen by IC	mg/L	0.28
Orthophosphate as P	mg/L	0.32
Potassium, Total, ICAP	mg/L	4.8
Silica	mg/L	9.9
Sodium, Total, ICAP	mg/L	94
Specific Conductance (@25 °C)	µS/cm	1000
Strontium, ICAP	mg/L	1.1
Sulfate	mg/L	240
Total Dissolved Solids (TDS)	mg/L	660
Total phosphorus as P	mg/L	ND (DL 0.02)
Total Suspended Solids (TSS)	mg/L	ND (DL 10.0)
Turbidity	NTU	1.1
Temperature	°F	65
Dissolved Oxygen	mg/L	10.36
pH	-	8.1

* Data from <http://www.cap-az.com/departments/water-operations/water-quality>

Table S2. Batch Bottle Experimental Matrices

Additives	Synthetic Water	Chloride-spiked Synthetic Water	Chloride- and NOM-spiked Synthetic Water	Natural CAP Water
NaHCO₃ (1 mM)	X	X	X	
Bromide (200 µg/L)	X	X	X	X
Chloride (20 mg/L)		X	X	
NOM (10 mg/L)			X	

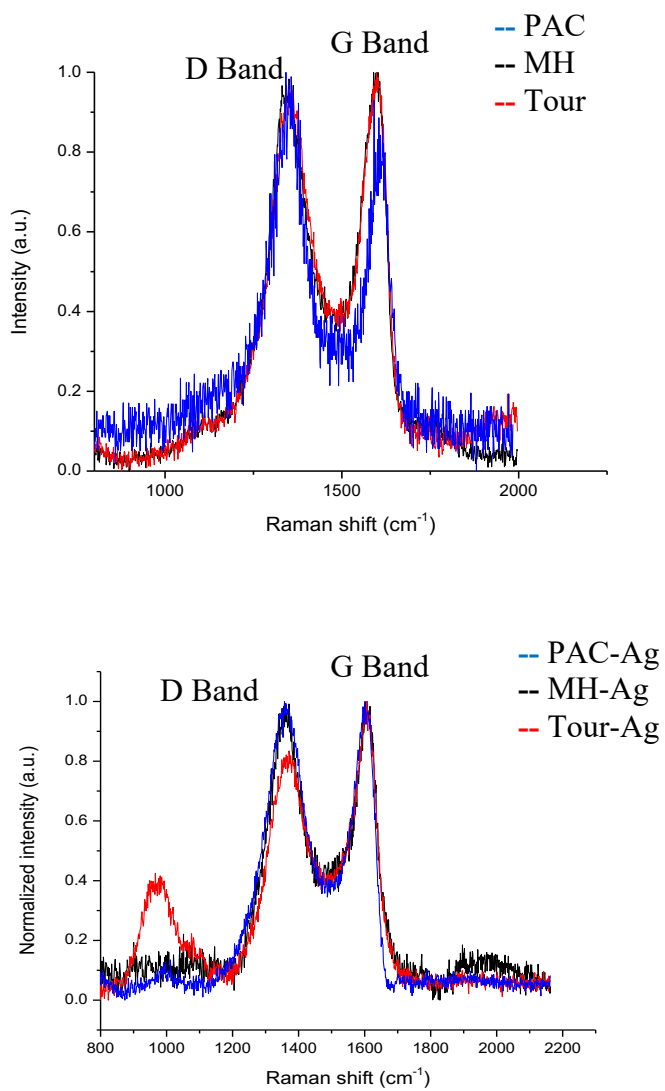


Figure S1. Raman Spectroscopy of Ag⁺ Impregnated and Non-Impregnated Carbonaceous Additives

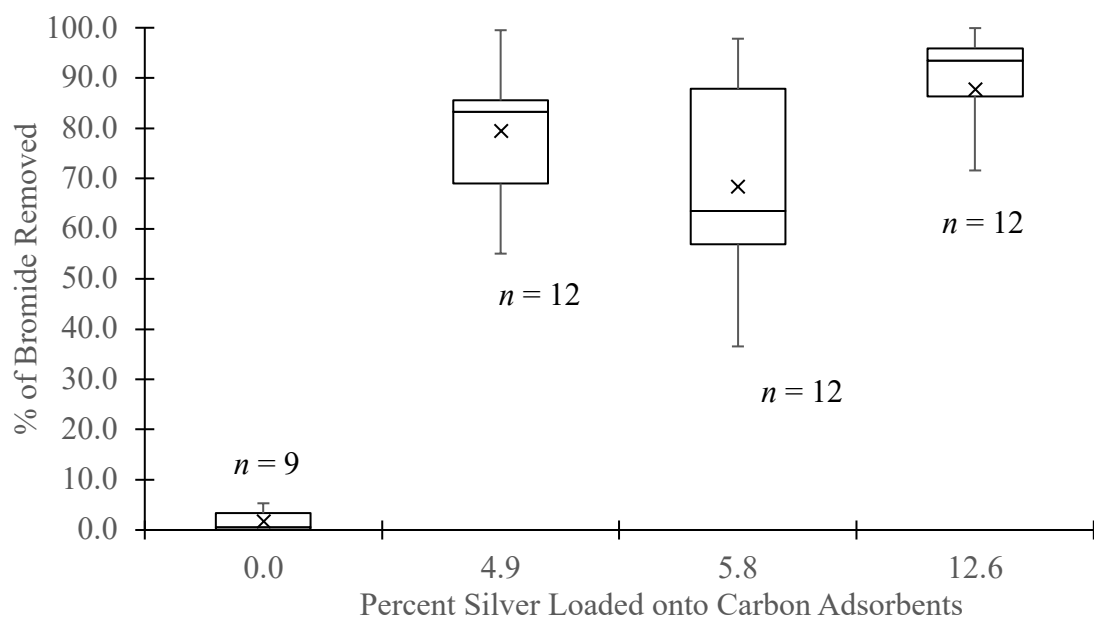


Figure S2. Bromide Removal as a Function of Ag^+ Loading on Carbon Adsorbents. “X” in each dataset represents the mean for that dataset.

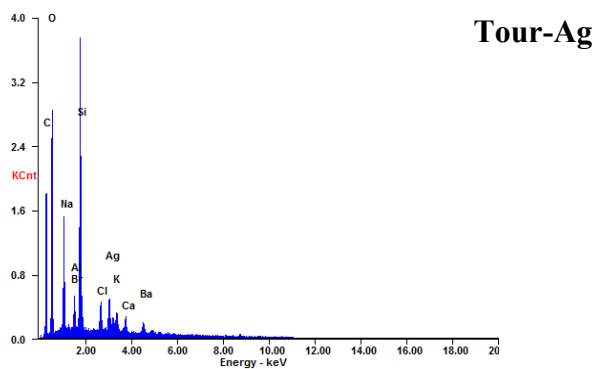
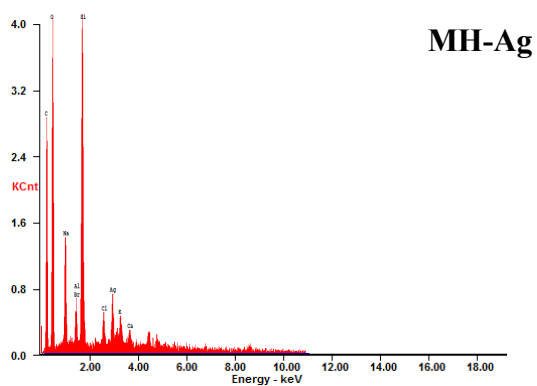
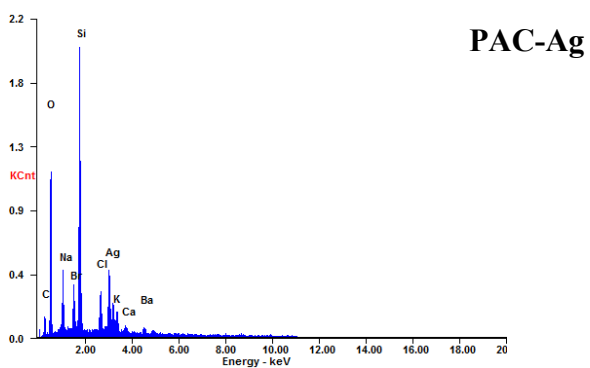
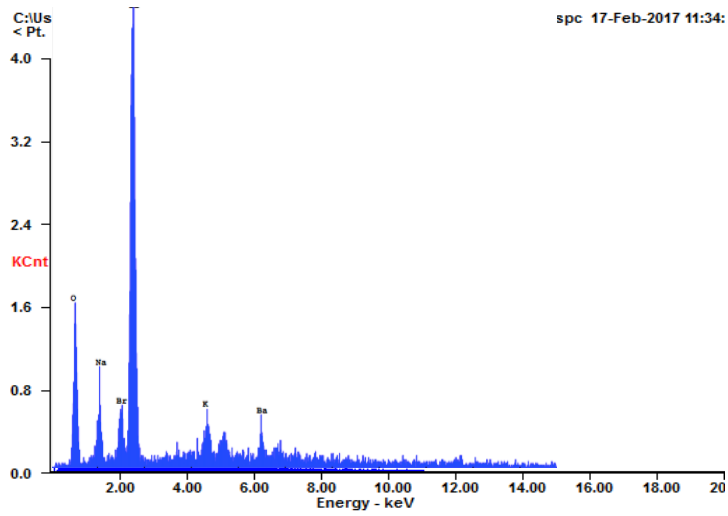
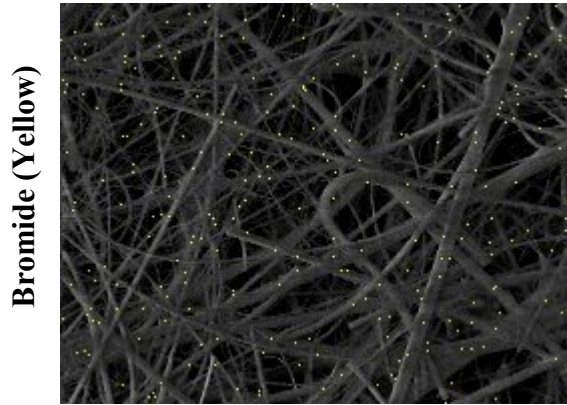


Figure S3. EDAX of Carbon Adsorbents Imaged on SEM. Experimental matrix is 1 mM NaHCO_3 spiked with 200 $\mu\text{g/L}$ Br^- and 20 mg/L Cl^- .

SEM/EDAX of Nylon Filters with no Carbon Adsorbents Present in Solution



CHAPTER 5: ANAEROBIC EFFECTS OF COLLOIDAL NANO-SILVER AND IONIC SILVER ON THE GUT MICROBIOME UNDER REALISTIC EXPOSURE CONDITIONS

- This chapter has not been published. Contributing Authors are Kidd, J., Ilhan, E., Krajmalnik-Brown, R., and Westerhoff, P. Target Journal: Environmental Science: Nano.
- My author contribution: Approximately 75% of the research and 90% of the text

5.1. Abstract

Two colloidal nanosilvers and an ionic silver were added to an anaerobic fecal consortium to contrast their impacts on the structure and function of fecal microbes after 24 hours of exposure. Silver doses (0.02, 0.2, and 2.0 mg L⁻¹) were selected to represent realistic exposures for oral dietary silver products. We observed decreasing shifts in gastrointestinal media pH and short chain fatty acid (SCFA) production after 24 hours. Gut flora species diversity was found to decrease when exposed to dietary nanosilver and ionic silver. There were also observable changes in the frequencies of gut flora at the phylum level. After 24 hours of silver exposure, there were observable decreases in *Firmicutes*, *Actinobacteria*, *Bacteriodes*, and *Cyanobacteria*, while also being observable decreases in *Proteobacteria*. Silver distribution tests with and without mucin present show that when gastrointestinal media contains mucin, there is a higher attachment of nanosilver and ionic silver to large, undissolved organic molecules in the media. When mucin is not present, there is a lower attachment of nanosilver and ionic silver to large, undissolved organic molecules in the media. These results indicate that nanosilver and ionic silver exposures to fecal microbes

reduce SCFA production and biodiversity of fecal microbes. Mucin in gastrointestinal media results in less silver free in gastrointestinal media.

5.2.Introduction

Engineered silver (Ag) ENMs are used consumer products and dietary supplements due to their redox-driven dissolution potential and release of silver ions, which provides antimicrobial properties. Despite their growing global use, Ag ENMs remain poorly understood to both regulators and scientists as there is little consensus on how Ag ENMs behave in the human body and the magnitude of which their use may contribute to gastrointestinal microbial resistance. Oral consumption and exposure of colloidal nanosilver can result in the flow of nanosilver and ionic silver from the mouth into the gastrointestinal (GI) tract. The GI tract is an important physical and biological barrier against Ag ENMs entering the circulatory system and the antimicrobial properties of Ag ENMs and associated silver ions may disrupt host homeostasis.

Recent studies have examined the sensitivity and impact of the human gut microbiome on overall human wellness. The gut microbiome plays a large role in host digestion and nutrition, influence immune system homeostasis, influence on cardiovascular diseases, link between changes in gut microbiome to changes in mood perceptions in the central nervous system (microbiome-gut-brain axis). Ag ENMs have been shown to cause microbial toxicity in aerobic environments due to the oxidation of Ag ENMs into their ionic Ag⁺ state which is the main theorized mechanism of microbial toxicity of Ag ENMs.

Little research has been done to examine Ag ENM toxicity to gut microbiomes in their natural anaerobic environment where the lack of oxygen reduces the likelihood of Ag oxidation, and the complex matrix of biomolecules facilitates heteroaggregation of Ag ENMs to mucin.

The goal of this research was to determine if Ag ENMs impact the diversity and function of a consortium of fecal microorganisms differently than ionic silver under realistic exposure conditions. Specific objectives included (1) characterization of two different, commercially available Ag ENMs and a commercially available ionic silver in gastrointestinal media, (2) determination of *in vitro* changes of fecal microorganism diversity after 24 hours of silver exposure by extracting microbial DNA from batch bottles and conducting DNA sequencing, (3) determination of changes in fecal microorganism activity by measuring short chain fatty acid (SCFA) production after 24 hours of silver exposure through biochemical characterization, (4) determination of the association of Ag ENMs and ionic silver to biomolecules present in gastrointestinal media after 24 hours of silver exposure.

5.3. Materials and Methods

5.3.1. Nanoparticle Selection and Characterization

Well-studied commercial grade citrate coated Ag (NanoComposix, NanoXact AGCN40) was selected as a control Ag nanoparticle. A dietary supplement Ag was purchased from Purest Colloids, and has previously been well characterized. Silver nitrate (Sigma Aldrich, CAS #7761-88-8) was used as a source of ionic silver. Characterization for the citrate coated Ag⁰ was provided by NanoComposix. Characterization for colloidal Ag⁰ was

previously reported in as the manufacturer (PurestColloids) only provides the hydrodynamic diameter of the Ag using dynamic light scattering. The characterization of both silver nanoparticles can be found in detail in the SI.

5.3.2. Preparation of Bench Scale Batch Serum Bottles

Gastrointestinal growth medium was made following the protocol from McDonald et al. 2013 for their twin-vessel single-stage chemostat model. A table of reagents for the media can be found in the SI. The growth medium was prepared to a volume of 5 liters and sterilized. After preparing the medium anaerobically under a stream of 20/80 % CO₂/N₂ gas, we distributed 100 mL of medium into triplicate 125-mL serum bottles for each testing condition and then adjusted the pH to 6.9-7.0 with 10% hydrochloric acid. Before inoculation of fecal inoculum, we flushed the headspace of the bottles with 20/80% CO₂/N₂ gas and equilibrated the bottle contents to atmospheric pressure (1 atm).

5.3.3. Collection and Preparation of Fecal Inocula

Fresh fecal samples were immediately placed into a -80C freezer upon collection. Approximately 500 mg of fecal material was pulled from each donor sample and mixed into 100 mL of anaerobic growth media to create a 10% (w/v) fecal slurry. The slurry was incubated at 37C on a rotational shaker for 24 hours. Approximately 1 mL of slurry was then transferred to a clean anaerobic growth media batch bottle and was incubated at 37C for 24 hours. This transfer process was repeated for a total of 5 transfers. At each inoculum transfer, the volume of gas produced was measured to ensure the fecal inoculum was acclimated to the media. The resulting fecal slurry after the 5 transfers was used as the

inoculum for the study. For batch bottles that required fecal inocula, 1 mL of inocula was added to 100 mL of sterile anaerobic growth media

5.3.4. Inoculation, Operation, and Sampling

Two rounds of testing were conducted for this study. A breakdown of testing parameters for each batch bottle can be found in Table S1. In the first study, we tested a variety of different experimental variables in triplicate (n=108). We tested three different silver types at three different silver concentrations (0.02, 0.2, and 2 mg L⁻¹). These batch bottle samples were tested in gastrointestinal media with and without fecal inoculum present. Control samples (n=30) were made and tested for nanosilver in anaerobic water, gastrointestinal anaerobic media without silver, and gastrointestinal anaerobic media with inoculum and without silver. The second study focused on the role of mucin within gastrointestinal media. The three different silver were added to triplicate batch bottles with fecal inoculum and no mucin at a concentration of 2 mg L⁻¹. Triplicate control samples (n=12) were gastrointestinal media (no mucin) with only the fecal inoculum and gastrointestinal media (no mucin) with only the silver added. Additional control experiments were run with mucin in anaerobic DI water. The three different silver were added to triplicate batch bottles at a concentration of 2 mg L⁻¹.

After batch bottle experiments had been incubated for 24 hours, the batch bottles were collected for sampling. Each bottle was inverted, and 1.5 mL of sample was taken using a syringe for each characterization parameter. The 1.5 mL samples were transferred to 2 mL centrifuge vials and stored at -80C until biochemical characterization analysis.

5.3.5. Biochemical Characterization

The pH of the aliquots collected for both time-points of 0 hours and 24 hours was measured using a pH meter (ThermoScientific Orion). In order to perform electron-equivalent mass balances, we used a HACH COD analysis kit (HACH Co, Loveland, CO, U.S.A) to measure the total chemical oxygen demand (COD) of the aliquots before filtering and soluble COD using after filtration with 0.2- μ m PVDF membranes (Acrodisc, LC 13 mm syringe filter) at both time-points of 0 hours and 24 hours. We calculated the electron equivalents of fermentation end products using the stoichiometric equations as specified in Rittmann and McCarty (Rittmann & McCarty, 2001). In order to determine short chain fatty acid (SCFA) fermentation end products, we diluted the aliquots into 10 mL of de-ionized water. After vortexing at least 1 min or until the sample was thoroughly homogenized, we collected 1.5 ml of the homogenized sample and centrifuged it at full speed ($16,100 \times g$) for 15 min at 4 °C. Then, we filtered supernatants through 0.2- μ m PVDF membrane filters and analyzed filtrates using High-Pressure Liquid Chromatography (HPLC) (LC-20AT, Shimadzu) equipped with a carbohydrate column (Aminex HPX-87H column, Biorad) as previously described (Lee *et al.*, 2008). Short-chain fatty acids (acetate, formate, butyrate, isobutyrate, isovalerate, valerate, propionate, lactate) were analyzed using 5 mM H₂SO₄ as the eluent, a 0.6-ml/min-flow rate, a column temperature of 50°C, and a 50-min run time. Hydrogen gas was measured from 200 μ L gas samples from the headspace of the batch bottles using a Shimadzu GC equipped with a thermal conductivity detector (GC-TCD). Statistical analysis was carried out using ANOVA followed by a post hoc chi-square test using the XLSTAT add-on in Microsoft Excel. For all analyses the level of significance was set at 5% ($p < 0.05$).

5.3.6. *Silver Distributions in Gastrointestinal Media*

Ag distributions in gastrointestinal media were studied through a filtration series of gastrointestinal media in batch bottles that were spiked with silver. 1mL of stock solution for each Ag type was added to 99mL of gastrointestinal media resulting in final silver concentrations of 0.02, 0.2, and 2.0 mg L⁻¹. The batch bottles were agitated for 24 hours under similar conditions to the initial study. Separate control vials of anaerobic water (99mL) were spiked with each Ag and analyzed with ICP-MS for Ag concentrations to estimate starting silver concentrations at T=0hrs and T=24hrs. Aliquots of 17mL of gastrointestinal media was collected for each batch bottle. Approximately 2mL of media was taken and stored for future analysis, while the remaining 15mL of media was filtered through 0.45-micron Whatman Nylon filters (Sigma Aldrich) to remove non-dissolved large organics. Approximately 2mL of media was taken and stored for future analysis, while the remaining 13mL of media was filtered through 30 kDa centrifugal ultrafilters (Millipore, Ultracel Regenerated Cellulose Membrane, >90% recovery, Burlington, MA, USA) to remove dissolved organics from the media. Approximately 2mL of media was taken and stored for future analysis after filtration. Analysis of silver concentrations was conducted by 2% HNO₃ acidification of samples followed by ICP-MS. A mass balance of Ag was conducted by quantifying the mass of Ag in media before and after each filtration step.

5.3.7. *DNA Extraction and Sequencing*

Microbial DNA was extracted from the aliquots sampled and saved from the batch bottles using a DNeasy® PowerSoil® Kit (Qiagen, CA) and followed the manufacturer's protocol

with no modifications. Bacterial community analysis was performed via next generation sequencing in MiSeq Illumina platform. Amplicon sequencing of the V4 region of the 16S rRNA gene was performed with the barcoded primer set 515f/806r designed by Caporaso et al. 2012 and following the protocol by the Earth Microbiome Project (EMP) (<http://www.earthmicrobiome.org/emp-standard-protocols/>) for the library preparation. PCR amplifications for each sample were done in triplicate, then pooled and quantified using Quant-iT™ PicoGreen® dsDNA Assay Kit (Invitrogen). 240 ng of DNA per sample were pooled and then cleaned using QIA quick PCR purification kit (QIAGEN). The PCR pool was quantified by Illumina library Quantification Kit ABI Prism® (Kapa Biosystems). The DNA pool was determined and diluted to a final concentration of 4 nM then denatured and diluted to a final concentration of 4 pM with 30% of PhiX. Finally, the DNA library was loaded in the MiSeq Illumina sequencer using the chemistry version 2 (2x150 paired end) and following the directions of the manufacturer

5.4. Results and Discussion

5.4.1. Changes in pH levels after 24 Hours of Silver Exposure

The pH of the gastrointestinal media was measured before and after 24 hours of Ag exposure. Figure 1A shows the comparison of pH levels for samples exposed to the three different Ag at three different concentrations. Abiotic control samples showed no significant decrease in pH levels after 24 hours of Ag exposure. There was no significant decrease in pH values for gastrointestinal media spiked with fecal microorganisms and each Ag type at concentrations of 0.02 mg L⁻¹ and 0.2 mg L⁻¹. For gastrointestinal media spiked with fecal microorganisms and each Ag type at a concentration of 2 mg L⁻¹, there

was a significant decrease in gastrointestinal pH compared to the control samples with no silver added (Figure 5-1A). Prior studies have shown that shifts in pH can influence the aggregation behavior of Ag nanoparticles, with the aggregation rate of Ag increasing with a decreasing pH in simulated gastric fluids [REF]. Alterations in pH levels in gastrointestinal media can impose selective pressure on fecal microorganism growth and the production and distribution of SCFA fermentation end products. Specifically, butyrate production typically occurs at mildly acidic pH levels [REF], while propionate production typically occurs at neutral pH [REF], and acetate production occurs at a range of pH depending on the microorganism that is producing acetate.

5.4.2. Changes in SCFA Production after 24 Hours of Silver Exposure

Fecal microbes can form metabolic networks in biofilms and their tolerance to changes in pH can alter SCFA production and alter other metabolic processes. The production of the SCFAs butyrate, propionate, and acetate were compared after 24 hours of Ag exposure at three different concentrations (Figure 5-1B). There was no statistically significant decrease in propionate production regardless of Ag type or concentration after 24 hours of exposure. There was a statistically significant decrease in butyrate production for all three Ag types at concentrations of 2 mg L⁻¹ after 24 hours of exposure; however, there was no decrease in butyrate production for Ag concentrations of 0.02 mg L⁻¹ and 0.2 mg L⁻¹. There was a statistically significant decrease in acetate production for all three Ag types at concentrations of 0.2 mg L⁻¹ and 2 mg L⁻¹; however, there was no decrease in acetate production for Ag concentrations of 0.02 mg L⁻¹.

5.4.3. Impact of Mucin on Distribution of Silver in Gastrointestinal Media

Intestinal mucin found in gastrointestinal media may be a hotspot for Ag association due to its barrier properties. Prior studies have shown that mucus is able to trap 200-nm Ag ENMs, reducing their interaction with the cellular membrane, resulting in lower levels of oxidative stress [REF]. Batch bottle studies were conducted to determine the association of Ag with and without mucin present. Filtration tests using 0.45-micron Nylon (removes non-dissolved organics) and 30kDa centrifugal filters (removes dissolved organics) were conducted to determine how much Ag is retained by and passes through each filter. Control samples with Ag-spiked DI water show that the majority of the three Ag pass through both filters (>99% recovery). In the presence of mucin, 87% of dietary Ag is retained by the 0.45-micron filter, and 12% of dietary Ag is further retained by the 30kDa filter. With no mucin present, 72% of dietary Ag is retained by the 0.45 micron-filter, and 23% of dietary Ag is further retained by the 30 kDa filter. For dietary silver, less than 1% of dietary Ag passes through the 30kDa filter when mucin is both present and not present in gastrointestinal media. In the presence of mucin, 95% of Ag-citrate is retained by the 0.45-micron filter, and 5% of Ag-citrate is further retained by the 30kDa filter. With no mucin present, 77% of Ag-citrate is retained by the 0.45 micron-filter, and 17% of dietary silver is further retained by the 30 kDa filter. For Ag-citrate, less than 1% of silver passes through the 30kDa filter when mucin is present and less than 5% of Ag-citrate passes through the 30kDa filter when mucin is not present in gastrointestinal media. In the presence of mucin, 94% of Ag-citrate is retained by the 0.45-micron filter, and 5% of Ag-citrate is further retained by the 30kDa filter. With no mucin present, 78% of Ag-citrate is retained by the 0.45 micron-filter, and 20% of dietary silver is further retained by the 30 kDa filter. For

Ag-citrate, less than 1% of silver passes through the 30kDa filter when mucin is present and less than 2% of Ag-citrate passes through the 30kDa filter when mucin is not present in gastrointestinal media. Because 0.45-micron filters are designed to remove non-dissolved organics, it is likely that the majority of each Ag in gastrointestinal media is associating with large non-dissolved organics (e.g. microbes, mucin). Additionally, there is an increase in each Ag that passes through the 0.45-micron filter when no mucin is present, which means that mucin is likely attributing to the high fraction of Ag retained by the 0.45-micron filter.

5.4.4. *Effect on Gastrointestinal Microbiome Diversity*

The fecal microorganism community biodiversity was evaluated using alpha rarefaction curves to determine species diversity for samples exposed to nanosilver and ionic silver (Figure 5-3). The Shannon Index Value, used to normalized community diversity as a function of sampling depth, of our control samples with no silver exposure was 2.10. We found that silver citrate exposure resulted in the lowest species richness, with a Shannon Index Value of 1.75. We found dietary silver (SIV = 2.38) and ionic silver (SIV = 2.37) to have a higher species diversity than our control gut flora.

Figure 5-4 shows the taxonomic bar chart for fecal microorganism community relative frequencies. For initial fecal microorganism stock community and primed fecal microorganism stock frequencies, there are high frequencies of Proteobacteria (~87%), which is commonly attributed to unhealthy communities or communities that are under stress [REF]. For control samples that were inoculated into gastrointestinal media for 24 hours without silver exposure, the fecal community relative frequency for Proteobacteria

decreases (~46%), while Firmicutes (~39%), Actinobacteria (~12%), and Bacteroidetes (~1%) increased compared to the stock fecal microorganisms. The relative frequencies of these samples is more aligned with prior studies that have evaluated fecal microorganism community diversity [REF]. For samples exposed to silver for 24 hours, the relative frequency of Proteobacteria increases compared to the control samples with no silver, while the relative frequency of Firmicutes, Actinobacteria, and Bacteroidetes decreases for all silver types and concentrations. This indicates that silver, regardless of type or concentrations elicits a selective pressure upon fecal microorganism communities.

5.5.Conclusions

Fecal microorganisms, after exposure to nanosilver and ionic silver for 24 hours, exhibit decreased pH and SCFA production. We observed decreases in pH and SCFA production of acetate and butyrate at nanosilver and ionic silver concentrations of 2 mg L^{-1} , which is the high range for expected concentrations of silver in the gut microbiome upon oral ingestion of dietary nanosilver supplements. Alpha rarefaction curves highlight that species diversity within the fecal microorganism community decreases when exposed to Ag-citrate and increases when exposed to dietary-Ag and ionic-Ag. Taxonomic bar charts show that silver exposure to fecal microorganisms for 24 hours alters the relative frequency of phylum-level microorganisms. These results indicate that silver, both in the nano form and ionic form, has an effect on the structure and function of fecal microorganisms and it will be important moving forward to understand the interactions between gastrointestinal media, mucus, fecal microbes and silver so that we can develop mathematical models and understand the mechanisms of nanosilver and ionic silver in this complex system.

5.6.Acknowledgements

This work was funded by the PLS alliance partnership between ASU, UNSW, and Kings College

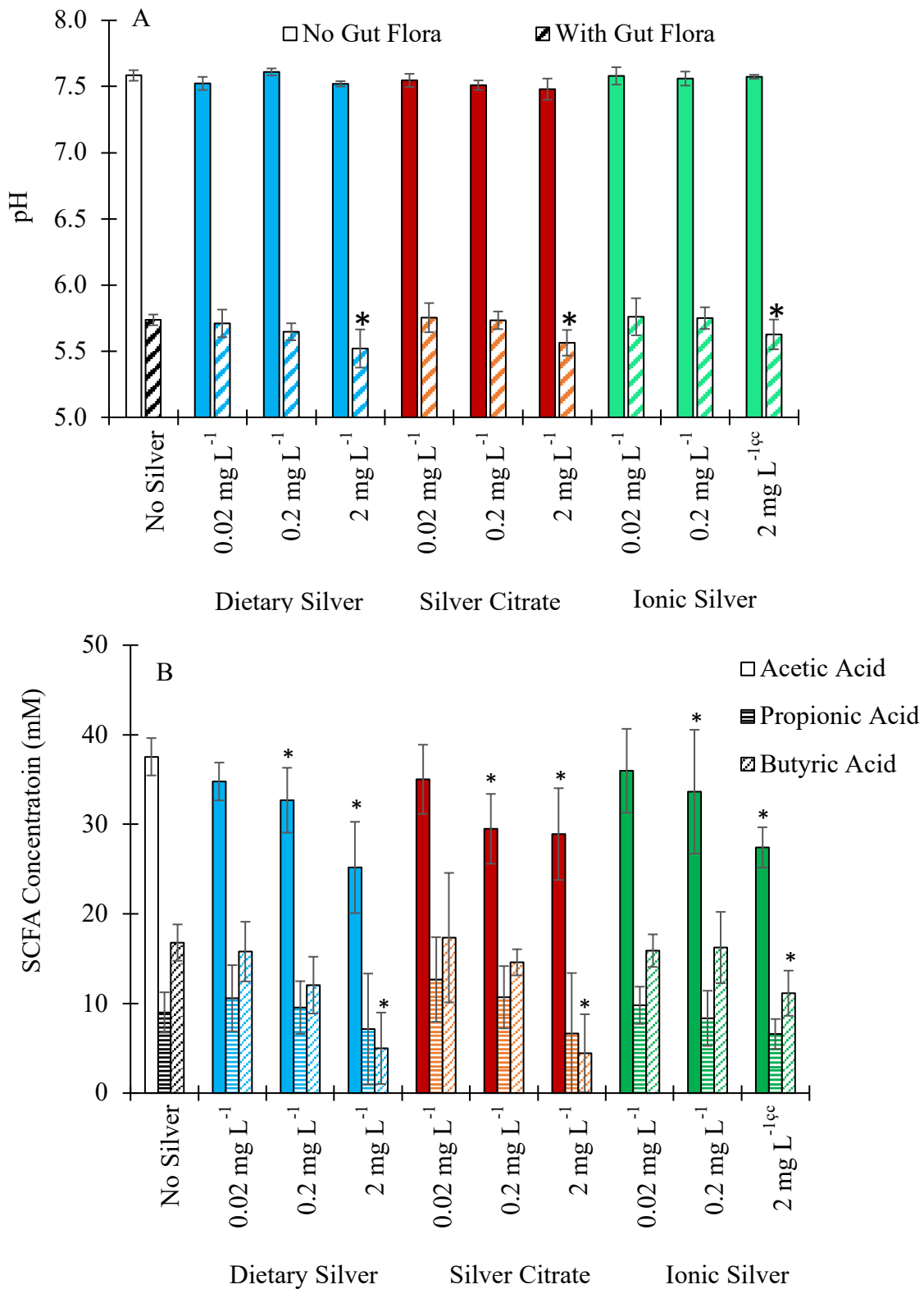


Figure 5-1. Changes in gastrointestinal (A) pH and (B) SCFA production after 24 hours of exposure to three silver types and concentrations.

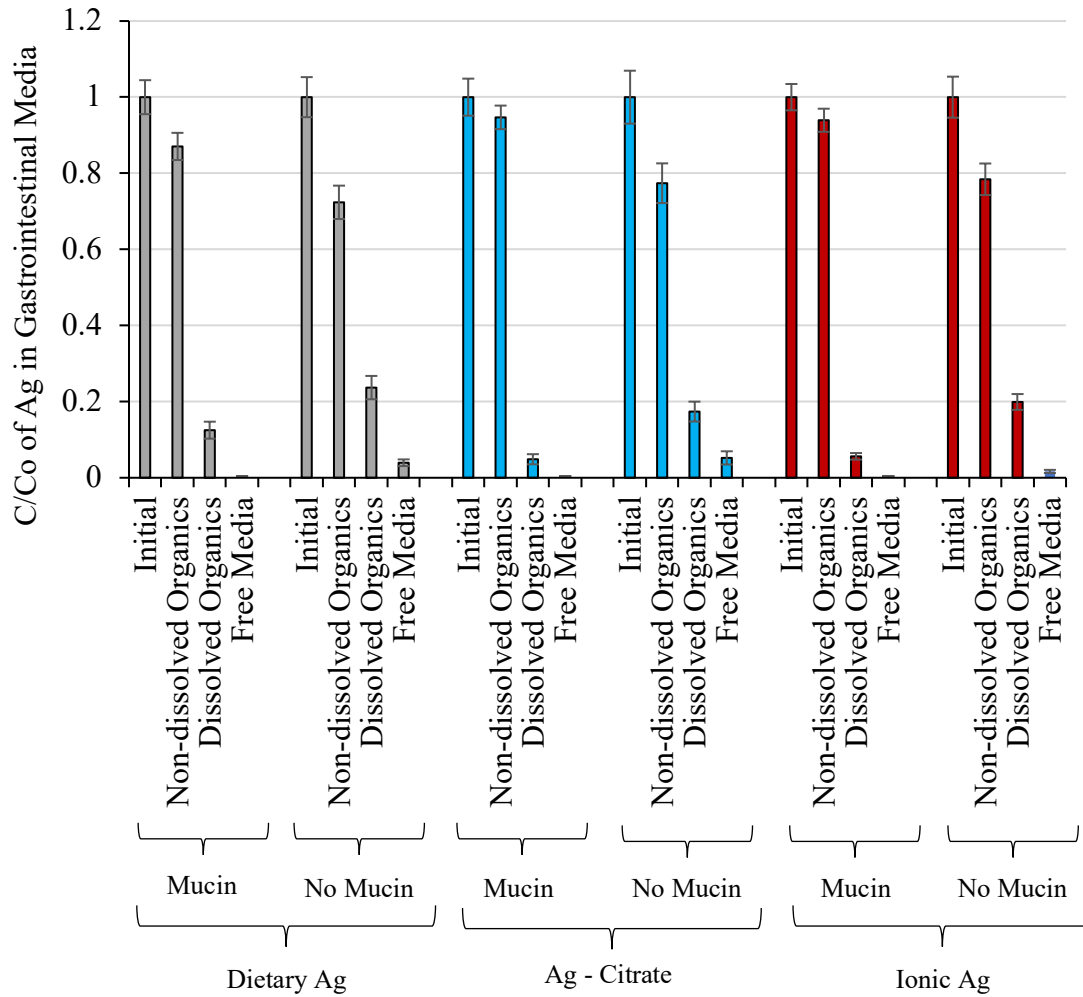


Figure 5-2. Ag distributions in gastrointestinal media with and without mucin after 24 hours of exposure

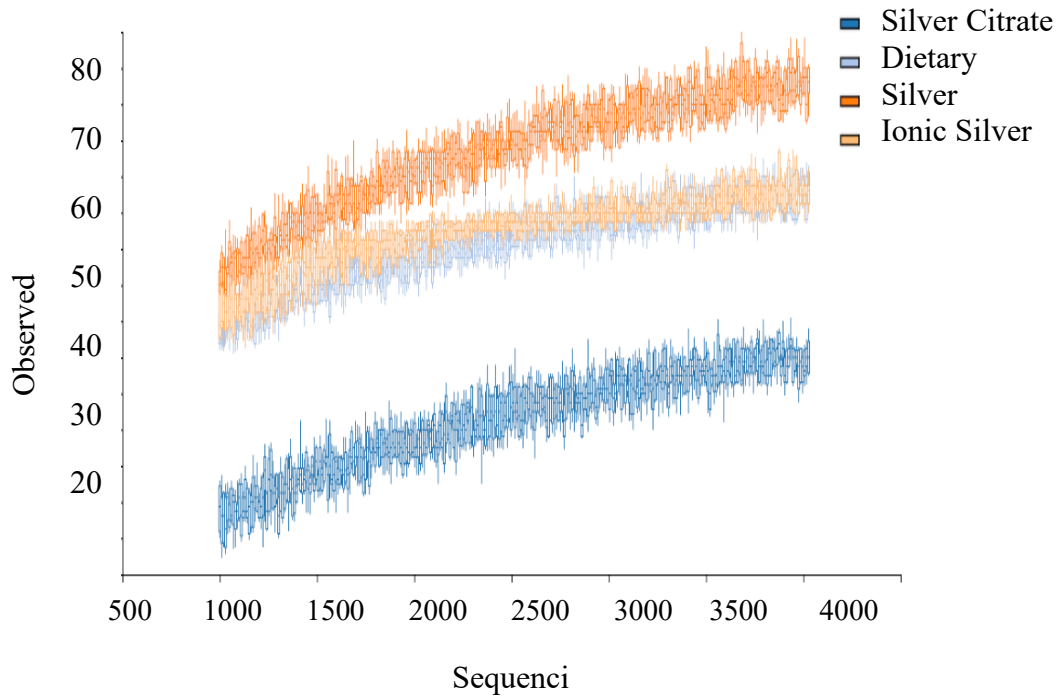


Figure 5-3. Alpha rarefaction curves of fecal microorganism communities to assess species richness after exposure of microorganisms to silver.

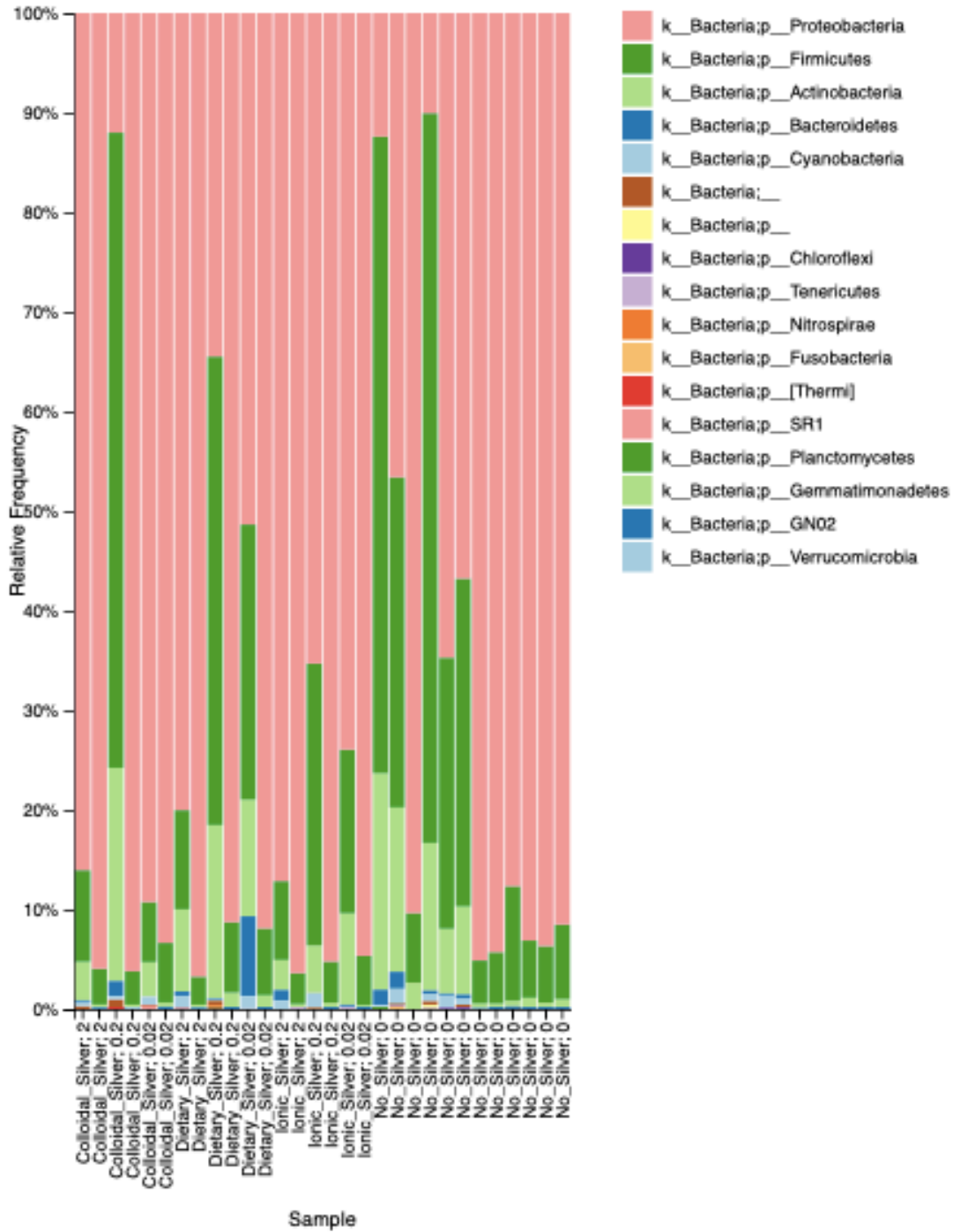


Figure 5-4. Relative frequencies of fecal microorganisms (phylum level) in control and experimental samples after 24 hours of silver exposures.

CHAPTER 6. SOCIETAL IMPLICATIONS OF NANO: PUBLIC PERCEPTIONS REGARDING THE USE OF NANOMATERIALS FOR DRINKING WATER TREATMENT

- This chapter has not been published. The manuscript was sent to NanoImpact, has been reviewed, and re-submitted with corrections. Contributing Authors are Kidd, J., Westerhoff, P., and Maynard, A.
- My author contribution: Approximately 100% of the research and 90% of the text

6.1. Abstract

Incorporating nanomaterials into point-of-use (POU) in-home water purification devices that treat well water or centrally-treated tap water offers new opportunities to meet growing customer demand for aesthetically pleasing and higher quality drinking water. While the technical performance and potential for nanomaterial release from POU devices have been studied, little is known about public acceptance of devices that use nanotechnology. We administered an 18-question survey of 1623 participants in four metropolitan areas—Phoenix, AZ (N=362); Houston, TX (N=380); Atlanta, GA (N=419); and Philadelphia, PA (N=415)—and one rural Arizona region (N=47) to assess perceptions around using nanomaterial-enabled POU devices. Approximately 90% of survey respondents had little to no prior knowledge of nanomaterials or their use in numerous consumer products ranging from POU water treatment devices to clothing or baby products. Survey respondents were more likely to purchase conventional drinking water purification devices than ones containing nanomaterials, but the majority of survey respondents (~64%) claimed they would likely or probably change their opinions around using nanomaterials to treat their drinking water if they were given more information about nanomaterials and

their role in treating drinking water. The results indicate that respondents are willing to change their minds if they are provided information around nanomaterials and their use in in-home water purification. When we incorporated responses regarding previous knowledge of nanomaterials, we found that the less knowledge respondents had of nanomaterials, the more willing they would be to use them to treat their drinking water. 65% of respondents with prior knowledge of nanomaterials were unwilling to drink water treated with nanomaterials. Respondents considered the safety of the device as being most important to them, followed closely by treated water taste. 30% of respondents stated that they would purchase the drinking water purification product with nanomaterials if it worked as effectively as a competitor and was half the price. 26% of respondents stated that they would purchase the drinking water purification product with nanomaterials if it worked twice as effectively as a competitor and was half the price. The findings are discussed in regard to specific adoption of nanotechnology in drinking water and also broader adoption and acceptance of emerging technologies that hold promise to improve environmental outcomes.

6.2. Introduction

Technical, economic, and customer aesthetic preferences are influencing treatment, distribution, and consumption of clean drinking water. Drinking water quality is affected by the emergence of previously un-monitored pollutants.^{1,2} Aging infrastructure^{3,4} is increasing the incidence of lead and copper contamination and is also increasing the presence of potentially harmful disinfection byproducts.^{5,6} Unregulated chemicals that affect taste or odor aesthetics of water influence the public's preference to drink bottled

water or utilize point-of-use (POU) treatment devices (e.g., ion exchange, reverse osmosis, activated carbon) to purify municipal tap water.¹⁻¹¹ In the United States of America (USA), over 40 million people rely on private wells as drinking water supplies,¹² and many of these homes also use POU devices. For several economic and resilience reasons, there is also increasing decentralization of purification technologies in municipal water distribution systems.¹³ In response to these drivers, the POU market for drinking water devices exceeds \$20M annually and is rapidly growing.¹⁴ Added functionality and product differentiation in POU devices are being developed to meet this growing global demand.

Incorporating nanomaterials into POU water purification devices offers new opportunities to advance drinking water treatment.¹⁵⁻²³ Precisely engineered nanomaterials can have physico-chemical properties (e.g., selective pollutant adsorption, catalytic surfaces, ferromagnetism, localized surface plasmon resonance)²³⁻²⁵ that lead to new and efficient drinking water purification processes. This specifically enables the advanced design of membranes,^{26,27} adsorption characteristics,²⁸ electrochemistry,^{29,30} and functionalized surfaces and coatings.³¹ Nanosilver,³² carbon nanotubes,³³ and other engineered nanomaterials^{34,35} are already being used in POU devices. Along with improved treatment of drinking water, additional emphasis has been placed on research projects that evaluate environmental health and nanomaterial safety,¹⁸ including the potential for nanomaterials to leach from devices into receiving waters³⁶ and their potential implications for human health.³⁷ Surveys conducted over a decade ago examined the risks and concerns of nanomaterial-based POU devices. However, the prior surveys focused on the lack of trust between consumers and the government as well as consumer perceptions that

nanomaterial-based POU devices were far from commercialization.³⁸ The social acceptance and concerns associated with nanomaterial-enabled POU devices have not previously been explored, even though nanotechnology has continued to advance over the last decade and consumer perceptions within drinking water communities is a well-studied field.³⁹ The potential economic and societal benefits of nanomaterial-enabled POU devices may not be realized if societal acceptance is not adequately addressed early in the development process.⁴⁰ While the commercialization of nanomaterial-enabled POU devices is strongly influenced by expert opinions regarding their societal acceptability, consumer acceptance ultimately dictates the success or failure of a technology.^{41,42}

We present the results from a consumer survey that explored concerns and acceptance of nanomaterial-enabled POU drinking water purification devices. Our analysis is based on a public survey of 1623 participants in four states in the USA. The study objectives were to (i) determine if consumer demographics are related to perceptions around using nanomaterials in POU devices for water purification, (ii) determine consumer perceptions about their drinking water quality, (iii) determine consumer knowledge of nanomaterials and their perceptions of nanomaterials in POU devices for water purification, and (iv) compare consumer perceptions of nanomaterial-based POU water purification devices to conventional POU water purification devices. Navigating the landscape around consumer acceptances and nanotechnology barriers is complex and answering these objectives provide one potential explanation to these concerns and barriers, We discuss findings in regard to specific adoption of nanotechnology in drinking

water and also broader adoption and acceptance of emerging technologies that hold promise to improve environmental outcomes.

6.3. Methods

6.3.1. Study Design and Sample Population

This study used an 18-question survey to explore public perceptions of and attitudes toward nanomaterial-based POU water treatment devices. The survey was conducted via an online survey platform⁴⁴ across four cities (Phoenix, AZ; Houston, TX; Atlanta, GA; and Philadelphia, PA) and one rural region (Northern Arizona) in the USA between July 1st and July 15th, 2018. Surveys were deployed by Survey Sampling International (SSI, headquartered in Shelton, CT). SSI's "open-door" sourcing obtains its sample from panels, social media, online communities, and affiliate partners. SSI ensures data integrity through timestamps to flag "speeders" and quality control questions to identify inattention. Data authentication occurs through several steps, including digital fingerprinting and matches against third-party databases.

A total of 1623 fully completed responses were collected: 362 responses were from Phoenix, AZ (pop.~4.8M), 380 from Houston, TX (pop.~6.9M), 419 from Atlanta, GA (pop.~5.9M), 415 from Philadelphia, PA (pop.~6.1M), and 47 from rural Northern Arizona (pop.~350K). These regions were selected to represent different climate zones and water resource availabilities.⁴⁵ Rural northern Arizona was predetermined as an area of interest for one of the geographical regions we surveyed due to smaller populations and historically different drinking water sources than urban regions. Survey respondent locations were determined by postal code. Responses with a postal code located outside the five regions

of interest were discarded from the study. To ensure anonymity, respondents were given a unique identification number when completing the survey. Institutional Review Board approval was received from the Office of Research Integrity and Assurance at Arizona State University.

6.3.2. Survey Design

The survey, which is provided in its entirety in the supplemental information, contained 18 questions that were separated into three sections. The first section asked six demographic questions, which were multiple choice close-ended questions with an option for “other” that included a free-response box. The second section asked three questions to assess the respondent’s satisfaction with drinking water quality. Two of the questions were multiple choice close-ended questions, and the third question used a Likert scale. The third section contained nine questions addressing nanomaterials and their applications in drinking water technologies. Five questions were multiple choice close-ended questions, and four questions were Likert scale questions. The survey was designed to target populations that would have the ability to purchase a POU drinking water purification device and as such, survey restrictions were placed so that survey takers were 18 years of age or older and were not incarcerated. The survey construction was pre-tested using a population of 30 undergraduate engineering students at Arizona State University before sent to SSI for distribution.

6.3.3. Survey Analysis

After the survey was completed, the data was transferred to a secure server and analyzed using the XLSTAT add-on on to Microsoft Excel 2016. Descriptive statistical analysis

occurred using ANOVA followed by a post hoc chi-square test. For Likert scale questions, a Mann Whitney U test was conducted. For all analyses, the level of significance was set at 5% ($p < 0.05$).

6.4. Results and Discussion

6.4.1. Response Rates and Respondent Demographics

Of the 1928 surveys that were submitted, a total of 1623 fully completed surveys were returned and analyzed. The 305 surveys that were not fully completed were discarded from the study. Table S1 shows the respondent demographics. We attempted to represent all demographics; however, there are some inconsistencies in the data set. The majority of respondents' age was in the 26 to 35 range (52% of sample population). The median household size was 2-3 people. There was an under-representation of respondents over the age of 65 (~ 1% of sample population) and respondents living in the rural northern Arizona (~3% of the sample population). There was an over-representation of homeowners (~54% of sample population). The majority of respondents (~52%) had an annual income below \$55,000, and the majority of respondents (>52%) also had less than an associate degree.

We looked at the regional locations of survey respondents and compared the average responses of each region for each survey question (Table S2). When asked "What is your level of satisfaction with the quality of your drinking water?", the respondents from rural northern Arizona were less satisfied with their drinking water than the other regions ($p=0.02$). When asked "How familiar are you with nanomaterials?", the respondents from rural northern Arizona had less average knowledge of nanomaterials than the other regions ($p=0.01$). When asked "Are you aware that some consumer products that include food,

cosmetics, and medicine contained nanomaterials?”, respondents from rural northern Arizona had less average awareness that those products contained nanomaterials than the other regions ($p=0.03$). When asked “Please rank the following technologies contained within in-home water purification devices in terms of how likely you are to select them to treat your drinking water.”, respondents from rural northern Arizona and Phoenix (Metro) regions were more likely to use reverse osmosis technologies than the other three regions ($p=1.00E-3$).

Respondents were given a list of 14 common drinking water contaminants and were asked “which drinking water contaminants are of most concern to you?”. There were no significant differences in responses from the different regions for the following contaminants: chromium, fluoride, salt, disinfection by-products, viruses, and bacteria. When asked about the color of water ($p=0.01$) and the taste of water ($p=1.00E-3$), Phoenix (Metro) and Houston (Metro) were more concerned than the other regions. When asked about the hardness of water ($p=1.91E-11$), nitrate ($p=0.02$), and arsenic ($p=0.03$), Phoenix (Metro) was more concerned than the other regions. When asked about the odor of water ($p=0.02$), Philadelphia (Metro) was less concerned than the other regions. When asked about pesticides ($p=0.01$) and pharmaceuticals ($p=0.05$), rural northern Arizona was less concerned than the other regions. For all other survey questions, we found no significant differences between respondents from different geographical regions.

6.4.2. Respondent Perceptions on Their Drinking Water Quality

Survey respondents were asked “Where do you typically get your drinking water from?”. Survey respondents selected all sources from which they obtain their drinking water, with the following results:

Bottled Water	Tap Water	Bottled Water and Tap Water	Private Well	Water Vendor
(41%)	> (28%)	> (17%)	> (4%)	> (2%)

The remaining 8% of respondents selected a combination of answers (e.g., tap water and water vendor or private well and bottled water). When asked about their level of satisfaction with their drinking water, 82% of respondents who drink only water from a vendor were satisfied with their water, 77% of respondents who drink only bottled water were satisfied with their water, and 71% of respondents who drink only tap water were satisfied with their water. Additionally, of those using only tap water, 11% were unsatisfied with their drinking water, which is the highest percentage among all drinking water sources.

Respondents were presented with a list of 14 of the U.S. Environmental Protection Agency (EPA) national primary drinking water regulations (NPDWRs) table of contaminants⁴⁷ and were asked to rate their level of concern for each contaminant. Figure 6-1 compares the level of concern of these 14 drinking water contaminants between respondents who drink bottled water versus those who drink tap water. Both groups identified bacteria, pesticides, the taste of water, and disinfection by-products as the four

most concerning contaminants. The level of concern for the remaining 10 drinking water contaminants varied for both groups. When we directly compared each group's level of concern for each contaminant, we found that respondents who drink bottled water were more concerned than those who drink tap water for all 14 drinking water contaminants. This corresponds with prior research where it was found that drinking water behaviors can be correlated with negative consumer-perceptions around chemicals being present in tap water⁴⁸⁻⁵² and mistrust in water suppliers supplying tap water.⁵³⁻⁵⁵

Previous research has also explored the relationship between drinking water consumption behaviors and economic factors (e.g., costs) and found higher incomes and living in urban areas are positively correlated with drinking bottled water.⁵⁶⁻⁵⁸ However, the results from our study did not match previous findings. We compared the average annual income of survey respondents from the five geographical locations (Figure S1) and found that there was a lower average annual income for respondents living in rural northern Arizona. When we compared drinking water source with average annual income, we found that for each income bracket below \$90,000 per year, there was a higher percentage of respondents who drink bottled water only than tap water only (Figure 6-2). For each income bracket above \$90,000 per year, there was a higher percentage of respondents who drink tap water only. When we compared drinking water sources with regional location, we found a higher percentage of respondents who drinking water from private wells in rural Arizona (~ 46%) compared to 13–20% from private wells in the four cities, and a lower percentage of respondents who drink bottled water (~33% in rural Arizona compared to 35-54% in the four cities) (Figure S1).

6.4.3. Public Knowledge of Nanomaterials and Their Use in Consumer Products

Based on our data, prior knowledge of nanomaterials factors into respondent concern of using nanomaterials in different consumer products. When respondents were asked about their familiarity with nanomaterials (Table S2), the majority of respondents (~53%) had never heard of nanomaterials while an additional 37% of respondents had heard of the term “nanomaterial” but either did not know or could not remember what it was. Thus, a combined 90% of respondents had little to no prior knowledge of nanomaterials and their use in consumer products.

Respondents were then asked if they were aware that some consumer products (e.g., food, cosmetics, medicine) contained nanomaterials. 50% of respondents stated they had no knowledge of nanomaterial use in the consumer products listed. 26% of respondents stated they knew that nanomaterials were in some of the consumer products listed. 13% of respondents stated they knew that nanomaterials were used in most of the consumer products listed. 11% of respondents stated they knew that nanomaterials were in all of the consumer products listed.

Figure 6-3 summarizes the concerns regarding nanomaterial use in different consumer products, which may be potentially harmful to the health of people who use them. The results indicate that the likelihood for nanomaterials to be ingested or exposure to sensitive populations (e.g., direct oral consumption, children) has a higher concern. Drinking water purification devices are most concerning for respondents, followed by baby products, food, and medicine. Cosmetics, clothing, and electronics were the least concerning products to respondents.

Respondents were then asked to indicate if they would use in-home water purification devices that use nanomaterials to treat their drinking water (Table 6-1). 23% of respondents stated they would not want to drink water treated with nanomaterials, 20% of respondents were hesitant, 42% of respondents were unsure, 9% of respondents were willing, but had reservations, and 7% of respondents were ready to drink water treated with nanomaterials. When we assessed these results in combination with responses about previous knowledge of nanomaterials, we found that the less knowledge respondents had of nanomaterials, the more willing they would be to drink water treated using them. Only 10% of respondents who had no prior knowledge of nanomaterials (53%, n=867) were unwilling to drink water treated with nanomaterials. Alternatively, 65% of respondents with prior knowledge of nanomaterials (47%, n=756) were unwilling to drink water treated with nanomaterials.

These results highlight that (i) nearly 90% of all respondents had little knowledge or had never heard of nanomaterials before, which means that their decision-making towards the use of nanomaterials to treat drinking water is likely a result of a number of different factors undetermined in this survey, (ii) responder concerns around nanomaterials in consumer products were similar regardless of their prior knowledge of nanomaterials, (iii) respondents were more concerned about nanomaterials if they could be ingested or come in contact with sensitive populations (e.g., oral consumption, children), and (iv) respondents were more concerned about using nanomaterials to treat drinking water than other consumer products, meaning that additional effort may be needed to ensure the safety of these water purification devices.

6.4.4. Public Perceptions of Nanotechnology Versus Conventional Water Purification Products

Respondents were asked what information they want before purchasing a drinking water purification device that uses nanomaterials to treat drinking water (Table S3). 13% of respondents stated they needed no additional information, 18% of respondents wanted more information on the use and benefits of nanomaterials in the device, 15% of respondents wanted more information on the potential risks of nanomaterials in the device, 7% of respondents wanted more information on how the nanomaterial-based device compares to other technologies, 5% of respondents wanted a certification of safety from the manufacturer, and 4% of respondents wanted a certification of safety from an independent organization. Additionally, 9% of respondents stated that they want all of the above, and 29% of respondents wanted a combination of two or more; although, no individual combination was greater than 4% of respondents.

Respondents were asked which specific features of an in-home water purification device that uses nanomaterials were most important to them. As shown in Figure 6-4, respondents identified device safety as being most important, followed closely by treated water taste. These two qualities were followed by treated water appearance, device price, whether the device operates without electricity, and device size/weight.

Respondents were asked to select from a series of conventional in-home water purification devices and determine how likely they would be to use the devices to treat their drinking water. As shown in Figure 6-5, respondents were most likely to use an in-home water purification device that utilizes natural solar light. This was followed closely

by reverse osmosis and activated carbon/charcoal. Respondents were least likely to use nanotechnology compared to alternative in-home water purification devices; however, nanotechnology had the least amount of responses for “highly unlikely” and had one of the highest number of responses for “neutral” compared to the other technologies.

Respondents were asked under which circumstances they would likely purchase an in-home water purification device that contained nanomaterials if available for purchase (Figure 6-6A). 30% of respondents stated that they would purchase the drinking water purification product with nanomaterials if it worked as effectively as a competitor and was half the price. 26% of respondents stated that they would purchase the drinking water purification product with nanomaterials if it worked twice as effectively as a competitor and was half the price. 15% of respondents stated that they would purchase the drinking water purification product with nanomaterials if it worked twice as effectively as a competitor and was the same price. 13% of respondents stated that they would purchase the drinking water purification product with nanomaterials if it worked as effectively as a competitor and was the same price. 16% of respondents stated that they would choose a competing product over one containing nanomaterials regardless of the efficiency or price.

Finally, respondents were asked if they believed their opinion of in-home water purification devices would change if they had more information on nanomaterials and their role in treating drinking water. As shown in Figure 6-6B, 31% of respondents replied, “definitely yes”, 33% of respondents replied, “probably yes”, 32% of respondents replied, “might or might not”, 3% of respondents replied, “probably not”, and 2% of respondents replied, “definitely not”. The results from this question indicate that respondents are willing

to change their minds if they are provided information around nanomaterials and their use in in-home water purification. However, these results contradict our findings in the previous section where 65% of respondents with prior knowledge of nanomaterials were unwilling to drink water treated with nanomaterials, while only 10% of respondents who had no prior knowledge of nanomaterials were unwilling to drink water treated with nanomaterials. These contradictions in responses indicate that consumer decisions to purchase nanomaterial-enabled POU devices to treat their drinking water may not be as simple as understanding what contaminants are concerning to them or how much knowledge they have about nanomaterials. There may be a complex combination of different factors that ultimately lead to a decision to purchase or not purchase these devices.

6.5.Conclusion

This study indicated that there are many consumer-related concerns around the use of nanomaterials within in-home water purification devices. Approximately 90% of respondents had little to no prior knowledge of nanomaterials or their use in consumer products. Secondly, the majority of respondents we surveyed use bottled water and are generally satisfied with their drinking water. Thirdly, respondents were more concerned about nanomaterials for applications where there is a higher potential for direct contact and exposure (e.g., baby products, food, drinking water purification).

While survey respondents indicated they had concern about the use of nanomaterials to treat drinking water, the majority of respondents indicated that if given more information about nanomaterials and their use in these products they would likely change their opinion on using nanomaterials to treat their drinking water if given more

information before purchasing the device. This suggests that nanomaterial-enabled POU water purification technologies have a place within the consumer market if specific concerns and barriers are addressed. One possibility is that if manufacturers provide more information about nanomaterial use along with information about potential nanomaterial benefits and risks, some consumer concerns over nanomaterial-enabled POU water purification technologies may be alleviated. However, there are studies with mixed reactions regarding educating the public on nanotechnology and whether or not it may not be the best mechanism to enhance adoption and acceptance^{58,59}. Alternatively, focusing efforts on reducing the costs and increasing the efficiency of these devices would support consumer acceptance. This study shows there are opportunities for manufacturers of nanomaterial-enabled POU water purification technologies to build trust with consumers by better understanding and responding to their concerns and hopes, while avoiding decisions that depend solely on assumptions of consumer behavior.

While this paper focused on use of nanotechnology in POU drinking water treatment, the results illustrated more broadly the public's knowledge of and willingness to use emerging technologies. Previous examples such as biotechnology (e.g., genetically modified organisms) demonstrate how public perceptions influence acceptance and regulation of new technologies within different parts of society (e.g., USA versus European Union), despite availability of the same scientific data on efficacy, risks, and ability to achieve broader societal goals (e.g., feeding a growing global population). Other emerging technologies (e.g., artificial intelligence, autonomous vehicles) could likely have environmental benefits, and presumably similar patterns in public knowledge and

acceptance exist as observed herein with nanotechnology. Specifically, the public likely knows little about the actual technology, and may express concern about the technology, but they would be more willing to accept the technology if they had more knowledge or if the technology had independent third-party validation. Thus, public surveys such as this play an important role in benchmarking society's acceptance of new technologies that have the potential to help protect human health.

6.6.Acknowledgements

This research was funded by the National Science Foundation through the Nanosystems Engineering Research Center for Nanotechnology-Enabled Water Treatment (EEC 1449500). Laurel Passantino provided technical editing.

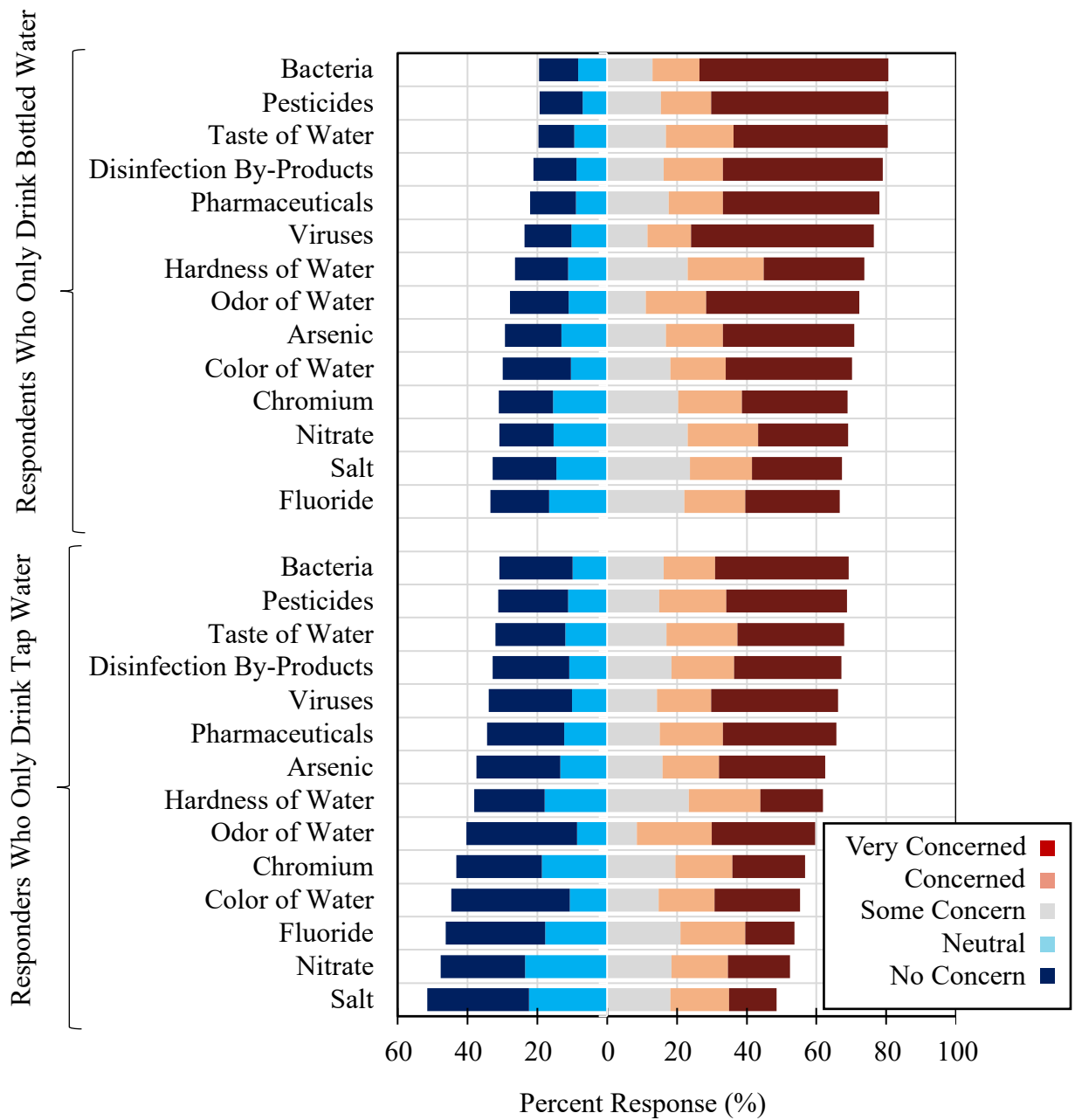


Figure 6-1. Survey respondent perceptions of fourteen common drinking water contaminants: a comparison between bottled water drinkers and tap water drinkers.

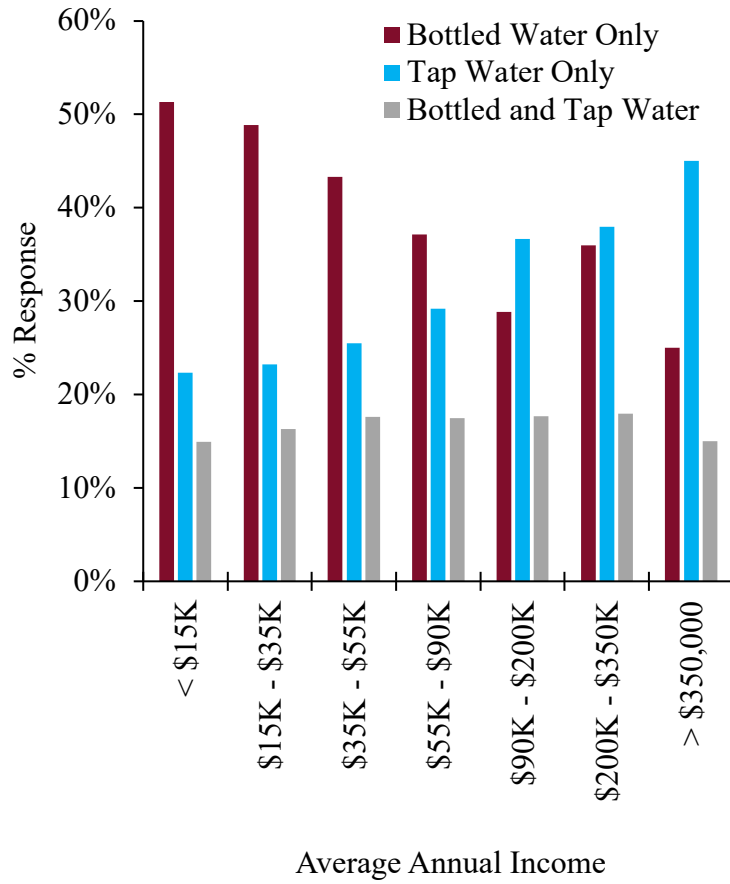


Figure 6-2. Survey respondent drinking water source by average annual income

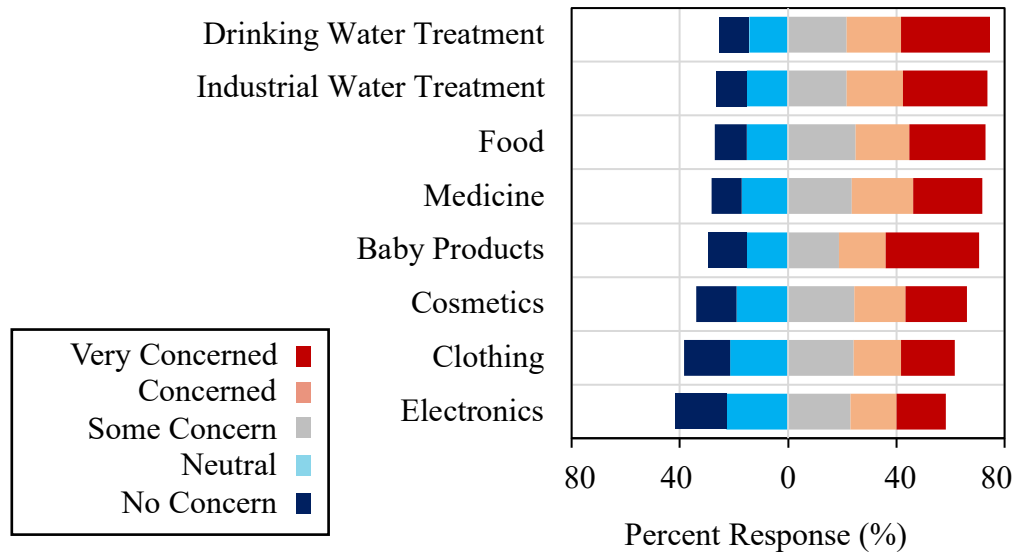


Figure 6-3. Percent response of respondent concerns towards the use of nanomaterials in various consumer products

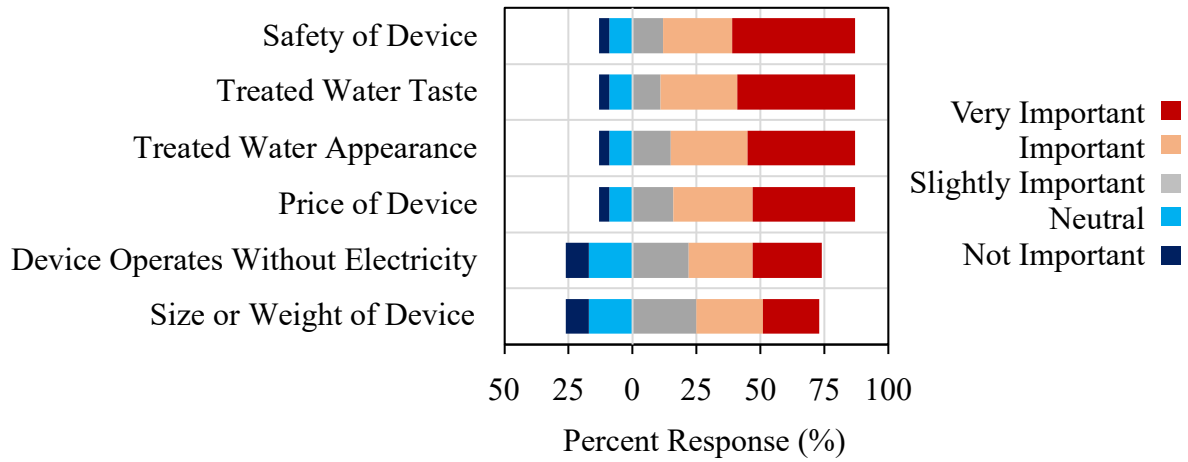


Figure 6-4. Respondents’ views on the importance of specific features of in-home water purification devices using nanomaterials

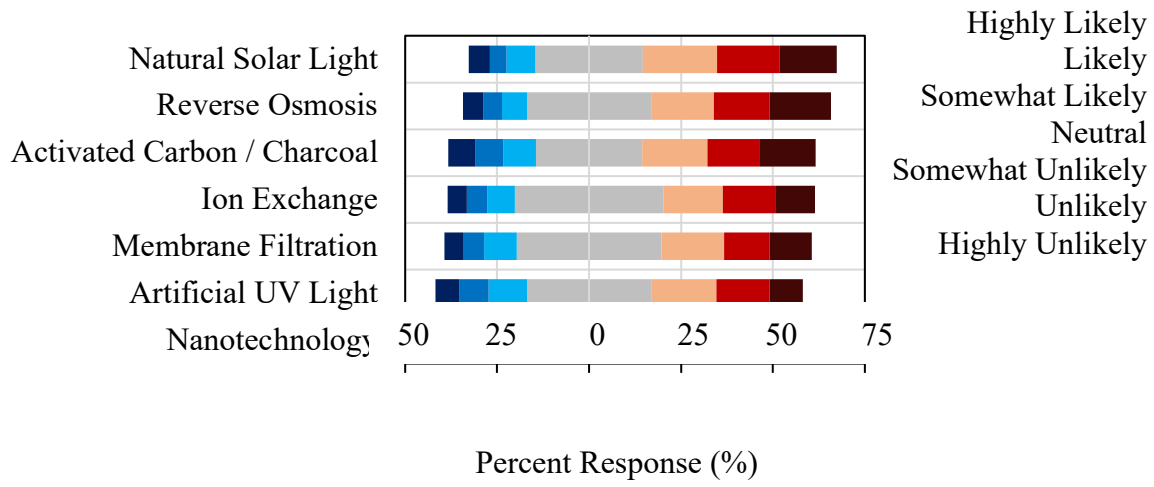


Figure 6-5. Respondents’ views on the likelihood they would purchase each in-home water purification device to treat their drinking water

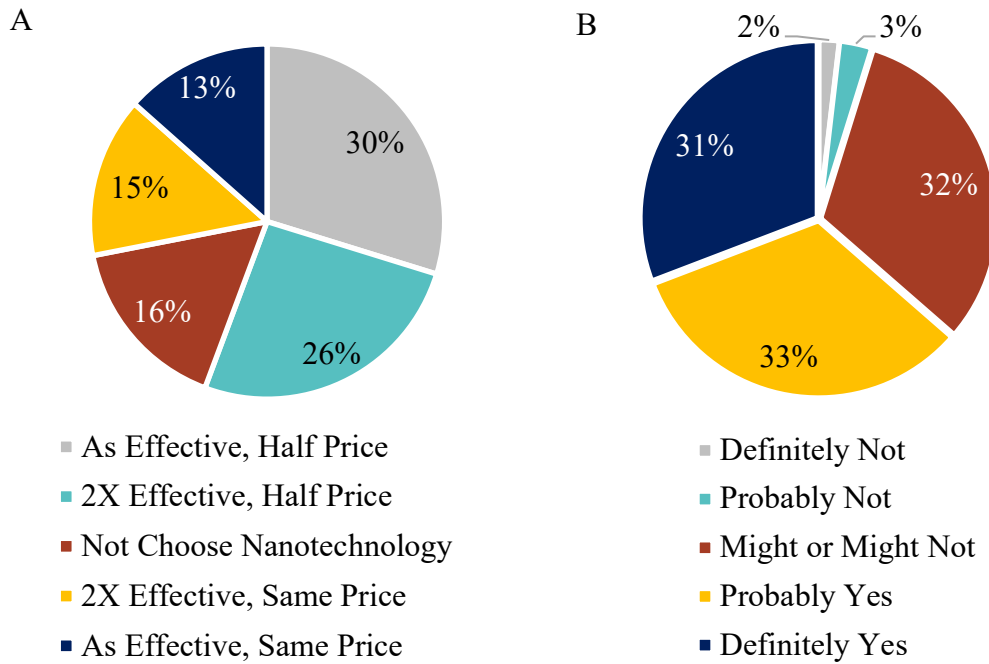


Figure 6-6. Respondents' answers to (a) circumstances (efficiency and price of device) where they would purchase a drinking water purification device that uses nanomaterials and (b) if their opinion on the use of in-home water purification devices that use nanomaterials to treat drinking water would change if they had more information on nanomaterials and their role in treating drinking water.

Table 6-1. Comparing survey responses of bottled water drinkers and tap water drinkers to whether they would use in-home water purification devices that use nanomaterials to treat their drinking water

Response	Responses (Bottled Water Only)	Responses (Tap Water Only)
I would not want to drink water treated with nanomaterials	227 (29%)	104 (20%)
I am hesitant about drinking water treated with nanomaterials	162 (20%)	91 (17%)
I am unsure about drinking water treated with nanomaterials	296 (37%)	249 (47%)
I am willing to drink water treated with nanomaterials, but have some reservations	75 (10%)	56 (11%)
I am ready to drink water treated with nanomaterials	33 (4%)	29 (5%)

6.7. Supplemental Information

Public Water Survey Questionnaire:

Question One: What is your age?

- Less than 18
- 18 – 25
- 26 – 35
- 36 – 45
- 46 – 55
- 56 – 65
- More than 65

Question Two: What is the 5-digit zip code of your current place of residence?

Question Three: Including yourself, how many people currently live in your household?

- 1
- 2 – 3
- 4 – 5
- 6 – 7
- More than 7

Question Four: What was the approximate annual income from employment and all other sources for all members of your household last year, before taxes?

- Less than \$15,000
- \$15,000 - \$35,000
- \$35,000 - \$55,000
- \$55,000 - \$90,000
- \$90,000 - \$200,000
- \$200,000 - \$350,000
- More than \$350,000

Question Five: What is the highest degree or level of school you have completed? (If you're currently enrolled in school, please indicate the highest degree you have received)

- Less than a high school diploma
- High school diploma or equivalent (e.g. GED)
- Some college, no degree
- Associate degree (e.g. AA, AS)
- Bachelor's degree (e.g. BA, BS)

- Master's degree (e.g. MA, MS, MEd)
- Professional degree (e.g. MD, DDS, DVM)
- Doctoral degree (e.g. PhD, EdD)

Question Six: Which of the following best describes your current housing status?

- Homeowner
- Renting a Home
- Renting an Apartment
- Living with Parents / Family
- Other, Please Specify: _____

Question Seven: Where do you typically get your drinking water from? Select all that apply:

- Tap water from your city
- Bottled water
- Water from a vendor (e.g. water delivery by company)
- Private well at your home
- Other, Please Specify: _____

Question Eight: What is your level of satisfaction with the quality of your drinking water?

- Extremely Satisfied
- Satisfied
- Neither Satisfied nor Dissatisfied
- Dissatisfied
- Extremely Dissatisfied

Question Nine: Which drinking water contaminants are of most concern to you?

	No Concern	Neutral	Some Concern	Concerned	Very Concerned
Color of water	<input type="radio"/>	<input type="radio"/>	<input type="radio"/>	<input type="radio"/>	<input type="radio"/>
Odor of water	<input type="radio"/>	<input type="radio"/>	<input type="radio"/>	<input type="radio"/>	<input type="radio"/>
Taste of water	<input type="radio"/>	<input type="radio"/>	<input type="radio"/>	<input type="radio"/>	<input type="radio"/>
Hardness of water	<input type="radio"/>	<input type="radio"/>	<input type="radio"/>	<input type="radio"/>	<input type="radio"/>
Nitrate	<input type="radio"/>	<input type="radio"/>	<input type="radio"/>	<input type="radio"/>	<input type="radio"/>
Arsenic	<input type="radio"/>	<input type="radio"/>	<input type="radio"/>	<input type="radio"/>	<input type="radio"/>
Chromium	<input type="radio"/>	<input type="radio"/>	<input type="radio"/>	<input type="radio"/>	<input type="radio"/>
Fluoride	<input type="radio"/>	<input type="radio"/>	<input type="radio"/>	<input type="radio"/>	<input type="radio"/>
Salt	<input type="radio"/>	<input type="radio"/>	<input type="radio"/>	<input type="radio"/>	<input type="radio"/>
Viruses	<input type="radio"/>	<input type="radio"/>	<input type="radio"/>	<input type="radio"/>	<input type="radio"/>
Bacteria	<input type="radio"/>	<input type="radio"/>	<input type="radio"/>	<input type="radio"/>	<input type="radio"/>
Disinfection By-Products	<input type="radio"/>	<input type="radio"/>	<input type="radio"/>	<input type="radio"/>	<input type="radio"/>
Pesticides	<input type="radio"/>	<input type="radio"/>	<input type="radio"/>	<input type="radio"/>	<input type="radio"/>
Pharmaceuticals	<input type="radio"/>	<input type="radio"/>	<input type="radio"/>	<input type="radio"/>	<input type="radio"/>

Question Ten: How familiar are you with nanomaterials?

- I have never heard of nanomaterials
- I have heard of nanomaterials, but don't remember what they are
- I have some idea of what nanomaterials are
- I know what nanomaterials are but don't understand their applications
- I know what nanomaterials are and understand their applications

Question Eleven: Are you aware that some consumer products that include food, cosmetics, and medicine contained nanomaterials?

- I had no previous knowledge
- I know that some of those products contain nanomaterials
- I know that most of those products contain nanomaterials
- I know that all those products contain nanomaterials

Question Twelve: Indicate your level of concern that nanomaterials in the following consumer products may be potentially harmful to the health of people who use them:

	Not at All	Neutral	Some Concern	Concerned	Very Concerned
Food	<input type="radio"/>	<input type="radio"/>	<input type="radio"/>	<input type="radio"/>	<input type="radio"/>
Medicine	<input type="radio"/>	<input type="radio"/>	<input type="radio"/>	<input type="radio"/>	<input type="radio"/>
Cosmetics	<input type="radio"/>	<input type="radio"/>	<input type="radio"/>	<input type="radio"/>	<input type="radio"/>
Clothing	<input type="radio"/>	<input type="radio"/>	<input type="radio"/>	<input type="radio"/>	<input type="radio"/>
Baby Products	<input type="radio"/>	<input type="radio"/>	<input type="radio"/>	<input type="radio"/>	<input type="radio"/>
Electronics	<input type="radio"/>	<input type="radio"/>	<input type="radio"/>	<input type="radio"/>	<input type="radio"/>
Drinking Water Treatment	<input type="radio"/>	<input type="radio"/>	<input type="radio"/>	<input type="radio"/>	<input type="radio"/>
Industrial Water Treatment	<input type="radio"/>	<input type="radio"/>	<input type="radio"/>	<input type="radio"/>	<input type="radio"/>

Question Thirteen: In-home water purification devices are devices under your sink, in a pitcher, in a refrigerator, and in your garage that further purify your drinking water. In your opinion, would you use in-home water purification devices that use nanomaterials to treat your drinking water?

- I would not want to drink water treated with nanomaterials
- I am hesitant about drinking water treated with nanomaterials
- I am unsure about drinking water treated with nanomaterials
- I am willing to drink water treated with nanomaterials, but have some reservations
- I am ready to drink water treated with nanomaterials

Question Fourteen: If you were to purchase an in-home water purification device that uses nanomaterials to treat drinking water, what information would you need before making that decision? Check all that apply:

- No need for additional information

- More information on the use and benefits of nanomaterials in the device
- Information on the potential risks of nanomaterials in the device
- Information on how the nanomaterial-based device compares to other technologies
- A certification of safety from the manufacturer
- A certification of safety from an independent organization
- Other, please specify: _____

Question Fifteen: Please rank the following qualities in terms of importance in an in-home water purification device that uses nanomaterials:

	Not Important	Neutral	Slightly Important	Important	Very Important
Safety of Device	<input type="radio"/>	<input type="radio"/>	<input type="radio"/>	<input type="radio"/>	<input type="radio"/>
Treated Water Taste	<input type="radio"/>	<input type="radio"/>	<input type="radio"/>	<input type="radio"/>	<input type="radio"/>
Treated Water Appearance	<input type="radio"/>	<input type="radio"/>	<input type="radio"/>	<input type="radio"/>	<input type="radio"/>
Size / Weight of Device	<input type="radio"/>	<input type="radio"/>	<input type="radio"/>	<input type="radio"/>	<input type="radio"/>
Device Operates Without Electricity	<input type="radio"/>	<input type="radio"/>	<input type="radio"/>	<input type="radio"/>	<input type="radio"/>
Price of Device	<input type="radio"/>	<input type="radio"/>	<input type="radio"/>	<input type="radio"/>	<input type="radio"/>

Question Sixteen: Please rank the following technologies contained within in-home water purification devices in terms of how likely you are to select them to treat your drinking water:

	Highly Unlikely	Unlikely	Somewhat Unlikely	Neutral	Somewhat Likely	Likely	Highly Likely
Activated Carbon / Charcoal	<input type="radio"/>	<input type="radio"/>	<input type="radio"/>	<input type="radio"/>	<input type="radio"/>	<input type="radio"/>	<input type="radio"/>
Artificial Ultraviolet Light	<input type="radio"/>	<input type="radio"/>	<input type="radio"/>	<input type="radio"/>	<input type="radio"/>	<input type="radio"/>	<input type="radio"/>
Natural Solar Light	<input type="radio"/>	<input type="radio"/>	<input type="radio"/>	<input type="radio"/>	<input type="radio"/>	<input type="radio"/>	<input type="radio"/>
Nanotechnology	<input type="radio"/>	<input type="radio"/>	<input type="radio"/>	<input type="radio"/>	<input type="radio"/>	<input type="radio"/>	<input type="radio"/>
Reverse Osmosis	<input type="radio"/>	<input type="radio"/>	<input type="radio"/>	<input type="radio"/>	<input type="radio"/>	<input type="radio"/>	<input type="radio"/>
Ion Exchange	<input type="radio"/>	<input type="radio"/>	<input type="radio"/>	<input type="radio"/>	<input type="radio"/>	<input type="radio"/>	<input type="radio"/>
Membrane Filtration	<input type="radio"/>	<input type="radio"/>	<input type="radio"/>	<input type="radio"/>	<input type="radio"/>	<input type="radio"/>	<input type="radio"/>

Question Seventeen: If in-home water purification devices that contained nanomaterials were available for purchase for treating drinking water, under which circumstance would you likely purchase one?

- The product with nanomaterials works as effectively as its competitor but is half the price
- The product with nanomaterials works twice as effectively as its competitor but is half the price
- The product with nanomaterials works twice as effectively as its competitor but is the same price
- The product with nanomaterials works as effectively as its competitor but is the same price

- I would choose a competing product over one containing nanomaterials regardless of the price or efficiency

Question Eighteen: Do you think that your opinion of in-home water purification devices that use nanomaterials to treat drinking water would change if you had more information on nanomaterials and their role in treating drinking water?

- Definitely yes
- Probably yes
- Might or might not
- Probably not
- Definitely not

Table S1. Demographics of Survey Respondents.

Regional Location		Home Ownership		Household Size	
Location	Response	Status	Response	Number of Residents	Response
Rural Northern Arizona	47 (3%)	Homeowner	885 (54%)	1	233 (14%)
Phoenix (Metro)	362 (22%)	Renting a Home	330 (20%)	2-3	839 (52%)
Houston (Metro)	380 (23%)	Renting an Apartment	317 (20%)	4-5	464 (28%)
Atlanta (Metro)	419 (26%)	Living with Parents/Family	57 (4%)	6-7	74 (5%)
Philadelphia (Metro)	415 (26%)	Other	34 (2%)	More than 7	13 (1%)

Annual Income		Education Level		Age	
Income	Response	Level	Response	Age Range	Response
Less than \$15,000	193 (12%)	Less than a high school diploma	70 (4%)	18-25	347 (21%)
\$15,000 - \$35,000	319 (20%)	High school diploma or equivalent	354 (22%)	26-35	541 (33%)
\$35,000 - \$55,000	310 (19%)	Some college, no degree	415 (26%)	36-45	255 (16%)
\$55,000 - \$90,000	451 (28%)	Associate's degree	180 (11%)	46-55	217 (13%)
\$90,000 - \$200,000	303 (18%)	Bachelor's degree	387 (24%)	56-65	256 (16%)
\$200,000 - \$350,000	32 (2%)	Master's degree	148 (9%)	65 and Older	7 (1%)
More than \$350,000	15 (1%)	Professional degree	34 (2%)		
		Doctoral degree	35 (2%)		

Table S3. Survey Responder Prior Knowledge of Nanomaterials

Response	Responses	Percentage
I have never heard of nanomaterials	867	53%
I have heard of nanomaterials, but don't remember what they are	293	18%
I have some idea of what nanomaterials are	310	19%
I know what nanomaterials are but don't know their applications	91	6%
I know what nanomaterials are and understand their applications	62	4%

Table S4. Information consumers want before purchasing a drinking water treatment device that uses nanomaterials to treat drinking water

- A No need for additional information
- B More information on the use and benefits of nanomaterials in the device
- C Information on the potential risks of nanomaterials in the device
- D Information on how the nanomaterial-based device compares to other technologies
- E A certification of safety from the manufacturer
- F A certification of safety from an independent organization

	A	B	C	D	E	F					
Number	219	302	242	121	79	66					
Percentage	13%	19%	15%	7%	5%	4%					
	BC	BD	BE	BF	CD	CE	CF	DE	DF	EF	
Number	67	5	10	6	26	13	15	16	6	14	
Percentage	4%	0%	1%	0%	2%	1%	1%	1%	0%	1%	
	BCD	BCE	BCF	BDE	BD	BE	CD	CD	CE	DE	
Number	62	21	27	2	6	2	5	10	14	9	
Percentage	4%	1%	2%	0%	0%	0%	0%	1%	1%	1%	
	BCDE	BCD	BDE	CDE							
Number	35	54	2	14							
Percentage	2%	3%	0%	1%							
	BCDE										
Number	153										
Percentage	9%										

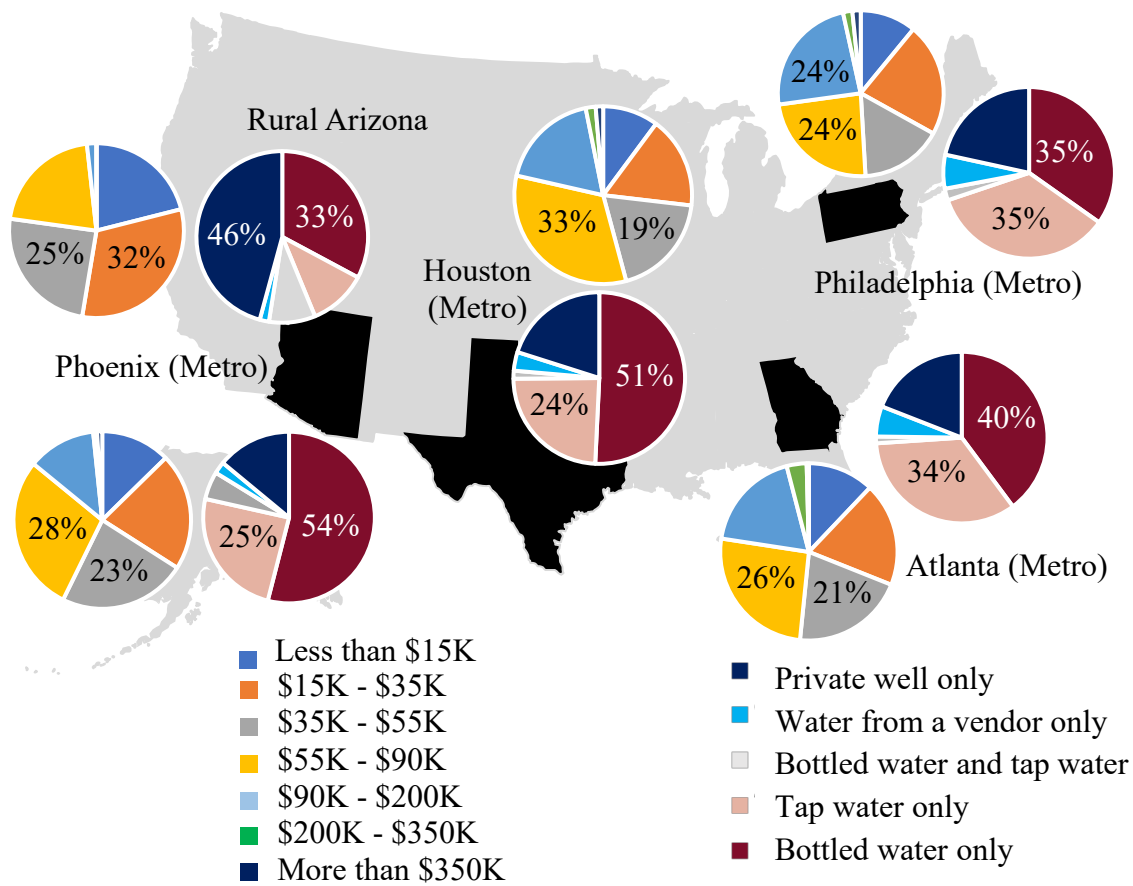


Figure S1. Drinking Water Source by Regional Location

CHAPTER 7: SOCIETAL PERCEPTIONS OF NANO: ARE INDUSTRIAL PERCEPTIONS FOR DRINKING WATER TREATMENT

NANOTECHNOLOGIES VALIDATED BY PUBLIC PERCEPTIONS?

- This chapter has not been published. The manuscript will be sent to NanoImpact once Chapter 9 has been accepted by reviewers. Contributing Authors are Kidd, J., Westerhoff, P., and Maynard, A.
- My author contribution: Approximately 100% of the research and 90% of the text

7.1. Abstract

Incorporating nanomaterials into point-of-use (POU) in-home water purification devices that treat well water or centrally-treated tap water is of importance to industry as they attempt to meet growing customer demand for higher quality drinking water. Due to lack of regulation of nanomaterials and public uncertainties around nanomaterials, little is known about industry perceived barriers towards bringing nanomaterial-enabled POU drinking water purification devices successfully to market. We administered a 14-question survey of 65 participants from different US-based industrial companies focused on drinking water purification. Results from the industry survey show that the major concern for industry are costs and public perceptions of nanomaterial-enabled POU devices for drinking water purification. Cost-specific barriers are conventional competing technologies and operational versus capital costs. When asked about ensuring safety of nanomaterial-enabled POU devices for drinking water treatment, 49% of respondents stated that governmental regulation of nanomaterials would be the preferred approach to ensure public safety, followed by the certification of POU devices (28%). Additionally, 57% of industry survey respondents were concerned or very concerned that public

perceptions will influence the long-term viability of nanomaterial-enabled POU devices for drinking water purification. When asked about specific nanomaterials and their potential use in POU devices for drinking water purification, industry survey respondents believe that nanomaterials with high concern for environmental health and safety (e.g. CNTs, Ag) are least likely to be accepted by the public for used in POU devices, with the exception of TiO₂ which was viewed as both a concern for environmental health and safety and public acceptance. Industry concerns and public concerns were compared to determine synergies and disconnects between both stakeholders. Both stakeholders are concerned about the safety of nanomaterial-enabled POU devices, but industry respondents prefer governmental oversight while public respondents prefer more information about nanomaterials. Additionally, public perceptions will influence long-term viability of nanomaterial-enabled POU devices, but ensuring that more information about nanomaterials is provided for the public or ensuring that devices are either more efficient or cost less than conventional competing technologies will likely allow for industry to overcome public concerns and ensure successful implementation of nanomaterial-enabled POU devices for drinking water purification. The findings are discussed in regard to specific adoption of nanotechnology in drinking water and also broader adoption and acceptance of emerging technologies that hold promise to improve environmental outcomes.

7.2. Introduction

Access to safe and readily-available drinking water is considered a basic human right. Yet, aging infrastructure, contaminated source waters, and low economic status of many

communities worldwide puts a heavy burden on global water systems to ensure safe drinking water. As of 2015, over 2 billion people worldwide relied on unmanaged drinking water services including over 500 million people collecting drinking water from unprotected wells and springs or untreated surface water intakes from lakes, rivers, and streams [WHO 2018]. To manage aging infrastructure and failing processes, tailored treatment approaches can offer benefits and relieve pressure for these

global water systems. Typical drinking water facilities rely on a variety of unit processes to handle a multitude of drinking water contaminants, specifically coagulation and sedimentation for turbidity, membranes and aeration for dissolved inorganics, filtration and disinfection for pathogens, and adsorption for dissolved organics. However, the costs of updating existing infrastructure and the energy requirements needed to maintain and operate these drinking water treatment processes is extensive.

The incorporation of nanomaterials into conventional water treatment devices provides the opportunity for improvement of advanced drinking water treatment and is typically used when (1) current technologies do not meet current or upcoming drinking water regulations, (2) there is a need to treat recalcitrant compounds (e.g. pharmaceuticals) that escape drinking water treatment facilities and hinder reuse, (3) it enhances the cost-effectiveness of the water treatment devices (e.g. less energy, less material), and (4) there is insufficient infrastructure in place at water treatment facilities and point-of-use (POU) treatment devices are used.

In circumstances where nanomaterials are used within POU treatment devices (e.g. under the sink filters), industry must navigate through a complex, risk landscape where the opportunities and uncertainties of nanotechnologies overlaps with public knowledge and concerns around nanomaterials and how their potential risks compare to their potential benefits. We previously explored the concerns and uncertainties of consumers around the use of nanomaterials in POU drinking water purification devices. Results from the study highlighted that the public has very little to no knowledge of nanomaterials, they have concerns around the use of nanomaterials in consumer products, and they would likely

purchase alternative point-of-use water purification devices over nanomaterial-enabled devices. In markets where consumer attitudes are likely to

dictate commercial success of applications, it is important to understand if industry concerns around using nanomaterials in their products is aligned or disconnected from consumer concerns.

Here, we present the results of research into barriers and concerns that industry member respondents have about the use of nanomaterials in POU drinking water purification devices. The objectives of the study were to (1) determine if industry demographics influence perceptions around the use of nanomaterials in POU devices for drinking water purification, (2) determine what industrial concerns and barriers there are around using nanomaterials in POU devices for drinking water purification (3) determine what industry believes to be the major industrial barriers towards bringing nanomaterial-enabled POU devices successfully to market, (4) determine what industry believes to be the major consumer barriers towards bringing nanomaterial-enabled POU devices successfully to market, and (5) determine where there are alignments and disconnects between industrial concerns and consumer concerns around nanomaterial-enabled POU drinking water purification devices.

7.3. Methods

7.3.1. Study Design and Sample Selection

This study was built around a 14-question survey designed to explore industrial perceptions of and attitudes toward nanomaterial-based POU water treatment devices amongst respondents. The survey was conducted via an online survey platform and distributed to U.S. based industrial companies between June 1st, 2018 and July 1st, 2018. Surveys were deployed by emailing an online link to Qualtrics^{XM} survey software on secure Arizona

State University servers. Data integrity is ensured through timestamps to flag “speeders”. Data was retained on secure Arizona State University servers and respondents were given an alternative ID to ensure anonymity.

An online link to the survey was sent via email to 300 U.S. based industrial companies who work with drinking water and industrial water treatment. The companies were instructed to distribute the link to different employees within their company. A total of 65 responses were collected. To ensure anonymity, respondents were given a unique identification number when completing the survey. Institutional Review Board approval was received from the Office of Research Integrity and Assurance at Arizona State University.

7.3.2. Survey Design

The survey contained 14 questions that were separated into four sections. The first section consisted of 3 demographic questions, which were multiple choice close-ended questions with an option for “other” to be openly filled in. The second section contained 3 questions that addressed the respondent’s concerns around industrial barriers to bringing nanomaterial-enabled POU drinking water purification devices to market. One question was a multiple choice close-ended question, the second question was a rank question, and the third question was a Likert scale question. The third section contained 4 questions addressing industrial concerns around public acceptance of nanomaterial-enabled POU devices for drinking water purification, which were a combination of 3 Likert scale questions and 1 rank question. The fourth section contained 4 questions that addressed industrial concerns and barriers towards using nanomaterials in POU drinking water

purification devices, which were a combination of 2 rank questions and 2 multiple-choice close-ended questions. The survey is provided in its entirety in the supplemental information.

7.3.3. *Survey Analysis*

After the survey was completed, the data was transferred to Microsoft Excel 2016 and analyzed using the XLSTAT add-on on a secure server. Descriptive statistical analysis was carried out using ANOVA followed by a post hoc chi-square test. For Likert scale questions, a Mann Whitney U test was conducted. For all analyses the level of significance was set at 5% ($p < 0.05$). Ranking question analysis was carried out by determining the rank score and rank distribution for each question. A score was calculated as follows:

$$\text{Rank Score} = X_1W_1 + X_2W_2 + X_3W_3 \dots X_nW_n$$

Where X is the response count for each answer choice and W is the weight of ranked position. The respondent's most preferred choice had the largest weight, and their least preferred choice had the lowest weight. For questions with six total responses, weights ranged from 1-6. Likewise, for questions with ten total responses, weights ranged from 1-10. Ranking questions were analyzed with the Friedman Test.

7.4. **Results and Discussion**

7.4.1. *Response Rates and Respondent Demographics*

A total of 65 fully completed surveys were returned and analyzed. The surveys that were not fully completed were discarded from the study. Table S1 compares respondents' job functions within their company and their company's role within the water treatment chain. The majority of survey respondents held a research and development (R&D) position

within their company (38%), followed by administration/management (26%), product development (14%), marketing/sales (12%), and finance/accounting (9%). Additionally, survey respondent companies have a role in the water treatment chain as a research, development, and deployment partner (29%), followed by equipment manufacturer (26%), end user (20%), service provider (17%), and manufacturer of nanomaterials and other advanced materials (8%). Survey respondents were then asked what type of water their company focuses on treating. The majority of respondents (57%) stated that their company focuses on treating both commercial potable water and industrial wastewater. 26% of respondents stated that their company focuses only on treating commercial potable water and 17% of respondents stated that their company focuses only on treating industrial wastewater.

7.4.2. Industrial Concerns around Barriers to Successful Implementation of Nanomaterial-Enabled POU Devices

Respondents were asked how concerned they were about six different factors creating a major barrier for them to successfully bring nanomaterial-enabled POU devices to market. Figure 7-1 shows the percent response of respondents to each factor. Costs were the most concerning to respondents followed by consumer fears and acceptance, environmental health and safety. Industrial scale manufacturing of nanomaterial-enabled POU devices was least concerning for respondents.

Respondents were then asked what the greatest concern was regarding the costs of successfully bringing nanomaterial-enabled POU devices to market (Figure S1). 35% of respondents stated that cheaper and/or alternative technologies were the greatest cost

concern for them, followed by operational costs versus capital costs (23%), industrial scale manufacturing (20%), complying with impending governmental regulations (14%), and regeneration costs of technologies (6%).

Respondents were then asked to rank by importance the information they would want from vendors supplying their company with nanomaterials to incorporate into their POU devices. Figure 7-2 shows the overall rank, rank distribution and score of the information respondents would want from nanomaterial vendors. Respondents valued environmental and human health impact assessments as the most important information they would want from vendors, followed by complete material characterization and information on the benefits and constraints of nanomaterials. These three factors had similar rankings among survey respondents. The sustainability, life cycle assessment, viability and stability of nanomaterials also had similar rankings to each other, but were significantly less important to respondents than the three highest ranking factors.

7.4.3. Industrial Concerns Around Public Acceptance and Perceptions of Nanomaterial-Enabled POU Devices

Respondents were asked what their preferred approach was to ensure nanomaterial-enabled POU devices for drinking water treatment were safe for public use (Figure S2). 49% of respondents stated that governmental regulation of nanomaterials would be the preferred approach to ensure public safety, followed by the certification of POU devices (28%), standard codes of conduct (18%), and state regulation of nanomaterials (5%).

Respondents were then asked what the likelihood was that the public would accept nanomaterial-enabled treatment devices used in a variety of different water treatment

sectors. Figure 7-3 shows the how concerned industry believes the public will be if nanomaterials are used to treat five different water sources. Industry believes that the majority of the public will have little to no concern about industry using nanomaterials to treat raw waters and industrial waters. Industry believes the level of public concern will increase when using nanomaterials to treat waters the public will likely come in contact with. The level of concern increases for municipal water treatment, point of entry (POE) devices, and POU devices.

Respondents were then asked if they believed public perceptions would influence long-term viability of nanomaterial-enabled POU devices for drinking water treatment (Table S2). Only 1% of respondents stated they believed there was no concern around public perceptions influencing POU viability long-term. On the other hand, 22% of respondents were very concerned, 35% of respondents were concerned, 31% of respondents had some concern, and 12% of respondents had little concern about public perceptions influencing POU viability long-term.

Respondents were then asked to rank what information they believe consumers would want to know before purchasing a nano-enabled POU device to treat their drinking water. Figure 7-4 shows the overall rank, rank distribution and score of the information respondents believe the public would want before purchasing a nano-enabled POU device to treat their drinking water. Industry believes that the public will value a label guaranteeing the safety of the POU device the most, followed by a label indicating nanomaterials are present in the device, and basic information about nanomaterials in the device. The

performance of nanomaterials in the POU device, the benefits of nanomaterials in the POU device, and the risks of nanomaterials in the POU device were valued the least by industry.

7.4.4. Industrial Concerns Around Nanomaterial-Specific Barriers, Risks and Perceptions of Using Nanomaterials in POU Devices to Treat Drinking Water

Survey respondents were given a list of the top ten manufactured nanomaterials released from commercial products and asked to rank them from 1-10 in terms of both their potential to cause environmental health and safety risks as well as public concern. Figure 7-5 illustrates the breakdown of industrial rankings of these ten nanomaterials. Industry respondents believe that carbon nanotubes (CNTs) and silver nanomaterials (Ag) have the highest potential to cause environmental health and safety concerns and have the lowest potential for public acceptance if used in POU drinking water devices. On the other hand, nanoclays and silica (SiO₂) have the lowest potential to cause environmental health and safety concerns and have the highest potential for public acceptance if used in POU drinking water devices. One nanomaterial of interest is titanium dioxide (TiO₂) which was ranked third by industry for having a high potential to cause environmental health and safety concerns, but was ranked fourth by industry for having a high potential to be accepted by the public if used in POU drinking water devices. This is likely due to TiO₂ currently being used in a wide variety of consumer products already (e.g. toothpaste, sunscreen).

Survey respondents were then asked if silver nanomaterials were used in water treatment devices, what would be the major barriers for treating drinking waters and industrial waters. Figure 6 illustrates the percent responses of industry respondents. Figure

7-6A shows that 42% of respondents believe that the major barrier for treating drinking water with silver nanomaterials is consumer perceptions and acceptance, followed by costs (23%), environmental and human health risks (17%), regulations (11%), and viability (5%). Figure 7-6B shows that 54% of respondents believe that the major barrier for treating industrial water with silver nanomaterials is costs, followed by environmental and human health risks (23%), viability (12%), regulations (5%), and consumer perceptions and acceptance (5%). These results indicate that perceived barriers around nanomaterial use to treat water may not be solely based on nanomaterial type, but rather other additional factors, including treated water type and costs.

7.4.5. Synergies and Disconnects Between Industry Concerns and Public Concerns

Regarding the Use of Nanomaterial-enabled POU Devices to Treat Drinking Water

We previously published work on a public survey (N=1623) on public perceptions for the use of nanomaterials for in-home POU drinking water purification devices. In that survey we determined that the majority of public respondents that took the survey had little to no prior knowledge about nanomaterials (~90%), they drank bottled water more than other drinking water sources and were generally satisfied with using bottled water more than tap water, they were more concerned about nanomaterials for applications where there is potential for direct contact and exposure, and they were more likely to use nanotechnologies to treat their drinking water if they were given more information about nanomaterials before purchasing POU devices.

There were similar questions in both the public survey and this industry survey to determine where synergies and disconnects are between both stakeholders around using

nanomaterials to treat drinking water and the perceptions and potential barriers there are as industry attempts to bring these technologies to market successfully. Both stakeholders agree that safety of a nanomaterial-enabled POU drinking water purification device is important for consumers. When asked about the most important characteristics of a POU device that uses nanomaterials, public survey respondents stated that the safety of the device was the most important characteristic. When asked about the best approaches for ensuring safety of these devices the majority of industry survey respondents (~42%) stated that governmental oversight would be the best approach for ensuring safety of these devices, followed by certification of products (~28%). Public survey respondents wanted more information about the use and benefits of nanomaterials (~19%), potential risks of nanomaterials in device (~15%), and information on how nanomaterial-enabled devices compare to conventional devices (~7%).

When asked about the long-term viability of nanomaterial-enabled POU devices to treat drinking water, ~56% of industry survey respondents were either concerned or very concerned about public perceptions influencing the long-term viability of these devices. While the majority of public survey respondents know little to nothing about nanomaterials (~90%), when asked about the likelihood they would use nanotechnology to treat their drinking water, ~35% of respondents would likely use nanotechnology, ~42% of respondents are neutral about using nanotechnology, and only ~22% of respondents would be unlikely to use nanotechnology. Public survey respondents also stated that they would purchase nanomaterial-enabled POU devices to treat their drinking water if the device works as effectively as competitors but is half the price (~30%) or is twice as effective as

competitors and is half the price (~26%). Only ~16% of public survey respondents stated they would not use nanotechnology to treat their drinking water. Additionally, ~95% of public survey respondents stated that if they were given more information about nanomaterials and their use in POU devices to treat drinking water they would likely change their opinion about nanomaterials. These results indicated that public perceptions of nanomaterial-enabled POU devices to treat drinking water are likely to influence long-term viability of these devices, but the lack of public knowledge of nanomaterials and a more neutral/positive perception towards nanotechnology by the public likely means that industry should be able to overcome consumer barriers for successful implementation of nanomaterial-enabled POU devices for drinking water purification.

7.5. Conclusions

This study indicated that there are many industry-related concerns around the use of nanomaterials within in-home water purification devices. Industry respondents believe the major barriers to nanomaterial-enabled POU devices to treat drinking water are costs and consumer perceptions. Regarding cost barriers for industry survey respondents, competition with conventional drinking water treatment devices is their major concern, followed by operational versus capital costs of establishing a nanomaterial-enabled POU device. Industry survey respondents were also concerned about the environmental health and safety of nanomaterials used in POU devices and the ability to fully characterize them, as they are most interested in obtaining environmental impact assessments and complete material characterization from vendors supplying them with nanomaterials to use in their POU drinking water purification devices. Industry survey respondents believe that the

closer nanomaterial-enabled POU devices are to direct consumer exposure, the less likely they are willing to use the device to treat their drinking water. Industry survey respondents also believe that public perceptions will have an influence on the long-term viability of nanomaterial-enabled POU devices. Industry survey respondents believe that nanomaterials with a likelihood for environmental health and safety concern (e.g. CNTs, Ag) are less likely to be accepted by the public and vice-versa, with the exception of TiO₂ which is likely due to its abundance in a variety of different consumer products already.

There are synergies and disconnects between industry survey respondents and public survey respondents. Both stakeholders were concerned with the safety of nanomaterial-enabled POU devices for the public, but their opinions on the method for ensuring safety of the devices is different as industry would prefer governmental oversight of POU devices and the public would prefer more information on nanomaterials and their use in POU devices. Additionally, public perceptions will influence the viability of nanomaterial-enabled POU devices for drinking water purification, but ensuring that more information about nanomaterials is provided for the public or ensuring that devices are either more efficient or cost less than conventional competing technologies will likely allow for industry to overcome public concerns and ensure successful implementation of nanomaterial-enabled POU devices for drinking water purification.

7.6. Acknowledgements

This research was funded by the National Science Foundation through the Nanosystems Engineering Research Center for Nano- Enabled Water Treatment (EEC 1449500).

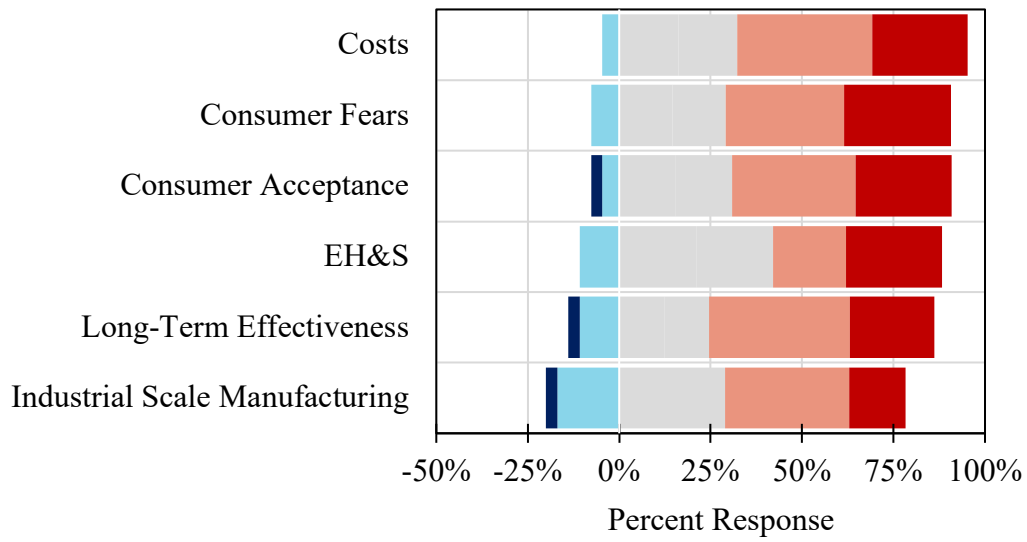


Figure 7-1. Industry concerns that the following factors may be major barriers to successful commercialization of nanomaterial-enabled POU devices.

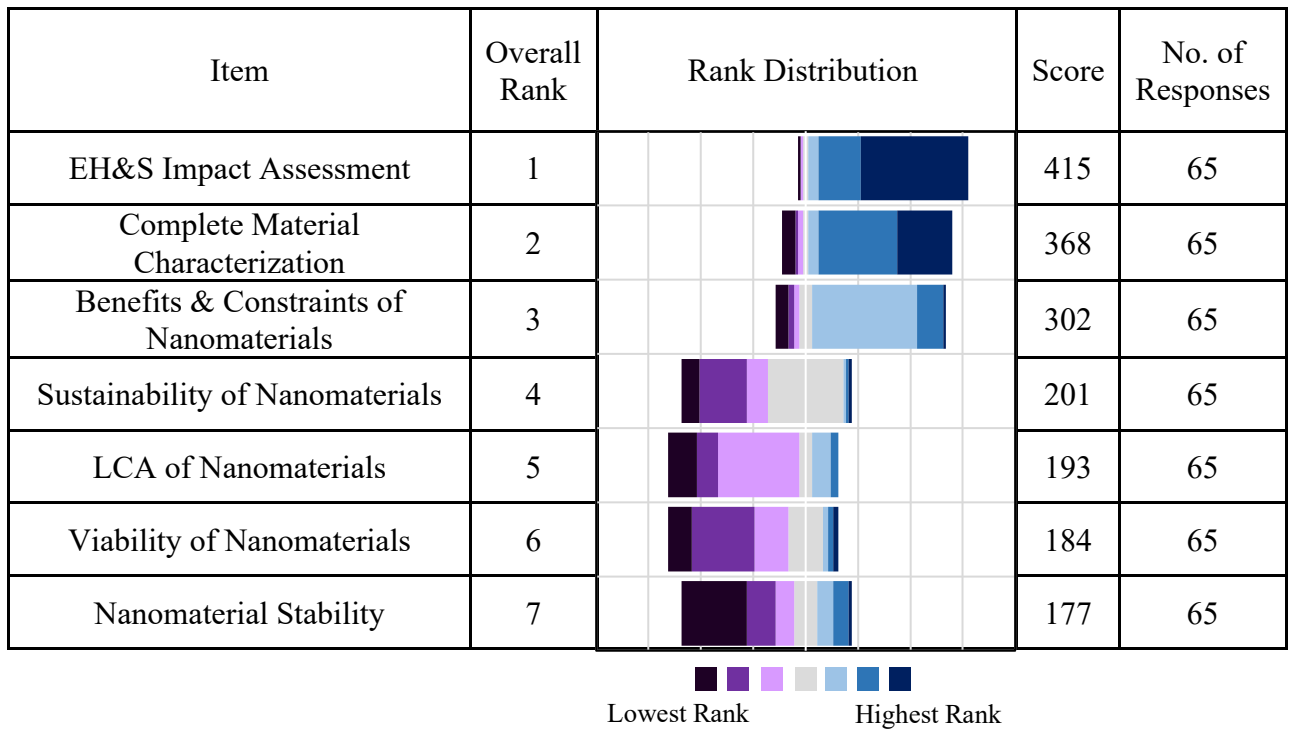


Figure 7-2. Industry rankings of the importance of information they want from vendors supplying them with nanomaterials to incorporate into POU devices

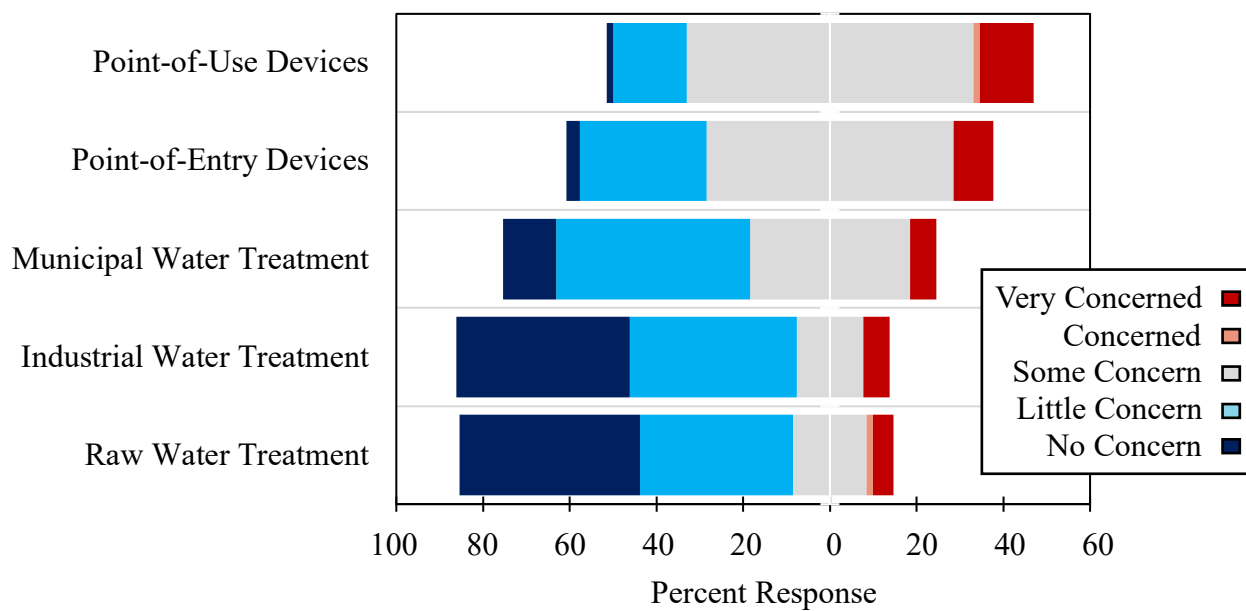


Figure 7-3. Industry beliefs of the level of public concern around using nanomaterial-enabled devices to treat different source waters

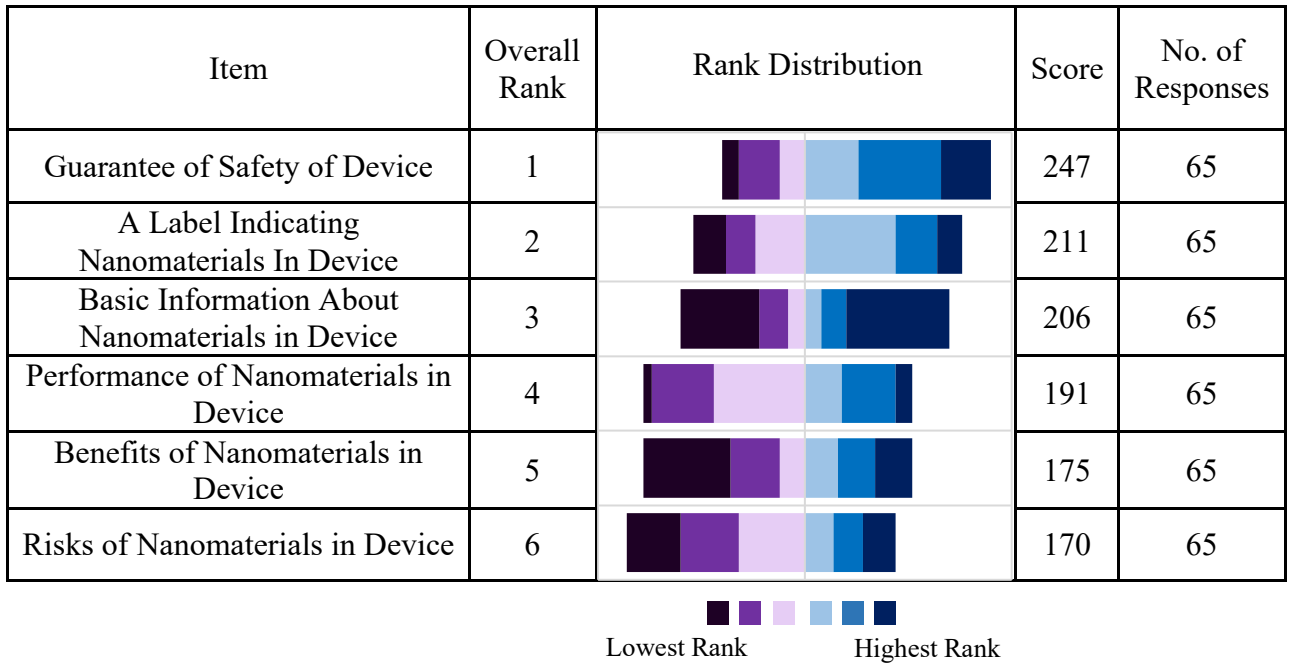


Figure 7-4. Industry rankings of the information they believe the public will want to know before purchasing a nanomaterial-enabled POU device to treat drinking water.

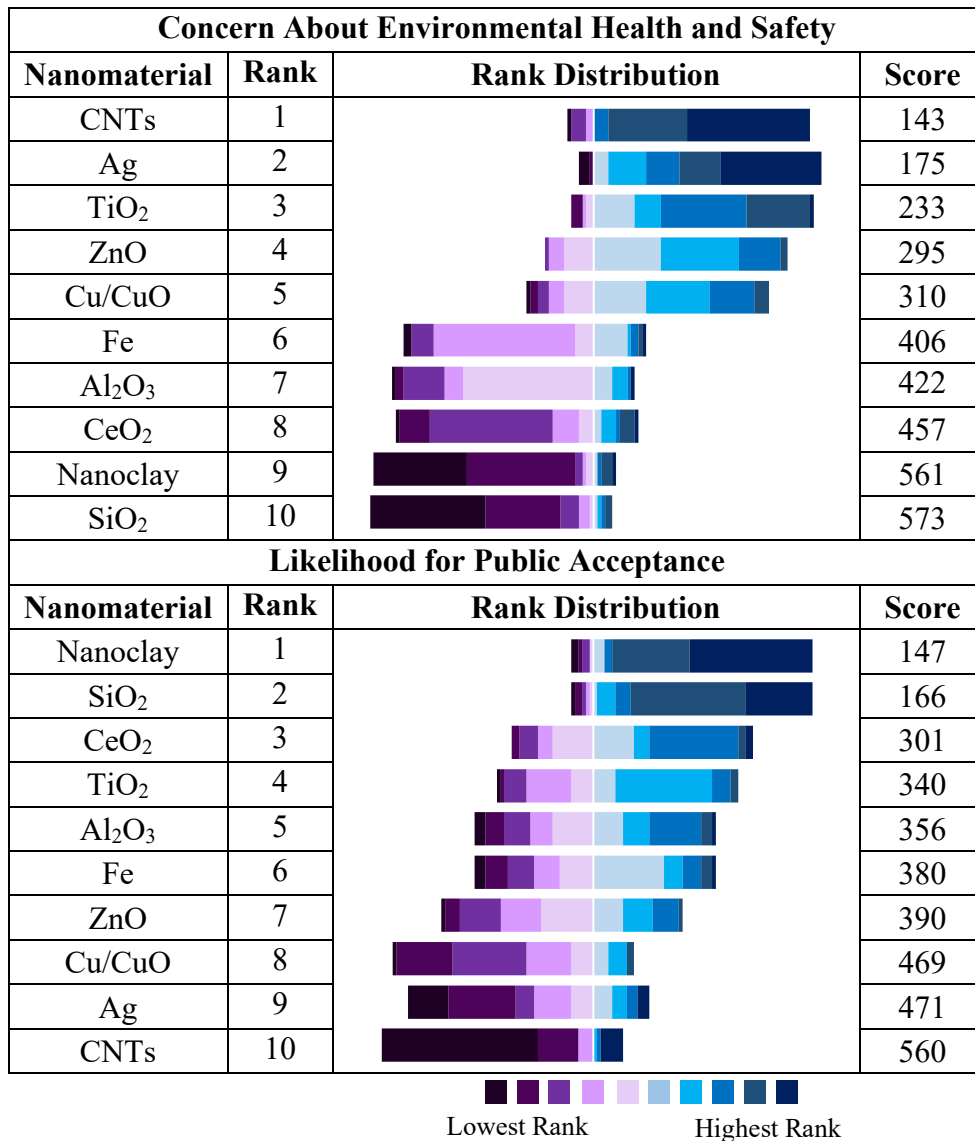
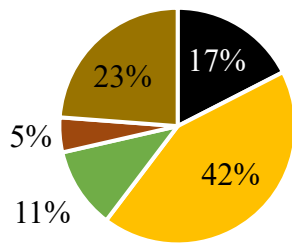
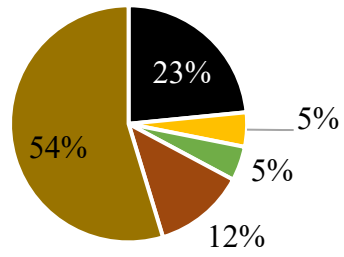


Figure 7-5. Industry rankings of ten commonly manufactured nanomaterials and their potential impact on environmental health and safety and their acceptance by the public if used in POU drinking water purification devices

A



B



- Environmental and Human Health Risks
- Consumer Perception and Acceptance
- Regulations
- Viability
- Costs

Figure 7-6. Industry survey respondents' percent response to the major barrier to successfully use silver nanomaterials to treat (A) drinking waters and (B) industrial waters

7.7. Supplemental Information

Survey Questions:

Question 1: Which one of the following best describes your job function?

- Administration / Management
- Finance/Accounting
- Human Resources
- Information Technology
- Marketing / Sales
- Product Development
- Quality Control
- Research and Development
- Other, Please Specify: _____

Question 2: Which of the following water resources is your company primarily concerned with?

- Industrial Waters
- Potable Waters
- Both
- Other, Please Specify: _____

Question 3: What is the primary role of your company within the water treatment value chain?

- Manufacturer of Nanomaterials and other Advanced Materials
- Research, Development, and Deployment Partner
- Equipment Manufacturer
- Service Provider
- End User
- Other, Please Specify: _____

Question 4: How concerned are you about the following factors creating major barriers to bringing nanotechnology water treatment devices to market successfully?

	No Concer n	Little Concer n	Some Concer n	Concer n	Very Concerned
Environmental Health & Safety	<input type="radio"/>	<input type="radio"/>	<input type="radio"/>	<input type="radio"/>	<input type="radio"/>
Industrial Scale Manufacturing	<input type="radio"/>	<input type="radio"/>	<input type="radio"/>	<input type="radio"/>	<input type="radio"/>
Long-Term Effectiveness	<input type="radio"/>	<input type="radio"/>	<input type="radio"/>	<input type="radio"/>	<input type="radio"/>
Consumer Acceptance	<input type="radio"/>	<input type="radio"/>	<input type="radio"/>	<input type="radio"/>	<input type="radio"/>
Consumer Fears	<input type="radio"/>	<input type="radio"/>	<input type="radio"/>	<input type="radio"/>	<input type="radio"/>
Costs	<input type="radio"/>	<input type="radio"/>	<input type="radio"/>	<input type="radio"/>	<input type="radio"/>

Question 5: In your opinion, what is the likelihood that members of public will accept nano-enabled water treatment devices used in the following water treatment sectors?

	Not Likely	Somewhat Likely	Likely	Very Likely
Raw Water Treatment	<input type="radio"/>	<input type="radio"/>	<input type="radio"/>	<input type="radio"/>
Industrial Water Treatment	<input type="radio"/>	<input type="radio"/>	<input type="radio"/>	<input type="radio"/>
Municipal Drinking Water Treatment	<input type="radio"/>	<input type="radio"/>	<input type="radio"/>	<input type="radio"/>
Point-of-Entry Devices	<input type="radio"/>	<input type="radio"/>	<input type="radio"/>	<input type="radio"/>
Point-of-Use Devices	<input type="radio"/>	<input type="radio"/>	<input type="radio"/>	<input type="radio"/>

Question 6: In your opinion, how concerned are you that public perceptions will influence the long-term viability of nano-enabled devices for water treatment applications?

- No Concern
- Little Concern
- Some Concern
- Concerned
- Very Concerned

Question 7: In your opinion please rank the following, from 1 (most important) to 6 (least important), in terms of the information you think consumers would want before purchasing nano-enabled water treatment devices for point-of-use drinking water?

	Most Important			Least Important		
	1	2	3	4	5	6
Risks of Nanomaterials used in the Device	<input type="radio"/>	<input type="radio"/>	<input type="radio"/>	<input type="radio"/>	<input type="radio"/>	<input type="radio"/>
Benefits of Nanomaterials used in the Device	<input type="radio"/>	<input type="radio"/>	<input type="radio"/>	<input type="radio"/>	<input type="radio"/>	<input type="radio"/>
Performance of Nanomaterials used in the Device	<input type="radio"/>	<input type="radio"/>	<input type="radio"/>	<input type="radio"/>	<input type="radio"/>	<input type="radio"/>
Basic Information about Nanomaterials used in Device	<input type="radio"/>	<input type="radio"/>	<input type="radio"/>	<input type="radio"/>	<input type="radio"/>	<input type="radio"/>
A label indicating there are Nanomaterials used in Device	<input type="radio"/>	<input type="radio"/>	<input type="radio"/>	<input type="radio"/>	<input type="radio"/>	<input type="radio"/>
A Guarantee of Safety for the Device	<input type="radio"/>	<input type="radio"/>	<input type="radio"/>	<input type="radio"/>	<input type="radio"/>	<input type="radio"/>

Question 8: In your opinion please rank the following, from 1 (most important) to 6 (least important), in terms of what information you would want from vendors supplying you with nanomaterials to incorporate into nano-enabled water treatment devices for point-of-use drinking water?

	Most Important			Least Important			
	1	2	3	4	5	6	7
Environmental and Human Health Impacts Assessment	<input type="radio"/>	<input type="radio"/>	<input type="radio"/>	<input type="radio"/>	<input type="radio"/>	<input type="radio"/>	<input type="radio"/>
Complete Material Characterization	<input type="radio"/>	<input type="radio"/>	<input type="radio"/>	<input type="radio"/>	<input type="radio"/>	<input type="radio"/>	<input type="radio"/>
Information on the Benefits and Constraints of the Material	<input type="radio"/>	<input type="radio"/>	<input type="radio"/>	<input type="radio"/>	<input type="radio"/>	<input type="radio"/>	<input type="radio"/>
Sustainability of the Material	<input type="radio"/>	<input type="radio"/>	<input type="radio"/>	<input type="radio"/>	<input type="radio"/>	<input type="radio"/>	<input type="radio"/>
Life Cycle Assessment of the Material	<input type="radio"/>	<input type="radio"/>	<input type="radio"/>	<input type="radio"/>	<input type="radio"/>	<input type="radio"/>	<input type="radio"/>
Viability of Materials	<input type="radio"/>	<input type="radio"/>	<input type="radio"/>	<input type="radio"/>	<input type="radio"/>	<input type="radio"/>	<input type="radio"/>
Material Stability	<input type="radio"/>	<input type="radio"/>	<input type="radio"/>	<input type="radio"/>	<input type="radio"/>	<input type="radio"/>	<input type="radio"/>

Question 9: In your opinion, what is your greatest concern regarding the costs of bringing nano-enabled water treatment technologies to market?

- Cheaper / Alternative Technologies
- Operational Costs vs. Capital Costs
- Industrial Scale Manufacturing
- Complying with Regulations
- Regeneration of Technology
- Other, Please Specify _____

Question 10: In your opinion, what do you believe is the preferred approach to ensure nano-enabled devices for water treatment are safe for public use?

- Certification of Products
- Standard Codes of Conduct
- State Regulation
- Governmental Regulation
- Other, Please Specify _____

Question 11: Previous Studies (i.e. Keller et al. 2013) have discussed If nano-enabled water treatment devices used these materials to treat drinking water, in your opinion how would you rank them, from 1 (highest) to 10 (lowest) in terms of their potential environmental and health risks and public acceptance:the global life cycle releases of the top 10 nanomaterials used in consumer products.

	Environmental and Health Risks	Public Acceptance
Ag ⁰	_____	_____
Al ₂ O ₃	_____	_____
CeO ₂	_____	_____
CNT	_____	_____
Cu + Cu Oxides	_____	_____
Fe + Fe Oxides	_____	_____
Nanoclays	_____	_____
SiO ₂	_____	_____
TiO ₂	_____	_____
ZnO	_____	_____

Question 12: Silver nanoparticles are being extensively studied for use in water treatment devices because of their antimicrobial properties. In your opinion, what is the major barrier to successfully using silver nanoparticles to treat industrial and potable water. Please choose one for each water type.

	Industrial Water	Potable Water
Environmental and Human Health Risks	<input type="radio"/>	<input type="radio"/>
Consumer Perception and Acceptance	<input type="radio"/>	<input type="radio"/>
Regulations	<input type="radio"/>	<input type="radio"/>
Viability	<input type="radio"/>	<input type="radio"/>
Cost	<input type="radio"/>	<input type="radio"/>
Other, Please Specify	_____	_____

Table S1. Comparison Between Job Function of Responders Within Company and Their Company's Role in the Water Treatment Chain.

Role of Company in Water Treatment Chain	Job Function Within Company					Total
	Admin.	R&D	Product Development	Finance / Accounting	Marketing / Sales	
Advanced Material Manufacturer	2 (3%)	0	3 (5%)	0	0	5 (8%)
R&D and Deployment Partner	5 (8%)	11 (17%)	1 (2%)	0	2 (3%)	19 (29%)
Equipment Manufacturer	4 (6%)	6 (9%)	3 (5%)	2 (3%)	2 (3%)	17 (26%)
Service Provider	4 (6%)	3 (5%)	0	1 (2%)	3 (5%)	11 (17%)
End User	2 (3%)	5 (8%)	2 (3%)	3 (5%)	1 (2%)	13 (20%)
Total	17 (26%)	25 (38%)	9 (14%)	6 (9%)	8 (12%)	65 (100%)

Table S2. Industry survey respondents' belief that public perceptions would influence long-term viability of nanomaterial-enabled POU devices for drinking water treatment

	No Concern	Little Concern	Some Concern	Concerned	Very Concerned
Number	0	8	20	23	14
Percentage	0%	12%	31%	35%	22%

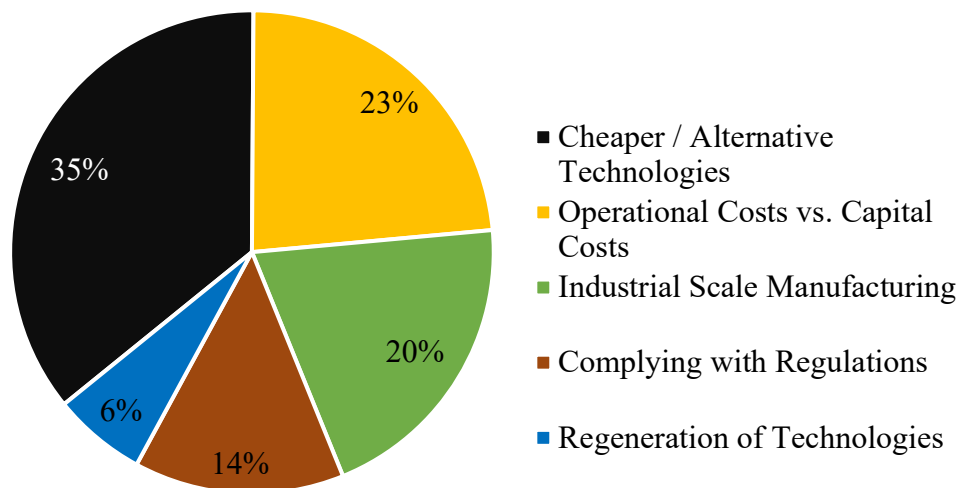


Figure S1. Industry survey respondents' greatest concern regarding the costs of bringing nanomaterial-enabled POU devices to market

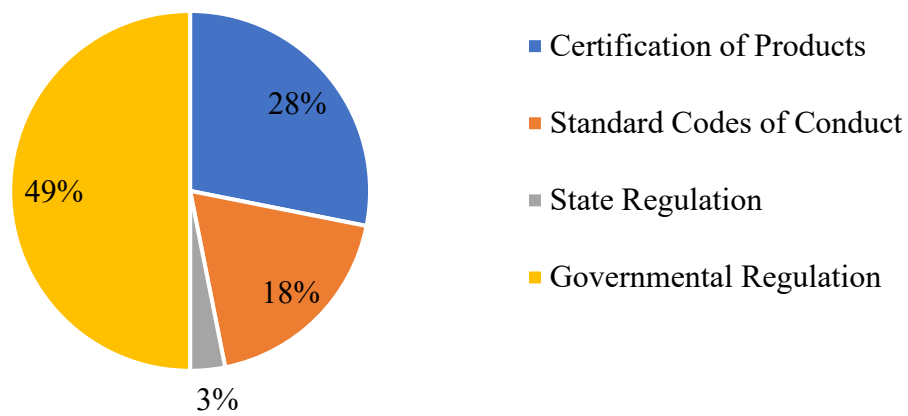


Figure S2. Industry survey respondents' preferred approach to ensure nanomaterial-enabled POU devices for drinking water treatment are safe for public use.

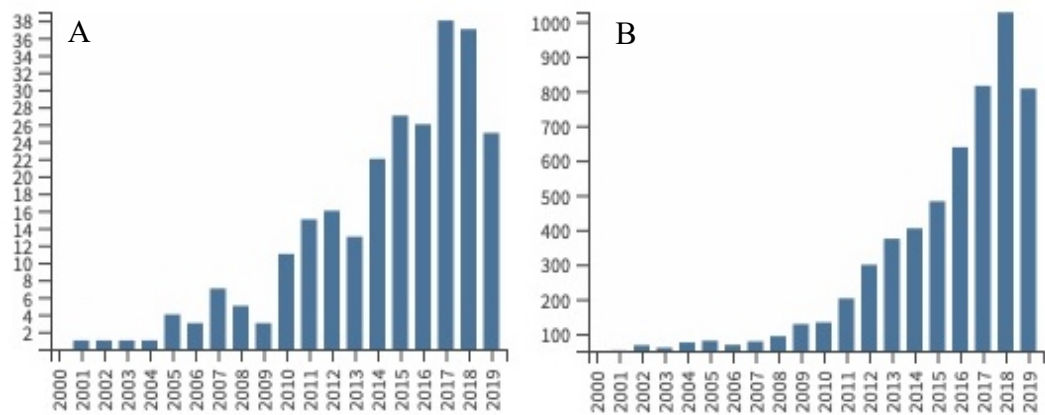


Figure S3. (A) Total publications by year and (B) summation of times cited by year for publications between 2000 and 2019. Key search topic was “silver drinking water treatment”

CHAPTER 8. SUMMARY

8.1. Introduction

The intentional use of nanomaterials within numerous technologies provides great potential to improve the quality of human life. Most research has focused on navigating the research space between the fundamental understanding of nanomaterial functional attributes and their use in different industrial-based and consumer-based technologies. Significantly less research has been done to understand what impact nanomaterials and their applications have from a societal perspective. The motivation of the work in this dissertation is to take an interdisciplinary approach to understand how nanomaterial functional attributes can improve the effectiveness of different technologies, what the intended/unintended consequences of these technologies are to the environment and human health, and how these consequences ultimately impact the decision-making of different stakeholders within society. This chapter incorporates findings from my dissertation with the existing literature to answer the guiding research questions proposed in Chapter 1. The overarching research question that guided this research was, “What are the environmental, human health, and societal impacts of metallic and carbon ENMs used in environmental remediation technologies and consumer products?”

8.2. Identifying Functional Assays to Predict ENM Behavior in the Environment

My first research question was, “Can nano-specific functional assays be developed to create activity profiles for a range of ENMs in order to provide a framework and estimations of likely nanomaterial disposition in the environment?” In Chapter 3, I developed and evaluated reproducibility and inter-correlation of 12 physical, chemical, and

biological functional assays in water for eight different engineered nanomaterials (ENMs) and interpreted results using activity-profiling radar plots. The functional assays were highly reproducible when run in triplicate (average coefficient of variation [CV] = 6.6%). Radar plots showed that each nanomaterial exhibited unique activity profiles (Figure 3-2).

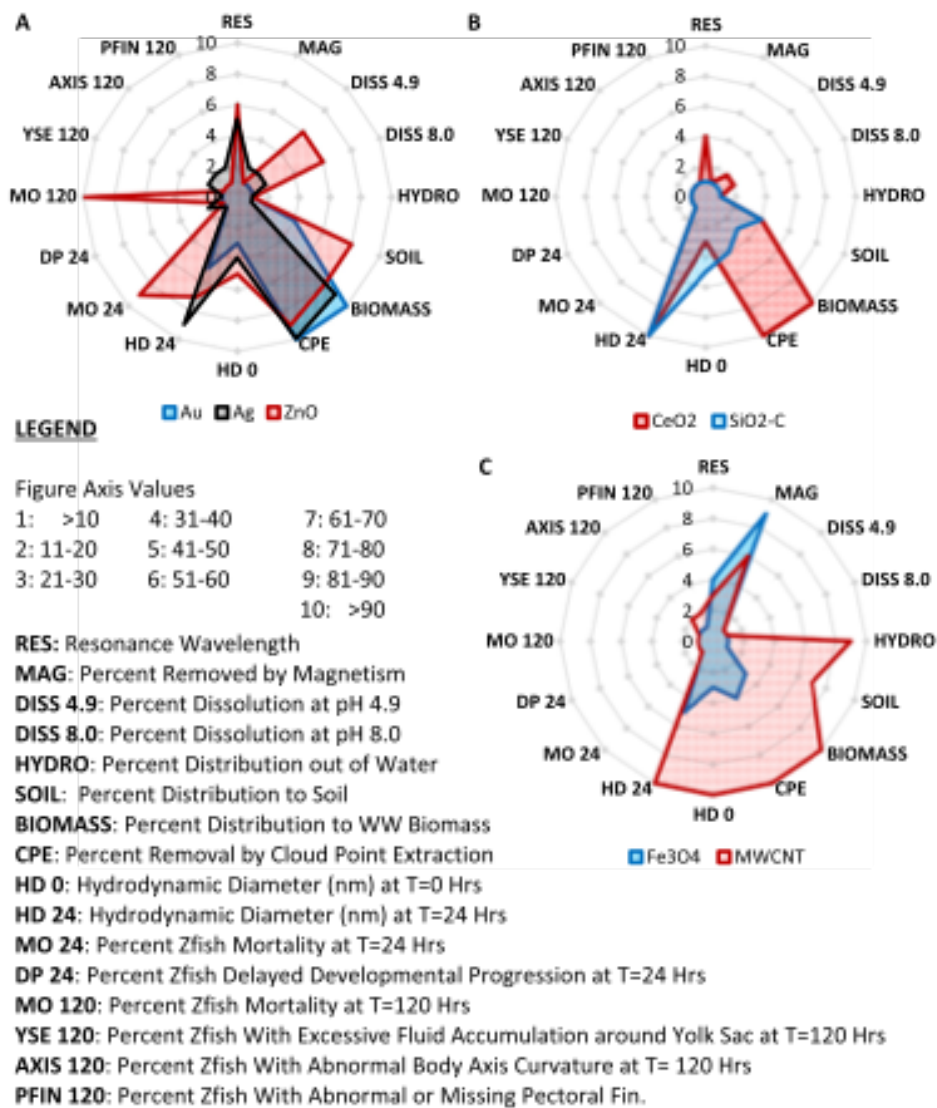


Figure 3-2. Activity profile radar plots for the comparison of behavioral trends of different engineered nanomaterials. (A) comparison of Au, Ag, and ZnO ENMs used as

antimicrobials, (B) comparison of CeO₂ and SiO₂-C ENMs used as chemical mechanical polishers, and (C) comparison of Fe₃O₄ and MWCNT ENMs used as adsorbents for water treatment

Reactivity assays showed dissolution or aggregation potential for some ENMs. Surprisingly, multi-walled carbon nanotubes (MWCNTs) exhibited movement in a magnetic field. We found high inter-correlations between cloud point extraction (CPE) and distribution to sewage sludge ($R^2 = 0.99$), dissolution at pH 8 and pH 4.9 ($R^2 = 0.98$), and dissolution at pH 8 and zebrafish mortality at 24 hpf ($R^2 = 0.94$). Additionally, most ENMs tend to distribute out of water and into other phases (i.e., soil surfaces, surfactant micelles, and sewage sludge). The activity-profiling radar plots provide a framework and estimations of likely ENM disposition in the environment.

8.3.Exploring Environmental Remediation Technologies Using Ionic Silver-Carbon Complexes

My second research question was, “Can silver impregnated graphene oxide remove bromide from surface waters with more efficiency than silver impregnated powder activated carbon in the presence of competing ions and natural organic matter?”. In Chapter 4, I compared the removal efficiency of bromide ions from surface water by silver impregnated 2D open graphene oxide and silver impregnated porous activated carbon particles. Batch studies were conducted to assess Br⁻ removal in model waters with Br⁻, chloride (Cl⁻), bicarbonate (HCO₃⁻), and/or NOM and natural surface waters. Carbon adsorbents without silver impregnation were unable to remove Br⁻ from surface water. In buffered ultrapure waters spiked with Br⁻, all Ag⁺ impregnated carbon adsorbents

performed well; however, the introduction of competing ions (Cl^-) and organics (NOM) and the use of natural CAP water significantly reduced the ability of PAC-Ag to remove Br^- from surface waters, which we attributed to its porous nature (Figure 4-2).

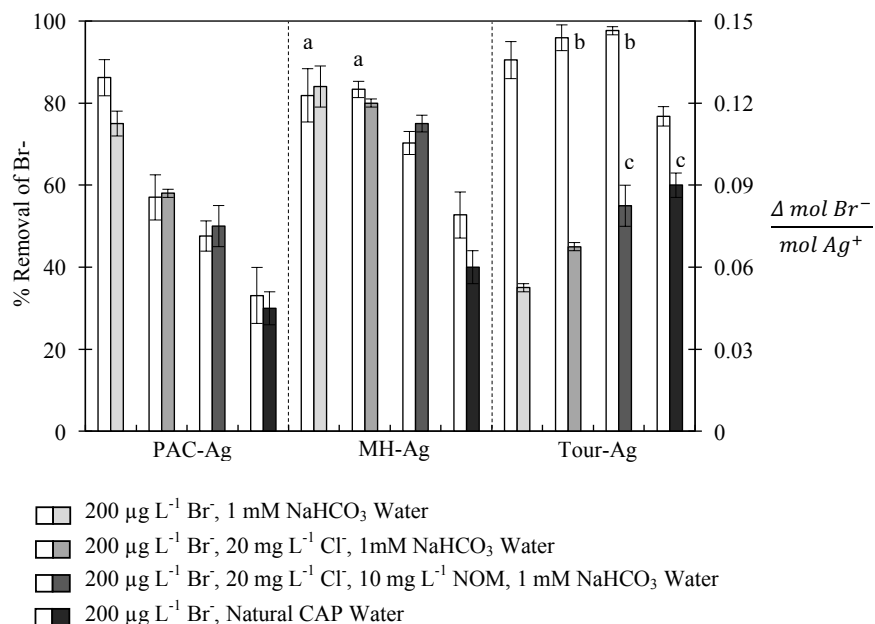


Figure 4-2. The removal of spiked Br^- ($200 \mu\text{g L}^{-1}$) in four different water matrices by 25 mg L^{-1} of Ag^+ impregnated PAC and GO after mixing for 4 hours in polypropylene batch bottles. The water matrix chemistry is provided in the legend. The white bars correspond to the left axis (% removal of Br^-), and the grey bars correspond to the right axis (Br^- removal capacity per mol of silver). The data represent average of experiment triplicates with error bars (total 1 standard deviation). Letters above bars indicate no statistical significance between data sets (one-way analysis of variance, 95% CI, ANOVA).

The sheet-like structure of MH-Ag and Tour-Ag provided the advantage of reducing the competition for adsorption sites compared to PAC-Ag. They performed as superior

adsorbents for Ag^+ based Br^- removal. Both MH-Ag and Tour-Ag showed the ability to remove more Br^- than PAC-Ag when competing ions and organics were present. All three silver impregnated adsorbents reduced Br^- in surface water when used in conjunction with alum during coagulation and flocculation, making silver impregnated GO a viable technology to be introduced into the current treatment processes framework of water treatment facilities. The mechanism for Br^- removal by silver impregnated GO appears to be initiated by Ag^+ leaching into solution, complexing with Br^- , and forming and precipitating AgBr salts. In complex waters with chloride and/or NOM present, $\text{AgCl}_{(s)}$ or Ag-NOM complexes likely compete with AgBr reactions. The likely minor pathways for Br^- removal are by Br^- complexing with Ag^+ on the adsorbent surface, which are shown in the SEM/EDAX images (Figure 4-4).

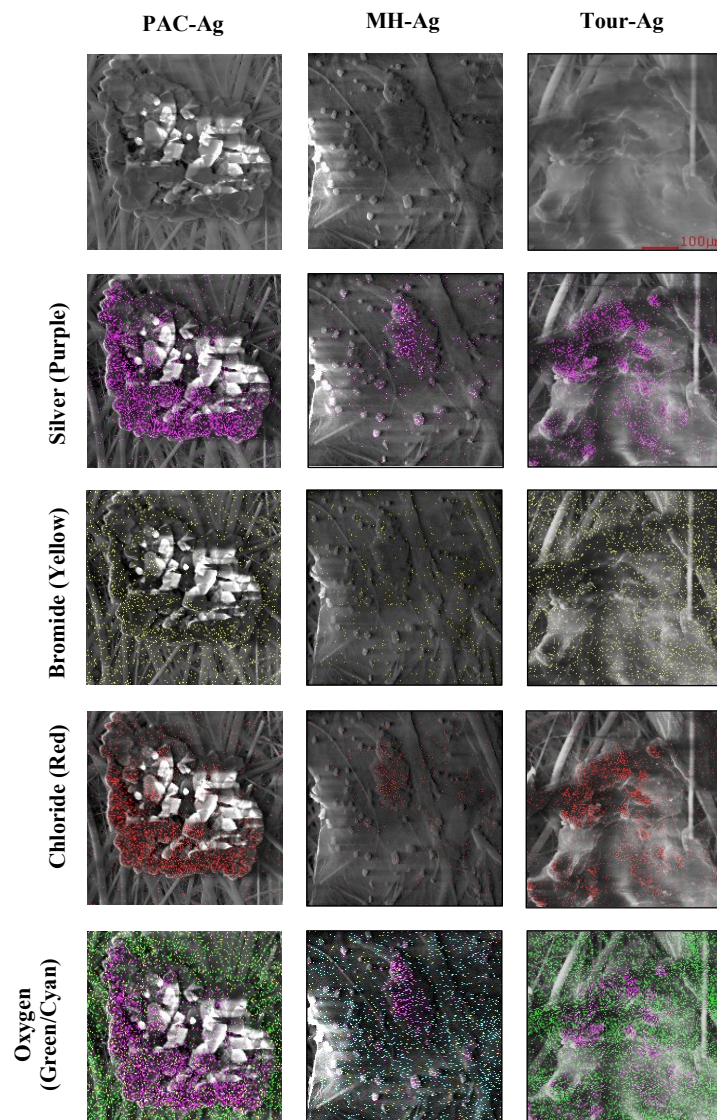


Figure 4-4. SEM images of PAC-Ag, MH-Ag, and Tour-Ag in 1 mM NaHCO₃ with 200 ug L⁻¹ bromide and 20 mg L⁻¹ chloride. Each figure is on the same scale (top right figure). Each column corresponds to an individual adsorbent. The first row is of SEM images with no EDAX elemental scanning, and the other rows show silver, bromide, chloride, or oxygen from EDAX elemental scanning.

8.4. Identifying the Effects of Ionic Silver and Nanosilver Exposures on Fecal Microorganism Structure and Function

My third research question was, “Do silver nanomaterials impact the structure and function of fecal microorganisms differently than ionic silver under realistic exposure conditions?”. In Chapter 5, I conducted bench scale anaerobic batch bottle studies to look at how exposing gut microbes to three different concentrations and types of silver impacted the pH and COD of the anaerobic system, as well as the production of short chain fatty acids (SCFAs) and biodiversity of the gut microbiome. We observed shifts in gastrointestinal pH (decrease) and SCFA production (decrease) when gut flora was exposed to 0.2 mg L⁻¹ and 2 mg L⁻¹ of nanosilver and ionic silver (Figure 5-1).

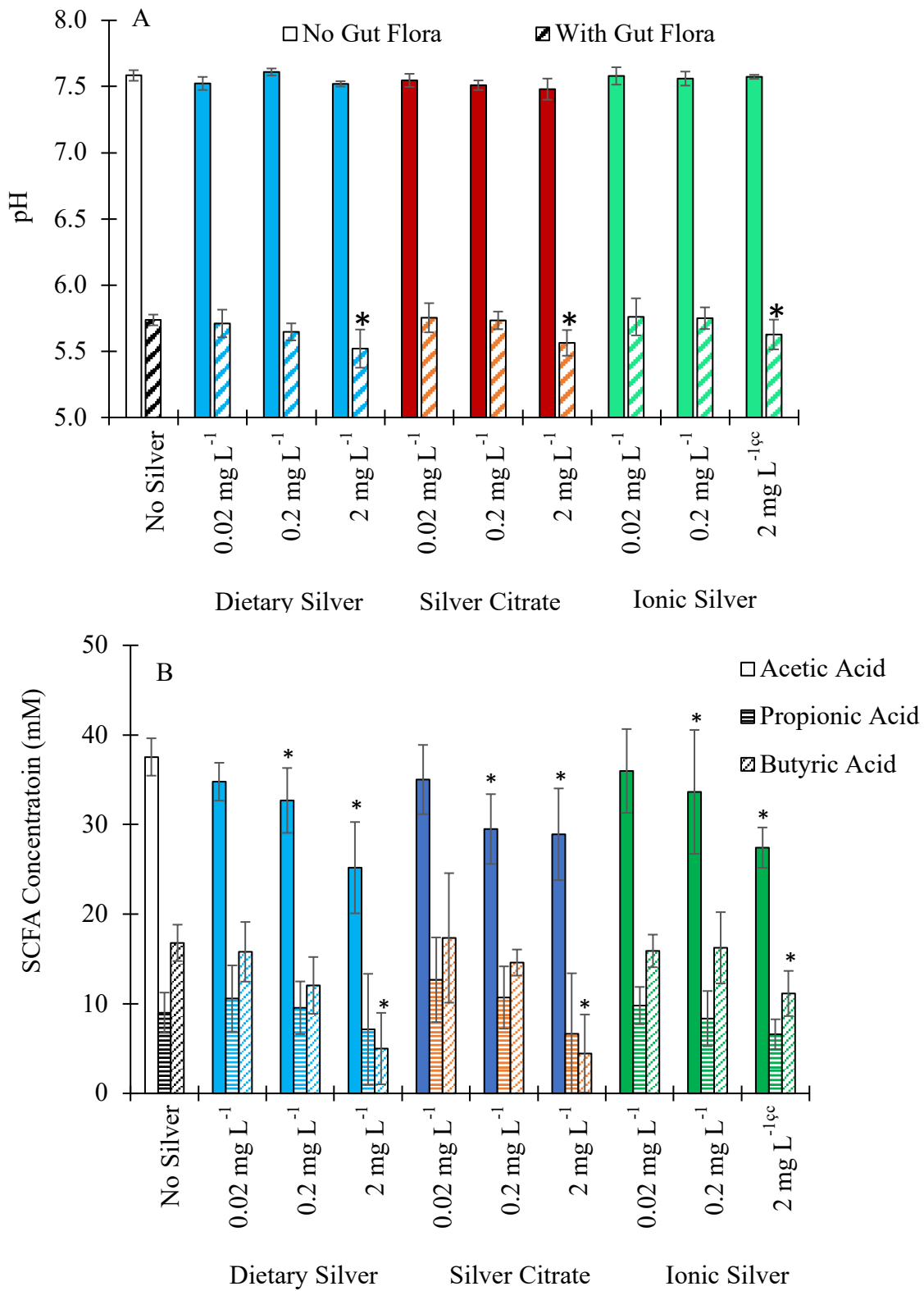


Figure 5-1. Changes in gastrointestinal (A) pH and (B) SCFA production after 24 hours of exposure to three silver types and concentrations.

Using Qiime for genetic analysis of the gut flora exposed to silver, we saw observable changes in frequencies of gut microbiomes (Figure 5-4). We observed that there are changes in community diversity among control samples and stock samples. We observed higher changes in community diversity when exposed to silver.

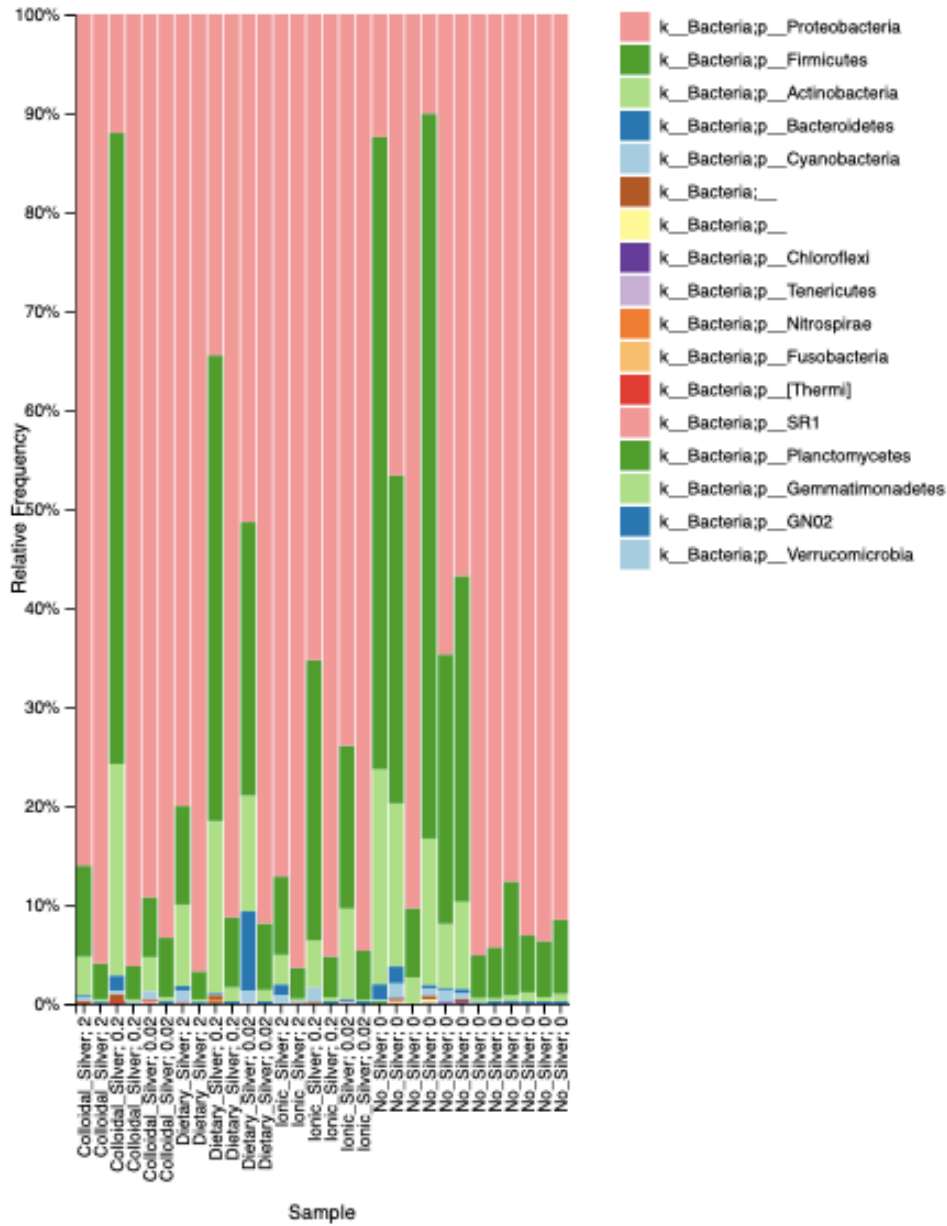


Figure 5-4. Relative frequencies of fecal microorganisms (phylum level) in control and experimental samples after 24 hours of silver exposures.

8.5. Comparison of Public and Industrial Barriers and Concerns Around the Use of ENMs in Small Scale Drinking Water Purification Devices

My fourth research question was, “What consumer concerns and barriers arise regarding the use of nanomaterials in point-of-use drinking water purification devices?”. In Chapter 6, I administered an 18-question survey of 1623 participants in four metropolitan areas—Phoenix, AZ, Houston, TX, Atlanta, GA, and Philadelphia, PA, and one rural Arizona region to assess perceptions around using nanomaterial-enabled POU devices. Approximately 90% of survey respondents had little to no prior knowledge of nanomaterials or their use in numerous consumer products ranging from POU water treatment devices to clothing or baby products. Survey respondents were more likely to purchase conventional drinking water purification devices than ones containing nanomaterials, but the majority of survey respondents (~64%) claimed they would likely or probably change their opinions around using nanomaterials to treat their drinking water if they were given more information about nanomaterials and their role in treating drinking water. The results indicate that respondents are willing to change their minds if they are provided information around nanomaterials and their use in in-home water purification. Respondents considered the safety of the device as being most important to them, followed closely by treated water taste (Figure 6-4).

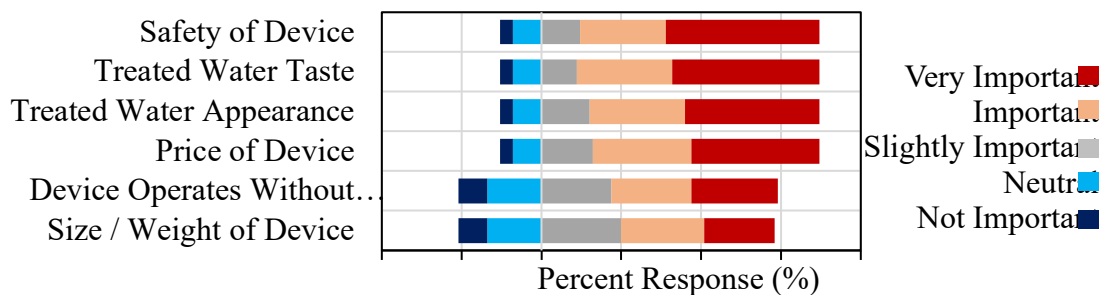


Figure 6-4. Respondents’ views on the importance of specific features of in-home water purification devices using nanomaterials

When we incorporated responses regarding previous knowledge of nanomaterials, we found that the less knowledge respondents had of nanomaterials, the more willing they would be to use them to treat their drinking water. 65% of respondents with prior knowledge of nanomaterials were unwilling to drink water treated with nanomaterials. 30% of respondents stated that they would purchase the drinking water purification product with nanomaterials if it worked as effectively as a competitor and was half the price. 26% of respondents stated that they would purchase the drinking water purification product with nanomaterials if it worked twice as effectively as a competitor and was half the price. The findings are discussed in regard to specific adoption of nanotechnology in drinking water and also broader adoption and acceptance of emerging technologies that hold promise to improve environmental outcomes.

My last research question was, “What are the overlaps and disconnects between industrial and consumer concerns and barriers regarding the use of nanomaterials in point-of-use drinking water purification devices?”. In Chapter 7, I administered a 14-question survey of 65 participants from different US-based industrial companies focused on drinking water purification. Results from the industry survey show that the major concern for industry are costs and public perceptions of nanomaterial enabled POU devices for drinking water purification. Cost-specific barriers are conventional competing technologies and operational versus capital costs. When asked about ensuring safety of nanomaterial enabled POU devices for drinking water treatment, 49% of respondents stated that governmental regulation of nanomaterials would be the preferred approach to ensure public safety, followed by the certification of POU devices (28%). Additionally, 57% of industry survey

respondents were concerned or very concerned that public perceptions will influence the long-term viability of nanomaterial enabled POU devices for drinking water purification. When asked about specific nanomaterials and their potential use in POU devices for drinking water purification, industry survey respondents believe that nanomaterials with high concern for environmental health and safety (e.g. CNTs, Ag) are least likely to be accepted by the public for used in POU devices, with the exception of TiO₂ which was viewed both a concern for environmental health and safety and public acceptance (Figure 10-5).

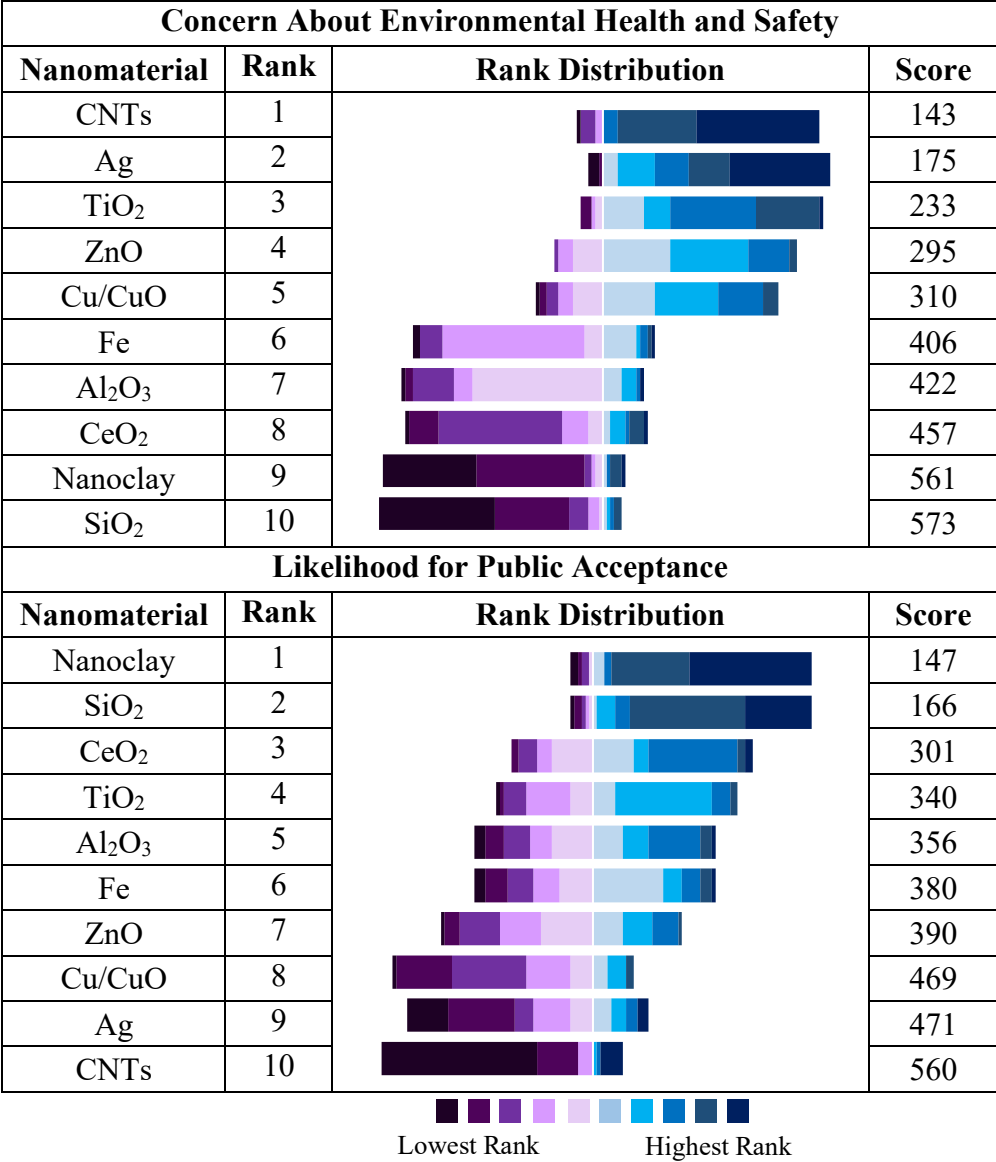


Figure 7-5. Industry rankings of ten commonly manufactured nanomaterials and their potential impact on environmental health and safety and their acceptance by the public if used in POU drinking water purification devices

Industry concerns and public concerns were compared to determine synergies and disconnects between both stakeholders. Both stakeholders are concerned about the safety

of nanomaterial enabled POU devices, but industry respondents prefer governmental oversight while public respondents prefer more information about nanomaterials. Additionally, public perceptions will influence long-term viability of nanomaterial-enabled POU devices, but ensuring that more information about nanomaterials is provided for the public or ensuring that devices are either more efficient or cost less than conventional competing technologies will likely allow for industry to overcome public concerns and ensure successful implementation of nanomaterial-enabled POU devices for drinking water purification. The findings are discussed in regard to specific adoption of nanotechnology in drinking water and also broader adoption and acceptance of emerging technologies that hold promise to improve environmental outcomes.

CHAPTER 9. CONCLUSIONS AND FUTURE RECOMMENDATIONS

9.1. Conclusions

This thesis was designed to gauge the efficacy of silver for surface water contaminant removal, evaluate societal concerns of silver use in consumer products and industrial processes, and accurately predict its environmental disposition in the environment for silver used in consumer products and industrial processes. By combining efforts to develop rapid assessment tools with wet-lab bench scale engineering of silver and industrial and consumer surveys, I was able to complete the goal of this dissertation. This work represents a novel, interdisciplinary approach to combine standard environmental engineering practices with social science practices to assess the impact of silver use in industrial processes and consumer products. Insights from this work point to improvement of knowledge on silver, its use, and concerns in industry and the public. A summary of key results is provided for each chapter in this thesis below:

9.1.1. Chapter 2 – Physico-chemical properties and their importance in the environment:

current trends in nanomaterial exposures

- Current exposure measurements and models, while not perfect, have given insight into ENM exposure in the environment. The state of science pertaining to ENM exposure is still in the infant stage but is quickly developing. Intrinsic ENM properties and extrinsic, matrix-sensitive properties can create unique exposure scenarios that are currently too complex for available methodologies.
- Currently, we are unable to determine whether specific ENM properties, or a combination of ENM properties, are responsible for ENM release and exposure

in the environment. Quantification of ENMs and ENM material properties requires a number of different analytical tools because of a lack of analytical tools capable of conducting analysis on more than one specific parameter. ENM transformations in the environment (i.e., dissolution, aggregation) are key components in altering the release potential of ENMs in products.

9.1.2. Chapter 3 – Developing and interpreting aqueous functional assays for comparative property-activity relationships of different nanomaterials

- We can develop rapid, high throughput assays for ENMs suspended in a standard 1 mM NaHCO₃ buffer
- We can developed a strategy to plot and interpret the outcomes of the functional assays by using activity-profiling radar plots.

9.1.4. Chapter 4 – Removal of bromide from surface water: comparison between silver impregnated graphene oxide and silver impregnated powder activated carbon

- The sheet-like structure of MH-Ag and Tour-Ag provided the advantage of reducing the competition for adsorption sites compared to PAC-Ag. They performed as superior adsorbents for Ag⁺ based Br⁻ removal.
- Both MH-Ag and Tour-Ag showed the ability to remove more Br⁻ than PAC-Ag when competing ions and organics were present.
- All three silver impregnated adsorbents reduced Br⁻ in surface water when used in conjunction with alum during coagulation and flocculation, making silver impregnated GO a viable technology to be introduced into the current treatment processes framework of water treatment facilities.

9.1.5. Chapter 5 – Anaerobic effects of colloidal nano-silver and ionic silver on the gut microbiome under realistic exposure conditions

- We observed shifts in gastrointestinal pH (decrease) and SCFA production (decrease) when gut flora was exposed to 0.2 mg L⁻¹ and 2 mg L⁻¹ of nanosilver and ionic silver
- We observed shifts in gut flora genetic diversity after exposure to nanosilver and ionic silver for 24 hours

9.1.6. Chapter 6 – Public perceptions regarding the use of nanomaterials for drinking water treatment

- Approximately 90% of respondents had little to no prior knowledge of nanomaterials or their use in consumer products.
- The majority of respondents we surveyed use bottled water and are generally satisfied with their drinking water.
- Survey respondents were more concerned about nanomaterials for applications where there is a higher potential for direct contact and exposure (e.g., baby products, food, drinking water purification).

9.1.7. Chapter 7 – Are industrial perceptions for drinking water treatment nanotechnologies validated by public perceptions?

- Survey respondents believe the major barrier to ENM-based POU devices to treat drinking water are the costs and consumer perceptions
- Survey respondents were concerned about environmental health and safety of nanomaterials used in POU devices and the ability to fully characterize them.

- Survey respondents believe public perceptions will have an influence on the long-term viability of ENM-based POU devices

9.2. Recommendation for Future Research

While this dissertation focuses on metallic and carbon nanomaterials, the amount of ENMs used in industry for remediation technologies and consumer products is almost limitless. The properties of nanomaterials and their activity in the environment and on human health may change over time or novel nanomaterials with new unique properties may be developed in the future. Based on the work presented in this dissertation, I have three recommendations for future work that would advance the state of knowledge in this dissertation further. My first recommendation would be to look at other nanoproducts used in dietary supplements for the gut microbiome other than nanosilver. Nano cellulose is an emerging food additive as it can be used as a low-calorie replacement for carbohydrate additives used as stabilizers, thickeners, and flavor carriers in a range of food products. Nanocellulose is carbon based and has a needle-like shape. These properties make nanocellulose hard to analyze on conventional instrumentation and has the potential to behave similarly to other needle-like materials (e.g. asbestos, carbon nanotubes). Conducting experimentation to examine the effect of nanocellulose on the gut microbiome would be an interesting study for future students at ASU. My second recommendation would be to re-evaluate the gut microbiome study in Chapter 5. While we took significant precaution in the experimental design and execution of the study, the initial results from

the study indicate that the gut flora was likely under tremendous stress as the genetic diversity of the gut flora was different than what is typically seen from healthy individuals. In our study we found that nanosilver and ionic silver cause a significant shift in gut flora biodiversity, altering the biodiversity of the flora similar to what would be expected in a healthy individual. This finding means that it would be important to determine if there was contamination in the anaerobic batch bottles during the study or during sampling and it would be of interest to repeat the study to compare results. Alternatively, if nanosilver and ionic silver are causing an improved result to gut microbiome biodiversity, could nanosilver or ionic silver be a therapeutic method to improve gut microbiome health. Understanding how nanosilver and ionic silver improve gut flora diversity would be an interesting study for the future. My last recommendation would be to conduct research that builds upon the work done with MWCNTs in Appendix B. While yttrium was chosen as the surrogate trace residual metal in this study, each MWCNT will have distinctive synthesis methods and thus will likely have unique trace residual metal compositions. It will be important moving forward to understand these differences between MWCNTs and whether a unified method can be developed to quantify MWCNTs through spICP-MS or ICP-MS using trace residual metals or whether trace residual metals like yttrium can be useful as a marker in standardized testing of MWCNTs moving forward.

REFERENCES

1. Keller, A., McFerran, S., Lazareva, A., and Suh, S. (2013). Global life cycle releases of engineered nanomaterials. *J. Nanopart. Res.*, **15**(6), 1–17
2. Sanz-Rodriguez, F., Martínez Maestro, L., Rocha, U., García Solé, J., Jacinto, C., Carmen Iglesias-de la Cruz, M., and Juarranz, A. (2012). Optimum quantum dot size for highly efficient fluorescence bioimaging. *J. Appl. Phys.*, **111**(2), 235131–235136.
3. Nick, S. T., Bolandi, A., Samuels, T. A., and Obare, S. O. (2014). Advances in understanding the transformation of engineered nanoparticles in the environment. *Pure Appl. Chem.*, **86**(7), 1129–1140.
4. Chen, Z., Forman, A. J., and Jaramillo, T. (2013). Bridging the gap between bulk and nanostructured impact of surface states on the electrocatalytic and photoelectrochemical properties of MoS₂. *J. Phys. Chem. C*, **117**(19), 9713–9722.
5. Kulagin, N., Goroshkova, L., and Hieckmann, E. (2012). Change in properties of nano and bulk SrTiO₃ crystals. *Can. J. Phys.*, **90**(7), 683–691.
6. Saafan, S. A., Assar, S. T., Moharram, B. M., and El Nimr, M. K. (2010). Comparison study of some structural and magnetic properties of nano-structured and bulk Li–Ni–Zn ferrite samples. *J. Magn. Magn. Mater.*, **322**(6), 628–632.
7. Kreyling, W. G., Semmler-Behnke, M., and Chaudhry, Q. (2010). A complementary definition of nanomaterial. *Nano Today*, **5**(3), 165–168.
8. Popma, J. R., Heugens, E. H. W., Rietveld, A. G., Oomen, A. G., Cassee, F. R., Meent, V. D., and Wijnhoven, S. W. P. (2012). Considerations on the EU definition of a nanomaterial: science to support policy making. *Regul. Toxicol. Pharm.*, **65**(1), 119–125.
9. Cao, G. (2004). *Nanostructures and Nanomaterials: Synthesis, Properties and Applications*, 1st Ed. (Imperial College Press, London, England).
10. Gregorczyk, K., and Knez, M. (2016). Hybrid nanomaterials through molecular and atomic layer deposition: top down, bottom up, and in-between approaches to new materials. *Prog. Mater. Sci.*, **75**, 1–37.
11. Roco, M. C. (2011). Nanotechnology: from discovery to innovation and socioeconomic projects. *Chem. Eng. Prog.* **107**(5), 21–27.

12. Roco, M. C., Mirkin, C. A., and Hersam, M. C. (2011). Nanotechnology research directions for societal needs in 2020: summary of international study. *J. Nanopart. Res.*, **13**(3), 897–919.
13. Roco, M. C. (2011). The long view of nanotechnology development: the national nanotechnology initiative at 10 years. *J. Nanopart. Res.*, **13**(2), 427–445.
14. Gottschalk, F., and Nowack, B. (2011). The release of engineered nanomaterials to the environment. *J. Environ. Monit.*, **13**(5), 1145–1155.
15. Losert, S., Hess, A., Ilari, G., von Goetz, N., and Hungerbuehler, K. (2015). Online characterization of nano-aerosols released by commercial spray products using SMPS–ICPMS coupling. *J. Nanopart. Res.*, **17**(7), 1–14.
16. Tromp, P. C., Oomen, A. G., Marvin, H. J. P., Rietveld, A., Oegema, G., Bouwmeester, H., and Kramer, E. (2012). Presence of nano-sized silica during in vitro digestion of foods containing silica as a food additive. *ACS Nano*, **6**(3), 2441–2451.
17. Al-Kattan, A., Wichser, A., Vonbank, R., Brunner, S., Ulrich, A., Zuin, S., and Nowack, B. (2013). Release of TiO₂ from paints containing pigment-TiO₂ or nano-TiO₂ by weathering. *Environ. Sci. Process. Impacts*, **15**(12), 2186–2193.
18. Gondikas, A. P., von der Kammer, F., Reed, R. B., Wagner, S., Ranville, J. F., and Hofmann, T. (2014). Release of TiO₂ nanoparticles from sunscreens into surface waters: a one-year survey at the old Danube recreational lake. *Environ. Sci. Technol.*, **48**(10), 5415.
19. Dahm, M. M., Evans, D. E., Schubauer-Berigan, M. K., Birch, M. E., and Deddens, J. A. (2013). Occupational exposure assessment in carbon nanotube and nanofiber primary and secondary manufacturers: mobile direct-reading sampling. *Ann. Occup. Hyg.*, **57**(3), 328–344.
20. Hicks, A. L., Gilbertson, L. M., Yamani, J. S., Theis, T. L., and Zimmerman, J. B. (2015). Life cycle payback estimates of nanosilver enabled textiles under different silver loading, release, and laundering scenarios informed by literature review. *Environ. Sci. Technol.*, **49**(13), 7529.
21. Wilson, M. J. (1999). The origin and formation of clay minerals in soils: past, present and future perspectives. *Clay Miner.*, **34**, 7–25.
22. Bargar, J., Bernier-Latmani, R., Giammar, D., and Tebo, B. (2008). Biogenic uraninite nanoparticles and their importance for uranium remediation. *Elements*, **4**, 407–412.
23. Buseck, P., and Pósfai, M. (1999). Airborne minerals and related aerosol particles: effects on climate and the environment. *Proc. Natl. Acad. Sci. U. S. A.*, **96**, 3372–3379.

24. Cavalli, F., Facchini, M., Decesari, S., et al. (2004). Advances in characterization of size-resolved organic matter in marine aerosol over the North Atlantic. *J. Geophys. Res.*, **109**, 21425.
25. Adegboyega, N., Sharma, V., Siskova, K., Vecerova, R., et al. (2014). Enhanced formation of silver nanoparticles in Ag⁺-NOM-iron (II, III) systems and antibacterial activity studies. *Environ. Sci. Technol.*, **48**, 3228–3235.
26. Yin, Y., Liu, J., and Jiang, G. (2012). Sunlight-induced reduction of ionic Ag and Au to metallic nanoparticles by dissolved organic matter. *ACS Nano*, **6**, 7910–7919.
27. Yucel, M., Gartman, A., Chan, C., and Luther, G. (2011). Hydrothermal vents as a kinetically stable source of iron-sulfide-bearing nanoparticles to the ocean. *Nat. Geosci.*, **4**, 367–371.
28. d’Almeida, G. A., and Schutz, L. (1983). Number, mass and volume distributions of mineral aerosol and soils of the Sahara. *J. Clim. Appl. Meteorol.*, **22**, 233–243.
29. Lungu, M., Neculae, A., Bunoiu, M., and Biris, C. (2015). *Nanoparticles’ Promises and Risks: Characterization, Manipulation, and Potential Hazards to Humanity and the Environment* (Springer InternationalSwitzerland), xiv, 355 p.
30. Shi, Z., Shao, L., Jones, T. P., and Lu, S. (2005). Microscopy and mineralogy of airborne particles collected during severe dust storm episodes in Beijing, China. *J. Geophys. Res.*, **110**, D01303.
31. Yano, E., Yokoyama, Y., Higashi, H., Nishii, S., Maeda, K., and Koizumi, A. (1990). Health effects of volcanic ash: a repeat study. *Environ. Health*, **45**, 367–373.
32. von der Kammer, F., Ferguson, P. L., Holden, P. A., Masion, A., Rogers, K. R., Klaine, S. J., Koelmans, A. A., Horne, N., and Unrine, J. M. (2012). Analysis of engineered nanomaterials in complex matrices (environment and biota): general considerations and conceptual case studies. *Environ. Toxicol. Chem.*, **31**, 32.
33. Wiesner, M. R., Lowry, G. V., Jones, K. L., Hochella, M. F. Jr, DiGiulio, R. T., Casman, E., and Bernhardt, E. S. (2009). Decreasing uncertainties in assessing environmental exposure, risk, and ecological implications of nanomaterials. *Environ. Sci. Technol.*, **43**, 6458.
34. Keller, A., McFerran, S., Lazareva, A., and Suh, S. (2013). Global life cycle releases of engineered nanomaterials. *J. Nanopart. Res.*, **15**(6), 1–17.

35. Hume, S. L., and Jeerage, K. M. (2013). Surface chemistry and size influence the release of model therapeutic nanoparticles from poly(ethylene glycol) hydrogels. *J. Nanopart. Res.*, **15**(5), 1–16.
36. Cho, E., Holback, H., Liu, K., Abouelmagd, S., Park, J., and Yeo, Y. (2014). Nanoparticle characterization: state of the art, challenges, and emerging technologies. *Mol. Pharmaceutics*, **10**(6), 2093–2110.
37. Baalousha, M., and Lead, J. (2015). *Characterization of Nanomaterials in Complex Environmental and Biological Media* (Elsevier, Amsterdam).
38. Lobos, J., and Velankar, S. (2014). How much do nanoparticle fillers improve the modulus and strength of polymer foams? *J. Cell. Plast.*, **1**, 1–32.
39. Dastjerdi, R., Montazer, M., and Shahsavan, S. (2009). A new method to stabilize nanoparticles on textile surfaces. *Colloids Surf. A*, **345**(1), 202–210.
40. Faure, B., Salazar-Alvarez, G., Ahniyaz, A., Villaluenga, I., Berriozabal, G., De Miguel, Y. R., and Naturvetenskapliga, F. (2013). Dispersion and surface functionalization of oxide nanoparticles for transparent photocatalytic and UV-protecting coatings and sunscreens. *Sci. Technol. Adv. Mater.*, **14**(2), 23001.
41. Faria, A. C. L., Bordin, Angelo Rafael de Vito, Pedrazzi, V., Rodrigues, R. C. S., and Ribeiro, R. F. (2012). Effect of whitening toothpaste on titanium and titanium alloy surfaces. *Braz. Oral Res.*, **26**(6), 498–504.
42. Gouda, M. (2012). Nano-zirconium oxide and nano-silver oxide/cotton gauze fabrics for antimicrobial and wound healing acceleration. *J. Ind. Text.*, **41**(3), 222–240.
43. Lee, S., Laldawngliana, C., and Tiwari, D. (2012). Iron oxide nano-particles-immobilized-sand material in the treatment of Cu contaminated waste waters. *J. Chem. Eng.*, **103**, 195–196.
44. Azad, M., Nasrollahi, S. A., and Firooz, A. (2014). Zinc oxide in sunscreen products. *Dermatol. Cosmet.*, **5**(1), 41–48.
45. Godlewski, M., Guziewicz, E., Kopalko, K., Łuka, G., Łukasiewicz, M. I., Krajewski, T., and Gierałowska, S. (2011). Zinc oxide for electronic, photovoltaic and optoelectronic applications. *Low Temp. Phys.*, **37**(3), 235–240.
46. Buffle, J., Wilkinson, K. J., Stoll, S., Filella, M., and Zhang, J. (1998). A generalized description of aquatic colloidal interactions: the three-colloidal component approach. *Environ. Sci. Technol.*, **32**(19), 2887–2899.

47. Zhou, W., Qi, S., Tu, C., Zhao, H., Wang, C., and Kou, J. (2007). Effect of the particle size of Al₂O₃ on the properties of filled heat-conductive silicone rubber. *J. Appl. Polym. Sci.*, **104**(2), 1312–1318.
48. Boutard, T., Rousseau, B., Couteau, C., Tomasoni, C., Simonnard, C., Jacquot, C., and Roussakis, C. (2013). Comparison of photoprotection efficiency and antiproliferative activity of ZnO commercial sunscreens and CeO₂. *Mater. Lett.*, **108**, 13–16.
49. Wong, A., Wijnands, S. F. L., Kuboki, T., and Park, C. B. (2013). Mechanisms of nanoclay-enhanced plastic foaming processes: effects of nanoclay intercalation and exfoliation. *J. Nanopart. Res.*, **15**(8), 1–15.
50. Kim, J., Shashkov, E. V., Galanzha, E. I., Kotagiri, N., and Zharov, V. P. (2007). Photothermal antimicrobial nanotherapy and nanodiagnostics with self-assembling carbon nanotube clusters. *Lasers Surg. Med.*, **39**(7), 622–634.
51. Nowack, B., David, R. M., Fissan, H., Morris, H., Shatkin, J. A., Stintz, M., and Brouwer, D. (2013). Potential release scenarios for carbon nanotubes used in composites. *Environ. Int.*, **59**, 1–11.
52. Martinet, C., Kassir-Bodon, A., Deschamps, T., Cornet, A., Le Floch, S., Martinez, V., and Champagnon, B. (2015). Permanently densified SiO₂ glasses: a structural approach. *J. Phys.*, **27**(32), 325401.
53. Mutsuga, M., Sato, K., Hirahara, Y., and Kawamura, Y. (2011). Analytical methods for SiO₂ and other inorganic oxides in titanium dioxide or certain silicates for food additive specifications. *Food Addit. Contam.*, **28**(4), 423–427.
54. Liu, J., and Hurt, R. H. (2010). Ion release kinetics and particle persistence in aqueous nano-silver colloids. *Environ. Sci. Technol.*, **44**(6), 2169–2175.
55. Sayle, T. X. T., Molinari, M., Das, S., Bhatta, U. M., Möbus, G., Parker, S. C., and Sayle, D. C. (2013). Environment-mediated structure, surface redox activity and reactivity of ceria nanoparticles. *Nanoscale*, **5**(13), 663–673.
56. Borm, P., Klaessig, F. C., Landry, T. D., Moudgil, B., Pauluhn, J., Thomas, K., Trottier, R., and Wood, S. (2006). Research strategies for safety evaluation of nanomaterials, part V: role of dissolution in biological fate and effects of nanoscale particles. *Toxicol. Sci.*, **90**, 23–32.
57. Murdock, R. C., Braydich-Stolle, L., Schrand, A. M., Schlager, J. J., and Hussain, S. M. (2008). Characterization of nanomaterial dispersion in solution prior to in vitro exposure using dynamic light scattering technique. *Toxicol. Sci.*, **101**, 239–253.

58. Li, Y., Zhang, W., Niu, J., and Chen, Y. (2012). Mechanism of photogenerated reactive oxygen species and correlation with the antibacterial properties of engineered metal-oxide nanoparticles. *ACS Nano*, **6**(6), 5164–5173.
59. Xiu, Z., Zhang, Q., Puppala, H., Colvin, V., and Alvarez, P. (2012). Negligible particle-specific antibacterial activity of silver nanoparticles. *Nano Lett.*, **12**(8), 4271–4275.
60. Stumm, W. (1997). Reactivity at the mineral-water interface: dissolution and inhibition. *Colloids Surf. A*, **120**(1), 143–166.
61. Rubasinghege, G., Lentz, R. W., Scherer, M. M., and Grassian, V. H. (2012). Simulated atmospheric processing of iron oxyhydroxide minerals at low pH: roles of particle size and acid anion in iron dissolution. *Proc. Natl. Acad. Sci. U. S. A.*, **107**, 6628–6633.
62. Liu, J., Sonshine, D. A., Shervani, S., and Hurt, R. H. (2010). Controlled release of biologically active silver from nanosilver surfaces. *ACS Nano*, **4**(11), 6903–6913.
63. Pokhrel, L. R., Dubey, B., and Scheuerman, P. R. (2013). Impacts of select organic ligands on the colloidal stability, dissolution dynamics, and toxicity of silver nanoparticles. *Environ. Sci. Technol.*, **47**(22), 12877–12885.
64. Hotze, E., Phenrat, T., and Lowry, G. (2010). Nanoparticle aggregation: challenges to understanding transport and reactivity in the environment. *J. Environ. Qual.*, **39**, 1909–1924.
65. Hahn, M., D. Abadzic, and C. O’Melia. (2004). Aquasols: on the role of secondary minima. *Environ. Sci. Technol.*, **38**, 5915–5924.
66. Barbot, E., Dussouillez, P., Bottero, J.-Y., and Moulin, P. (2010). Coagulation of bentonite suspension by polyelectrolytes or ferric chloride: floc breakage and reformation. *Chem. Eng. J.*, **156**, 83–91.
67. Wu, W., Giese, R., and van Oss, C. (1999). Stability versus flocculation of particle suspensions in water-correlation with the extended DLVO approach for aqueous systems, compared with classical DLVO theory. *Colloids Surf. B*, **14**, 47–55.
68. Wouterse, M., Velzeboer, I., Meent, D., Koelmans, A. A., and Quik, J. T. K. (2014). Heteroaggregation and sedimentation rates for nanomaterials in natural waters. *Water Res.*, **48**(1), 269–279.
69. Li, Z., Greden, K., Alvarez, P. J. J., Gregory, K. B., and Lowry, G. V. (2010). Adsorbed polymer and NOM limits adhesion and toxicity of nano scale zerovalent iron to E. coli. *Environ. Sci. Technol.*, **44**(9), 3462–3467.

70. Badawy, A., Scheckel, K., Suidan, M., and Tolaymat, T. (2012). The impact of stabilization mechanism on the aggregation kinetics of silver nanoparticles. *Sci. Total Environ.*, **429**, 325–331.
71. Buffle, J., Wilkinson, K. J., Stoll, S., Filella, M., and Zhang, J. (1998). A generalized description of aquatic colloidal interactions: the three-colloidal component approach. *Environ. Sci. Technol.*, **32**(19), 2887–2899. Qi, Y., Du, N., Zhang, H., Wang, J., Yang, D., and Yang, Y. (2012). Nanostructured hybrid cobalt oxide/copper electrodes of lithium-ion batteries with reversible high-rate capabilities. *J. Alloys Compd.*, **521**, 83–89.
72. Keller, A., Wang, H., Zhou, D., et al. (2010). Stability and aggregation of metal oxide nanoparticles in natural aqueous matrices. *Environ. Sci. Technol.*, **44**(6), 1962–1967.
73. Dalai, S., Pakrashi, S., Kumar, R., Chandrasekaran, N., and Mukherjee, A. (2012). A comparative cytotoxicity study of TiO₂ nanoparticles under light and dark conditions at low exposure concentrations. *Toxicol. Res.*, **1**, 116–130.
74. Lyon, D., and Alvarez, P. (2008). Fullerene water suspension (nC) exerts antibacterial effects via ROS-independent protein oxidation. *Environ. Sci. Technol.*, **42**(21), 8127–8132.
75. Cronholm, P., Karlsson, H. L., Hedberg, J., Lowe, T. A., Winnberg, L., Elihn, K., Wallinder, I. O., and Möller, L. (2013). Intracellular uptake and toxicity of Ag and CuO nanoparticles: a comparison between nanoparticles and their corresponding metal ions. *Small*, **9**(7), 970–982.

76. Parsons, J., Lopez, M., Gonzalez, C., Peralta-Videa, J., and Gardea-Torresdey, J. (2010). Toxicity and biotransformation of uncoated and coated nickel hydroxide nanoparticles on mesquite plants. *Environ. Toxicol. Chem.*, **29**(5), 1146–1154.
77. Preister, J. H., Ge, Y., Mielke, R., Horst, A., et al. (2012). Soybean susceptibility to manufactured nanomaterials with evidence for food quality and soil fertility interruption. *Proc. Natl. Acad. Sci. U. S. A.*, **109**(37), 2451–2456.
78. Lee, W., An, Y., Yoon, H., and Kweon, H. (2008). Toxicity and bioavailability of copper nanoparticles to the terrestrial plants mung bean (*Phaseolus radiatus*) and wheat (*Triticum aestivum*): plant agar test for water-insoluble nanoparticles. *Environ. Toxicol. Chem.*, **7**(9), 1915–1921.
79. Kashiwada, S., Ariza, M. E., Kawaguchi, T., Nakagame, Y., et al. (2012). Silver nanocolloids disrupt medaka embryogenesis through vital gene expressions. *Environ. Sci. Technol.*, **46**, 6278–6287.
80. George, S., Lin, S., Ji, Z., Thomas, C. R., Li, L., Mecklenburg, M., et al. (2012). Surface defects on plate-shaped silver nanoparticles contribute to its hazard potential in a fish gill cell line and zebrafish embryos. *ACS Nano*, **6**, 3745–3759.
81. Unrine, J. M., Tsyusko, O. V., Hunyadi, S. E., Judy, J. D., and Bertsch, P. M. (2010). Effects of particle size on chemical speciation and bioavailability of copper to earthworms (*Eisenia fetida*) exposed to copper nanoparticles. *J. Environ. Qual.*, **39**, 1942–1953.
82. Gottschalk, F., Sonderer, T., Scholz, R. W., and Nowack, B. (2009). Modeled environmental concentrations of engineered nanomaterials (TiO₂, ZnO, Ag, CNT, fullerenes) for different regions. *Environ. Sci. Technol.*, **43**(24), 9216–9222.
83. Velzeboer, I., Quik, J. T. K., van de Meent, D., and Koelmans, A. A. (2014). Rapid settling of nanoparticles due to heteroaggregation with suspended sediment. *Environ. Toxicol. Chem.*, **33**(8), 1766–1773.
84. Liu, H. H., and Cohen, Y. (2014). Multimedia environmental distribution of engineered nanomaterials. *Environ. Sci. Technol.*, **48**(6), 3281–3292.
85. Praetorius, A., Tufenkji, N., Goss, K. U., Scheringer, M., von der Kammer, F., and Elimelech, M. (2014). The road to nowhere: equilibrium partition coefficients for nanoparticles. *Environ. Sci. Nano*, **1**(4), 317–323.
86. Montano, M., Ranville, J., Lowry, G., Blue, J., Hiremath, N., Koenig, S., and Tuccillo, M. (2014). Detection and characterization of engineered nanomaterials in the

environment: current state-of-the-art and future directions report. U.S. Environmental Protection Agency, Washington, DC, EPA/600/R-14/244.

87. Irin, F., Shrestha, B., Cañas, J. E., Saed, M. A., and Green, M. J. (2012). Detection of carbon nanotubes in biological samples through microwave-induced heating. *Carbon*, **50**(12), 4441.
88. Doudrick, K., Herckes, P., and Westerhoff, P. (2012). Detection of carbon nanotubes in environmental matrices using programmed thermal analysis. *Environ. Sci. Technol.*, **46**(22), 12246–12253.
89. Bertsch, P., and Hunter, D. (2001). Applications of synchrotron based x-ray microprobes. *Chem. Rev.*, **101**, 1809–1842.
90. Jawor, A., and Hoek, E. M. V. (2010). Removing cadmium ions from water via nanoparticle-enhanced ultrafiltration. *Environ. Sci. Technol.*, **44**(7), 2570–2576.
91. Nazar, M. F., Shah, S. S., Shah, A., Eastoe, J., and Khan, A. M. (2011). Separation and recycling of nanoparticles using cloud point extraction with non-ionic surfactant mixtures. *J. Colloid Interface Sci.*, **363**(2), 490–496.
92. Hendren, C., Lowry, G., Unrine, J., and Wiesner, M. (2015). A functional assay-based strategy for nanomaterial risk forecasting. *Sci. Total Environ.*, **536**, 1029–1037.
93. Westerhoff, P., and Nowack, B. (2013). Searching for Global Descriptors of Engineered Nanomaterial Fate and Transport in the Environment. *Accounts of Chemical Research*, **46**(3), pp. 844–853.
94. Yokel, R. A., and MacPhail, R. C. (2011). Engineered nanomaterials: Exposures, hazards, and risk prevention. *Journal of Occupational Medicine and Toxicology*, **6**(1), pp. 7-7.
95. Naldoni, A., Allieta, M., Santangelo, S., Marelli, M., Fabbri, F., Cappelli, S., and Dal Santo, V. (2012). Effect of nature and location of defects on bandgap narrowing in black TiO₂ nanoparticles. *Journal of the American Chemical Society*, **134**(18), pp. 7600-7603
96. Zhang, H., Ji, Z., Xia, T., Meng, H., Low-Kam, C., Liu, R., and Nel, A. E. (2012). Use of metal oxide nanoparticle band gap to develop a predictive paradigm for oxidative stress and acute pulmonary inflammation. *ACS Nano*, **6**(5), pp. 4349-4368
97. George, S., Pokhrel, S., Ji, Z., Henderson, B. L., Xia, T., Li, L., and Mädler, L. (2011). Role of Fe doping in tuning the band gap of TiO₂ for the photo-oxidation-induced

- cytotoxicity paradigm. *Journal of the American Chemical Society*, 133(29), pp. 11270-11278.
98. Gottschalk, F., Sonderer, T., Scholz, R. W., and Nowack, B. (2009). Modeled environmental concentrations of engineered nanomaterials (TiO₂, ZnO, Ag, CNT, fullerenes) for different regions. *Environmental Science and Technology*, 43(24), pp. 9216-9222.
 99. Darlington, T. K., Neigh, A. M., Spencer, M. T., Guyen, O. T., and Oldenburg, S. J. (2009). Nanoparticle characteristics affecting environmental fate and transport through soil. *Environmental Toxicology and Chemistry*, 28(6), pp. 1191-1199.
 100. Praetorius, A., Scheringer, M., and Hungerbühler, K. (2012). Development of Environmental Fate Models for Engineered Nanoparticles: A Case Study of TiO₂ Nanoparticles in the Rhine River. *Environmental Science and Technology*, 46(12), pp. 6705-6713.
 101. Selick, Harold E., Alan P. Beresford, and Michael H. Tarbit. (2002). The emerging importance of predictive ADME simulation in drug discovery. *Drug Discovery Today*, 7(2), pp. 109-116.
 102. Yu, H., and Adedoyin, A. (2003). ADME-Tox in drug discovery: integration of experimental and computational technologies. *Drug Discovery Today*, 8(18), pp. 852-861.
 103. Mandrell, D.; Truong, L.; Jephson, C.; Sarker, M. R.; Moore, A.; Lang, C.; Simonich, M. T.; and Tanguay, R. L. (2012). Automated Zebrafish Chorion Removal and Single Embryo Placement: Optimizing Throughput of Zebrafish Developmental Toxicity Screens. *Jala*, 17, (1), pp. 66-74.
 104. Truong, L.; Tilton, S. C.; Zaikova, T.; Richman, E.; Waters, K. M.; Hutchison, J. E.; and Tanguay, R.L. (2013). Surface functionalities of gold nanoparticles impact embryonic gene expression responses. *Nanotoxicology*, 7(2), pp. 192-201.
 105. Cassano, A., Robinson, M., Palczewska, A., Puzyn, T., Gajewicz, A., Tran, L., Manganelli, S., and Cronin, M.. (2016). Comparing the CORAL and Random Forest Approaches for Modelling the In Vitro Cytotoxicity of Silica Nanomaterials. *Alternative to Lab Animals: ATLA*, 44(6), pp. 533.
 106. Goldberg, E., Scheringer, M., Bucheli, T., and Hungerbuhler, K. (2015). Prediction of nanoparticle transport behavior from physicochemical properties: machine learning provides insights to guide the next generation of transport models. *Environmental Science: Nano*, 2(4), pp. 352-360.

107. Winkler, David. (2016). Recent advances, and unresolved issues, in the application of computational modelling to the prediction of the biological effects of nanomaterials. *Toxicology and Applied Pharmacology*, 299, pp. 96-100.
108. Allan, S. E.; Smith, B. W.; Tanguay, R. L.; and Anderson, K. A. (2012). Bridging environmental mixtures and toxic effects. *Environmental Toxicology and Chemistry*, 31(12), pp. 2877-2887.
109. Kim, K., Truong, L., Wehmas, L., and Tanguay, R. L. (2013). Silver nanoparticle toxicity in the embryonic zebrafish is governed by particle dispersion and ionic environment. *Nanotechnology*, 24(11), pp. 115101
110. Chen, J. F.; Das, S. R.; La Du, J.; Corvi, M. M.; Bai, C. L.; Chen, Y. H.; Liu, X. J.; Zhu, G. N.; Tanguay, R. L.; Dong, Q. X.; and Huang, C. J. (2013). Chronic PFOS exposures induce life stage-specific behavioral deficits in adult zebrafish and produce malformation and behavioral deficits in F1 offspring. *Environmental Toxicology and Chemistry*, 32(1), pp. 201-206.
111. Corvi, M. M.; Stanley, K. A.; Peterson, T. S.; Kent, M. L.; Feist, S. W.; La Du, J. K.; Volz, D. C.; Hosmer, A. J.; and Tanguay, R. L. (2012). Investigating the Impact of Chronic Atrazine Exposure on Sexual Development in Zebrafish. *Birth Defects Research Part B-Developmental and Reproductive Toxicology*, 95(4), pp. 276-288.
112. Kim, K. T.; Jang, M. H.; Kim, J. Y.; Xing, B. S.; Tanguay, R. L.; Lee, B. G.; and Kim, S. D. (2012). Embryonic toxicity changes of organic nanomaterials in the presence of natural organic matter. *Science of the Total Environment*, 426, pp. 423-429.
113. Liu, R.; Lin, S. J.; Rallo, R.; Zhao, Y.; Damoiseaux, R.; Xia, T.; Lin, S.; Nel, A.; and Cohen, Y. (2012). Automated Phenotype Recognition for Zebrafish Embryo Based In vivo High Throughput Toxicity Screening of Engineered Nano-Materials. *PLoS One*, 7, (4).
114. Corredor, C., Borysiak, M. D., Wolfer, J., Westerhoff, P., and Posner, J. D. (2015). Colorimetric detection of catalytic reactivity of nanoparticles in complex matrices. *Environmental Science and Technology*, 49(6), pp. 3611-3618
115. Khaksar, M., Boghaei, D. M., and Amini, M. (2015). Synthesis, structural characterization and reactivity of manganese tungstate nanoparticles in the oxidative degradation of methylene blue. *Comptes Rendus Chimie*, 18(2), pp. 199-203

116. Sabry, R. S., Al-Haidarie, Y. K., and Kudhier, M. A. (2016). Synthesis and photocatalytic activity of TiO₂ nanoparticles prepared by sol–gel method. *Journal of Sol-Gel Science and Technology*, 78(2), pp. 299-306
117. Nel, A., Madler, L., Velegol, D., Xia, T., Hoek, E., Somasundaran, P., Klaessig, F., Castranova, V., and Thompson, M. (2009). Understanding biophysicochemical interactions at the nano-bio interface. *Nature Materials*, 8, pp. 543-557
118. Xiao, Y., and Wiesner, M. R. (2012). Characterization of surface hydrophobicity of engineered nanoparticles. *Journal of Hazardous Materials*, pp. 215-216
119. Hristovski, K., Westerhoff, P., and Posner, J. (2011). Octanol-water distribution of engineered nanomaterials. *Journal of Environmental Science and Health, Part A: Toxic/Hazardous substances and environmental engineering*. 46(6), pp. 636-647
120. Shahbazi-Gahrouei, D., Abdolahi, M., Zarkesh-Esfahani, S., Laurent, S., Sermeus, C., and Gruettner, C. (2013). Functionalized nanoparticles for the detection and quantitative analysis of cell surface antigen. *BioMed Research International Volume 2013*.
121. Park, H., Hwang, M., and Lee, K. (2013). Immunomagnetic nanoparticle-based assays for detection of biomarkers. *International Journal of Nanomedicine*. 8, pp. 4543-4552
122. Liu, X., and Chen, K.L. (2015). Interactions of Graphene oxide with model cell membranes: probing nanoparticle attachment and lipid bilayer disruption. *Langmuir*, 31(44), pp. 12076-86.
123. Hendren, C., Lowry, G., Unrine, J., and Wiesner, M. (2015). A functional assay-based strategy for nanomaterial risk forecasting. *Science of the Total Environment*, 536, pp. 1029-1037.
124. Crittenden, J., Smetana, S., and Pandit, A. (2014). Target Plots for Environmentally Responsible Selection of Chemicals. Center for Sustainable Engineering Electronic Library for Educational Modules.
125. Speed, D., et al. (2015). Physical, chemical, and in vitro toxicological characterization of nanoparticles in chemical mechanical planarization suspensions used in the semiconductor industry: towards environmental health and safety assessments. *Environmental Science Nano*, 2(3): pp. 227-244.
126. Lee, S., et al. (2014). Nanoparticle Size Detection Limits by Single Particle ICP-MS for 40 Elements. *Environmental Science and Technology*, 48(17): pp. 10291-10300.

127. Bi, X.Y., et al. (2014). Quantitative resolution of nanoparticle sizes using single particle inductively coupled plasma mass spectrometry with the K-means clustering algorithm. *Journal of Analytical Atomic Spectrometry*, 29(9): p. 1630-1639.
128. Mitrano, D.M., et al. (2013). Silver nanoparticle characterization using single particle ICP-MS (SP-ICP-MS) and asymmetrical flow field flow fractionation ICP-MS (AF4-ICP-MS) (vol 27, pg 1131, 2012). *Journal of Analytical Atomic Spectrometry*, 28(12): pp. 1949.
129. Reed, R. B., Ladner, D. A., Higgins, C. P., Westerhoff, P., and Ranville, J. F. (2012). Solubility of nano-zinc oxide in environmentally and biologically important matrices. *Environmental Toxicology and Chemistry*, 31(1), pp. 93-99
130. Doudrick, K., P. Herckes, and P. Westerhoff. (2012). Detection of Carbon Nanotubes in Environmental Matrices Using Programmed Thermal Analysis. *Environmental Science and Technology*, 46, pp. 12246-12253
131. Environmental Protection Agency. (1992). Toxicity Characteristic Leaching Procedure. Method 1311. Found online at: <https://www.epa.gov/sites/production/files/2015-12/documents/1311.pdf>
132. Telgmann, L., Nguyen, M., Shen, L., Yargeau, V., Hintelmann, H., and Metcalfe, C. (2016). Single particle ICP-MS as a tool for determining the stability of silver nanoparticles in aquatic matrixes under various environmental conditions, including treatment by ozonation. *Analytical and Bioanalytical Chemistry*, 408(19), pp. 5169-5177
133. Liu, J., and Hurt, R. (2010). Ion release kinetics and particle persistence in aqueous nano-silver kinetics. *Environmental Science and Technology*, 44(6), 2169-2175
134. Duester, L., Fabricius, A., Jakobtorweihen, S., Philippe, A., Weigl, F., Wimmer, A., Schuster, M., Nazar, M. (2016). Can cloud point-based enrichment, preservation, and detection methods help to bridge gaps in aquatic nanometrology? *Analytical and Bioanalytical Chemistry*, 408, pp. 7551-7557
135. Kiser, M., Ladner, D., Hristovski, K., and Westerhoff, P. (2012). Nanomaterial transformation and association with fresh and freeze-dried wastewater activated sludge: implications for testing protocol and environmental fate. *Environmental Science and Technology*, 46(13), pp. 7046-7053
136. Kiser, M., Ryu, H., Jang, H., Hristovski, K., and Westerhoff, P. (2010). Biosorption of nanoparticles to heterotrophic wastewater biomass. *Water Research*, 44(14), pp. 4105-4114

137. Garner, K., Suh, S., Lenihan, H., and Keller, A. (2015). Species sensitivity distributions for engineered nanomaterials. *Environmental Science and Technology*, 49, pp. 5753-5759
138. Bai, W., Zhang, Z., Tian, W. et al. (2010). Toxicity of zinc oxide nanoparticles to zebrafish embryo: a physicochemical study of toxicity mechanism. *Journal of Nanoparticle Research*, 12, pp. 1645-52
139. Shaw, B., and Handy, R. (2011). Physiological effects of nanoparticles on fish: a comparison of nanometals versus metal ions. *Environment International*. 37(6), pp. 1083-1097
140. Uebe, R., and Schuler, D. (2016). Magnetosome biogenesis in magnetotactic bacteria. *Nature Reviews Microbiology*, 14(10), pp. 621-637.
141. G. D. Douglas, A. E. Bence, R. C. Prince, S. J. McMillen and E. L. Butler, Environmental stability of selected petroleum hydrocarbon source and weathering ratios, *Environ. Sci. Technol.*, 1996, 30, 2332–2339.
142. R. Munter, Advanced oxidation processes—current status and prospects, *Proc. Est. Acad. Sci., Chem.*, 2001, 50, 59–80.
143. K. Urum, S. Grigson, T. Pekdemir and S. McMenamy, A comparison of the efficiency of different surfactants for removal of crude oil from contaminated sites, *Chemosphere*, 2006, 62, 1403–1410.
144. Z. Wang, M. Fingas and D. S. Page, Oil spill identification, *J. Chromatogr. A*, 1999, 843, 369–411.
145. Y. C. Chien, Field study of in situ remediation of petroleum hydrocarbon contaminated soil on site using microwave energy, *J. Hazard. Mater.*, 2012, 199–200, 457–461.
146. S. Mutyala, C. Fairbridge, J. R. Jocelyn Pare, J. M. R. Belanger, S. Ng and R. Hawkins, Microwave applications to oil sands and petroleum: A review, *Fuel Process. Technol.*, 2010, 91, 127–135.
147. R. Naidu, Recent advances in contaminated site remediation, *Water, Air, Soil Pollut.*, 2013, 224, 1705.
148. A. Abramovitch, L. Chang-Qing, E. Hicks and J. Sinard, In situ remediation of soils contaminated with toxic metal ions using microwave energy, *Chemosphere*, 2003, 53, 1077–1085.

149. D. A. Jones, T. P. Lelyveld, S. D. Mavrofidis, S. W. Kingman and N. J. Miles, Microwave heating applications in environmental engineering—a review, *Resour., Conserv. Recycl.*, 2002, 34, 75–90.
150. X. Liu and G. Yu, Combined effect of microwave and activated carbon on the remediation of polychlorinated biphenyl-contaminated soil, *Chemosphere*, 2006, 63, 228–235.
151. D. Li, Y. Zhang, X. Quan and Y. Zhao, Microwave thermal remediation of crude oil contaminated soil enhanced by carbon fiber, *J. Environ. Sci.*, 2009, 21, 1290–1295.
152. Z. Kawala and T. Atamaczuk, Microwave enhanced thermal decontamination of soil, *Environ. Sci. Technol.*, 1998, 32, 2602–2607.
153. T. Kim, J. Lee and K.-H. Lee, Microwave heating of carbon- based solid materials, *Carbon Lett.*, 2014, 15, 15–24.
154. J. A. Menendez, A. A. B. Fidalgo, F. L. Zubizarreta, E. G. Calvo and J. M. Bermudez, Microwave heating processes involving carbon materials, *Fuel Process. Technol.*, 2010, 91, 1–8.
155. J. Chen, S. Xue, Y. Song, M. Shen, Z. Zhang, T. Yuan, F. Tian and D. Dionysiou, Microwave-induced carbon nanotubes catalytic degradation of organic pollutants in aqueous solution, *J. Hazard. Mater.*, 2016, 310, 226–234.
156. F. Irin, B. Shrestna, J. E. Canas, M. A. Saed and M. J. Green, Detection of carbon nanotubes in biological samples through microwave-induced heating, *Carbon*, 2012, 50, 4441–4449.
157. S. Li, F. Irin, F. O. Atore, M. J. Green and J. E. Canas-Carell, Determination of multi-walled carbon nanotube bio- accumulation in earthworms measured by a microwave- based detection technique, *Sci. Total Environ.*, 2013, 445– 446, 9–13.
158. E. J. G. Santos and E. Kaxiras, Electric-field dependence of the effective dielectric constant in graphene, *Nano Lett.*, 2013, 13, 898–902.
159. U. Weissker, S. Hampel, A. Leonhardt and B. Buchner, Carbon nanotubes filled with ferromagnetic materials, *Materials*, 2010, 3, 4387–4427.
160. C. G. Jou, C. R. Wu and C. L. Lee, Application of microwave energy to treat granular activated carbon content with chlorobenzene, *Environ. Prog. Sustainable Energy*, 2010, 29, 272–277.

161. S. Yuan, M. Tian and X. Lu, Microwave remediation of soil contaminated with hexachlorobenzene, *J. Hazard. Mater.*, 2006, B137, 878–885.
162. H. C. Chang, C. J. G. Jou and C. L. Lee, Treatment of heavy oil contaminated sand by microwave energy, *Environ. Eng. Sci.*, 2011, 28, 869–873.
163. O. G. Apul, P. Dahlen, A. Delgado, F. Sharif and P. Westerhoff, Treatment of heavy, long-chain petroleum-hydrocarbon impacted soils using chemical oxidation, *J. Environ. Eng.*, 2016, 040160065.
164. A. G. Delgado, D. Fajardo-Williams, S. C. Papat, C. I. Torres and R. Krajmalnik-Brown, Successful operation of continuous reactors at short retention times results in high-density, fast-rate *Dehalococcoides* dechlorinating cultures, *Appl. Microbiol. Biotechnol.*, 2014, 98, 2729–2737.
165. T. Chen, B. M. Yavuz, A. G. Delgado, A. J. Proctor, J. Maldonado, Y. Zuo, P. Westerhoff, R. Krajmalnik-Brown and B. E. Rittmann, Ozone enhances the bioavailability of heavy hydrocarbons in soil, *J. Environ. Eng. Sci.*, 2016, 11, 7–17.
166. P. P. Falciglia, G. Ursom and F. G. A. Vagliasindi, Microwave heating remediation of soils contaminated with diesel fuel, *J. Soils Sediments*, 2013, 13, 1396–1407.
167. P. P. Falciglia and F. G. A. Vagliasindi, Remediation of hydrocarbon polluted soils using 2.45 GHz frequency-heating: Influence of operating power and soil texture on soil temperature profiles and contaminant removal kinetics, *J. Geochem. Explor.*, 2015, 151, 66–73.
168. Amy, G., Siddiqui, M.S., Zhai, W., DeBroux, J., and Odem, W. (1994). *Survey of bromide in drinking water and impacts on DBP formation*. American Water Works Association.
169. Apul, O., Wang, Q., Zhou, Y., and Karanfil, T. (2013). Adsorption of aromatic organic contaminants by graphene nanosheets: Comparison with carbon nanotubes and activated carbon. *Water Research*, 47(4), pp. 1648-1654.
170. Chen, C., Apul, O., and Karanfil, T. (2016). Removal of bromide from surface waters using silver impregnated activated carbon. *Water Research*.
171. Das, M., Sarma, R., Saikia, R., Kale, V., Shelke, M., and Sengupta, P. (2011). Synthesis of silver nanoparticles in an aqueous suspension of graphene oxide sheets and its antimicrobial activity. *Colloids and Surfaces B: Biointerfaces*, 83(1), pp. 16-22.

172. Davis, S. N., Whittemore, D. O., and Fabryka-Martin, J. (1998). Uses of chloride/bromide ratios in studies of potable water. *Ground Water*, 36 (2), pp. 338-350.
173. Dreyer, D., Todd, A., and Bielawski, C. (2014). Harnessing the chemistry of graphene oxide. *Chemical Society Reviews*, 43(15), pp. 5288-5310.
174. Ersan, G., Kaya, Y., Apul, O., and Karanfil, T. (2016). Adsorption of organic contaminants by graphene nanosheets, carbon nanotubes and granular activated carbons under natural organic matter preloading conditions. *Science of the Total Environment*, 565, pp. 811-817.
175. Fehn, U., Snyder, G., and Egeberg, P. K. (2000). Dating of pore waters with ¹²⁹I: relevance
176. Ferrar, K. J., Michanowicz, D. R., Christen, C. L., Mulcahy, N., Malone, S. L., and Sharma, R. K. (2013). Assessment of effluent contaminants from three facilities discharging Marcellus Shale wastewater to surface waters in Pennsylvania. *Environmental Science and Technology*, 47(7), pp. 3472-3481.
177. Ferrari, A. (2007). Raman spectroscopy of graphene and graphite: disorder, electron-phonon coupling, doping and nonadiabatic effects. *Solid State Communications*, 143(1), pp. 47-57.
178. Ferrari, A., and Basko, D. (2013). Raman spectroscopy as a versatile tool for studying the properties of graphene. *Nature Nanotechnology*, 8(4), pp. 235-246.
179. for the origin of marine gas hydrates. *Science*, 289(5488), pp. 2332-2335.
180. Frommer, M. A., and Dalven, I. (2000). *U.S. Patent No. 6,071,415*. Washington, DC: U.S. Patent and Trademark Office.
181. Guo, F., Creighton, M., Chen, Y., Hurt, R., and Kulaots, I. (2014). Porous structures in stacked, crumpled and pillared graphene-based 3D materials. *Carbon*, 66, pp. 476-484.
182. Harkness, J., Dwyer, G., Warner, N., Parker, K., Mitch, W., and Vengosh, A. (2015). Iodide, bromide, and ammonium in hydraulic fracturing and oil and gas wastewaters: environmental implications. *Environmental Science & Technology*, 49 (3), pp. 1955-1963
183. He, D., Garg, S., and Waite, D. (2012). H₂O₂-mediated oxidation of zero-valent silver and resultant interactions among silver nanoparticles, silver ions, and reactive oxygen species. *Langmuir*, 28 (27), pp. 10266-10275

184. Kampioti, A. A., and Stephanou, E. G. (2002). The impact of bromide on the formation of neutral and acidic disinfection by-products (DBPs) in Mediterranean chlorinated drinking water. *Water Research*, 36 (10), pp. 2596–2606.
185. Katz, B. G., Eberts, S. M., and Kauffman, L. J. (2011). Using Cl/Br ratios and other indicators to assess potential impacts on groundwater quality from septic systems: a review and examples from principal aquifers in the United States. *Journal of Hydrology*, 397 (3), pp. 151-166.
186. Kolker, A., Quick, J., Senior, C., and Belkin, H., (2012). Mercury and halogens in coal—Their role in determining mercury emissions from coal combustion: U.S. Geological Survey Fact Sheet 2012–3122, 6 p.
187. Li, Q., Snoeyink, V., Marinas, B., and Campos, C. (2003). Pore blockage effect of NOM on atrazine adsorption kinetics of PAC: The roles of PAC pore size distribution and NOM molecular weight. *Water Research*, 37(20), pp. 4863-4872.
188. Marcano, M., Kosynkin, D., Berlin, J., Sinitskii, A., Sun, Z., Slesarev, A., Alemany, L., Lu, W., and Tour, J. (2010). Improved Synthesis of Graphene Oxide. *ACS Nano*, 4 (8), pp. 4806-4814
189. McTigue, N. E., Cornwell, D. A., Graf, K., and Brown, R. (2014). Occurrence and consequences of increased bromide in drinking water sources. *American Water Works Association*, 106 (11), pp. E492-E508.
190. Minear, R. A., and Amy, G. (1995). *Disinfection By-Products in Water Treatment: The Chemistry of Their Formation and Control*. CRC Press.
191. Mullaney, J. R., Lorenz, D. L., and Arntson, A. D. (2009). *Chloride in groundwater and surface water in areas underlain by the glacial aquifer system, northern United States*. Reston, VA: US Geological Survey.
192. Norman, W. D., Jasinski, R. J., and Nelson, E. B. (1996). *U.S. Patent No. 5,551,516*. Washington, DC: U.S. Patent and Trademark Office.
193. Perreault, F., De Faria, A. F., and Elimelech, M. (2015). Environmental applications of graphene-based nanomaterials. *Chemical Society Reviews*, 44(16), pp. 5861-5896.
194. Pham, C., Eck, M., and Krueger, M. (2013). Thiol functionalized reduced graphene oxide as a base material for noel graphene-nanoparticle hybrid composites. *Chemical Engineering Journal*, 231, pp. 146-154.

195. Plewa, M. J., Wagner, E. D., Muellner, M. G., Hsu, K. M., and Richardson, S. D. (2008). Comparative mammalian cell toxicity of N-DBPs and C-DBPs. *Urbana*, 51, pp. 61801.
 196. Polo, A., Velo-Gala, I., Sanchez-Polo, M., von Gunten, U., Lopez-Penalver, J., and Rivera-Utrilla, J. (2016). Halide removal from aqueous solution by novel silver-polymeric materials. *Science of the Total Environment*, 573, pp. 1125-1131.
 197. Richardson, S. D., Fasano, F., Ellington, J. J., Crumley, F. G., Buettner, K. M., Evans, J., and McKague, A. B. (2008). Occurrence and mammalian cell toxicity of iodinated disinfection byproducts in drinking water. *Environmental Science and Technology*, 42 (22), pp. 8330-8338.
 198. Richardson, S., and Postigo, C. (2017). Liquid Chromatography-Mass Spectrometry of Emerging Disinfection By-products. *Comprehensive Analytical Chemistry*, 79.
 199. Sawade, E., Fabris, R., Humpage, A., and Drikas, M. (2016). Effect of increasing bromide concentration on toxicity in treated drinking water. *Journal of Water and Health*, 14(2), pp. 183-191.
 200. Soltermann, F., Abegglen, C., Götz, C. W., and von Gunten, U. (2016). Bromide sources and loads in Swiss surface waters and their relevance for bromate formation during wastewater ozonation. *Environmental Science and Technology*, 50, pp. 9825-9834.
 201. Tung, V., Allen, M., Yang, Y., and Kaner, R. (2008). High-throughput solution processing of large-scale graphene. *Nature Nanotechnology*, 4, pp. 25 - 29
 202. Westerhoff, P., Yoon, Y., Snyder, S., and Wert, E. (2005). Fate of endocrine-disruptor, pharmaceutical, and personal care product chemicals during simulated drinking water treatment processes. *Environmental Science and Technology*, 39 (17), pp. 6649-6663.
 203. Wilson, J., and VanBriesen, J. (2012). Oil and gas produced water management and surface drinking water sources in Pennsylvania. *Environmental Practice*, 14 (4), pp. 288-300.
 204. Wilson, J., and VanBriesen, J. (2013). Source water changes and energy extraction activities in the Monongahela River, 2009–2012. *Environmental Science & Technology*, 47 (21), pp. 12575-12582.
- Winid, B. (2015). Bromine and water quality—Selected aspects and future perspectives. *Applied Geochemistry*, 63, pp. 413-435.

205. Yang, Y., Komaki, Y., Kimura, S. Y., Hu, H. Y., Wagner, E. D., Mariñas, B. J., and Plewa, M. J. (2014). Toxic impact of bromide and iodide on drinking water disinfected with chlorine or chloramines. *Environmental Science and Technology*, 48 (20), pp. 12362-12369.
206. Zhai, H., Zhang, X., Zhu, X., Liu, J., and Ji, M. (2014). Formation of brominated disinfection byproducts during chloramination of drinking water: New polar species and overall kinetics. *Environmental Science and Technology*, 48(5), pp. 2579-2588
207. Zhao, G., Li, J., Ren., Chen, C., and Wang, X. (2011). Few-Layered Graphene oxide nanosheets as superior sorbents for heavy metal ion pollution management. *Environmental Science and Technology*, 45 (24), pp. 10454-10462.
208. Mohammadzadeh, F., Jahanshahi, M., and Rashidi, A. Preparation of nanosensors based on organic functionalized MWCNT for H₂S detection. *Applied Surface Science* **2012**, 259, pp. 159-165
209. Dorraji, S., Ahadzadeh, I., and Rasoulifard, M. Chitosan/polyaniline/ MWCNT nanocomposite fibers as an electrode material for electrical double layer capacitors. *International Journal of Hydrogen Energy* **2014**, 39(17), pp. 9350-9355.
210. Asmatulu, R., Mahmud, G. A., Hille, C., and Misak, H. E. Effects of UV degradation on surface hydrophobicity, crack, and thickness of MWCNT-based nanocomposite coatings. *Progress in Organic Coatings* **2011**, 72(3), pp. 553-561
211. Kuznetsov, A. A., Lee, S. B., Zhang, M., Baughman, R. H., and Zakhidov, A. Electron field emission from transparent multiwalled carbon nanotube sheets for inverted field emission displays. *Carbon* **2010**, 48(1), pp. 41-46
212. Mueller, N., and Nowack, B. Exposure modelling of engineered nanoparticles in the environment. *Environmental Science and Technology* **2008**, 15(42), pp. 4447-4453
213. Gottschalk, F., Sonderer, T., Scholz, R., and Nowack, B. Modeled environmental concentrations of engineered nanomaterials (TiO₂, ZnO, Ag, CNT, Fullerenes) for different regions. *Environmental Science and Technology* **2009**, 43(24), pp. 9216-9222
214. Petersen, E., Zhang, L., Mattison, N., O'Carroll, D., Whelton, A., Uddin, N., Nguyen, T., Huang, Q., Henry, T., Holbrook, D., and Chen, K. Potential Release Pathways, Environmental Fate, and Ecological Risks of Carbon Nanotubes. *Environmental Science and Technology* **2011**, 45(23), pp. 9837-9856.

215. Garner, K., Suh, S., Lenihan, H., and Keller, A. Species sensitivity distributions for engineered nanomaterials. *Environmental Science and Technology* **2015**, 49, pp. 5753-5759
216. Jackson, P., Jacobsen, N., Baun, A., Birkedal, R., Kuhnel, D., Jensen, K., Vogel, U., and Wallin, H. Biaccumulation and ecotoxicity of carbon nanotubes. *Chemistry Central Journal* **2013**, 7, pp. 154-175
217. Kiser, M. A., Ladner, D. A., Hristovski, K. D., and Westerhoff, P. Nanomaterial transformation and association with fresh and freeze-dried wastewater activated sludge: Implications for testing protocol and environmental fate. *Environmental Science and Technology*, **2012**, 46(13), pp. 7046
218. Kiser, M. A., Westerhoff, P., Benn, T., Wang, Y., Pérez-Rivera, J., and Hristovski, K. Titanium nanomaterial removal and release from wastewater treatment plants. *Environmental Science and Technology* **2009**, 43(17), pp. 6757-6763
219. Westerhoff, P. K., Kiser, M. A., and Hristovski, K. Nanomaterial removal and transformation during biological wastewater treatment. *Environmental Engineering Science* **2013**, 30(3), pp. 109-117
220. Yang, Y., Yu, Z., Nosaka, T., Doudrick, K., Hristovski, K., Herckes, P., and Westerhoff, P. Interaction of carbonaceous nanomaterials with wastewater biomass. *Frontiers of Environmental Science and Engineering* **2015**, 9(5), pp. 823-831
221. Petersen, E., Cervantes, D., Bucheli, T., Elliott, L., Fagan, J., Gogos, A., Hanna, S., Kagi, Ralf, Mansfield, E., Bustos, A., Plata, D., Reipa, V., Westerhoff, P., and Winchester, M. Quantification of carbon nanotubes in environmental matrices: current capabilities, cases studies and future prospects. *Environmental Science and Technology* **2016**, 50(9), pp. 4587-4605
222. Reed, R. B., Goodwin, D. G., Marsh, K. L., Capracotta, S. S., Higgins, C. P., Fairbrother, D. H., and Ranville, J. F. Detection of single walled carbon nanotubes by monitoring embedded metals. *Environmental Science: Processes and Impacts* **2013**, 15(1), pp. 204-213.
223. Montano, M. D.; Badiei, H. R.; Bazargan, S.; Ranville, J. Improvements in the detection and characterization of engineered nanoparticles using spICP-MS with microsecond dwell times. *Environmental Science: Nano* **2014**, 1(4), pp. 338-346.
224. Wang, J., Lankone, R., Reed, R., Fairbrother, H., and Ranville, J. Analysis of single-walled carbon nanotubes using spICP-MS with microsecond dwell time. *NanoImpact* **2016**, 1, pp. 65-72

225. Kiser, M. A., Ryu, H., Jang, H., Hristovski, K., and Westerhoff, P. Biosorption of nanoparticles to heterotrophic wastewater biomass. *Water Research* **2010**, 44(14), pp. 4105-4114
226. Doudrick, K., Herckes, P., and Westerhoff, P. Detection of carbon nanotubes in environmental matrices using programmed thermal analysis. *Environmental Science and Technology* **2012**, 46(22), pp. 12246-12253
227. Corredor, C., Hou, W., Klein, S., Moghadam, B., Goryll, M., Doudrick, K., Westerhoff, P., and Posner, J. Disruption of model cell membranes by carbon nanotubes. *Carbon* **2013**, 60, pp. 67
228. Silva, R. M., Doudrick, K., Franzi, L. M., TeeSy, C., Anderson, D. S., Wu, Z., and Pinkerton, K. E. Instillation versus inhalation of multiwalled carbon nanotubes: Exposure-related health effects, clearance, and the role of particle characteristics. *ACS Nano* **2014**, 8(9), pp. 8911-8931
229. Doudrick, K., Nosaka, T., Herckes, P., and Westerhoff, P. Quantification of graphene and graphene oxide in complex organic matrices. *Environmental Science: Nano* **2015**, 2(1), pp. 60-67
230. Ge, C., Lao, F., Li, W., Li, Y., Chen, C., Qiu, Y., Mao, X., Li, B., Chai, Z., and Zhao, Y. Quantitative Analysis of Metal Impurities in Carbon Nanotubes: Efficacy of Different Pretreatment Protocols for ICPMS Spectroscopy. *Analytical Chemistry* **2008**, 80 (24), pp. 9426-9434.
231. Lee, S., Bi, X., Reed, R., Ranville, J., Herckes, P., and Westerhoff, P. Nanoparticle size detection limits by single particle ICP-MS for 40 elements. *Environmental Science and Technology* **2014**, 48(17), 10291-10300.
232. Bi, X., Lee, S., Ranville, J. F., Sattigeri, P., Spanias, A., Herckes, P., and Westerhoff, P. Quantitative resolution of nanoparticle sizes using single particle inductively coupled plasma mass spectrometry with the K-means clustering algorithm. *Journal of Analytical Atomic Spectrometry* **2014**, 29(9), 1630-1639.
233. Mitrano, D. M., Ranville, J. F., Bednar, A., Kazor, K., Hering, A. S., and Higgins, C. P. Tracking dissolution of silver nanoparticles at environmentally relevant concentrations in laboratory, natural, and processed waters using single particle ICP-MS (spICP-MS). *Environmental Science: Nano* **2014**, 1(3), 248-259.
234. Westerhoff, P., Lee, S., Yang, Y., Gordon, G., Hristovski, K., Halden, R., and Herckes, P. Characterization, recovery opportunities, and valuation of metals in

- municipal sludges from US wastewater treatment plants nationwide. *Environmental Science and Technology* **2015**, 49, pp. 9479-9488
235. Pace, H., Rogers, N., Jarolimek, C., Coleman, V., Higgins, C., and Ranville, J. Determining transport efficiency for the purpose of counting and sizing nanoparticles via single particle inductively coupled plasma mass spectrometry. *Analytical Chemistry* **2011**, 83 (24), pp. 9361-9369.
 236. Eatemadi, A., Daraee, H., Karimkhanloo, H., Kouhi, M., Zarghami, N., Akbarzadeh, A., Abasi, M., Hanifehpour, Y., and Joo, S. *Nanoscale Research Letters* **2014**, 9(1), pp. 393-406
 237. Kateb, B., Yamamoto, V., Alizadeh, D., Zhang, L., Manohara, H., Bronikowski, M., and Badie, B. Multi-walled carbon nanotube (MWCNT) synthesis, preparation, labeling, and functionalization. *Methods in Molecular Biology* **2010**, 651, pp. 307-317
 238. Kiser, M.A., et al., Biosorption of nanoparticles to heterotrophic wastewater biomass. *Water Research*, 2010. **44**(14): p. 4105-4114.
 239. Kiser, M.A., et al., Titanium Nanomaterial Removal and Release from Wastewater Treatment Plants. *Environmental Science & Technology*, 2009. **43**(17): p. 6757-6763.
 240. Keller, A.A. and A. Lazareva, Predicted releases of engineered nanomaterials: From global to regional to local. *Environ. Sci. Tech. Letters*, 2014. **1**(1): p. 65-70.
 241. Mueller, N.C. and B. Nowack, Exposure modeling of engineered nanoparticles in the environment. *Environmental Science & Technology*, 2008. **42**(12): p. 4447-4453.
 242. Piccinno, F., et al., Industrial production quantities and uses of ten engineered nanomaterials in Europe and the world. *Journal of Nanoparticle Research*, 2012. **14**(9).
 243. Gottschalk, F., T. Sun, and B. Nowack, Environmental concentrations of engineered nanomaterials: Review of modeling and analytical studies. *Environmental Pollution*, 2013. **181**: p. 287-300.
 244. Reed, R.B., et al., Solubility of nano-zinc oxide in environmentally and biologically important matrices. *Environmental Toxicology and Chemistry*, 2012. **31**(1): p. 93-99.
 245. Robichaud, C.O., et al., Estimates of Upper Bounds and Trends in Nano-TiO₂ Production As a Basis for Exposure Assessment *Environ. Sci. Technol.*, 2009.

- 43**(12): p. 4227-4233.
246. Kaegi, R., et al., Fate and transformation of silver nanoparticles in urban wastewater systems. *Water Research*, 2013. **47**(12): p. 3866-3877.
247. Thalmann, B., et al., Sulfidation Kinetics of Silver Nanoparticles Reacted with Metal Sulfides. *Environmental Science & Technology*, 2014. **48**(9): p. 4885-4892.
- Conway, J.R., et al., Aggregation, Dissolution, and Transformation of Copper Nanoparticles in Natural Waters. *Environmental Science & Technology*, 2015. **49**(5): p. 2749-2756.
248. Hong, J., et al., Toxic effects of copper-based nanoparticles or compounds to lettuce (*Lactuca sativa*) and alfalfa (*Medicago sativa*). *Environmental Science-Processes & Impacts*, 2015. **17**(1): p. 177-185.
249. Lenton, S., et al., A review of the biology of calcium phosphate sequestration with special reference to milk. *Dairy Science & Technology*, 2015. **95**(1): p. 3-14.
250. Miretzky, P. and A. Fernandez-Cirelli, Phosphates for Pb immobilization in soils: a review. *Environmental Chemistry Letters*, 2008. **6**(3): p. 121-133.
251. Piccoli, P. and P. Candela, Apatite in felsic rocks – a model for the estimation of initial halogen concentrations in the bishop tuff (long valley and tuolumne intrusive suite(sierra-nevada batholith) magmas. *American Journal of Science*, 1994. **294**(1): p. 92-135.
252. Vance, M.E., et al., Nanotechnology in the real world: Redeveloping the nanomaterial consumer products inventory. *Beilstein Journal of Nanotechnology*, 2015. **6**: p. 1769-1780.
253. e-Bashan, L.E. and Y. Bashan, Recent advances in removing phosphorus from wastewater and its future use as fertilizer (1997-2003). *Water Research*, 2004. **38**(19): p. 4222-4246.
254. Wiesner, M.R., et al., Meditations on the Ubiquity and Mutability of Nano-Sized Materials in the Environment. *Acs Nano*, 2011. **5**(11): p. 8466-8470.
255. Boisson, J., et al., Evaluation of hydroxyapatite as a metal immobilizing soil additive for the remediation of polluted soils. Part 1. Influence of hydroxyapatite on metal exchangeability in soil, plant growth and plant metal accumulation. *Environmental Pollution*, 1999. **104**(2): p. 225-233.
256. Fuller, C.C., et al., Mechanisms of uranium interactions with hydroxyapatite:

- Implications for groundwater remediation. 2002. **36**(2): p. 158-165.
257. Fan, X., D.J. Parker, and M.D. Smith, Adsorption kinetics of fluoride on low cost materials. *Water Research*, 2003. **37**(20): p. 4929-4937.
258. SCCS, Opinion on Hydroxyapatite (nano). 2015, European Union Scientific Committee on Consumer Safety: Luxembourg. p. 55.
259. Straub, D.A., Calcium supplementation in clinical practice: a review of forms, doses, and indications. *Nutrition in Clinical Practice*, 2007. **22**(3): p. 286-296.
260. Ruegsegger, P., A. Keller, and M.A. Dambacher, COMPARISON OF THE TREATMENT EFFECTS OF OSSEIN-HYDROXYAPATITE COMPOUND AND CALCIUM-CARBONATE IN OSTEOPOROTIC FEMALES. *Osteoporosis International*, 1995. **5**(1): p. 30-34.
261. Yang, Y., et al., Characterization of Food-Grade Titanium Dioxide: The Presence of Nanosized Particles. *Environmental Science & Technology*, 2014. **48**(11): p. 6391-6400.
262. Yang, Y., et al., Survey of food-grade silica dioxide nanomaterial occurrence, characterization, human gut impacts and fate across its lifecycle. *Science of the Total Environment*, in-press (2016).
- Canady, R. and L. Tsytsikova, NanoRelease Food Additive: Supporting methods to measure food nanomaterials. *Abstracts of Papers of the American Chemical Society*, 2013. **245**.
263. Singh, G., et al., Measurement Methods to Detect, Characterize, and Quantify Engineered Nanomaterials in Foods. *Comprehensive Reviews in Food Science and Food Safety*, 2014. **13**(4): p. 693-704.
264. Szakal, C., et al., Measurement of Nanomaterials in Foods: Integrative Consideration of Challenges and Future Prospects. *ACS Nano*, 2014. **8**(4): p. 3128-3135.
265. Yada, R.Y., et al., Engineered Nanoscale Food Ingredients: Evaluation of Current Knowledge on Material Characteristics Relevant to Uptake from the Gastrointestinal Tract. *Comprehensive Reviews in Food Science and Food Safety*, 2014. **13**(4): p. 730-744.
266. Bass, J.K. and G.M. Chan, Calcium nutrition and metabolism during infancy. *Nutrition*, 2006. **22**(10): p. 1057-1066.

267. Nguyen, T.T.P., et al., A comprehensive review on in vitro digestion of infant formula. *Food Research International*, 2015. **76**: p. 373-386.
268. Lonnerdal, B., Effects of milk and milk components on calcium, magnesium, and trace element absorption during infancy. *Physiological Reviews*, 1997. **77**(3): p. 643-669.
269. Abrams, S.A., Building bones in babies: Can and should we exceed the human milk-fed infant's rate of bone calcium accretion? *Nutrition Reviews*, 2006. **64**(11): p. 487-494.
270. Thompkinson, D.K. and S. Kharb, Aspects of infant food formulation. *Comprehensive Reviews in Food Science and Food Safety*, 2007. **6**(4): p. 79-102.
271. Greer, F.R., CALCIUM, PHOSPHORUS, AND MAGNESIUM - HOW MUCH IS TOO MUCH FOR INFANT FORMULAS. *Journal of Nutrition*, 1989. **119**(12): p. 1846-1851.
272. Moy, R.J.D., Iron fortification of infant formula. *Nutrition Research Reviews*, 2000. **13**(2): p. 215-227.
273. Ai, K., Y. Liu, and L. Lu, Hydrogen-Bonding Recognition-Induced Color Change of Gold Nanoparticles for Visual Detection of Melamine in Raw Milk and Infant Formula. *Journal of the American Chemical Society*, 2009. **131**(27): p. 9496-+.
274. Ding, N., et al., Colorimetric Determination of Melamine in Dairy Products by Fe(3)O(4) Magnetic Nanoparticles-H(2)O(2)-ABTS Detection System. *Analytical Chemistry*, 2010. **82**(13): p. 5897-5899.
275. Gossner, C.M.-E., et al., The Melamine Incident: Implications for International Food and Feed Safety. *Environmental Health Perspectives*, 2009. **117**(12): p. 1803-1808.
276. Guan, N., et al., Melamine-Contaminated Powdered Formula and Urolithiasis in Young Children. *New England Journal of Medicine*, 2009. **360**(11): p. 1067-1074.
277. Mauer, L.J., et al., Melamine Detection in Infant Formula Powder Using Near- and Mid-Infrared Spectroscopy. *Journal of Agricultural and Food Chemistry*, 2009. **57**(10): p. 39743980.
278. Sun, F., et al., Analytical methods and recent developments in the detection of melamine. *Trac-Trends in Analytical Chemistry*, 2010. **29**(11): p. 1239-1249.
279. Venkatasami, G. and J.R. Sowa, Jr., A rapid, acetonitrile-free, HPLC method for

- determination of melamine in infant formula. *Analytica Chimica Acta*, 2010. **665**(2): p. 227-230.
280. Marques, M.R.C., R. Loebenberg, and M. Almukainzi, Simulated Biological Fluids with Possible Application in Dissolution Testing. *Dissolution Technologies*, 2011. **18**(3): p. 15-28.
281. Weir, A., et al., Titanium Dioxide Nanoparticles in Food and Personal Care Products. *Environ. Sci. Tech.*, 2012. **46**(4): p. 2242-2250.
282. Yang, Y., et al., Characterization of Food-Grade Titanium Dioxide: The Presence of Nanosized Particles. *Environmental Science & Technology*, 2014. **48**(11): p. 6391-6400.
283. Wigginton, N.S., K.L. Haus, and M.F. Hochella, Aquatic environmental nanoparticles. *J. Environ. Monit.*, 2007. **9**: p. 1306–1316.
284. Montano, M.D., et al., Improvements in the detection and characterization of engineered nanoparticles using spICP-MS with microsecond dwell times. *Environmental Science-Nano*, 2014. **1**(4): p. 338-346.
285. Bi, X.Y., et al., Quantitative resolution of nanoparticle sizes using single particle inductively coupled plasma mass spectrometry with the K-means clustering algorithm. *Journal of Analytical Atomic Spectrometry*, 2014. **29**(9): p. 1630-1639.
286. Pace, H.E., et al., Single Particle Inductively Coupled Plasma-Mass Spectrometry: A Performance Evaluation and Method Comparison in the Determination of Nanoparticle Size. *Environmental Science & Technology*, 2012. **46**(22): p. 12272-12280.
287. Hasselov, M., et al., Nanoparticle analysis and characterization methodologies in environmental risk assessment of engineered nanoparticles. *Ecotoxicology*, 2008. **17**(5): p. 344-361.
288. Arvidsson, R., et al., Challenges in Exposure Modeling of Nanoparticles in Aquatic Environments. *Human and Ecological Risk Assessment*, 2011. **17**(1): p. 245-262.
289. Zhang, Y., et al., Synthesis of nanorod and needle-like hydroxyapatite crystal and role of pH adjustment. *Journal of Crystal Growth*, 2009. **311**(23-24): p. 4740-4746.
290. Sadat-Shojai, M., et al., Synthesis methods for nanosized hydroxyapatite with diverse structures. *Acta Biomaterialia*, 2013. **9**(8): p. 7591-7621.
291. Garner, K.L., et al., Species Sensitivity Distributions for Engineered

- Nanomaterials. *Environmental Science & Technology*, 2015. **49**(9): p. 5753-5759.
292. Keller, A.A., et al., Global life cycle releases of engineered nanomaterials. *Journal of Nanoparticle Research*, 2013. **15**(6).
293. Schriks, M., Heringa, M., van der Kooi, M., de Voogt, P., and van Wezel, A. (2010). Toxicological relevance of emerging contaminants for drinking water quality. *Water Research*, 44(2), pp. 461-476
294. Zodrow, K., Li, Q., Buono, R., Chen, W., Dalgger, G., Duenas-Osorio, L., Elimelech, M., Huang, X., Jiang, G., Kim, J., Logan, B., Sedlak, D., Westerhoff, P., and Alvarez, P. (2017). Advanced materials, technologies, and complex systems analyses: Emerging opportunities to enhance urban water security. *Environmental Science and Technology*, 51(18), pp. 10274-10281
- Lee, E., and Schwab, K. (2005). Deficiencies in drinking water distribution systems in developing countries. *Journal of Water and Health*, 3(2), pp. 109-127
295. Kessler, R. (2011). Stormwater strategies: cities prepare aging infrastructure for climate change, National Water Advisory Council, a514-a519.
296. Barber, L., Hladik, M., Vajda, A., Fitzgerald, K., and Douville, C. (2015). Impact of Wastewater Infrastructure Upgrades on the Urban Water Cycle: Reduction in Halogenated Reaction Byproducts following Conversion from Chlorine Gas to Ultraviolet Light Disinfection. *Science of the Total Environment*, 529, pp. 264-274
297. Grigg, N. (2005). Institutional analysis of infrastructure problems: case study of water quality in distribution systems. *Journal of Management in Engineering*, 21(4), pp. 152-158.
298. Cuppett, J., Duncan, S., and Dietrich, A. (2006). Evaluation of copper speciation and water quality factors that affect aqueous copper tasting response. *Chemical Senses*, 31(7), pp. 689-697
299. Dietrich, A., and Burlingame, G. (2015). Critical review and rethinking of USEPA secondary standards for maintaining organoleptic quality of drinking water. *Environmental Science and Technology*, 49(2), pp. 708-720
300. Heim, T., and Dietrich, A. (2007). Sensory aspects and water quality impacts of chlorinated and chloraminated drinking water in contact with HDPE and cPVC pipe. *Water Research*, 41(4), pp. 757-764

301. Saylor, A., Prokopy, L., and Amberg, S. (2011). What's wrong with the tap? Examining perceptions of tap water and bottled water at Purdue University. *Environmental Management*, 48(3), pp. 588-601
302. Whelton, A., Dietrich, A., Burlingame, G., Schechs, M., and Duncan, S. (2007). Minerals in drinking water: impacts on taste and importance to consumer health. *Water Science and Technology*, 55(5), pp. 283-291
303. World Health Organization (2000). Global water supply and sanitation assessment 2000 report. ISBN 92-4-156202-1
304. Zhou, H., and Smith, D. (2002). Advanced technologies in water and wastewater treatment. *Journal of Environmental Engineering and Science*, 1(4), pp. 247-264
305. Alspach, B., and Juby, G. (2018). Cost-effective ZLD technology for desalination concentrate management. *Journal-American Water Works Association*, 110(1), pp. 37-47
306. U.S. Geological Survey. (2015). Public supply and domestic water use in the United States. Retrieved from: <https://pubs.usgs.gov/of/2017/1131/ofr20171131.pdf>
307. Rice, J., and Westerhoff, P. (2015). Spatial and temporal variation in de facto wastewater reuse in drinking water systems across the U.S.A. *Environmental Science and Technology*, 49(2), pp. 982-989
308. Markets and Markets. (2019). Point-of-use water treatment systems market by device, technology, application, and region – forecast to 2023. Retrieved from Markets and Markets database.
309. Adeleye, A., Conway, J., Garner, K., Huang, Y., Su, Y., and Keller, A. (2016). Engineered nanomaterials for water treatment and remediation: costs, benefits, and applicability. *Chemical Engineering Journal*, 286, pp. 640-662
310. Gehrke, I., Geiser, A., and Somborn-Schulz, A. (2015). Innovations in nanotechnology for water treatment. *Nanotechnology Science and Applications*, 8, pp. 1-17.
311. Alvarez, P., Chan, C., Elimelech, M., Halas, N., and Villagran, D. (2018). Emerging opportunities for nanotechnology to enhance water security. *Nature Nanotechnology*, 13(8), pp. 634-641
312. Westerhoff, P., Alvarez, P., Li, Q., Gardea-Torresdey, J., and Zimmerman, J. (2016). Overcoming implementation barriers for nanotechnology in drinking water treatment. *Environmental Science: Nano*, 3, pp. 12411-1253

313. Zhang, H., Chen, B., and Banfield, J. (2010). Particle size and pH effects on nanoparticle dissolution. *Journal of Physical Chemistry*, 114(35), pp. 14876-14884
314. Bi, X., Ma, H., and Westerhoff, P. (2018). Dry powder assay rapidly detects metallic nanoparticles in water by measuring surface catalytic reactivity. *Environmental Science and Technology*, 52(22), pp. 13289-13297
315. Medvedeva, I., Bakhteeva, I., Zhakov, S., Revvo, A., Uimin, M., Yermakov, A., Byzov, I., Mysik, A., Schchegoleva, N. (2015). Separation of Fe₃O₄ nanoparticles from water by sedimentation in a gradient magnetic field. *Journal of Water Resource and Protection*, 7, pp. 111-118
316. Jeong, S., Shin, H., Jo, Y., Kim, Y., Kim, S., Lee, W., ... and An, H. (2018). Plasmonic silver nanoparticle-impregnated nanocomposite BiVO₄ photoanode for plasmon-enhanced photocatalytic water splitting. *The Journal of Physical Chemistry C*, 122(13), pp. 7088-7093.
317. Werber, J., Osuji, C., and Elimelech, M. (2016). Materials for next-generation desalination and water purification membranes. *Nature Reviews Materials*, 1(5), pp. 16018
318. Perreault, F., Jaramillo, H., Xie, M., Ude, M., Nghiem, L., and Elimelech, M. (2016). Biofouling mitigation in forward osmosis using graphene oxide functionalized thin-film composite membranes. *Environmental Science and Technology*, 50(11), pp. 5840-5848
319. Kidd, J., Barrios, A., Apul, O., Perreault, F., and Westerhoff, P. (2018). Removal of bromide from surface water: comparison between silver-impregnated graphene oxide and silver-impregnated powder activated carbon. *Environmental Engineering Science*, 35(9)
320. Garcia-Segura, S., Lanzarini-Lopes, M., Hristovski, K., and Westerhoff, P. (2018). Electrocatalytic reduction of nitrate: fundamentals to full-scale water treatment applications. *Applied Catalysis B: Environmental*, 236, pp. 546-568
321. Vahid, B., and Khataee, A. (2013). Photoassisted electrochemical recirculation system with boron-doped diamond anode and carbon nanotubes containing cathode for degradation of a model azo dye. *Electrochimica Acta*, 88, pp. 614-620
322. Neamtu, M., Nadejde, C., Hodoroaba, V., Schneider, R., Verestiuc, L., and Panne, U. (2018). Functionalized magnetic nanoparticles: synthesis, characterization, catalytic application and assessment of toxicity. *Scientific Reports*, 8, pp. 6278

323. Dankovich, T., and Gray, D. (2011). Bactericidal paper impregnated with silver nanoparticles for point-of-use water treatment. *Environmental Science and Technology*, 45(5), pp. 1992-1998
324. Das, R., Eaqub, M., Hamid, S., Ramakrishna, S., and Chowdhury, Z. (2014). Carbon nanotube membranes for water purification: a bright future in water desalination. *Desalination*, 336, pp. 97-109
325. Dankovich, T., and Smith, J. (2014). Incorporation of copper nanoparticles into paper for point-of-use water treatment. *Water Research*, 63, pp. 245-251
326. Lu, H., Wang, J., Stoller, M., Wang, T., Bao, Y., and Hao, H. (2016). An overview of nanomaterials for water and wastewater treatment. *Advances in Materials Science and Engineering*, doi: [10.1155/2016/4964828](https://doi.org/10.1155/2016/4964828)
327. Bi, Y., Han, B., Zimmerman, S., Perreault, F., Sinha, S., and Westerhoff, P. (2018). Four release tests exhibit variable silver stability from nanoparticle-modified reverse osmosis membranes. *Water Research*, 143, pp. 77-86.
328. Ahamed, M., AlSalhi, M., and Siddiqui, M. (2010). Silver nanoparticle applications and human health. *Clinica Chimica Acta*, 411(23), pp. 1841-1848.
329. Turgeon, S., Rodriguez, M., Thériault, M., and Levallois, P. (2004). Perception of drinking water in the Quebec City region (Canada): the influence of water quality and consumer location in the distribution system. *Journal of Environmental Management*, 70(4), pp. 363-373.
330. Doria, M. (2010). Factors influencing public perception of drinking water quality. *Water Policy*, 12(1), pp. 1-19.
331. Teillet, E., Urbano, C., Cordelle, S., and Schlich, P. (2010). Consumer perception and preference of bottled and tap water. *Journal of Sensory Studies*, 25(3), pp. 463-480.
332. MacOubrie, J. (2004). Public perceptions about nanotechnology: Risks, benefits and trust. *Journal of Nanoparticle Research*, 6(4), pp. 395-405.
333. Renn, O., and Roco, M. (2006). Nanotechnology and the need for risk governance. *Journal of Nanoparticle Research*, 8(2), pp. 153-191.
334. Gupta, N., Fischer, A., and Frewer, L. (2015). Ethics, risk and benefits associated with different applications of nanotechnology: a comparison of expert and consumer perceptions of drivers of societal acceptance. *NanoEthics*, 9(2), pp. 93-108.

335. Evans, J., and Mathur, A. (2005). The value of online surveys. *Internet Research*, 15(2), pp. 195-219
336. Rice, J., Wutich, A., White, D., and Westerhoff, P. (2016). Comparing actual de facto wastewater reuse and its public acceptability: A three city case study. *Sustainable Cities and Society*, 27, pp 467-474.
337. Liu, M., and Wronski, L. (2018). Trap questions in online surveys: Results from three web survey experiments. *International Journal of Market Research*, 60(1), pp. 32–49.
338. U.S. Environmental Protection Agency (2009). National primary drinking water regulation table, EPA 816-F-09-004. Retrieved from: <https://www.epa.gov/ground-water-and-drinking-water/national-primary-drinking-water-regulation-table>
339. York, A., Barnett, A., Wutich, A., and Crona, B. (2011). Household bottled water consumption in Phoenix: a lifestyle choice. *Water International*, 36(6), 708-718.
340. Doria, M. (2006). Bottled water versus tap water: understanding consumers' preferences. *Journal of Water and Health*, 4(2), pp. 271-276.
341. Platikanov, S., Hernández, A., González, S., Cortina, J. L., Tauler, R., and Devesa, R. (2017). Predicting consumer preferences for mineral composition of bottled and tap water. *Talanta*, 162, pp. 1-9.
342. Ward, L., Cain, O., Mullally, R., Holliday, K., Wernham, A., Baillie, P., and Greenfield, S. (2009). Health beliefs about bottled water: a qualitative study. *BMC Public Health*, 9(1), pp. 196.
343. Pierce, G., and Gonzalez, S. (2017). Mistrust at the tap? Factors contributing to public drinking water (mis) perception across US households. *Water Policy*, 19(1), pp. 1-12.
344. Doria, M., Pidgeon, N., and Hunter, P. (2009). Perceptions of drinking water quality and risk and its effect on behaviour: A cross-national study. *Science of the Total Environment*, 407(21), pp. 5455-5464.
345. Parag, Y., and Roberts, J. (2009). A battle against the bottles: building, claiming, and regaining tap-water trustworthiness. *Society and Natural Resources*, 22(7), pp. 625-636.
346. Johnstone, N., and Serret, Y. (2012). Determinants of bottled and purified water consumption: results based on an OECD survey. *Water Policy*, 14(4), pp. 668-679.

347. Kriström, B. (2013). Greening Household Behaviour: Overview from the 2011 Survey, chapter Household behaviour and energy use
348. Yoo, S., and Yang, C. (2000). Dealing with bottled water expenditures data with zero observations: a semiparametric specification. *Economics Letters*, 66(2), pp. 151-157
349. Currall, S., King, E., Lane, N., Madera, J., and Turner, S. (2006). What drives public acceptance of nanotechnology? *Nature Nanotechnology*, 1, pp. 153-155
350. Boholm, A., and Larsson, S. (2019). What is the problem? A literature review on challenges facing the communication of nanotechnology to the public. *Journal of Nanoparticle Research*, 21, pp. 86-107

APPENDIX A

CARBONACEOUS NANO-ADDITIVES AUGMENT MICROWAVE-ENABLED
THERMAL REMEDIATION OF SOILS CONTAINING PETROLEUM

CARBONACEOUS NANO-ADDITIVES AUGMENT MICROWAVE-ENABLED THERMAL REMEDIATION OF SOILS CONTAINING PETROLEUM

This chapter has been published as Apul, O., Delgado, A., **Kidd, J.**, Alam, F., Dahlen, P., and Westerhoff, P. (2016). Carbonaceous Nano-additives Augment Microwave-Enabled Thermal Remediation of Petroleum Hydrocarbon Containing Soils. *Environmental Science Nano*, 3, pp. 997-1002.

My author contribution: Approximately 85% of the research and 10% of the text

Abstract

Remediating soils contaminated with heavy hydrocarbons (C_{12} – C_{40}) from petrochemical exploration activities is a major environmental challenge across the globe. This study evaluated microwave irradiation in the presence of nano- and macro-scale graphitic additives as a rapid remediation technology for removing heavy hydrocarbons from soil. Adding inert materials (i.e., glass wool fibers or washed silica sand) as controls had no effect on total petroleum hydrocarbons (TPH) removal upon microwave irradiation. Carbonaceous nanomaterials (i.e., carbon nanotubes, graphene nanosheets, and carbon nanofibers) because of their favorable dielectric properties showed extraordinary heating performances when mixed with soil and microwave irradiated. As a result, adding these carbonaceous nanomaterials to contaminated soils removed more TPH compared with macro-scale carbonaceous additives. TPH concentrations decreased from 11000 to between 2000 and 6000 mg TPH kg^{-1} soil within one minute using carbon nanomaterial additives and a 2.45 GHz, 1000 W conventional microwave oven. In separate experiments, this technology de- creased TPH from 2500 to 650 mg TPH kg^{-1} soil from soils containing recalcitrant, non-biodegradable fractions of TPH. Large scale microwave systems are

available, and hold promise for remediating soils when used in conjunction with carbon nanomaterials.

Introduction

Long chain, heavy petroleum hydrocarbons in soils create a persistent environmental liability; these heavier fractions are less prone to natural weathering processes including volatilization, biodegradation, and dissolution.^{1,2} Since the early 1960s, nearly 6.8×10^8 kg of oil have spilled into United States soils from pipeline breaks or seepage from corroded lines. In addition, nearly 1.0×10^9 kg oil have spilled into United States marine waters, which often ends up on land unless contained or recovered after the spill.^{3,4} Of particular concern are petroleum residuals containing 12 to 40 carbon chain lengths (C_{12} – C_{40}) because of their low volatility and biodegradability. Microwave-enabled thermal treatment of petroleum hydrocarbon-containing soils is a cost- and time- effective remediation solution,^{5–7} and it has been investigated in bench-scale batch experiments, pilot-scale tests, and field- scale tests.^{5,8–12} Microwave-enabled thermal treatment of petroleum hydrocarbon-containing soils (i) decomposes polar and polarizable hydrocarbon components, which are more susceptible to microwave heating, (ii) evaporates volatile components regardless of their affinity to microwave energy because of locally heated regions of the surrounding environment, and (iii) co-evaporates non-volatile components that can be stripped with the steam generated from evaporation of water molecules.

Microwave-enabled heating introduces an electromagnetic field to the target matrix and generates heat via two predominant mechanisms: (i) polar molecules (i.e., compounds with permanent and induced dipoles such as water or chlorinated organics) rotate

erratically to align themselves to the incoming dielectric field, physical resistance causes friction, and subsequent heat release elevates the temperature of the molecules and their surroundings; and (ii) free electrons of charged particles (i.e., freely moving charged particles within a region such as π electrons of

graphitic carbon surface) trying to couple to the changes of electric field dissipate energy in the form of heat.^{13,14}

Overall, carbonaceous nano additives augment localized heating, which further enhances these processes. The heat induction, which is the ability to suppress electromagnetic radiation and convert it to thermal energy, is dictated by the dielectric properties of compounds of subject. Dielectric properties of compounds are generally controlled by their polarity and morphology.¹² The selective nature of microwave heating can further be localized by utilizing additives with favorable dielectric properties. A common class of microwave absorbers are graphitic allotropes of carbon. A wide variety of carbon materials, including newer generation carbon nanomaterials (e.g., carbon nanotubes, graphene nanosheets, superfine powdered activated carbons), have unique structural and electrical properties. The generous electron budget on the graphene layers of sp-2 hybridized carbon network and freely floating π -electrons on their surfaces make carbonaceous materials exceptional candidates for microwave absorbers.^{13,15} Therefore, graphitic carbon nanomaterials are promising additives for microwave-enabled soil remediation.^{16–19} To the best of our knowledge, new generations of carbon nanomaterials have not yet been investigated as additives for microwave-enabled thermal remediation of soils.

Microwave heating utilizing additives with dielectric properties is being investigated at an increasing pace in diverse fields.¹⁴ However, only a small number of studies demonstrate the use of charcoal,⁸ carbon fibers,¹¹ and granular activated

carbons^{10,20} as additives to augment microwave heating for soil remediation.^{5,21,22} This study investigated carbonaceous nanomaterials as additives to augment microwave-enabled thermal treatment of petroleum soils because carbon nanomaterials with exceptional electron budget on the π -orbitals can show

extraordinary heating performance when mixed with soil. The performance of carbon nanomaterials was compared against previously-reported macro-scale carbons and inert materials. The primary objective of this study was to provide a bench-scale proof-of-concept evaluation of novel carbonaceous nanomaterials as additives to augment microwave heating and enhance removal of total petroleum hydrocarbons (TPH) from contaminated soils within brief irradiation times. The long-term objective of this work is to develop a microwave-based technology that exploits the nano properties of graphitic carbon allotropes and is energy efficient, effective, rapid, and suitable for field deployment. In order to achieve those goals, this study serves to (i) provide evidence on the effectiveness of carbon nanomaterials as additives to microwave-enabled thermal remediation, (ii) identify the critical properties of select carbon nanomaterials, and (iii) provide some insight to the mechanism of hydrocarbon removal during microwave-enabled thermal remediation.

Materials and Methods

Materials

The soil used in this study was a homogenous mixture of samples obtained from multiple locations at a decommissioned oil field in the United States and contained 11000 mg kg^{-1} TPH. The sand/silt/clay soil matrix was contaminated with a 40 API gravity crude oil and had been weathering in situ at the field site. The soil had 33.8% w/w water holding capacity. Additional soil characterization is available in prior publications.²³ Experiments were conducted with two soils from the same source (as-received or after aerobic

biodegradation). Soil was biodegraded by providing a source of macronutrients, trace minerals, and vitamin solutions as described

elsewhere²⁴ and mixing twice weekly. The TPH concentration of the biodegraded soil was $2481 \pm 192 \text{ mg kg}^{-1}$. Additional biodegradation details are in the SI section.

One type of multi-walled carbon nanotubes (NC7000, labeled as MWCNT-1) was obtained from Nanocyl SA (Nanocyl SA, Sambreville, Belgium). Carbon nanofibers (iron-free, conical >99%, diameter 100 nm, length 20–200 μm , pore size $0.075 \text{ cm}^3 \text{ g}^{-1}$) and the second type of multi-walled carbon nanotubes (labeled as MWCNT-2; 95% carbon content trace metal basis, outer diameter 7–15 nm, inner diameter 3–6 nm, length 0.5–200 μm) were purchased from Sigma Aldrich (St. Louis, MO). Powdered activated carbon (PAC 20B) was purchased from Cabot Norit Americas Inc. (Boston, MA). Super-fine powdered activated carbon (SPAC) was obtained by pulverizing PAC 20B to submicron particle sizes via wet milling. Graphene (N006-010-P) and graphene oxide (N002-PDE) were purchased from Angstrom Materials (Dayton, OH). Food grade charcoal (bamboo activated charcoal powder, mesh 325) was purchased from Charcoal House, LLC (Crawford, NE). Washed silica sand (mesh no.: 40–60) and glass wool fibers were used as controls. The additive materials were utilized as received from the manufacturer without any physical or chemical preconditioning in our laboratory.

Microwave treatment

Five grams of contaminated soil (containing 18.7 wt% moisture) was placed into a 40 mL glass vial or porcelain crucible dish with no cap or cover. Additives (1–5% w/w) were manually mixed into the soil matrix to ensure sample homogeneity. The vials were placed on rotating glass dolly of the household Hamilton Beach microwave oven (Glen Allen, VA; Model No.: P100N30ALS3B, 2.45 GHz, 1000 W output) in a laboratory hood and set

to the desired experimental time (varying between 15 seconds to 5 minutes). The active power generated by the microwave was measured online by Kill A Watt® (P3 International). Soil temperature

measurements were obtained immediately following treatment using a handheld, VWR non-contact infrared digital temperature gun (Radnor, PA).

Total petroleum hydrocarbons (TPH) analysis

Soil sample TPH concentrations were analyzed by an independent analytical lab (Eurofins Lancaster Laboratories; Lancaster, PA) or in-house. For external laboratory analysis, bulk soil preparation (SW-846 5035A Modified) and extractable petroleum hydrocarbon detection for soils (SW-846 3546) were followed. All TPH concentrations were corrected according to surrogate (i.e., o-terphenyl) recovery percentages, which ranged from 64 to 93%. For in-house analysis, one gram of soil was dried with sodium sulfate and extracted with dichloromethane (DCM) in a Gerhardt® Soxtherm automatic extractor (Gerhardt Analytical System, Königswinter, Germany).²⁵ Prior to extraction, samples were spiked with 50 μL of 1-chlorooctadecane and o-terphenyl from 1000 mg L^{-1} stock solutions to verify recovery. All TPH concentrations were corrected according to average surrogate recoveries, which ranged from 74% to 92%. The DCM extract was concentrated to 1 mL final volume, filtered through a 0.2 μm PTFE filter, and analyzed on a GC-FID (Shimadzu GC2010, Shimadzu Corp., MD, USA). All TPH concentrations were reported per dry weight of the soil. Additional details on the in-house TPH extraction method are provided in the SI. Student's t-test was employed for statistical hypothesis testing when evaluating the significant differences between datasets.

Results and Discussion

Microwave-enabled thermal treatment of soils containing petroleum hydrocarbons

Petroleum hydrocarbon-containing soils with ten different additive materials were irradiated in a microwave for 60 seconds. Fig. 1 shows the TPH concentrations before and after microwave treatment. Microwave treatment of soil with no additives showed no detectable decrease in TPH

concentration. Likewise, addition of controls had no decrease in TPH after microwave treatment indicating the bulk density or the morphology of inert controls does not contribute to TPH removal. Similarly, macro-scale carbon additives (PAC, SPAC, and charcoal) showed no statistically significant ($\alpha = 0.05$) decrease in TPH after 60 seconds of microwave treatment. Treatments with some carbonaceous nano additive showed TPH removal up to 82%. The TPH concentrations were significantly ($p < 0.05$) lower than initial TPH concentration when graphene, MWCNT-1, or carbon nanofiber was added. Graphene and MWCNT-1 performed best. Differences in additive performance were attributed to the varying morphology and dielectric properties of selected additives. These results suggest that the unique dielectric properties of these carbonaceous nano-additives can be exploited for augmenting microwave irradiation soil remediation techniques.

The MWCNT type made a difference in microwave-enabled remediation. Menendez et al.¹⁴ reported a wide range of dielectric tangent losses (0.25–1.44) for carbon nanotubes. This variability can be attributed to the morphological differences of the tubes or the unpredictable cluster formation of the nanotubes. Further evaluation is required to understand which properties of MWCNT-1 (vs. MWCNT-2) augmented thermal remediation.

Selected residual TPH distributions showing carbon chain lengths before microwave treatment (untreated soil) and after 60 second microwave treatment (graphene and carbon nano-fiber additives) are presented in Fig. 2. The shorter chain hydrocarbon concentrations were smaller than longer chain hydrocarbons after microwave treatment. For example, TPH removal percentages in C12–C20, C20–C28, and C28–C36 carbon

chain length fractions were 94%, 81%, and 73%, respectively, for graphene and 66%, 55%, and 38%, respectively, for carbon nanofibers. The shorter chain hydrocarbons appear more prone to microwave-enabled thermal remediation with additives.

Bulk soil temperatures rose to 190 °C when irradiated with some of the additives (i.e., graphene, MWCNT-1 or carbon nanofibers) and rose only to 40–50 °C with no additive. During irradiation a thick, black colored gas was emitted from the soil almost immediately. This gas is presumably a mixture of volatilized hydrocarbons, steam from soil moisture, and gaseous oxidation products. At this exploratory stage, the flue gas was not captured for further analysis; however, its composition would elucidate whether the heavy hydrocarbons were volatilized, oxidized to shorter chain (more volatile) components, or completely mineralized to CO₂. Another visual observation was the generation of white or light blue colored sparks, especially when graphenes and MWCNTs were irradiated. The sparks were attributed to graphitic carbon allotropes reflecting microwave radiation fractions where delocalized π -electrons can move freely, enabling them to jump out and ionize the surrounding atmosphere. These sparks are defined as microplasmas (i.e., plasmas confined to a small region that last for a fraction of a second).¹⁴

Two control additives with poor microwave responsiveness, washed silica sand (dense particles resembling activated carbon) and glass wool fibers (loose and cottony fibers resembling carbon fibers), showed no notable performance, confirming their low microwave heating capacities; however, it is difficult to make conclusive statements because several other carbonaceous materials (PAC, SPAC, Charcoal) also did not perform well in the 60 second microwave tests. Longer microwave irradiation times could be applied with similar additives; however, it was decided that further exploration of these control additives would not be included in this study. Error bars represent heterogeneity of

TPH within soil samples, which occurs due to variations in soil properties (particle size, composition) and way the TPH spill or mixing induces macro-scale heterogeneities of real field samples. This is the very nature of actual heavy hydrocarbon contaminated soils, which differs from mechanistic studies that may use simpler

background matrices (e.g., silica sand containing crude oil). Recoveries of internally spiked compounds with the soils were used to compute TPH concentrations. Statistical analysis was conducted to differentiate effects of TPH soil heterogeneity from effects of microwave treatment in the presence of different additives. A 15-minute irradiation time was investigated using 10% w/w granular activated carbon additive, and TPH removal greater than 90% was achieved. The resulting chromatograms and experimental details of the granular activated carbon test are provided in Fig. S1 in ESI. The granular activated carbon test results demonstrate that macro-scale graphitic materials can also remove TPH, but the prolonged irradiation process is more energy intensive and would directly influence the cost of the treatment.

Regardless of particle size and graphitic properties, graphene oxide, charcoal, PAC, and SPAC did not perform well as dielectric additives under tested conditions. Two possible reasons for the lower performance could be: (i) the considerably higher density and sphere-like morphology of activated carbon or charcoal particles, and (ii) the presence of oxygen on the surface of graphene oxide. However there is not enough evidence at this stage to make a conclusive statement regarding the poor performance of these additives.

Effect of operational parameters

Performance of microwave-enabled thermal treatment is influenced by operational parameters including (i) microwave energy input or heating time, (ii) dielectric additive amount, (iii) moisture content, and (iv) microwave frequency.^{10,12} Irradiation time as an operational parameter will affect cost and must therefore be considered in balance with remediation efficiency. Previously, 15-minute irradiation was applied using granular

activated carbon additives and removed TPH from soil as described in Fig. S1 in ESI; dielectric nano-additives showed similar performances with much shorter irradiation times. For 1% MWCNT-1, increasing the microwave irradiation time from 15 seconds to 30 and 60 seconds increased TPH removal from 20% to 30% and 60%, respectively (see Fig. S2 in ESI†). Longer irradiation times increased the temperature due to the increase in the specific energy input as previously reported in the literature.^{26,27} An average of 1678 W power input (see the online power measurements in Fig. S3 in ESI†) from microwave introduced 0.007 kW h (i.e., 24.2 kJ) energy in 15 seconds, whereas increasing the irradiation time to 30 and 60 seconds increased the energy input to 0.013 kW h and 0.027 kW h, which yields to 2.7 and 5.4 kW h kg⁻¹ soil, respectively.

Higher concentrations of nano additives may allow more contact with soil due to abundance of additive mass, resulting in more heating during irradiation. Increasing MWCNT-1 mass per unit soil from 1 wt% to 2.5% and 5% increased TPH removal from 35% to 45% and 70%, respectively (see Fig. S4 in ESI).

Soil moisture content is another important operational parameter because water has a high dielectric tangent loss and can contribute to microwave heating and stripping of hydrocarbons during evaporation; conversely, it can serve as a heat sink and decrease the soil temperature. TPH removal was not notably different when microwave heating was applied to soils at 0, 20, and 60% of the soil water holding capacity (see Fig. S5 in ESI†). A detailed investigation is required to understand the effect of moisture content on microwave-enabled thermal treatment of soils containing petroleum hydrocarbons.

Microwave-enabled thermal treatment of bioremediated soils with additives

Bioremediation is a common low-cost strategy to remove a portion of TPH from contaminated soils, but a non- biodegradable TPH fraction persists and causes regulatory challenges or issues associated with use or disposal of the soils. To investigate the effect of microwave irradiation on persistent components of bioremediated soils containing TPH, a bioremediated soil was exposed to five minutes of microwave irradiation. The post-treatment average TPH concentrations (\pm standard deviation from triplicate treatments) with and without MWCNTs were 644 ± 230 and $2072 \pm 45 \text{ mg kg}^{-1}$, respectively. Adding MWCNT-1 improved TPH reduction from 17% to 74%. This substantial performance increase was attributed to the superior dielectric properties of graphitic allotropes of carbon nanotubes, confirming the ability to convert microwave radiation to conventional heat. Fig. S6 provides chromatograms obtained after bioremediation and after subsequent microwave irradiation. The majority of lighter TPH fractions that elute early in the gas chromatography run are removed during bioremediation, indicating that heavier, longer-chain TPH fractions are more persistent as expected. Adding MWCNTs in combination with microwave irradiation removed petroleum hydrocarbons, including the most recalcitrant fractions that were eluting after 30 minutes. Microwave irradiation with MWCNTs following bioremediation was capable of removing more than 90% of the TPH from impacted soil.

This study demonstrated the extraordinary thermal properties of carbonaceous nanomaterials and their ability to enhance the microwave-enabled thermal remediation of petroleum hydrocarbon-containing soils. Switching from macro-scale to nano-scale carbonaceous materials can shorten the irradiation times and decrease the energy intensity

of the process dramatically. Additionally, some of the tested nano-additives significantly increased the performance of microwave treatment of biodegraded soils containing recalcitrant petroleum hydrocarbons. The demonstrated technology has the potential for scale-up to an ex-situ setting where soil is conveyed into a field-scale microwave oven for continuous remediation of soils containing petroleum hydrocarbons. The conveyor belt material can be coated with fabricated carbon nanomaterials or external additives can be used to avoid addition of nanoparticles into the soil matrix.

A mechanistic evaluation of select nano-additives is going to be conducted by systematically obtaining physicochemical, electrical and thermal properties of nano-additives and testing their microwave responsiveness for thermal remediation of soils containing petroleum hydrocarbons. Complementary tests will be conducted in simpler background matrices (i.e., nano-additives on treatment of silica sand that is synthetically contaminated with a specific geographic crude oil source) to gain a mechanistic insight. From a field deployment perspective, our future work is going to evaluate the trade-offs between addition of persistent nanoparticles into the soil matrix versus application of recoverable materials. In addition to the oncoming mechanistic studies and industrial scale microwave devices, investigation of microwave field uniformity and temperature induced change uniformity will be critically evaluated.

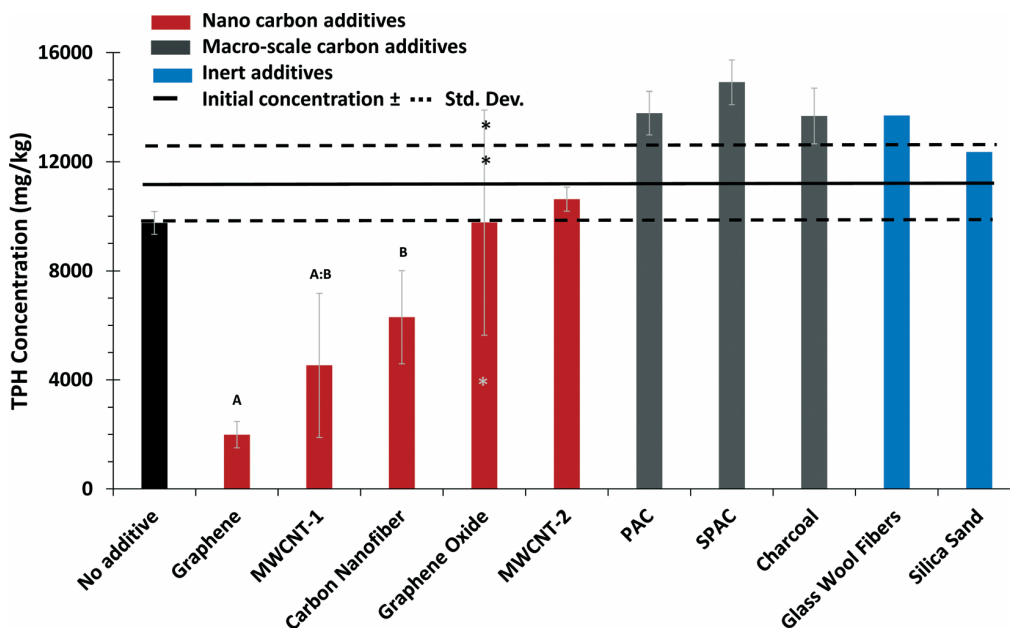


Fig. 1 TPH concentrations in soil after 60 second microwave treatment with 2.5 wt% dielectric additives and corresponding controls with inert or no additives. Error bars indicate standard deviation of triplicate experiments. Indicator letters (A and B) show treatments that are significantly lower than initial TPH concentration at 95% level of significance ($p < 0.05$) where same letters indicate statistical indifference. Asterisks (*) indicate the TPH concentrations of the triplicate treatments causing the large error bar on graphene oxide treatment. Solid and dashed lines indicate initial TPH concentration \pm standard deviation of triplicate measurements. MWCNT: multi-walled carbon nanotubes, PAC: powdered activated carbon, SPAC: superfine powdered activated carbon.

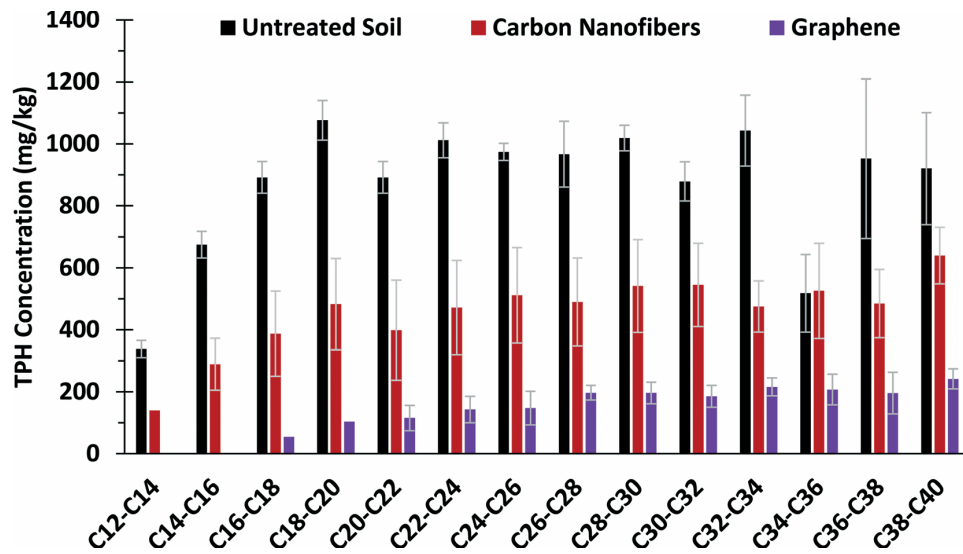


Fig. 2 TPH concentration by carbon chain length in soil before and after 60 second microwave treatment for select carbonaceous materials. Error bars indicate standard deviation of triplicate experiments.

Acknowledgements

This work was supported by the National Science Foundation (EEC-1449500) Nanosystems Engineering Research Center for Nanotechnology Enabled Water Treatment (NEWT) at Arizona State University. Preliminary efforts by Matthew Fesko while at ASU helped initiate this research. Editorial assistance from Laurel Passantino is appreciated.

Supplemental Information

Biodegradation Procedure for Soils Containing Petroleum Hydrocarbons

Soil was biodegraded in a 1.5 L glass pan containing 1.25 kg of soil. Each kg of soil was dosed with 10 mL of macronutrient solution, 1 mL Trace A solution, 1 mL Trace B solution, and 1 mL vitamin mix solution for bacterial growth. The composition of these solutions was published previously ^{S1}. The soil was mixed/tilled twice weekly to oxygenate, and DI water was provided to maintain the moisture content at 60-80% of the soil water holding capacity (i.e., 15- 18% w/w). Incubations were performed for 120 days at 30° C in the dark.

Extraction and Quantification of Total Petroleum Hydrocarbons from Soil

One gram of soil was dried with sodium sulfate and extracted with dichloromethane (DCM) in a Gerhardt[®] Soxtherm automatic extractor (Gerhardt Analytical System, Königswinter, Germany). The DCM extract was concentrated to 1 mL final volume, filtered through a 0.2- μ m PTFE filter, and analyzed on a GC-FID (Shimadzu GC2010, Shimadzu Corp., MD, USA) equipped with a Restek Rxi[®]-1HT column (30 m x 0.25 mm x 0.25 μ m). The GC-FID analytical method was developed according to the extractable petroleum hydrocarbons standard method ^{S2}. TPH was defined as the collective concentration of all compounds eluting from n-nonane (C₉) to n-tetracontane (C₄₀). Calibration curves were generated to obtain calibration factors using an alkane C₉-C₄₀ standard mixture (Sigma-Aldrich Co. Ltd.; St. Louis, MO) at six different concentrations between 2 and 200 mg/L. All TPH concentrations were reported per dry weight of the soil.

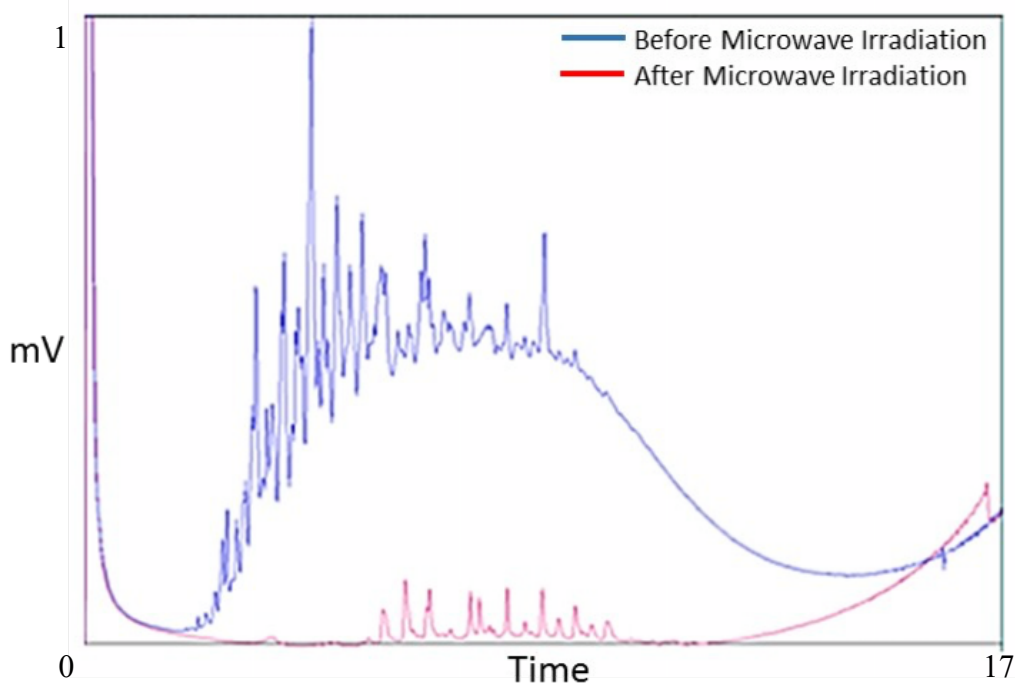


Figure S1. Chromatograms of soils containing petroleum hydrocarbons before and after 15-minute microwave irradiation enhanced with granular activated carbon. Microwave treatment of soils using granular activated carbons as additives: two grams of contaminated soil (containing 14,000 mg/kg TPH, 12.5% soil moisture) were placed into a 40 ml borosilicate VOA vial. Calgon granular activated carbon (10% w/w) was added to the soil matrix and manually mixed to ensure sample homogeneity. The vials were placed on a rotator disk in a household Hamilton Beach (Glen Allen, VA; Model No: P100N30ALS3B, 2.45 GHz, 1000-W output) microwave oven in a laboratory hood and set to 15 minutes. Residual TPH chromatograms were generated in-house using SRI 8610C Gas Chromatograph with Restek MXT-1HT SimDist column (10m, 0.53 mmID, 0.21 μ m df). Temperature programming was: 40-380 $^{\circ}$ C at 20 $^{\circ}$ C/min (total 17-minute run time) with gas flow rates of helium carrier 10 ml/min, hydrogen 20 ml/min, and air 230 ml/min.

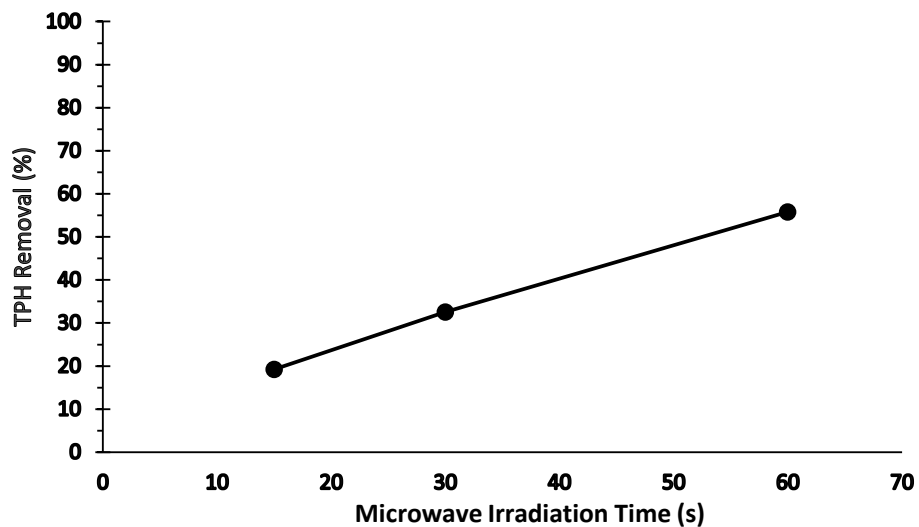


Figure S2. Effect of Microwave irradiation time on TPH removal. The solid line is drawn to guide the eye. MWCNT-1 (1% w/w) was used as dielectric additive.

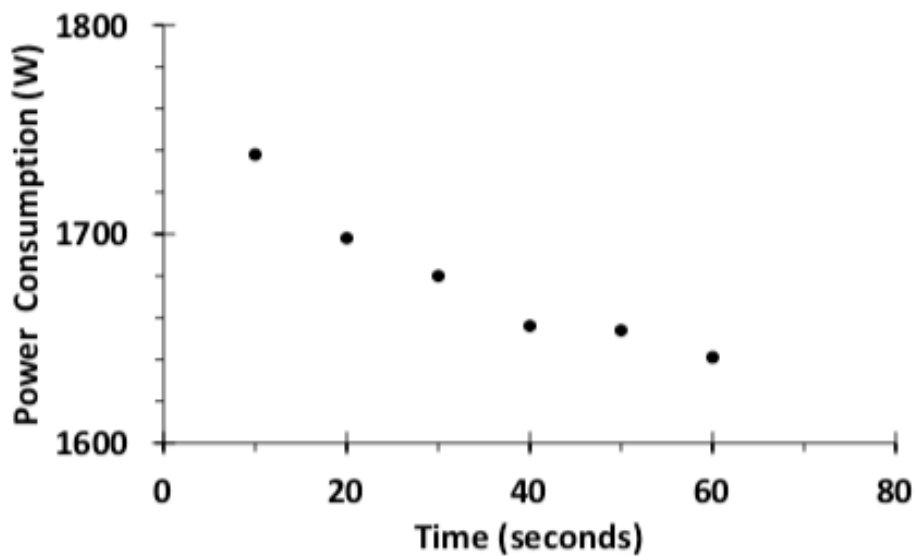


Figure S3. The online power measurements of the microwave oven when it was set to run for 60-seconds with no power adjustment.

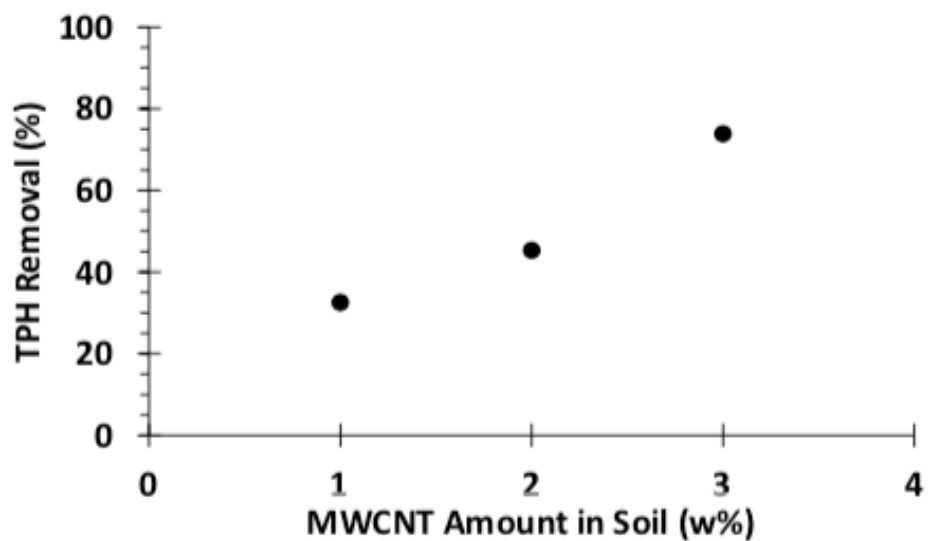


Figure S4. Effect of dielectric additive (MWCNT-1) amount on TPH removal. Thirty-second microwave irradiation was applied to all samples.

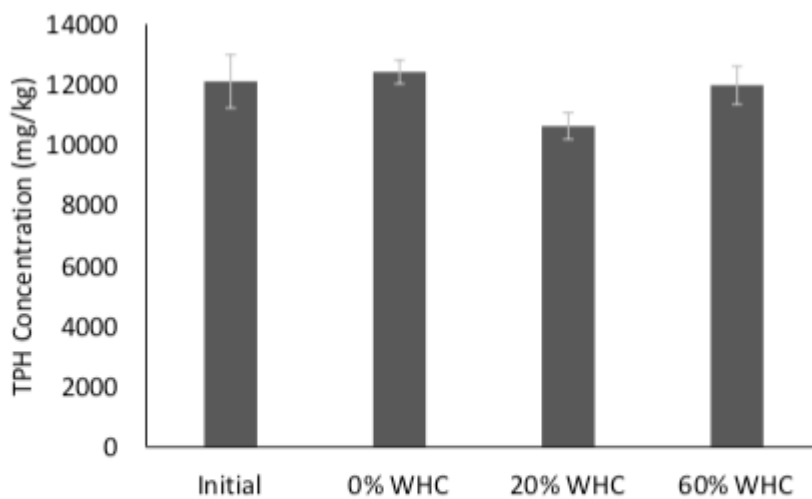


Figure S5. Effect of moisture content, reported as soil water holding capacity (WHC), on TPH removal after 60 second microwave irradiation with MWCNT-2 as the additive. Error bars indicate standard deviation of triplicate experiments.

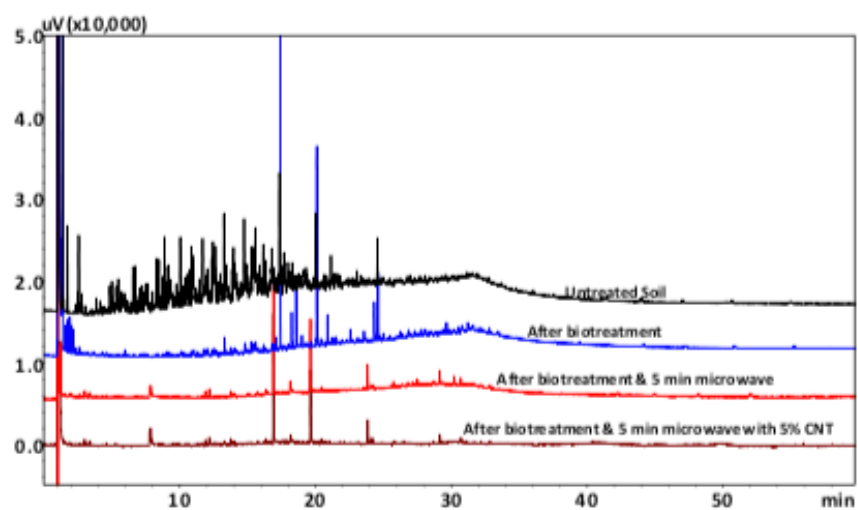


Figure S6. Chromatograms of TPH-containing soils after biotreatment and consecutive microwave treatment with and without carbon nanotubes. The baseline is shifted along the y-axis to allow better visual comparison.

APPENDIX B

YTTRIUM RESIDUES IN MWCNT ENABLE ASSESSMENT OF MWCNT
REMOVAL DURING WASTEWATER TREATMENT

YTTRIUM RESIDUES IN MWCNT ENABLE ASSESSMENT OF MWCNT REMOVAL DURING WASTEWATER TREATMENT

- This chapter has been published as **Kidd, J., Bi, Y., Hanigan, D., Herckes, P., and Westerhoff, P. (2019).** Yttrium residues in MWCNTs enable assessment of MWCNT removal during wastewater treatment. *Nanomaterials*, 9, pp. 670-683
- My author contribution: Approximately 60% of the research and 80% of the text

Abstract

Many analytical techniques have limited sensitivity to quantify multi-walled carbon nanotubes (MWCNTs) at environmentally relevant exposure concentrations in wastewaters. We found that trace metals (e.g., Y, Co, Fe) used in MWCNT synthesis correlated with MWCNT concentrations. Because of low background yttrium (Y) concentrations in wastewater, Y was used to track MWCNT removal by wastewater biomass. Transmission Electron Microscopy (TEM) imaging and dissolution studies indicated that the residual trace metals were strongly embedded within the MWCNTs. Yttrium concentration in MWCNTs was $76 \mu\text{g g}^{-1}$, and single particle mode inductively coupled plasma mass spectrometry (spICP-MS) was shown viable to detect Y-associated MWCNTs. The detection limit of the specific MWCNTs was $0.82 \mu\text{g L}^{-1}$ using Y as a surrogate, compared with $> 100 \mu\text{g L}^{-1}$ for other techniques applied for MWCNT quantification in wastewater biomass. MWCNT removal at wastewater treatment plants (WWTPs) was assessed by dosing MWCNTs ($100 \mu\text{g L}^{-1}$) in water containing a range of biomass concentrations obtained from wastewater return activated sludge (RAS) collected from a local WWTP. Using high volume to surface area reactors (to limit artifacts of MWCNT loss due to vessel walls) and adding 5 g L^{-1} of total suspended solids (TSS) of

RAS (3-hour mixing) reduced the MWCNT concentrations from $100 \mu\text{g L}^{-1}$ to $2 \mu\text{g L}^{-1}$.

The results provide environmentally relevant insight into the fate of

MWCNTs across their end of life cycle and aid in regulatory permits that require estimates of engineered nanomaterial removal at WWTPs upon accidental release into sewers from manufacturing facilities.

Introduction

Multi-walled carbon nanotubes (MWCNTs) consist of multiple rolled layers (concentric tubes) of graphene, which bring rise to their unique material properties (e.g., high thermal conductivity, elasticity, tensile strength, microwave absorbency, etc.). MWCNTs are being widely considered in numerous applications such as nanosensors [1], nanocomposite materials [2], paint or other coatings [3], and field-emission displays [4]. Manufacturing processes often combine MWCNT into stock solutions containing surfactants to maintain their dispersions or into polymers, which prevents working with dry MWCNT powders. Accidental MWCNT spills at manufacturing facilities can result in discharges to sewers, which flow to local wastewater treatment plants (WWTPs). In direct spillage scenarios into rivers or lakes, predicted MWCNT concentration ranges in surface waters may be in the microgram per liter ($\mu\text{g L}^{-1}$) range [5,6], which is 10–1000 times lower than MWCNT levels estimated to cause adverse biological responses in aquatic organisms [7-9]. However, in situations where MWCNT spills occur within industrial facilities, a short duration influx of MWCNTs at higher concentrations can occur at WWTPs. If not removed at WWTPs, short duration releases of MWCNTs into receiving waters could occur. Evaluating MWCNT removal in bench scale conditions can approximate full scale operations and provide useful information on what might be expected at full scale [10]. While research has shown that WWTPs can remove > 90% of many types of nanoparticles

due to their association with wastewater activated sludge and its subsequent physical separation [11-13], industry needs validated methods to estimate nanoparticle removal at WWTPs, similar to strategies employed for chemical pollutant removal tests (e.g., OPPTS 835.1110 EPA 712-C-98-298).

Current analytical techniques to detect and quantify carbon nanoparticles include programmed thermal analysis (PTA), Raman spectroscopy, spectroscopic absorbance, and microwave treatment with thermal analysis, but most available techniques have detection limits in solid matrices and water on the order of 10–100 mg kg⁻¹ or 0.1–10 mg L⁻¹, respectively [14]. Recent studies evaluated the ability of single particle inductively coupled plasma-mass spectrometry (spICP-MS) to detect residual trace catalytic metals (e.g., Fe, Y, Ni, Co, Mo) that persisted in single walled carbon nanotubes (SWCNTs) at ng L⁻¹ levels in an aqueous matrix [15-17]. Therefore, we explored spICP-MS and ICP-MS directly for the detection of known specific commercial MWCNTs in complex wastewater matrices.

The goal of this research was to demonstrate the use of metals as a surrogate measurement for MWCNT concentrations and use the measurements to assess the fate of MWCNTs at WWTPs under realistic MWCNT sewage concentrations. Specific objectives included (1) to select a trace rare earth element (REE) residual in MWCNTs as a surrogate for MWCNT quantification in wastewater by ICP-MS, (2) to determine the association of the selected REE (yttrium) and MWCNTs using transmission electron microscopy (TEM) before and after dissolution studies, (3) to determine the removal of MWCNTs with wastewater RAS, and (4) to use MWCNT removal results to predict conditions following an industrial spill scenario.

Materials and Methods

Preparation of MWCNT Solutions

A MWCNT working solution was prepared by diluting a commercial 5% MWCNT solution (Altana) to approximately 200 mg L⁻¹ using 18.2 M Ω -cm Nanopure water in 50 mL polypropylene centrifuge tubes. The MWCNT working solution was hand shaken and then immersed in a batch sonicator (Branson 5800) to disperse MWCNT particles. A test solution was prepared following prior research for wastewater biomass-nanoparticle removal evaluation [18], using 1 mM NaHCO₃ (pH 7.4) prepared in Nanopure water (\geq 18.2 M Ω -cm). Four vial types were used in these experiments: (1) 50 mL polystyrene centrifuge vials, (2) 40 mL borosilicate vials with septa screw cap, (3) 40 mL amber glass vials with Teflon septa screw cap, and (4) a standard jar test apparatus (Phipps and Bird) with six 2 L polyethylene vessels.

Return Activated Sludge (RAS) Stock Preparation

RAS was collected in 1 L Nalgene HDPE wide mouth bottles from a metro-Phoenix region secondary WWTP practicing nitrification and denitrification. The same approach was used previously for nanoparticle-WWTP studies [10,11,18]. Immediately after collection, the sample bottles were placed in an ice cooler (approx. 4 °C) and returned to the lab where they were stored in the 4 °C fridge. Within 24 hours, the solids visually settled, and the wastewater supernatant was decanted. The RAS was re-suspended in 400 mL of 1 mM NaHCO₃ solution, allowed to settle, and the supernatant discarded again. This was repeated for a total of three rinses. A final RAS stock suspension was then made in a 1 L Nalgene HDPE bottle with the 1 mM NaHCO₃ solution. To determine the concentration of the biomass suspension (g TSS L⁻¹), the collected biomass was stirred with a stir bar to shear

larger particles and obtain more uniform particle size. 10 mL of biomass sample were vacuum filtered with a 0.45-micron glass fiber filter, followed by 3 rinses of the filter using 10 mL of Nanopure water. The filter with biomass was then carefully removed, placed into an aluminum weighing dish, and dried at 105 °C until the change in biomass weight between sampling periods (10 min) was less than 4% of total sample weight. The weight of the dry biomass was recorded, and the concentration of dry biomass was calculated (g TSS L⁻¹). The stock RAS suspension was then diluted with 1 mM NaHCO₃ solution to achieve a TSS concentration equal to the desired TSS concentration in the experimental samples. New diluted stocks were made from the original stock for each experimental RAS concentration. The new RAS stocks were stored in the 4 °C fridge until the experiment was conducted. We completed the experiment within 24 hours of rinsing and diluting the RAS stock solutions.

Quantification Techniques for MWCNTs

Light Scattering Detection and Programmed Thermal Analysis of MWCNTs

To supplement the use of trace elements for MWCNT detection, MWCNTs were also quantified using UV-Vis spectroscopy and PTA [19]. For UV-Vis spectroscopy, calibration curves were made by creating a dilution series from the 200 mg L⁻¹ MWCNT stock solution in 1 mM NaHCO₃ matrix solution. The dilution series was scanned at wavelengths from 300 to 800 nm (Figure S1). For PTA, the 5% MWCNT solution and a MWCNT powder were analyzed. Both samples used the same manufactured MWCNTs. The MWCNT solution was dried at 105 °C until the change in dry weight measured between 24-hour time points was < 4%. The two MWCNTs were placed in a furnace and

heated in the absence and then presence of oxygen following the methodology outlined previously for PTA detection of MWCNTs (Figure S2) [19-22].

Microwave Digestion of MWCNTs

Soluble metal residuals present on MWCNTs were quantified by ICP-MS after microwave digestion. Briefly, ~0.1 g of 5% MWCNT solutions were digested in 10 mL HNO₃ (70%) with a CEM MARS 5 microwave accelerated reaction system (1200 watts, 2450 MHz) at 170 °C for 40 minutes. After cooling, the digested samples were diluted in 2% HNO₃ and analyzed for 30 common metals using a Thermo Scientific X-Series II ICP-MS. Previous study indicates that this method yields reliable results for the quantification of metal contents in CNTs [23]. Of the 54 elements scanned, only a few elements were found in measurable concentrations in this product.

Dissolution Tests and TEM Imaging to Assess Residual Metal Association with MWCNTs

To determine association of metal residuals with the MWCNTs, two 40 mL solutions of MWCNTs (1 mg L⁻¹) were suspended in 50 mL polystyrene centrifuge vials at different pH values: 2% HNO₃ (pH 2) and 1 mM NaHCO₃ (pH 7.4). Solutions were shaken for 24 hours to evaluate mechanical and/or chemical release of metal catalysts. 15 mL of each solution were passed through a 30 kDa ultrafilter using a centrifuge for 15 minutes at 5000 G (Millipore, Ultracel Regenerated Cellulose Membrane, > 90% recovery) to separate remaining MWCNT particulates and nano-scale or dissolved metals. The permeate was analyzed by spICP-MS. The remaining 25 mL of MWCNT solutions not used in the ultrafiltration process were evaluated with a Philips CM200 TEM coupled with energy

dispersive X-ray spectroscopy (EDAX). Samples were placed on copper TEM grids (2% HNO₃ sample was neutralized with NaOH salt before placement on grids) and analyzed.

Single Particle ICP-MS and ICP-MS Analysis of Yttrium

We operated ICP-MS in single particle mode following methods published previously [15,24-26] and followed the approach of analyzing for trace metals in MWCNTs as demonstrated for SWCNTs [15,17]. For samples analyzed with spICP-MS, if the sample contains dissolved metals, the ions will be distributed homogeneously within the solution, producing a consistent intensity signal vs. time across readings. However, if the sample contains particles, the metal atoms within the sample are no longer distributed homogeneously. Instead the metals are present as discrete particulates and, once ionized, move through the mass analyzer to the detector as a cluster of ions. This cluster of ions results in a spike above the background, where the pulse corresponds to an individual particle and the background represents the “dissolved” metals in solution.

Of the six metal residuals (⁵⁹Co, ⁶⁰Ni, ⁶⁸Zn, ⁸⁹Y, ⁹⁰Zr, and ⁹⁵Mo) that were physically bound to the MWCNTs, we determined that yttrium (Y) would be best used as an indicator of this specific MWCNT for quantification because it has the highest sensitivity on ICP-MS (see Results) and also a low background concentration of yttrium present in wastewater sludge [27]. Analysis by spICP-MS was performed on non-digested samples using a Thermo Scientific X-Series II (Waltham, MA) in time-resolved data acquisition mode with a dwell time of 10 ms following methodologies described elsewhere [28]. In brief, samples were placed in polypropylene sample tubes in Nanopure water, and the tubes were placed in a sonicating bath for 15 minutes. Samples were then immediately pumped into the

instrument, and the spectra for ^{89}Y were recorded. We used three times the standard deviation of the spectra to delineate MWCNT pulses from background dissolved metal. We also measured total dissolved ^{89}Y concentrations in MWCNT suspension by ICP-MS by diluting the MWCNT stock solution to between 0.001 to 100 $\mu\text{g L}^{-1}$. A linear calibration curve was made between diluted MWCNT concentrations and yttrium responses (in counts per second, cps) (Figure S3). Then we calculated a minimum detection level (MDL) following EPA procedure of running 10 replicate samples. The MWCNT stock solution was diluted to roughly 2 $\mu\text{g L}^{-1}$ to determine the MDL (0.49 $\mu\text{g L}^{-1}$). Because we found that the Y was easy to dissolve, biomass partitioning experiments were analyzed by first exposing the biomass/CNT mixture to 2% nitric acid, followed by filtration through 30 kDa ultrafilters and ICP-MS analysis.

MWCNT-RAS Batch Interaction Experiments

For experiments conducted in 40 mL glass and amber vials with septa screw caps, triplicate samples with 35 mL of wastewater biomass to achieve desired final biomass concentrations of 0, 0.5, 1.0, 2.0, 3.0 and 5.0 g TSS L^{-1} . The MWCNT solution (5 mL) was added to a final MWCNT concentration of 100 $\mu\text{g L}^{-1}$ for a total reactor volume of 40 mL. Triplicate controls with wastewater biomass only and nanoparticle solution only were also performed. Vials were sealed and secured on a rotator table for 3 hours at 45 revolutions per minute (rpm). After mixing, the samples equilibrated in the lab for 1 hour to allow for biomass settling, and a 10 mL supernatant aliquot was taken and centrifuged at 150 G for 10 minutes to settle any remaining biofloc in the supernatant. The samples were transferred to clean

vials and acidified with 2% HNO₃ for 24 hours to release yttrium from the MWCNTs. Samples were passed through 30 kDa ultrafilters and analyzed using ICP-MS.

For jar test experiments, a standard jar test apparatus (Phipps and Bird) was used with six 2 L vessels. Each jar was given a different biomass concentration (0, 0.5, 1.0, 2.0, 3.0, and 5.0 g TSS L⁻¹), and these biomass concentrations were made up to 1.8 L in 1 mM NaHCO₃ matrix solution. The no biomass control contained 1.8 L of 1 mM NaHCO₃ matrix solution. The experiments were run in triplicate (n=18). After biomass was added at specified concentrations, 200 mL of 1 mg L⁻¹ MWCNT solution were added to each reactor to give a final MWCNT concentration of 100 µg L⁻¹ and a final reactor volume of 2 L. The jar apparatus mixing was continuous at 45 rpm for 3 hours. The apparatus was turned off, and the biomass settled for 1 hour. 50 mL of supernatant from each jar test reactor was placed into a 50 mL polystyrene centrifuge vial and centrifuged at 150 G to separate the remaining biofloc from the solution. The supernatants were then acidified with 2% HNO₃ for 24 hours and filtered through 30 kDa ultrafilters prior to ICP-MS analysis of dissolved yttrium concentrations. Randomly chosen samples were also analyzed for ⁸⁹Y using spICP-MS to confirm removal of pulses originating from yttrium in the MWCNTs.

Results and Discussion

Characterization of MWCNTs and the Trace Metal Residuals Associated with MWCNTs

Elemental content of the MWCNTs determined by ICP-MS after microwave digestion are summarized in Table 1. Of the 54 elements scanned, only a few elements were found in measurable

concentrations in this product. Quantitative analyses were conducted for ^{59}Co , ^{60}Ni , ^{68}Zn , ^{89}Y , ^{90}Zr , and ^{95}Mo (Table 1).

Table 1. Contents of trace metal residual elements in MWCNTs determined by ICP-MS.

Metal	Concentration ($\mu\text{g g}^{-1}$)	*Sensitivity Regression Equation	*Sensitivity R^2 Value
Fe	9363 ± 578	-	-
Y	76.19 ± 5.93	$1.90\text{E}+04\text{X} + 1.07\text{E}+03$	0.99
Zr	1253 ± 75.31	$1.00\text{E}+04\text{X} + 2.35\text{E}+03$	0.99
Co	153.3 ± 6.47	$6.17\text{E}+03\text{X} + 2.57\text{E}+03$	0.99
Zn	10.47 ± 5.32	$8.96\text{E}+01\text{X} + 9.73\text{E}+02$	0.78
Ni	5.06 ± 0.41	$9.71\text{E}+02\text{X} + 1.82\text{E}+02$	0.99
Mo	1.19 ± 0.07	$2.72\text{E}+02\text{X} + 4.36\text{E}+00$	0.99

Concentration data expressed as Mean \pm S.D. of three independent measurements ($\mu\text{g g}^{-1}$)

*Data obtained from Figure 1

Iron (Fe) was found at the highest concentration ($\sim 9.36 \text{ mg g}^{-1}$) followed by Zr ($\sim 1.25 \text{ mg g}^{-1}$), Co ($153 \mu\text{g g}^{-1}$), Y ($76.2 \mu\text{g g}^{-1}$), Zn ($10.5 \mu\text{g g}^{-1}$), Ni ($5.1 \mu\text{g g}^{-1}$), and Mo ($1.2 \mu\text{g g}^{-1}$). We presume these residuals are catalyst impurities in the metals used in MWCNT synthesis rather than intentionally added by manufacturers. These results align well with reports of yttrium and cobalt in SWCNTs [15,17] Figure 1 shows the sensitivity of these three metal residuals by ICP-MS after microwave digestion of the CNT.

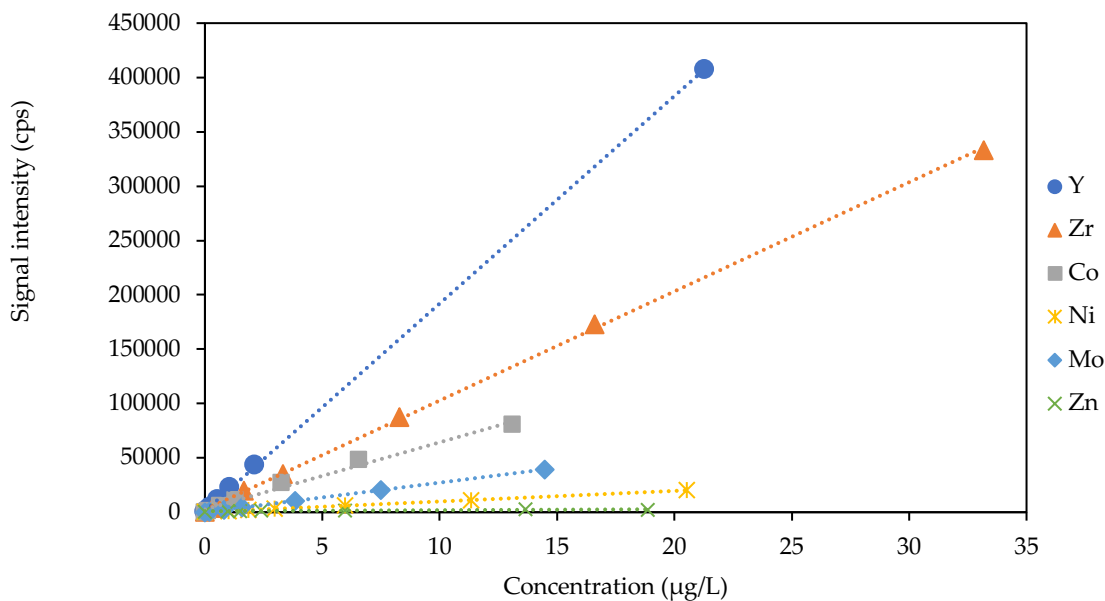


Figure 1. Sensitivity of trace metal residuals (Y, Zr, Co, Ni, Mo, Zn) using ICP-MS. The ratio of net signal to concentration is the sensitivity of each element.

Sensitivity was found by comparing the ratio of their net signal (counts per second) to concentration ($\mu\text{g L}^{-1}$) and is important because the quantitation limit of elements by ICP-MS is primarily set by sensitivity. We chose to normalize instrument response to the MWCNT concentration rather than to a neat metal standard because the manufacturer MWCNT solution matrix is unknown, causing unknown ionization or instrumental effects that would not be present for a neat solution. Yttrium had the highest sensitivity of the three metal residuals, followed by zirconium and cobalt. We previously found that yttrium had the lowest “enrichment factors, EF” in wastewater sludge [27], and here we found that yttrium was a feasible residual metal candidate to quantify MWCNT concentrations using spICP-MS and ICP-MS.

TEM images and their corresponding EDAX for the 5% MWCNT solution are shown in Figure 2. The TEM images are representative of analytical replicates taken from the stock solution. The average width of the MWCNTs was found to be 18 ± 3 nm, and the length was between 50 and 5000 nm. Additional TEM images are in Figure S4. EDAX detected Zirconium (Zr), Aluminum (Al), and Oxygen (O) with lower levels of phosphorus (P), Iron (Fe), and Silica (Si) present in the dense regions embedded within the MWCNTs. Trace metals quantified by ICP-MS were not detected by EDAX, which often is only sensitive at $> 0.5\%$ weight.

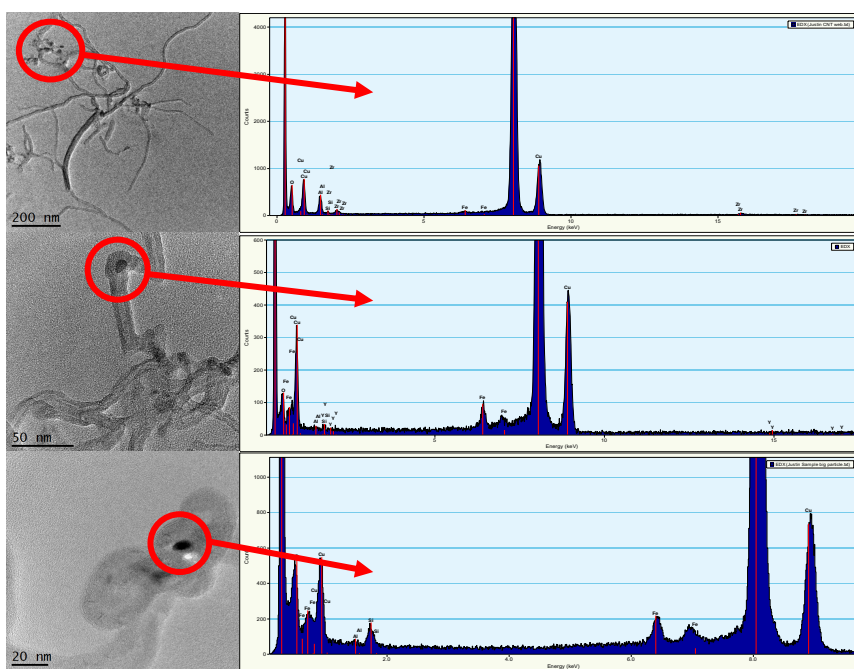


Figure 2. TEM imaging of 5% MWCNT stock solution and corresponding EDAX of highlighted TEM images. Dense (darker) regions on MWCNTs are residual trace metals remaining after MWCNT synthesis.

Association of Yttrium with MWCNTs

Dissolution experiments using MWCNTs were performed to determine if yttrium was mobilized into water or retained on the MWCNTs. In control experiments, we expected that dissolved yttrium would pass through the 30 kDa ultrafilters; however, if Y remained associated with the MWCNTs it would be retained by the 30 kDa ultrafilters. All of the ^{89}Y standard passed through the ultrafilter, confirming that dissolved yttrium is not retained or sorbed by the ultrafilter (> 90% recovery).

To determine the initial yttrium pulses present, 15 mL of the MWCNT solution was analyzed with spICP-MS (Figure 3A). A large number of pulses were present, and the signal (y-axis) baseline was between 40,000 and 60,000 cps for the yttrium response. After filtering 15 mL of the MWCNT solution through a 30 kDa ultrafilter (Figure 3B), there were virtually no pulses, and a baseline of < 1000 cps. When the remaining 15 mL of the MWCNT solution was acidified in 2% HNO_3 for 24 hours and filtered through the 30 kDa filters (Figure 3C), there were no pulses present, but the baseline shifted from < 1000 cps to approximately 40,000 cps. Taken together, we concluded that in 1 mM NaHCO_3 , yttrium was physically bound with MWCNTs and did not pass through the filter into the permeate. Once the MWCNTs were acidified with 2% HNO_3 , the yttrium dissolved and passed through the ultrafilter, further indicating that yttrium was associated with the MWCNTs.

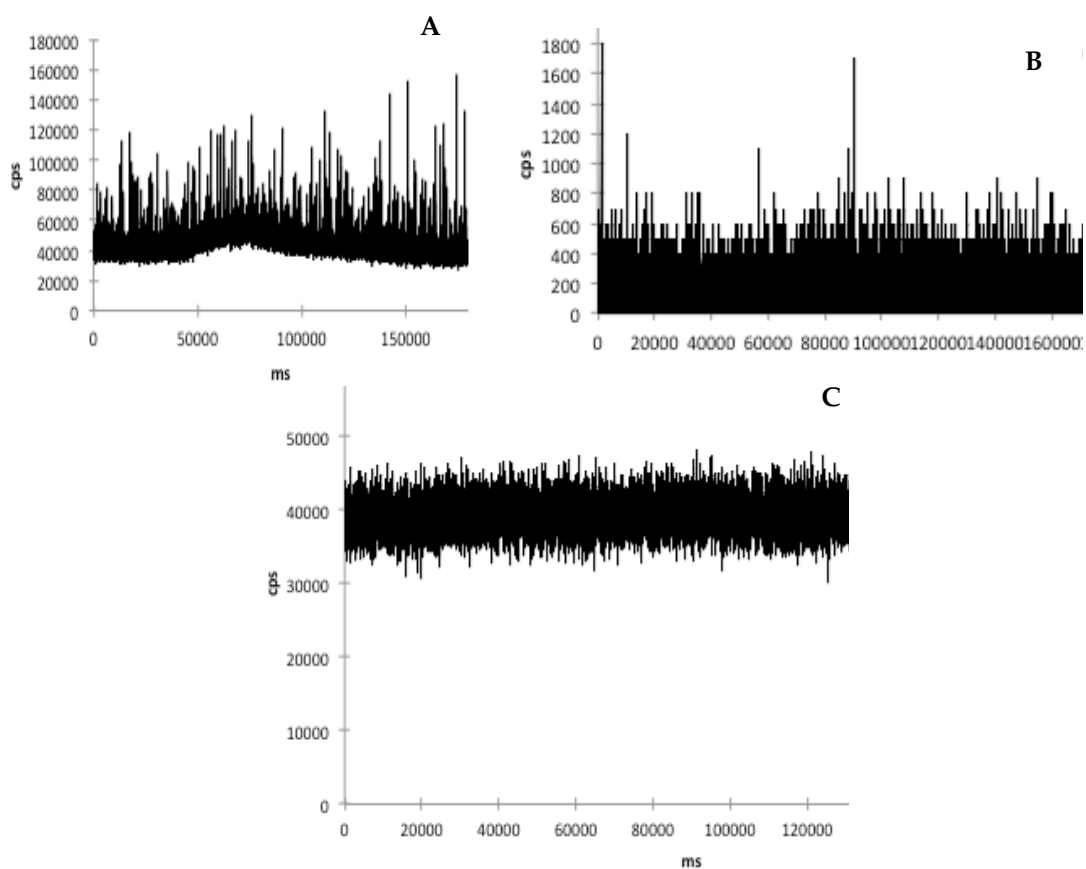


Figure 3. Yttrium spICP-MS data of an (A) undissolved initial MWCNT sample, (B) undissolved MWCNT permeate, and (C) 2% HNO₃ dissolved MWCNT permeate passed through a 30 kDa ultrafilter, showing that yttrium did not pass through the ultrafilter unless acidified and dissolved by 2% HNO₃.

To determine if yttrium leached from the MWCNTs over time, MWCNTs were spiked into either 1 mM NaHCO₃ or 2% HNO₃ solutions, and TEM/EDAX was conducted at time points of 0 hours and 24 hours (Figure 4). Figures 4A-C show TEM and EDAX images of

MWCNTs in 1 mM NaHCO₃ and 2% HNO₃ after the initial spike of MWCNTs into solution. Figures 4D-F show TEM and EDAX images of MWCNTs in 1 mM NaHCO₃ and 2% HNO₃ after 24 hours. In 1 mM NaHCO₃ solution, MWCNTs still contained residual metals (Fe, Al, etc...) after 24 hours, and there was no change in MWCNT morphology. In 2% HNO₃ solution, no MWCNTs remained at either time point (0 hours and 24 hours). Instead, we observed bundles of metal catalysts in solution. We concluded that the residual metals were tightly associated with the MWCNTs in 1 mM NaHCO₃ and were not likely to leach into solution during our wastewater activated sludge experiments under 24 hours. We also concluded that the low pH of the 2% HNO₃ solution caused metal dissolution from the MWCNTs.

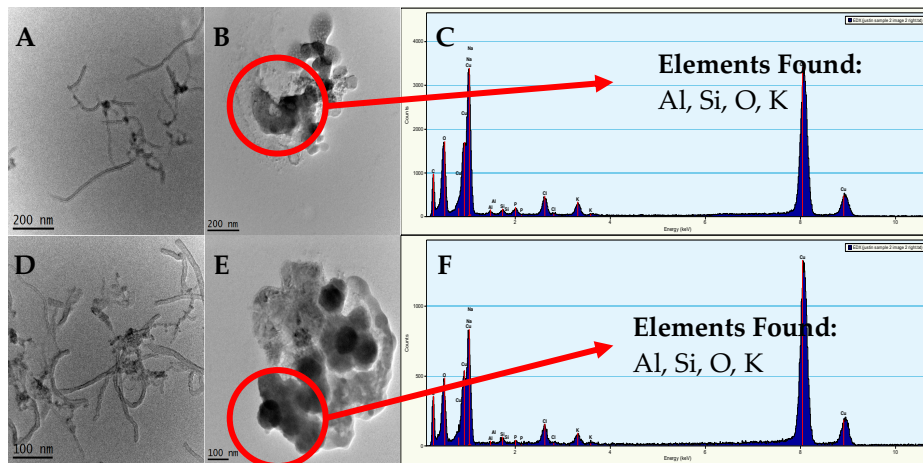


Figure 4. (A) TEM image of MWCNT in 1 mM NaHCO₃ matrix solution after initial spike (< 1 hour), (B) TEM image of MWCNT in 2% HNO₃ matrix solution after initial spike (< 1 hour), (C) EDAX of MWCNT from image B, (D) TEM image of MWCNT in 1 mM NaHCO₃ matrix solution after 24 hours, (E) TEM image of MWCNT in 2% HNO₃ matrix solution after 24 hours, (F) EDAX of MWCNT from Image E.

Quantification of Yttrium in MWCNT by spICP-MS and ICP-MS

We investigated using spICP-MS to quantify Y in MWCNTs. ^{89}Y showed a linear relationship for MWCNT solutions between 50 ng L^{-1} and $20 \text{ } \mu\text{g L}^{-1}$ (Figure 5). Increasing MWCNT concentration led to more pulses, with yttrium pulses used as a measurement of MWCNT concentration. The total pulse intensity within a specified run time were integrated by the number of pulses and used to correlate with MWCNT concentrations using the same approach for SWCNTs [15,17]. Following EPA method 200.8, an MDL for MWCNTs was calculated to be $0.82 \text{ } \mu\text{g L}^{-1}$ (Figure S5).

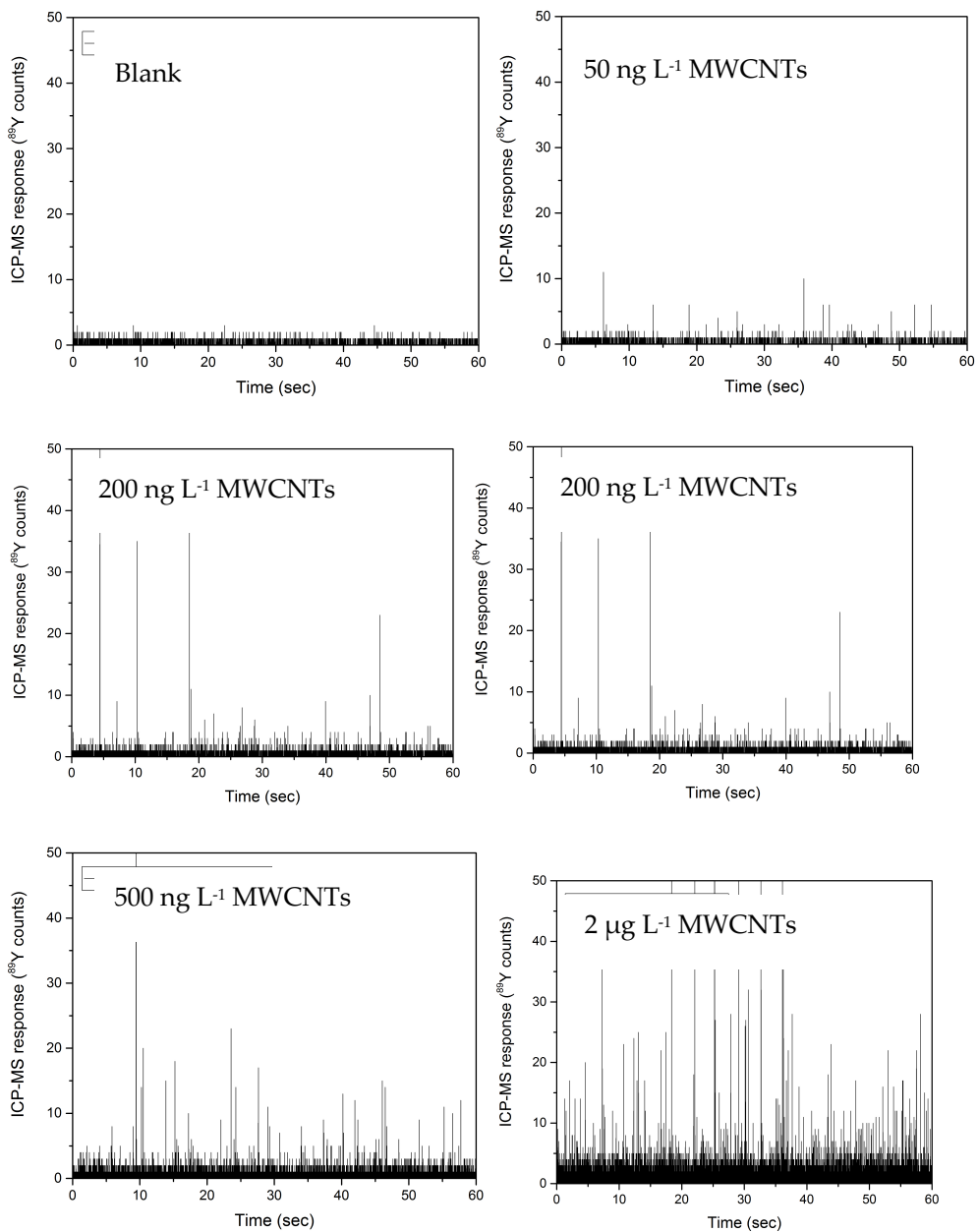


Figure 5. Single particle ICP-MS detection using ^{89}Y of MWCNTs in solution across a range of concentrations plus a control (blank) sample.

Separately we determined if dissolved yttrium, after acidification, could be quantified by ICP-MS instead of using spICP-MS because conventional ICP-MS is more commonly available in industry and commercial analytical labs. The 5% MWCNT solution was diluted in ultrapure water to $2 \mu\text{g L}^{-1}$, and a dilution series was made and acidified for 24 hours with 2% nitric acid to determine an MDL. Ten replicate samples were run, and ^{89}Y ICP-MS responses were measured. The average response was $2.12 \pm 0.29 \mu\text{g L}^{-1}$ with a variance of 0.0849 and a calculated MDL of $0.8 \mu\text{g L}^{-1}$. Additional experiments were performed using a $5 \mu\text{g L}^{-1}$ MWCNT solution, which yielded an MDL of $0.49 \mu\text{g L}^{-1}$. As shown below, there was no Y detected in the supernatant of control experiments with wastewater biomass (i.e., absence of MWCNT). The ICP-MS method reduced the time required to analyze MWCNTs compared to spICP-MS because the spICP-MS used in this study requires additional external calculations outside of the instrument software to separate real pulses from particles versus baseline pulses. For spICP-MS, additional work is needed to calculate the efficiency of particle transport that reaches the detector. This requires purchasing and injecting particles of known size and concentration. As a result, we used ICP-MS rather than spICP-MS to analyze MWCNT removal by RAS (described below) by quantifying dissolved yttrium remaining in supernatant. There was not a need to use spICP-MS in a quantitative manner. However, selected split samples analyzed using spICP-MS drew the same MWCNT removal conclusions as conventional ICP-MS analysis using Y, providing another indicator that yttrium is associated with MWCNTs.

6.4.1. Removal Efficiency of MWCNTs by Return Activated Sludge

Figure 6 presents MWCNT removal by RAS in 40 mL polystyrene centrifuge vials, 40 mL glass vials, 40 mL amber vials, and 2L polyethylene vials. Background yttrium concentrations in RAS were below the detection limit of ICP-MS. For the polystyrene centrifuge vials, only 25% of the MWCNTs spiked into the control samples (MWCNTs were added without RAS present) were detected in the supernatant by ICP-MS. The MWCNT loss was attributed to sorption on the polystyrene vial wall. In the experimental samples with low RAS biomass concentrations and in polystyrene vials, there was further decrease in MWCNTs from the supernatant. However, at RAS concentrations above 3 g L⁻¹, we observed higher concentrations of MWCNTs in the supernatant.

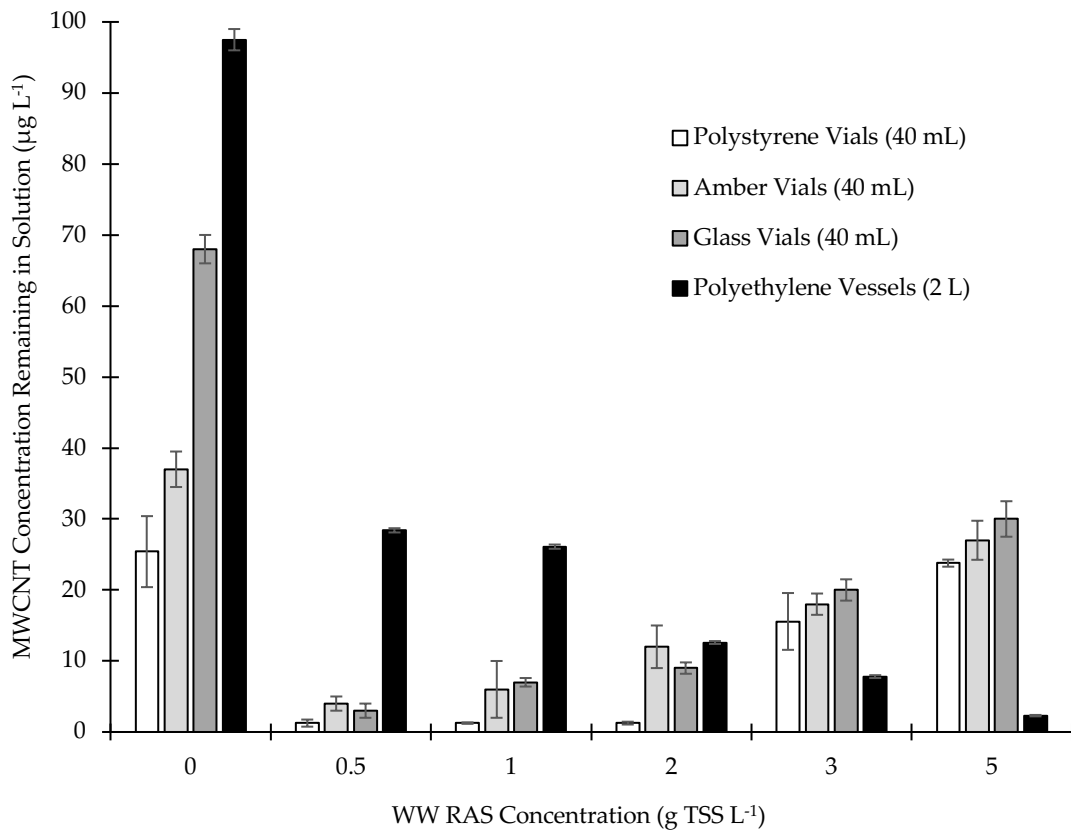


Figure 6. Replication of MWCNT adsorption to WW Biomass Using Different Container Vessels

The experiments were repeated using glass vials and amber glass vials (Figure 6). There appeared to be less adsorption of MWCNTs to the vial wall in the control samples (no RAS) for both the amber vials and the glass vials compared with the polystyrene vials. The amber vials had ~ 36% MWCNTs remaining in solution without biomass. The glass vials had ~ 70% MWCNTs remaining in solution without biomass. Similar to polystyrene vials, at RAS concentrations above 3 g L^{-1} , we observed higher concentrations of MWCNTs in the supernatant for both amber and glass vials.

We suspected that any surface may exhibit affinity for a fixed mass of MWCNTs. Therefore, we decreased the reactor surface area to volume ratio by using 2 L polyethylene reactor vessels ($0.85 \text{ cm}^2/\text{cm}^3$) instead of 40 mL vials ($3.06 \text{ cm}^2/\text{cm}^3$). All samples were analyzed for dissolved Y, and a subset of samples were also analyzed by spICP-MS to confirm the presence/absence of MWCNTs in samples. Our control sample (no RAS) showed negligible loss of MWCNTs to vessel walls as $> 95\%$ of MWCNTs spiked into 2 L vessel remained in solution.

The RAS reduced the MWCNT concentrations from $100 \text{ } \mu\text{g L}^{-1}$ to between $27 \text{ } \mu\text{g L}^{-1}$ and $2.2 \text{ } \mu\text{g L}^{-1}$ in the 2 L polyethylene reactor vessels (Figure 6). This indicates that as the RAS concentration increased, we achieved near complete MWCNT removal (97.7% MWCNT removal at 5 g TSS L^{-1} RAS). Based on triplicate experiments followed by yttrium analysis using ICP-MS and ANOVA ($> 95\%$ confidence), there was high

reproducibility of the tests. These results showed that MWCNTs were well removed by wastewater RAS, showing consistency with previously published findings [13].

Implications of Using Yttrium as a Trace Residual Metal to Quantify MWCNT Removal by Wastewater Biomass

After completing WWTP RAS batch scale experiments, we considered a manufacturing spill scenario to understand how the RAS removal test strategy employed here could aid industry in meeting potential regulatory requirements. Obtaining EPA approval for use of nanomaterials may require estimating concentrations of MWCNTs in rivers receiving treated wastewater effluent from facilities impacted by industrial discharges. We considered a relatively small community of 20,000 residents. Assuming an average of 50 gallons per capita of sewage production, this equates to a 1 MGD WWTP. This is a common lower design capacity of activated sludge WWTPs. The scenario considered one 55-gallon drum of a 5% MWCNT solution leaked or spilled before being discharged to the sewer system over 24 hours. In this scenario, the average MWCNT concentration entering the WWTP would be roughly 100–150 $\mu\text{g L}^{-1}$.

We considered a manufacturing spill scenario to understand how the RAS removal test strategy employed here could aid industry in meeting potential regulatory requirements. Based upon results in Figure 6, an activated sludge WWTP operating at a biomass concentration of 1 to 3 g TSS L^{-1} would adsorb > 95% of the MWCNTs and would result in 2–30 $\mu\text{g L}^{-1}$ being released to receiving waters. MWCNTs at 2–30 $\mu\text{g L}^{-1}$ would be below quantification limits by UV-Vis, Raman, PTA, etc (Figures S1 and S2). Because yttrium concentrations in wastewater are < 1 $\mu\text{g L}^{-1}$ [27] the measurement of yttrium by

ICP-MS or spICP-MS may be viable. Reported aquatic toxicity of MWCNTs are $> 50 \mu\text{g L}^{-1}$, and thus even without in-stream dilution, the spill event would be below this potential regulatory limit, even though the MWCNT concentration was $> 100 \mu\text{g L}^{-1}$ entering the WWTP in the raw sewage.

Conclusions

Detection and quantification of known commercially available MWCNTs at environmentally relevant concentrations ($< 50 \mu\text{g L}^{-1}$) using residual yttrium was found to be possible using both conventional ICP-MS and spICP-MS. Additionally our detection limit of $2.5 \mu\text{g L}^{-1}$ was lower than many reported MWCNT concentrations in surface waters. TEM imaging and dissolution studies showed that metal catalysts were physically bound to the MWCNT in bundles indicating that they can be used as proxies for MWCNT quantification. In the net removal experiments, we observed that adding wastewater RAS at $500 \text{ mg TSS L}^{-1}$ to 5 g TSS L^{-1} to solutions containing

100 $\mu\text{g L}^{-1}$ MWCNT removed the MWCNT, with the RAS concentration at 5g TSS L^{-1} removing MWCNTs to below threshold reporting levels. This method is only applicable in lab experiments with known MWCNT where Y content is a known constant. It is not applicable for full scale monitoring at WWTPs because every MWCNT will have its own signature (e.g., REE content or thermal properties).

While yttrium was chosen as the surrogate trace residual metal in this study, each MWCNT will have distinctive synthesis methods [29,30] and thus will likely have unique trace residual metal compositions. It will be important moving forward to understand these differences between MWCNTs and whether a unified method can be developed to quantify MWCNTs through spICP-MS or ICP-MS using trace residual metals or whether trace residual metals like yttrium can be useful as a marker in standardized testing of MWCNTs moving forward.

Acknowledgements

This research was partially funded by the U.S. Environmental Protection Agency (RD 83558001) and the National Science Foundation through the Nanosystems Engineering Research Center for Nano-Enabled Water Treatment (EEC 1449500).

Supplemental Information

Light Scattering Detection of MWCNTs

UV-Vis light scattering was first investigated to detect MWCNTs in solution. MWCNTs exhibit a broad response between 300 and 800 nm wavelengths (Figure S1A). Calibration curves were generated for both 300 nm and 400 nm wavelengths (Figure S1B) and were linear between 1 and 10 mg L⁻¹. Based upon the absorbance of MWCNTs and background absorbance of treated wastewater, the UV-Vis method for MWCNT determination was deemed valid only to ~ 0.5 mg L⁻¹ of MWCNT.

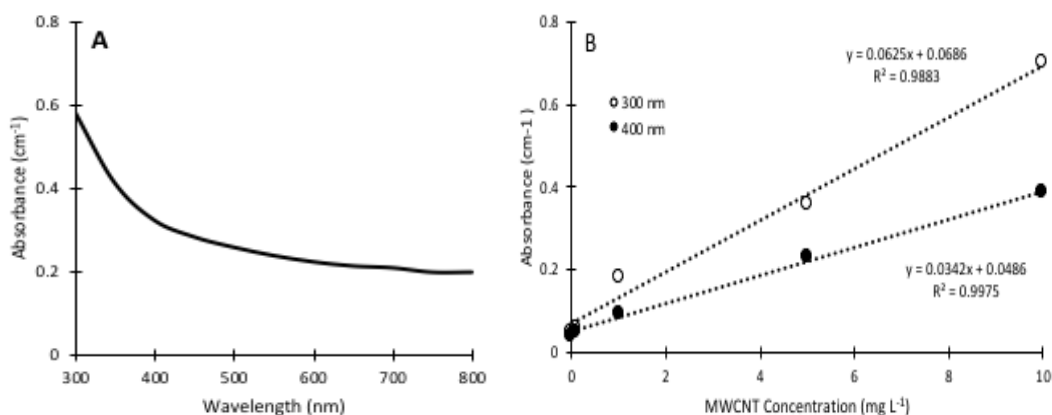


Figure S1. The left figure (A) shows the UV-Vis spectra for 10 mg L⁻¹ MWCNT on a 300–800 nm wavelength scan. There is no optimal peak, so calibration curves in the right figure (B) were made for MWCNT at 300 nm and 400 nm wavelengths. These are commonly used wavelengths for carbon nanotubes.

Programmed Thermal Analysis of MWCNTs

PTA was also attempted to quantify MWCNTs in water. Figure S2 shows PTA temperature profile applied (black line) and two PTA thermograms with a flame ionization detector (FID) carbon signal response (y-axis) for a dry MWCNT and then the material dried from the 5% MWCNT solution. The dry (powder) MWCNT product (red line) had a low response in the inert gas range (0–450 seconds) and then two peaks in the presence of oxygen gas (450–1000 seconds), which is typical of relatively pure CNTs with low organic content. The PTA thermogram for the MWCNT 5% solution (blue line) had a large response in the inert gas region, which is typical when organic compounds are present, and then a response that is shifted towards higher temperatures during exposure to the oxygen gas environment. The high background organic content from the surfactant used to stabilize the MWCNTs prevented the use of PTA for quantifying MWCNTs in water.

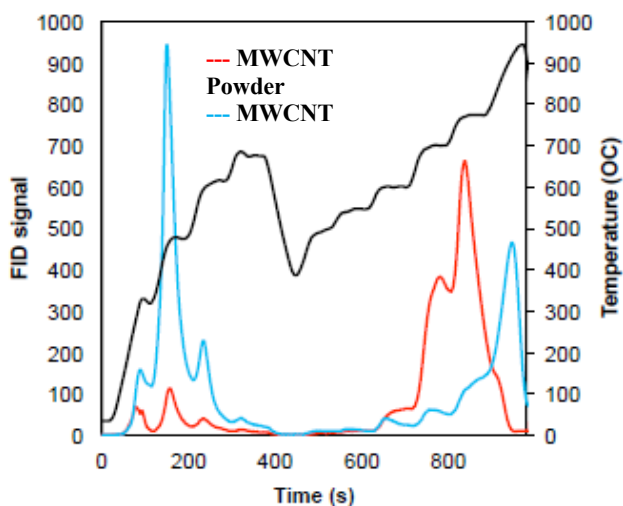


Figure S2. PTA temperature profile (black line) and FID signal response thermograms for two MWCNT products, one dry (red-line) and one liquid (blue-line).

Calibration Curve for ^{89}Y Pulse Counts (spICP-MS) Versus Dissolved Y Concentrations (ICP-MS)

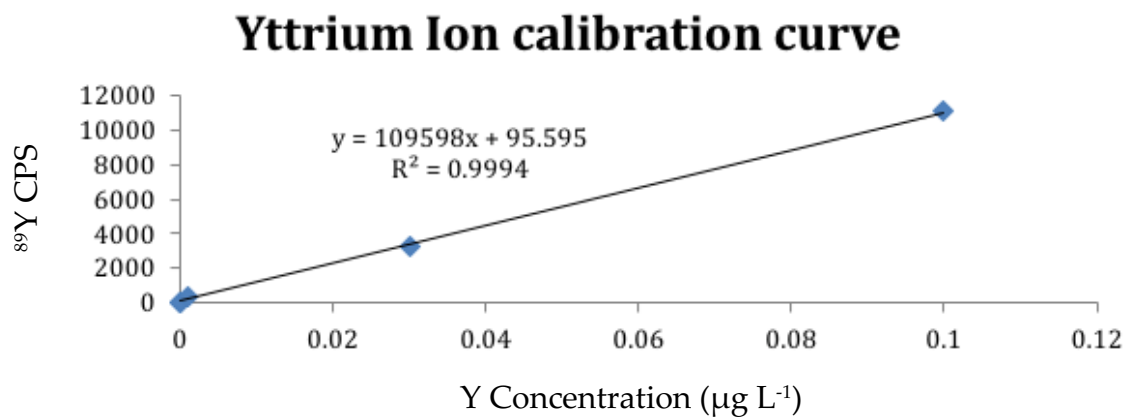


Figure S3. Calibration Curve for ^{89}Y pulse counts (spICP-MS) versus dissolved Y concentrations (ICP-MS). This calibration curve was used to determine MWCNTs remaining in solution with ICP-MS. The 5% MWCNT solution was diluted to between 0.001 and 0.10 $\mu\text{g L}^{-1}$.

TEM Images of MWCNT Solution

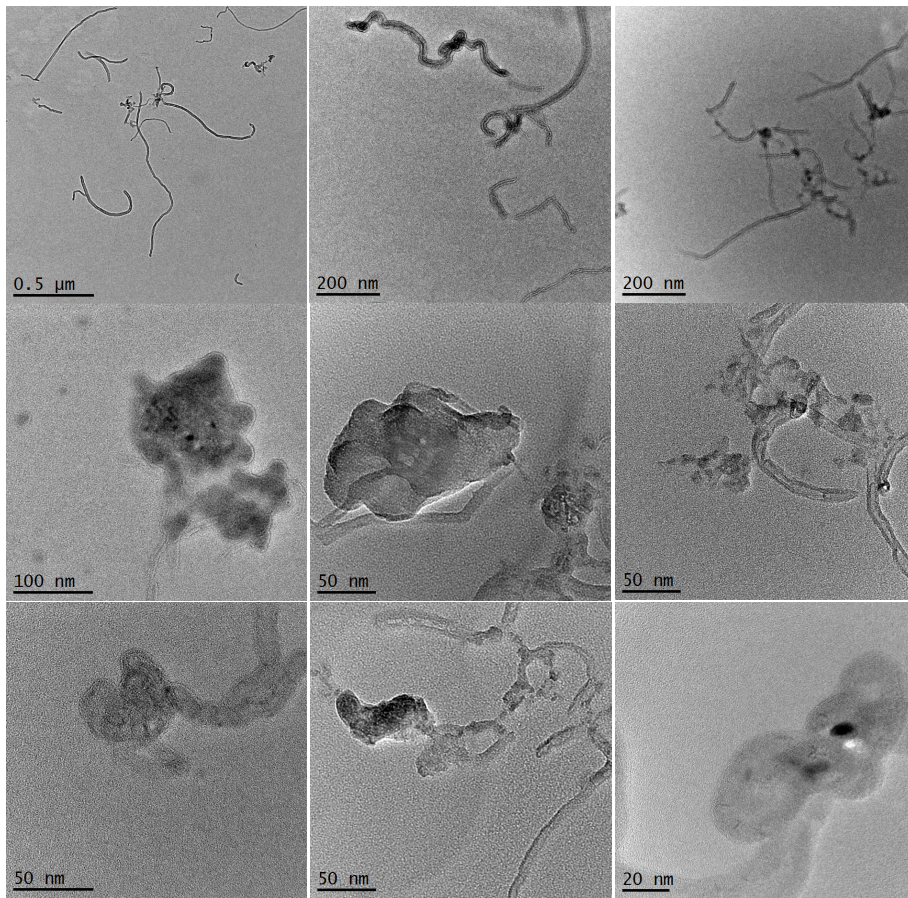


Figure S4. TEM images of MWCNTs in 1 mM NaHCNO₃ matrix solution.

Detection Limit Calculations for ^{89}Y by spICP-MS for MWCNTs

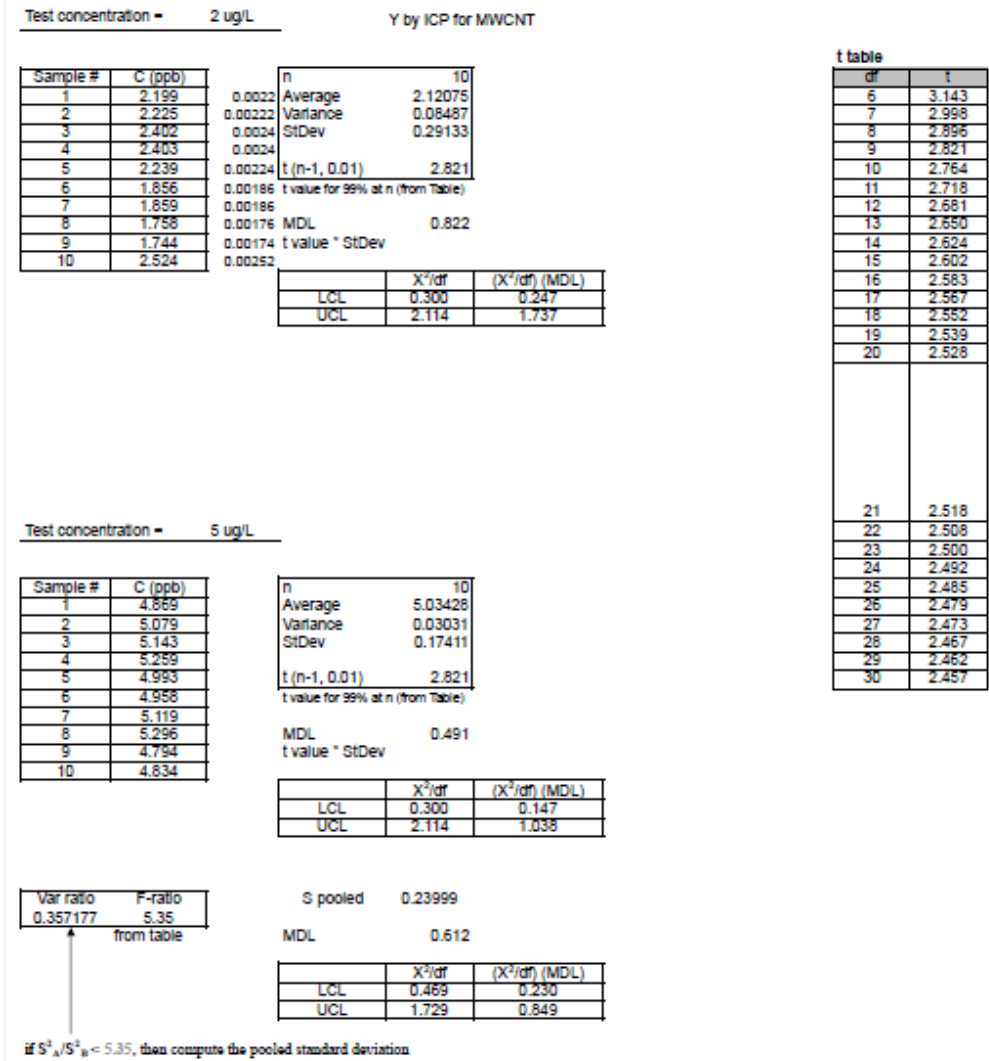


Figure S6. Raw data for calculating minimum detection limits of MWCNT 5% solution using ^{89}Y measurements on spICP-MS.

APPENDIX C

DETECTION AND DISSOLUTION OF NEEDLE-LIKE HYDROXYAPATITE NANOMATERIALS IN INFANT FORMULA

DETECTION AND DISSOLUTION OF NEEDLE-LIKE HYDROXYAPATITE

NANOMATERIALS IN INFANT FORMULA

- This chapter has been published as Schoepf, J., Bi, Y., **Kidd, J.**, Herckes, P., Hristovski, K., and Westerhoff, P. (2017). Detection and dissolution of needle-like hydroxyapatite nanomaterials in infant formula. *NanoImpact*, 5, pp. 22-28.
- My author contribution: Approximately 20% of the research and 5% of the text

Abstract

The unknowns surrounding presence, composition and transformations during the use phase of engineered nanoparticles (ENPs) in consumer products raises potential human and environmental health concerns and public discourse. This research developed evidence and confirmatory analytical methods to determine the presence and composition of ENPs in a consumer product with a complex organic matrix (six different infant formula samples). Nano-scale crystalline needle-shaped hydroxyapatite (HA; appx. 25 nm × 150 nm) primary particles, present as aggregates (0.3–2 μm), were detected in half the samples. This is the first report of these ENPs in infant formula. Dissolution experiments with needle-shaped HA were conducted to assess potential transformations of nano-HA particles. Rapid dissolution of needle-shaped HA occurred only under lower pH conditions present in simulated biological fluids (acidic gastric fluids), but not in simulated drinking water (near-neutral pH). Other non-nanosized HA minerals exhibited less dissolution under the same low pH conditions. This work demonstrates the occurrence of engineered nanomaterials in the food supply of a sensitive population (infants) and the need to consider transformations in nanomaterials that occur during use, which result in different exposures between pristine/as-produced ENPs and nanomaterials after passing through the human gut.

Introduction

Many minerals exist in both natural and engineered nanoparticle (ENP) forms. While the occurrence of naturally occurring nanoparticles (e.g., hematite, hydroxyapatite) is well recognized in natural systems, the environmental behavior of ENPs raises new regulatory and health concerns. These concerns primarily stem from existing knowledge gaps in understanding the ENP risks, which could be summarized in two categories: (1) discovering where ENPs are used in commerce and hence might enter the environment, and (2) elucidating ENP transformations from pristine materials, to synthesis in the lab or factory, and through use and end-of-life phases. We and others have previously shown that silicon- and titanium-oxide ENPs exist in foods, are ingested by humans, and pass through wastewater treatment plants, which results in their release to surface waters and terrestrial systems where sewage solids are land applied (Kiser et al., 2010; Kiser et al., 2009; Keller and Lazareva, 2014; Mueller and Nowack, 2008; Piccinno et al., 2012; Gottschalk et al., 2013; Reed et al., 2012; Robichaud et al., 2009). These two ENPs undergo little dissolution (i.e., transformation) during this process, which differs from antimicrobials like silver, copper, or zinc nanomaterials (Kaegi et al., 2013; Thalmann et al., 2014; Conway et al., 2015; Hong et al., 2015).

Calcium phosphate minerals are an example of solids present in nature and used in environmental remediation/treatment processes (Lenton et al., 2015; Miretzky and Fernandez-Cirelli, 2008; Piccoli and Candela, 1994; Vance et al., 2015; de-Bashan and Bashan, 2004; Wiesner et al., 2011) or human nutritional supplements. Intentional formation of calcium phosphate is used to immobilize heavy metals in soil (Boisson et al.,

1999; Fuller, 2002), remove fluoride from water to protect public health, (Fan et al., 2003) or remove phosphate from waste-waters to limit the eutrophication potential of wastewater discharges (de- Bashan and Bashan, 2004). Calcium phosphate, also referred as tricalcium phosphate (TCP), is used as a leavening agent in foods, a polishing material in toothpaste, an antioxidant activity promoter and texture stabilizer in canned vegetables, a firming agent or to avoid formation of clumps in food. Hydroxyapatite (HA; $\text{Ca}_5(\text{PO}_4)_3$ or $\text{Ca}_5(\text{PO}_4)_3(\text{OH})$) is a common form of calcium phosphate. Many people take calcium supplements, including calcium carbonate, calcium citrate and hydroxyapatite forms, but the literature is mixed on which form leads to greater bioavailable calcium for health bone development (Straub, 2007; Ruegsegger et al., 1995). In other applications, nano- forms of calcium minerals have raised concern. For example, the European Union Scientific Committee on Consumer Safety 2015 opinion on nano-HA states that the safety of its use in oral and cosmetic products cannot be currently decided due to limitations in available data, including the exact size, shape and crystallinity of the nano-HA, but that the available information indicates nano-HA in needle form is potentially toxic when used in dermally-applied cosmetic products (SCCS, 2015).

Calcium is an essential element for all biological organisms, and is widely used in human food supplements. For example, infant formula is intended to be the sole nutrition source for infants for the first 12 months. Although regulations (e.g. 21 CFR 107.100 in the USA) stipulate the elements required in the infant formula, they lack guidance on the type or size of the compounds used to provide the nutrients. Regulations refer to HA as generally regarded as safe (GRAS); however, new bottom up manufacturing processes that create

nanomaterials compared to top down processes create new concerns if the GRAS status applies. Given potential toxicity concerns raised in the EU on nano-needle-shaped hydroxyapatite in products intended for human use, the need for infants to have calcium and other elements (P, Fe) in their diets, and potential transformations for HA under different pH conditions, we undertook a study to separate and identify HA and other nanomaterials in powdered infant formulas. This challenging work with infant formulas that contain salts, sparingly soluble minerals, fats and other components is a precursor to understanding the occurrence and role of nano-scale HA minerals in complex environmental matrices (soil, biota, and water).

To identify initially unknown nanomaterials in infant formula, samples were separated by centrifugation after dispersing powders in water and then analyzed by transmission electron microscopy (TEM) with energy dispersive X-ray spectroscopy (EDS) and X-ray diffraction (XRD). Findings from these samples were compared against reference calcium phosphate materials. We focused on HA because it was found in three out of six samples, although it has not yet been widely considered by the health and safety exposure community as a risk in the food supply system. Within a complex food matrix, HA nanoparticles are difficult to be detected using conventional analytical paradigms. A secondary focus was the dissolution of HA in synthetic biological fluids to explore potential transformation in human body of these nano- and micron- sized minerals. Because the intended function of calcium phosphate in infant formula is to promote nutrient uptake, we used aqueous matrices representing simple drinking water and simulated gastric fluids. Understanding nanomaterial transformations during their intended use emerges as a critical discussion and

conclusion point around the benefits of using nanotechnology (e.g., rapid dissolution of HA to deliver calcium and phosphate ions).

Materials and Methods

Chemicals

Six infant formulas from different companies (Gerber, Similac, Enfamil, and Well Beginnings) were purchased in the United States and identified, for confidentiality, as S1–S6. Samples S1–S5 were dry powders, and S6 was a liquid concentrate. Dry powders and a liquid concentrate were chosen to compare suspected different additives used for each product. Three reference powder samples of food-grade calcium phosphate, labeled as hydroxyapatite, were procured from three different vendors. Samples R1 (American Elemental) and R2 (Hebei Shunye Import and Export Limited Company) were labeled as 99% pure and containing needle-like nano-HA. Sample R3 (NOW Foods) was an HA supplement provided in a gelatin pill capsule; only the contents of an opened capsule were used in analysis and dissolution tests.

Electron microscopy analysis

Infant formula (0.15 g) samples S1–6 and HA reference samples R1–3 were suspended in 40 mL ultrapure water (18.2 M Ω cm, Nanopure Infinity, Barnstead) and sonicated (80 W/L, Branson Ultrasonic Bath, Emerson) for 30 min to disperse particles. This mass to liquid ratio was used to parallel work other food samples analyzed by our group (Yang et al., 2014a; Yang et al., 2016a). Additional electron microscopy experiments were conducted at solid to liquid ratios based upon recommended sample preparation on the infant formula packaging, and showed no dependence of outcomes on solid to liquid ratios.

Other detailed control and validation experiments are summarized in Table SI.4 and described in the Results section.

Step-by-step description of sample preparation of electron microscopy samples are summarized in Figs. SI.2 through SI.5. Briefly, samples in 50 mL vials were centrifuged at $F = 14.000$ G for 15 min. The organics-rich supernatant was poured off, leaving a pellet of particulate matter at the bottom of the centrifuge tube. The pellet was re-suspended in 20 mL ultrapure water and inverted by hand for 30 s, then 50 μ L volumes were pipetted onto a copper/lacey carbon transmission electron microscopy (TEM) grid and allowed to air-dry overnight. Microscopy was performed on a Philips CM200 HR-TEM with energy dispersive X-ray spectroscopy (EDS). To confirm HA was not an artifact from sample preparation, a pure powder reference sample of HA was procured, deposited on a SEM stub (Fig. SI.3) and directly analyzed as a powder by scanning electron microscopy (SEM; FEG XL30 ESEM with EDS system) with energy dispersive spectroscopy. Mean particle diameter, particle size distributions, and cumulative distribution below 100 nm were determined by manually measuring the particles sizes of 250 particles from the images using ImageJ software and conducting statistical analysis.

Sample preparation for confirmation and quantification of hydroxyapatite

Fig. SI.6 provides a step-by-step description of sample preparation. To determine the relative amount of hydroxyapatite nanoparticles in infant formula, 10 g of each formula sample (six in total) was weighed into 50 mL centrifuge tubes with 40 mL of ultrapure water (18.2 M Ω cm, Nanopure Infinity, Barnstead). The mixed samples were then centrifuged for 20 min at $F = 14.000$ G to separate lighter components. The pellet collected

at the bottom of centrifuges was washed three additional times with UP water. The washed pellet was freeze-dried under vacuum for 48 h (FreeZone Freeze Dry System, Labconco), weighed, and compared with the weight of starting material to calculate the relative concentration of collected minerals. The mineral phases of pellets and reference powders were prepared (Fig. SI.7) and analyzed using powder X-ray diffraction (pXRD) using a Siemens D5000 diffractometer with a monochromated Cu-K α radiation at 40 kV and 30 mA. Each sample was scanned at 2 θ values from 10° to 70° to collect diffractograms, which were compared with the diffraction patterns of standard materials in ICDD database.

Dissolution experiments using hydroxyapatite in aqueous media

Ultrapure water and simulated biological fluids were used to examine the dissolution potential of the two reference HA and calcium bio-availability after ingestion. A detailed procedure is outlined in Fig. SI.1. A Fed-State Gastric Fluid (Fed-SGF, pH 5.0) and a Fasted-State Gastric Fluid (Fast-SGF, pH ~ 1.6) were prepared following recipes reported previously (Marques et al., 2011) and detailed in Table SI.1. For HA dissolution, 40 mL of the media was placed in 50 mL plastic centrifuge vials followed by the addition of 8 mg of reference HA to achieve a final concentration of 200 mg/L. The HA concentration was chosen to represent the serving size of HA per serving of infant formula. Immediately after mixing HA with simulated media, the suspensions were placed on a rotational shaker (45 rpm). The fed-state gastric fluid and fasted-state gastric fluid were rotated for 2 h to mimic the average contact time of food in the human stomach (Marques et al., 2011). Within 5 min of the completion of mixing, 15 mL of each suspension was filtered through 30 kDa centrifugal ultrafilters (NMWL = 30 K Da, ultracel regenerated cellulose, EMD Millipore)

at $F = 4000$ G for 12 min. A HA dose of 200 mg/L was added to the aqueous chemistry described in Table SI.1. The solution collected for each filtered sample was diluted in 2% nitric acid and analyzed for dissolved calcium and phosphorous concentrations by inductively coupled plasma mass spectrometry (ICP-MS, X-Series-II, Thermo Scientific). Control experiments were performed to understand potential impact of matrix effects (DI water, 1 mM NaHCO_3 , biological fluids) on permeation of dissolved Ca^{2+} through the ultrafilter or matrix effects due to calcium precipitation. Details and results provided in Supplemental Information (Table SI.2) concluded that there were no matrix effects in DI water, 1 mM NaHCO_3 , or gastric fluids (pH 1.6 or 5.0), and N90% of the spiked Ca^{2+} was recovered.

Results and Discussion

Presence of nanomaterials in powder formulas

Detecting nanomaterials in complex matrices is a challenge (Singh et al., 2014; Szakal et al., 2014; Yada et al., 2014). Initially, powder formula samples were analyzed by scanning electron microscopy (SEM), but the amount of organic material prevented meaningful imaging from carbon contamination (see Table SI.4), the deposition of carbonaceous material by the electron beam from cracking of carbon-carbon bonds present on the sample and carbon residual within the vacuum of

the sampling chamber of the microscope (Ennos, 1953). To overcome these issues and achieve high quality TEM images and meaningful elemental analysis of solids, infant formula samples were added to water and then followed protocols described in the Methods section. Results are discussed in two parts. First, the observed results show needle-like HA is present in some infant formula samples. Second, experiments demonstrate such structures are not artifacts of sample preparation.

TEM images in Fig. 1 are representative of multiple (typically N 10) images taken across several TEM grids of each sample. All six infant formula samples contained Ca and P as determined by EDS (Table 1), suggesting the presence of Ca-containing minerals. In addition, SiO₂ nanoparticles were found to be present in one sample (S4) and had similar size (~ 7 nm) and shape with this nanomaterial in other foods (Yang et al., 2016b). Titanium and oxygen containing material was detected in the liquid formula (S6) and was consistent with TiO₂ nanomaterials in foods reported in the literature (Yang et al., 2014a; Weir et al., 2012). Previous studies in food samples discuss occurrence and characterization of SiO₂ and TiO₂ materials (Yang et al., 2016b; Weir et al., 2012; Yang et al., 2014b), and therefore are not discussed further here.

The three most prevalent elements in colloids detected on the TEM grids were calcium, phosphorous and oxygen, and these were associated with the colloidal materials having two general shapes (needle-like or spherical). Fig. SI.8 shows representative TEM with EDS spectra for these colloidal materials and additional TEM images of the samples. S1, S2, and S3 samples contained needle-like shaped particles 10– 30 nm in width and 100–300 nm in length, creating impressions of dendritic networks. The size and shape of

HA in S3 were nearly identical to the needle-like hydroxyapatite reference (R1 and R2) samples (Fig. 1). Additional TEM of the three reference materials are shown in Fig. SI.9. Samples R1 and R2 containing nearly exclusively needle-like shaped HA whereas sample R3 contains only a few needle-like structures but mostly other micro-crystalline HA structures. This mineral phase, however, was not observed in S1 and S2, although TEM characterization suggested its presence.

XRD data for each sample and reference material are presented in Fig. 2. Initial XRD performed on the entire powdered infant formula samples exhibited a broad peak due to all the salts and organic materials. Therefore, XRD analysis for the infant formula samples were conducted on a purified pellet (Fig. 2 for S1–S6), but it was feasible to conduct XRD directly without sample pretreatment for the three reference HA. Fig. SI.10 shows XRD diffraction pattern confirming the presence of a single-phase hydroxyapatite ($\text{Ca}_5(\text{PO}_4)_3(\text{OH})$) in the three reference materials. The two needle-like hydroxyapatite reference samples (R1 and R2) have sharper diffraction peaks compared to the spherical counterpart which contains only a few needle-like structures but mostly other micro-crystalline HA structures (R3), suggesting larger crystallite sizes of R1 and R2 than R3. The micro-crystalline R3 sample was found to have similar morphology within S5, both displaying spherical shapes. Of the six infant formula samples (S1–S6) in Fig. 2, one or both forms of calcium were observed (calcite or calcium hydroxyapatite). XRD analysis unambiguously confirmed the presence of hydroxyapatite in S3 based upon library matches (Fig. 2). Samples S5 appeared to be mostly calcium hydroxyapatite, whereas other samples appear to contain a mixture of calcite and calcium hydroxyapatite. In S5 sample, however,

the calcium phosphate was dispersed in larger aggregates composed of organics and calcium material and mainly composed of monetite minerals (CaHPO_4) based upon XRD analysis.

Together, TEM and XRD analyses provide evidence that needle-shaped Ca-containing nanomaterials are present in 3 out of 6 infant formulas (S1, S2, and S3), likely in the form of HA or HA/calcite mixture. To assess the quantity of nano-scale needle-like HA in the samples, materials were separated from the rest of formula constituents via repeated sonication, centrifugation, and washing (Fig. SI.6). The minimum concentration of HA in S3 was estimated to be ~ 0.4 wt% based on the mass of insoluble pellet. The HA mass recovered in pellets from samples S1 and S6 was < 0.1 wt%, and even less mass was recovered from the other samples.

The presence of needle-like HA in the infant formula was unexpected. Therefore, an extensive array of experiments was performed using S3 and R1 to confirm their presence in the samples and demonstrate they were not artifacts of sample preparation. Complete details are provided in Supplemental Information text and summarized in Table SI.4. First, to assess the potential for artifacts or transformations in nanomaterial morphology and size experienced in sample preparation, hydroxyapatite reference materials were purchased and analyzed using the same sample preparation as the infant formulas (sonication, centrifugation, decantation, and resuspended (following steps in Fig. SI.2). During the same sample preparation, the needle-like and spherical reference materials maintained their size and morphology through the process, concluding sample preparation did not alter the nanomaterials in the infant formula. SEM analysis directly on the infant

formula powder was not able to detect needle-like HA because of the presence of salts and organics in the powder, where HA accounts for <0.4% of the dry mass of powder. Therefore, dispersion of the powder in water and separation of solids was necessary (see discussion related to Figs. SI.12–17).

Second, the infant formula (S3) was prepared at a higher solid to liquid ratio (6 g instead of 0.15 g in 40 mL of water) to represent the recommended ratio to prepare the infant formula as described on the package label. The samples were mixed by hand but not sonicated. Liquid was then either pipetted (20 mL) directly onto a TEM grid or centrifuged (4050 G for 4 h) onto a TEM grid placed in the bottom of the centrifuge vial. In both cases, TEM analysis of the grids detected nano needle-like HA (Table SI.4). Thus, neither the solid-to-liquid ratio nor method of preparing the TEM grid lead to artifacts in needle-like HA detection.

Third, evidence exists that needle-like HA could form due to sonication (Zhang et al., 2009; Sadat-Shojai et al., 2013; Cao et al., 2005). To demonstrate that sonication did not induce needle-like HA formation, experiments on dispersed S3 were performed. Sample S3 was prepared for TEM analysis following our original method (Fig. SI.2) that included sonication, compared against the sample procedure without sonication. Fig. SI.11 shows nearly identical TEM images from these comparative experiments. Nano needle-like HA is present both with and without sonication. Thus, this confirms that sonication of the infant formula added to water under the conditions applied herein does not lead to artifacts related to needle-like HA formation. Upon further inspection of the literature on needle-like HA synthesis, conditions (sonication power of 300 watts for 3 h and 333 °K) required to

produce needle-like HA during sonication do not exist during our preparation of sample S3 (Fig. SI.2 where sonication power 80 watts for 30 min and 300 °K).

Fourth, additional experiments were conducted to confirm our sample pretreatment did not in-situ produce needle-like HA due to the presence of dissolved calcium and phosphorous in the presence of other salts or organic macromolecules that might be present in infant formula. Sample S3 was dispersed in water and needle-like HA centrifuged out, into a pellet, following our original methodology. To the supernatant, absent of needle-like HA pellet, which still contains macromolecules and other inorganics, calcium and phosphorus ions were added to the supernatant at a 1.67 mol ratio (the optimum ratio for HA synthesis (Sadat-Shojai et al., 2013)) and then bath sonicated. Subsequent centrifugation and TEM inspection did not detect HA on the TEM grid. Thus, neither sonication alone nor sonication in the presence of other inorganic/organic components present in the infant formulas could produce nano needle-like HA artifacts, under the sample preparation conditions used in our work.

Dissolution potential for hydroxyapatite as a function of pH in biologically relevant media

High surface area or high aspect ratio of nanomaterials can increase the rate of mineral dissolution and result in the release of soluble ions (Conway et al., 2015; Cornelis et al., 2012; Zhang et al., 2011; Li et al., 2013; Brasiliense et al., 2016). While dissolution of nanomaterials can result in toxic responses for some metals (e.g., silver, zinc, copper) for other ENPs, we hypothesized that a beneficial reason of adding needle-like HA nanomaterials to the infant formula may be to increase dissolution potential of the mineral phase and bioavailability of calcium and phosphate. Therefore, dissolution experiments for

the reference needle-like (R1) and spherical (R3) hydroxyapatite materials were conducted in simulated drinking waters and biological fluids. The dissolution potential of HA in each matrix was based upon permeation of calcium ion through the 30 kDa ultrafilter. The HA nanomaterials have larger radii than the pore size of 30 kDa filters (~2 nm), allowing for the size exclusion of HA ions and colloidal HA (Erickson, 2009). Controlled experiments described in Supplemental Information confirm that matrix effects do not influence Ca^{2+} permeation across these ultrafilters under the operating conditions tested.

Fig. 3 shows that dissolution of hydroxyapatite occurs in the two gastric fluids, while b 6% of the HA dissolves in 1 mM NaHCO_3 and permeates the ultrafilters. In the pH 5.0 gastric fluid, N60% of needle-like HA (R1) and b 50% of the spherical HA (R3) dissolves. At pH 1.6, similar levels of needle-like HA (R1) dissolution occurs but a higher amount of dissolution occurs for spherical HA (R3). Similar patterns in UF permeation of phosphate during these tests were also observed (Fig. SI.18). Visual observations during the experiments indicate more rapid changes for R1 than R3 samples. Both samples were white and cloudy initially, but R1 became clear in b1 min

whereas the change in visibility took 1–2 h for R3 (see supplemental information Figs. SI.19–20). The two-hour period is physiologically relevant for the contact time for food and acidic gastric fluids (Marques et al., 2011). These visual observations may indicate disaggregation or dissolution. Measurement of dynamic light scattering after each dissolution test indicated a significant decrease in mean diameters for the needle-like HA reference material (Fig. SI.19), which could indicate either disaggregation or dissolution. Overall, the quantitative data for calcium and phosphorous, as indicators of HA, presented in Fig. 3 were supportive of qualitative visual observations.

Attempts were made to differentiate ionic from colloidal forms of Ca and P using single-particle ICP-MS, which is a powerful tool for analysis of many nanoparticles in aqueous media (Reed et al., 2012; Montano et al., 2014; Bi et al., 2014; Pace et al., 2012; Hasselov et al., 2008; Arvidsson et al., 2011). However, the minimum detection of Ca and P elements and associated mineral forms were more than several hundred nanometers due to the response factors of the ICP-MS (Singh et al., 2014). This highlights an important research need to improve sensitivity of spICP-MS for materials like HA.

Thermodynamic chemical equilibrium modeling (Visual MINTEQ (ver. 3.1)) predicts complete dissolution of HA in either gastric fluid (Fig. SI.22). The discrepancies between model predictions and experimental observations (Fig. 3) indicate that the dissolution of HA in the simulated gastric fluids may have kinetic limitations or differences in solubility products for different aspect ratio HA or presence of non-crystalline forms of calcium phosphate solids. In comparison to two other calcium minerals (i.e., calcite, monetite) identified in infant formula, hydroxyapatite has the lowest solubility at pH N 5.4

(Fig. SI.22). However, in both gastric fluids, all calcium minerals are predicted to dissolve completely at equilibrium with a serving concentration of 2 mM Ca in infant formula. Future research is needed to quantify the rates of dissolution for these two different HA morphologies.

The calcium bioavailability of different minerals cannot be concluded until additional kinetic studies are performed. However, the comparison between R1 (needle-like) and R3 (spherical) samples of HA (confirmed by XRD) suggest a priori assumptions about thermodynamic stability constants may not be appropriate for different shapes of HA. The dissolution mechanisms of calcium phosphate nanomaterials with respect to shape are not well understood. However, dissolution of high aspect ratio (i.e. needle-shaped) metal oxide nanoparticles have been reported to dissolve preferentially from each of the two ends (Cwiertny et al., 2009). Numerous methodologies exist to synthesize calcium phosphate, including those to produce needle-like nanostructures (Zhang et al., 2009; Sadat-Shojai et al., 2013), and it appears these different shapes could impact ability to dissolve in the acid biological fluids.

Human exposure impact of findings

TEM detected the presence of nanoparticles in all six samples. Results show that hydroxyapatite was detected in multiple samples at levels on the order of 0.1 to ~ 0.4 wt%. Other samples contained calcite, monetite, silica dioxide, and titanium dioxide at lower levels. Most attention was placed on hydroxyapatite because the presence of calcium nanomaterials in infant formula has not been reported previously. In the authors opinion, hydroxyapatite (needle-like structure) may be intentionally used in infant formula because

of its rapid (almost instantaneous) dissolution potential in gastric fluids at and below pH 5. However, further research is needed to prove this hypothesis. Previous research suggests hydroxyapatite dissolution provides favorable stoichiometric ratios of bioavailable Ca and P (Greer, 1989; Moy, 2000; Thompkinson and Kharb, 2007). Slower dissolution of spherical hydroxyapatite may not provide as much nutritional benefit. Additional techniques are needed to measure needle-like particles as FFF-ICP-MS, and spICP-MS measure particle size, but not morphology resulting in difficulty interpreting results for needle-like materials.

Others have reported the global production of many types of ENMs, yet these reports exclude needle-like hydroxyapatite (Vance et al., 2015; Garner et al., 2015; Keller et al., 2013) while one report quantifies the amount of HA in the USA entering the environment from the use in toothpaste to be between 18 and 19 metric tons per year in 2013 (Keller et al., 2014). The 2013 global market for infant formula was approximately \$41 Billion (US dollar), and growing rapidly in Asia and other markets (Kent, 2015). Based upon the prevalence of the material in infant formula alone, the global annual production is likely to be on the order of carbon nanotubes, in the range of thousands of metric tons per year (see Supplemental Information).

The dissolution potential of needle-like HA under mildly acidic conditions raises a number of issues for assessing the impact of these types of nanomaterials. First, the US EPA Toxic Substances Control Act (Section 8 rule for nanomaterials) may exclude, from being classified as nanomaterials, substances which dissociate completely in water. The needle-like HA examined here would be difficult to classify, because it did not rapidly

dissolve in water at near neutral pH, but did dissolve rapidly under mildly acidic conditions where it was intended to be used (i.e., digestive tract). Further proposed rule changes would exclude substances from being classified as nanomaterials which do not exhibit new properties when their size falls in the range of 1–100 nm. For HA it appears that the needle-like shape is intended to increase the rate of dissolution in acidic conditions, and this needle-like structure is specifically synthesized by controlled chemical and heating conditions through a new bottom up manufacturing process compared to standard top down processes. Therefore, needle-like HA could pose a challenge to proposed classification systems under this rule for ENPs in the USA.

Second, evaluating the toxicity in mammalian cell culture of needle-like hydroxyapatite may give very different results from in vivo administration, where acidic conditions in gastro-intestinal tracts would apparently rapidly transform (i.e., dissolution) the size of this HA engineered nanoparticle. Calcium ions are absorbed by the small intestine by passive diffusion and active transport (Bronner, 2009; Pansu et al., 1983), but recrystallization of HA may occur. If there is a high concentration of phosphate and calcium ions in the small intestine under alkaline conditions, you can get precipitation of HA (Jaeger and Robertson, 2004). This could impact the effects of HA on the gut microbiome because they would be exposed to non-dissolved (i.e., near pristine) forms of the ENP. Thus working with ENPs like needle-like HA raises challenges to appropriately track dosimetry throughout toxicological testing (Pal et al., 2015; Cohen et al., 2015; DeLoid et al., 2014).

Finally, elements in other nanomaterials (silver, copper, zinc, cadmium, etc.) can dissolve out of nanomaterials based upon variable environmental conditions. Whereas

redox conditions in solution can control the ionic release (Ag^+ , Cu^{2+} , Zn^{2+} , etc.) from these ENPs, dissolution of calcium and phosphate ions from HA appears to be controlled by its pH-dependent solubility rather than redox conditions in water. The needle-like HA structure may have different K_{SP} values compared against other calcium phosphate forms, or may just influence the relative dissolution kinetics. Fortunately, calcium and phosphorous are not toxic like other metals.

Table 1
Sample and reference material characteristics from label information, TEM/SEM*, and EDS**.

Sample ID	Manufacturer brand/Product ID # Product & label information	Elements detected**	Like by nano-scale minerals/elements	Dimension of primary particles*	Dimension of aggregates*
S1	<i>Powder formula</i> (120 mg Ca; 66 mg P; 1.8 mg Fe)	Ca, P, O	Nano needle-like HA	13 nm (width) by 110 nm (length)	320–1627 nm
S2	<i>Powder formula</i> (82 mg Ca; 44 mg P; 1.9 mg Fe)	Ca, P, Si, and O	Nano needle-like HA	28 ± 5 nm (width) by 160 ± 30 nm (length)	391–1026 nm
S3	<i>Powder formula</i> (67 mg Ca; 38 mg P; 1.5 mg Fe)	Ca, P, and O	Nano needle-like HA	28 ± 7 nm (width) by 237 ± 119 nm (length)	211–1722 nm
S4	<i>Powder formula</i> (82 mg Ca; 110 mg P; 1.9 mg Fe)	Si, O, Ca, P, and K	Nano SiO ₂	Spherical diameter: 7 ± 1 nm	None
S5	<i>Powder formula</i> (72 mg Ca; 40 mg P; 1.5 mg Fe)	Ca, P, Ti, Al, Si, S, K	Spherical nano Ca, P unknown	30–35 nm 10–30 nm	1000–2000 nm 1000–2000 nm
S6	<i>Liquid Formula</i> (78 mg Ca; NA mg P; 1.8 mg Fe)	Ca, O	Nano TiO ₂ Nano Ca, O particles	16–530 nm 590 ± 126 nm	None 1184–2647 nm
R1	Hydroxyapatite reference (American Elements Inc.)	Ca, P, O	Nano needle-like HA	30 ± 5 nm (width) by 131 ± 25 nm (length)	141–1786 nm
R2	Hydroxyapatite reference (Chinese supplier)	Ca, P, O	Nano needle-like HA	30 ± 6 nm (width) by 126 ± 28 nm (length)	220–1322 nm
R3	Hydroxyapatite dietary supplement (NOW, Australia)	Ca, P, O	Spherical HA	Diameter: 20 ± 5 nm	225–837 nm

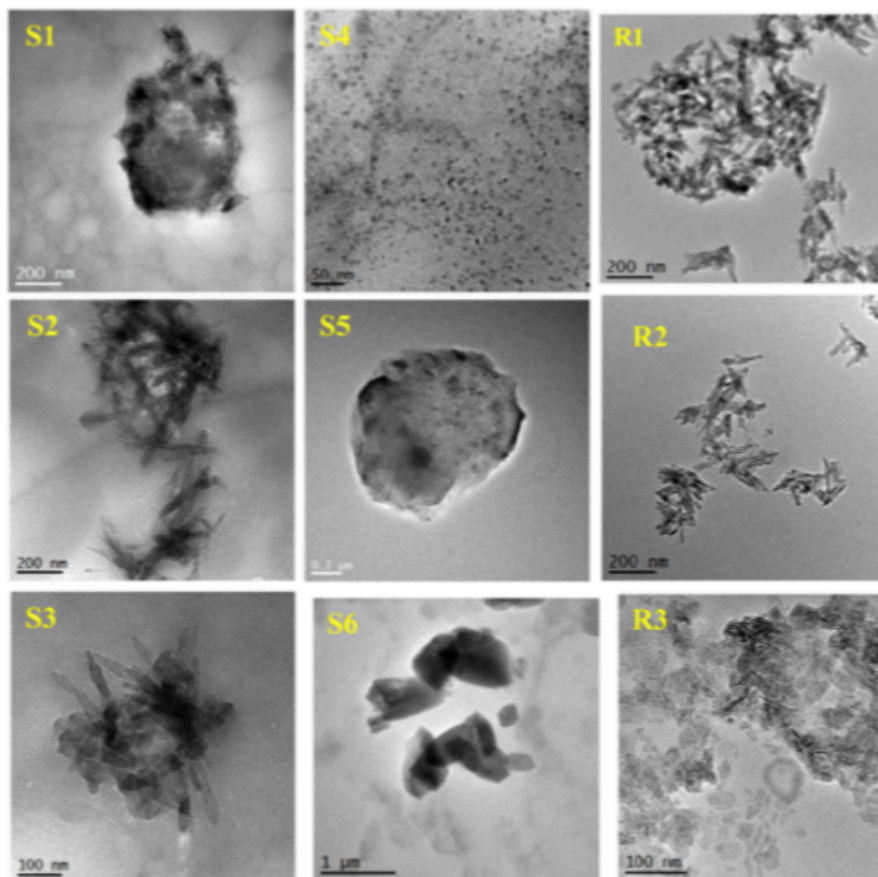


Fig. 1. Transmission electron micrographs of particles separated from infant formulas (S1–S6) and reference samples (R1–R3). EDS results summarized in Table 1.

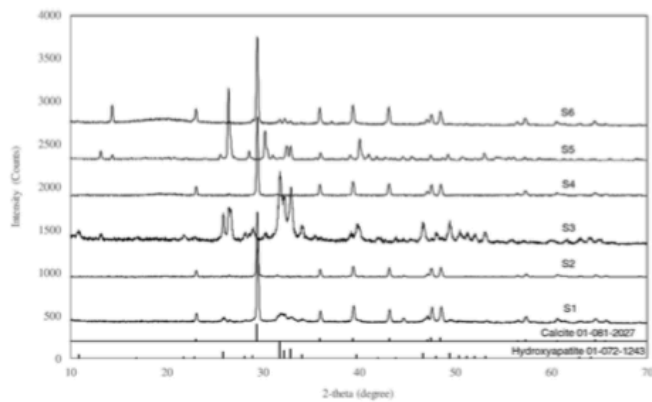


Fig. 2. X-ray diffraction patterns of dominant mineral content separated from the six infant formula products and reference XRD patterns for calcite and hydroxyapatite.

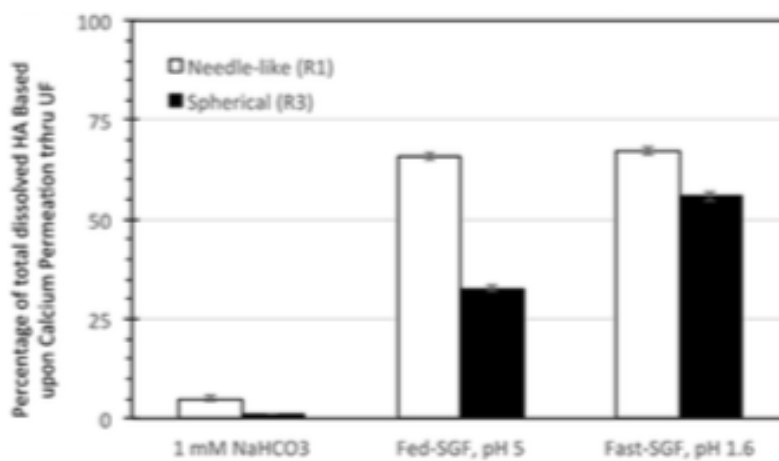


Fig. 3. Percentage of total dissolved hydroxyapatite in the three simulated fluids based upon percentage of calcium in the ultrafilter permeate relative to the added mass (100 mg HA/L and measured by ICP-MS) present as calcium.

Acknowledgements

Funding was provided from the US Environmental Protection Agency through the STAR program (RD83558001) and the National Science Foundation through the Nano-Enabled Water Treatment Technologies Nanosystems Engineering Research Center (EEC-1449500) and CBET 1336542. Assistance from Ian Illuminati from Friends of the Earth is appreciated. We gratefully acknowledge the use of the facilities within the LeRoy Eyring Center for Solid State Science at Arizona State University.

Supplemental Information

Background Information on Calcium Phosphate in Foods and Infant Formula Composition

The European Union codes food additives with E-numbers. For example, color additives are all in the E100 series, preservatives are in the E200 series, and anti-oxidants in the E300 series. Because of their versatile use, calcium based additives occur across multiple series, including calcium carbonate for color (E170), preservatives (e.g., calcium sorbate, sulfite), anti-oxidants (calcium ascorbate), emulsifiers (E404 calcium alginate), and other uses (E333 calcium citrate; E327 calcium lactate; E538 calcium oxide; E341 calcium phosphate). Other uses include acid, acidity regulators, anti-caking agents, anti-foaming agents, bulking agents, carriers and carrier solvents, emulsifying salts, firming agents, flavor enhancers, flour treatment agents, foaming agents, glazing agents, humectants, modified starches, packaging gases, propellants, raising agents, and sequestrates.

Calcium phosphate (E341), also known as tricalcium phosphate (TCP), in foods is used as a leavening agent, a polishing material in toothpaste, antioxidant activity promoter and texture stabilizer in canned vegetables, a firming agent or to avoid formation of clumps in foods. Calcium phosphate can be produced through crushing bones or engineered into specific mineral shapes and crystallinity, yet little information is available from manufacturers or suppliers. Unlike other food grade metal-based or metal oxide materials that do not dissolve in water, calcium phosphate is generally referred to as hardly soluble in water but easily dissolved in dilute acids. A large fraction of these other food-grade additives are crystalline and have primary particles below 100 nm in at least one dimension

[2-7]. Hydroxyapatite (HA) can be purchased in various forms, including nano-needle-like crystals that are aggregated together. However, little information exists on the forms of calcium phosphate (i.e., hydroxyapatite) in foods, how to detect it, and whether it undergoes transformations during use or consumption. The scientific community learned many lessons on the significance of nanomaterial transformations with nano-metals (silver, copper, zinc), fullerenes (C_{60} versus hydroxylated C_{60}), and others. Environmental conditions in natural systems (groundwater, lakes, rivers, air, sediments), engineered systems (sewers and wastewater treatment plants), biota (bacteria, fish), and within humans (e.g., protein corona) are critical in understanding the true exposure and toxicity of nanomaterials.

Infant formula is intended to be the sole source of nutrition for infants for the first 12 months leading to heavy regulations requiring sufficient nutrition testing before being marketed. According to Code of Federal Regulations (CFR) Title 21, Volume 2 (21 CFR 107.100), infant formula must have calcium, phosphorus, magnesium, iron, zinc, manganese, copper, iodine, sodium, potassium, and chloride. Although regulation exists on the elements required in the infant formula, guidance lacks on the type or size of the compounds used to provide the nutrients.

Infants receive most of their diet from milk, including the elements calcium and iron [8, 9]. Most infant formulas contain higher concentrations of nutritional elements than those of breast milk because knowledge of how infants utilize these elements is limited [10, 11]. The composition of infant formula is complex [12] and varies by brands [13], including the ratios of calcium to phosphate. Iron fortified infant formulas are also common

and recommended at 4 to 12 mg/L [14]. Despite the essential need of Ca, P, and Fe, little information exists on the mineral forms and sizes for materials in foods generally, and infant formulas specifically. Calcium phosphate is identified on powder infant formulas in the USA, yet little information exists on the mineral form.

Environmental pollutants can occur in infant formula. Lead is carefully measured because of its strong binding capacity with calcium phosphate. Extreme contamination was reported from melamine in infant formula in 2008 which led to rapid development of analytical techniques using conventional strategies and nano-sensing platforms [15-21]. However, there currently is little information or analytical detection strategies for nanomaterials in general, calcium phosphate mineral forms more specifically, for foods (including infant formula).

ADDITIONAL METHOD DETAILS

Composition fluids used to evaluate HA dissolution

Four primary solutions were used to conduct HA dissolution tests. First, ultrapure (Millipore) water (DI) without pH adjustment pH ~ 5.8 prior to any HA addition. Chemistries for the other three solutions are summarized in Table SI.1. Figure SI.1 outlines the step-by-step procedure for conducting the experiments.

Table SI.1 Composition of simulated fluid (pH adjusted with HCl/NaOH)

Bicarbonate Buffer Matrix Fluid, pH 8.0	
Composition	Concentration
Sodium bicarbonate	1 mM

Simulated Gastric Fluid (SGF), Fasted-State, pH 1.6 [22]	
Composition	Concentration
Sodium taurocholate	80 μ M
Lecithin	20 μ M
Sodium chloride	34.2 mM
Pepsin	0.1 g/L

Simulated Gastric Fluid (SGF), Fed-State, pH 5.0 [22]	
Composition	Concentration
Sodium chloride	237 mM
Acetic acid	17.12 mM
Sodium acetate	29.75 mM

<p>1) Media Preparation: The 1mM NaHCO₃ buffer solution and the two gastric fluids were prepared using the recipes found in Table SI.1 in clean 1L glass bottles</p>	<p>4) Centrifugation of Samples: After shaking, 15mL of solution was added immediately to 30kDa ultracentrifugal filters and centrifuged at F=4,000G for 12 minutes.</p>
<p>2) Addition of Materials: The media solutions were added to clean 50mL plastic centrifuge vials up to 40mL. HAp was weighed out and added in to the media at a 200mg/L concentration</p>	<p>5) Analysis Preparation of Samples: The solution that passed through the filters was collected and acidified with 2% HNO₃ for 24 hours. The samples were analyzed using ICP-MS</p>
<p>3) Simulated Mixing of Samples: The media vials were closed and placed in an end-over-end rotational shaker at 45RPM for 2 hours</p>	

Figure SI.1 Summary of sample preparation for dissolution potential

Ultrafiltration Efficiency Control Experiments

Calcium ion filtering efficiency of 30kDa centrifugal ultrafilters was evaluated by spiking 2 mM of Ca (as CaCl₂) to the three media solutions and mixing for 2 hours as in the original dissolution experiments. The concentration of Ca²⁺ spike was selected to be equivalent with the Ca concentration in 200 mg/L HA added in the original experiments. No phosphorous was added, so we could explicitly determine Ca filter efficiency without concern about calcium phosphate solid precipitation. After the 2 hour mixing time, samples were placed in the ultrafilters and centrifuged at F=4,000G for 12 minutes (same conditions as original experiments). Both filtrate and retentate were collected and analyzed by ICP-MS for total dissolved Ca concentration after acidification in 2% nitric acid.

Results shown in Table SI.2 indicate there were no matrix effects in DI water, 1 mM NaHCO₃, or gastric fluids (pH 1.6 or 5.0), and >90% of the spiked Ca²⁺ was recovered. The slightly lower calcium concentrations in 1 mM NaHCO₃ may be due to precipitation of calcium carbonate, which was slightly oversaturated under the solution conditions examined (Log SI = 0.4). As expected in ultrafiltration tests, the concentration of calcium in permeate and retentate were equivalent. Parallel experiments with simulated saliva (Table SI.3) indicated loss of spiked calcium ion, which we attribute to oversaturation of calcium hydroxyapatite (Log SI ~12). This would precipitate and be trapped on the filter. For this reason, although we conducted experiments with simulated saliva in addition to the fluids listed in Table SI.1, we do not report dissolution potential of reference HA in saliva based upon ultrafiltration data.

Table SI.2 – Ultrafiltration efficiency control tests based upon 2 mM CaCl₂ spike. Sample treatment was identical to methodology where 200 mg/L of HA was added (2 hour mixing then centrifuged with F=4000G for 12 minutes)

Matrix description	Ultrafiltration sample	Dissolved Calcium concentration (mM)
DI water	Permeate	1.80
	Retentate	1.86
1 mM NaHCO ₃	Permeate	1.79
	Retentate	1.81
Gastric Fluid (pH 5)	Permeate	1.96
	Retentate	1.98
Gastric Fluid (pH 1.6)	Permeate	1.77
	Retentate	1.95
Saliva fluid*	Permeate	0.173
	Retentate	0.106

Table SI.3 - Composition of Simulated Saliva Fluid (SSF) pH 7.4 [22]

Composition	Concentration (g/L)
Unadjusted pH = 7.4	--
Potassium chloride	0.720
Calcium chloride dihydrate	0.220
Sodium chloride	0.600
Potassium phosphate monobasic	0.680
Sodium phosphate dibasic	0.866
Potassium bicarbonate	1.500
Potassium thiocyanate	0.060
Citric acid	0.030

Results and Discussion Points

Electron microscopy results and demonstration that needle-like HA observed in samples were not artifacts of sample preparation

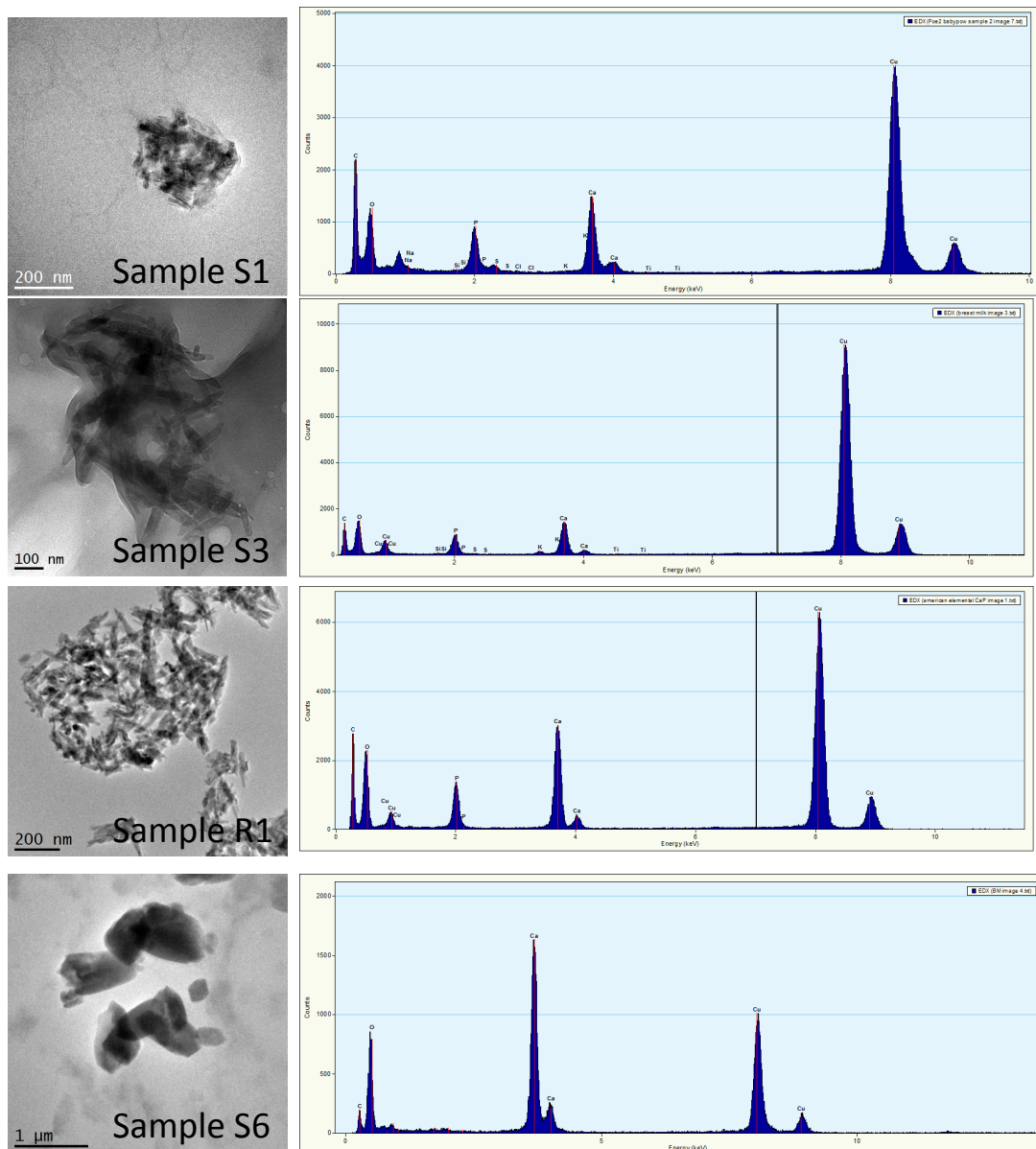


Figure SI.8A TEM and EDS on Calcium Containing Colloidal Material

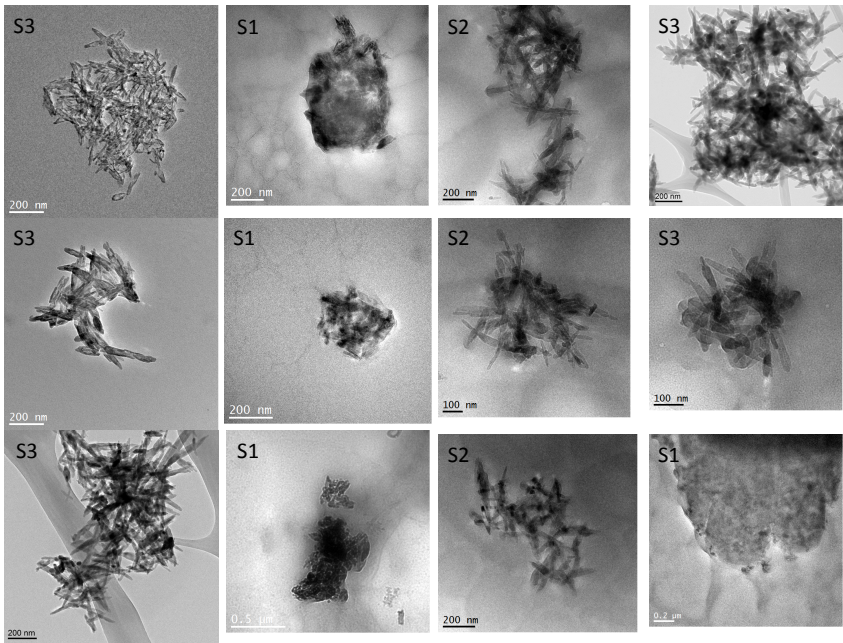


Figure SI.8B Additional TEM images from infant formula

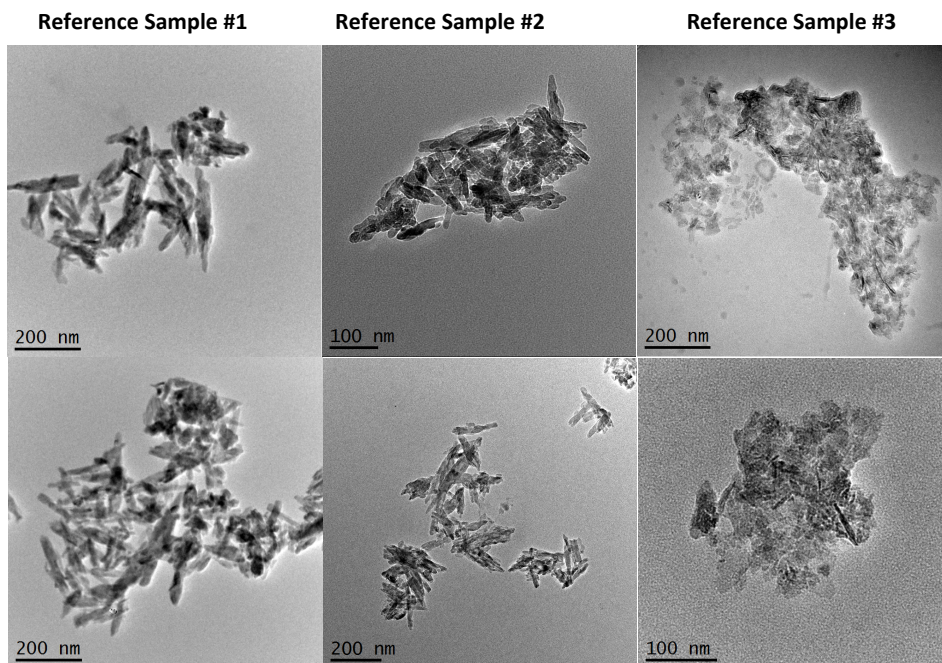


Figure SI.9 TEM of two reference samples containing nearly all needle-like HA (#1 and #2) and a third reference material containing mostly non-needle-like and spherical HA (#3).

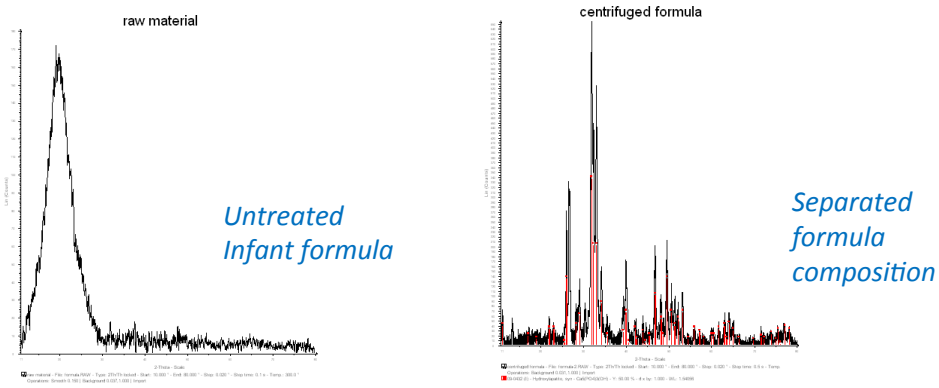
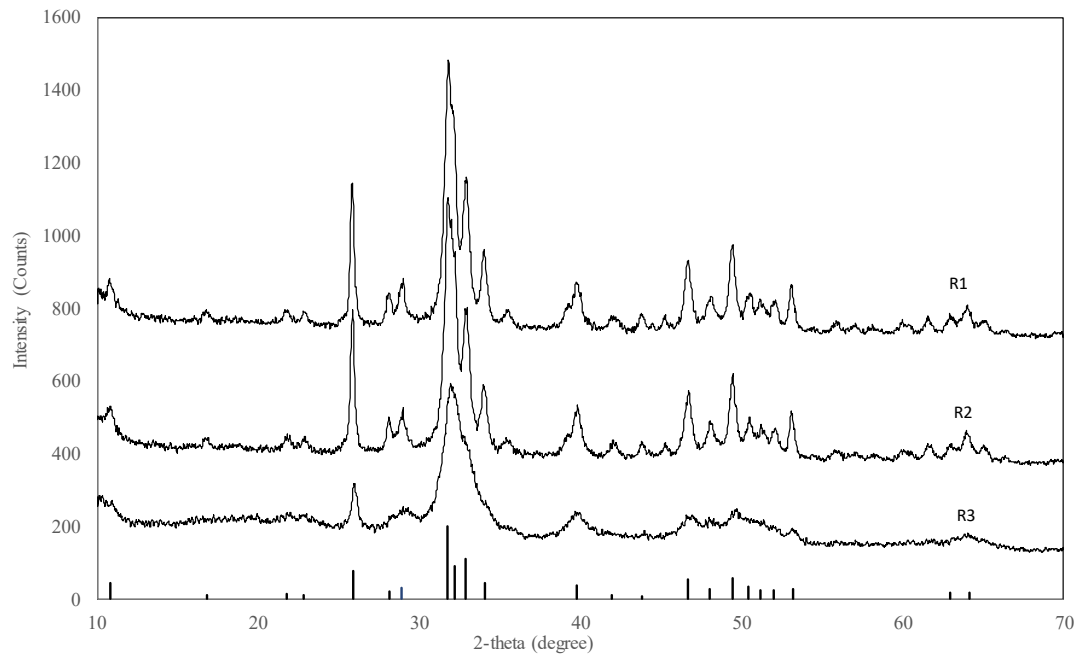


Figure SI.10. X-ray diffraction patterns of (A) three hydroxyapatite standard reference materials used to simulate hydroxyapatite nanoparticles in infant formula and reference XRD pattern for hydroxyapatite, and (B) powder infant formula (S3) versus centrifuged pellet from S3.

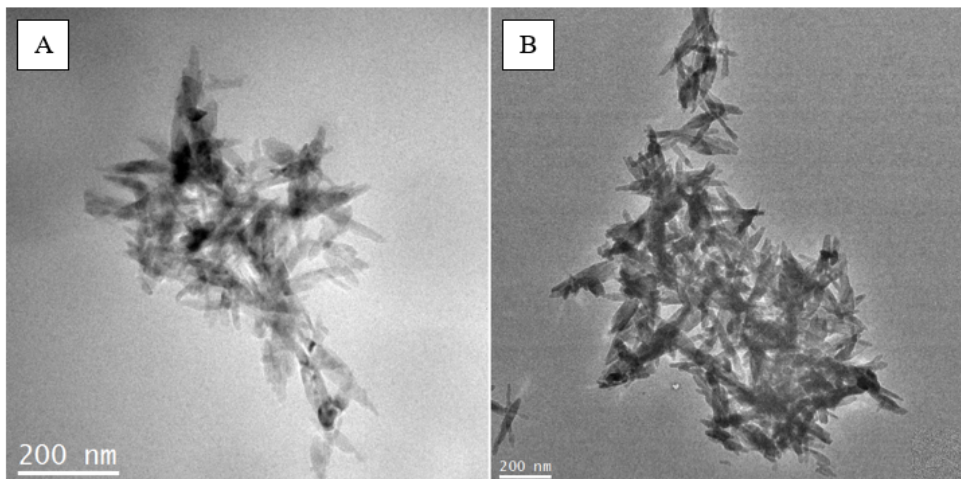


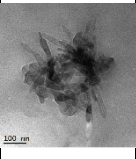
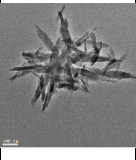
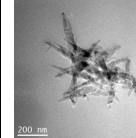
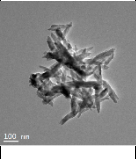
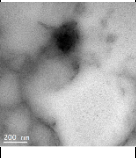
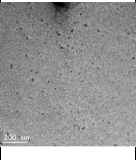
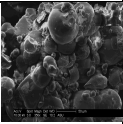
Figure SI.11 TEM of sample S3 following sample preparation outlined in Figure SI.2 but (A) without sonication versus (B) with sonication. Needle-like HA is present in both images and demonstrates sonication did not induce formation of this structure.

Seven additional results are presented (see table below). The overall conclusions of this work support the additional finding that needle-like HA are present in some of the infant formula, and are not artifacts of TEM sample preparation. Step-by-step methods are described in Figures SI.1 through SI.5. A summary of the results are now included in the supplemental results section (and Table SI.4). Primary conclusions from the seven experiments include the following:

1. 0.15 gram of sample S3 was placed in 40 mL and sonicated and prep'd for TEM following the original method in the paper. TEM found needle-like HA.
2. Same as #1 but without sonication. TEM found needle-like HA, and we can conclude that sonication did not form needle-like HA.
3. Same as #2 but we excluded centrifugation and just added 20 uL of sample onto the TEM grid. TEM found needle-like HA. Therefore, neither sonication nor centrifugation lead to any artifacts.
4. Here the infant formula was prepared by adding the volume/mass to water ratio specified on the infant formula packaging as the “recipe” to prepare the liquid infant formula. Then we applied a completely different centrifugation method presented on-line by EAWAG (<https://www.youtube.com/watch?v=PplBIJ7zCCA>) after a 100x dilution of the sample. TEM found needle-like HA. Using demonstrates the solid to liquid ratio does not lead to needle-like HA artifacts.
5. 0.15 gram of sample S3 was placed in 40 mL and sonicated/centrifuged as outlined in the original manuscript. The solid pellet was removed. Then we added dissolved calcium chloride and sodium phosphate salts into the supernatant, where any organic polymers would still be present. The concentrations of these added salts were based upon the mass of solids removed as the pellet. The sample was re-sonicated and centrifuged. The small pellet was then analyzed by TEM. Needle-like HA was *not* detected. This demonstrates that needle-like HA was not generated as an artifact from dissolve Ca/P in the infant formula.

6. Same as #5 above but instead of spiking calcium chloride and sodium phosphate salts into sample S3 (which contained needle-like HA), the test was performed using sample S6 (did not contain needle-like HA, but contained complex organics, etc. in the infant formula). Sample S6 was placed in 40 mL and sonicated/centrifuged as outlined in the original manuscript. The solid pellet was removed. Then we added dissolved calcium chloride and sodium phosphate salts into the supernatant, where any organic polymers would still be present. The concentrations of these added salts were based upon the mass of solids removed as the pellet. The sample was re-sonicated and centrifuged. The small pellet was then analyzed by TEM. Needle-like HA was *not* detected. This demonstrates that needle-like HA was not generated as an artifact from dissolve Ca/P in the infant formula.
7. A 1cm by 1cm piece of double sided carbon tape was placed on to an aluminum SEM stub. Infant formula (sample S3 which contained needle-like HA) was placed in a plastic weighing boat. The aluminum stub with carbon tape was pushed into the infant formula, allowing the dry powder to stick to the carbon tape. The aluminum stub with infant formula powder tape was placed inside the SEM (XL30 ESEM with EDAX) for analysis. No need-like HA was observed. This is attributed to presence of large amounts of other salts and organic materials which dominate by weight over needle-like HA. This was the original motivation for conducting TEM analysis on suspended liquid sample which has the ability, during sample preparation, to separate salts and dissolved organics from nano- and larger scale particles.

Table SI.4 – Summary of experiments to validate that needle-like HA is not an artifact from electron microscopy sample preparation

Sample	Sonication	Centrifugation	TEM Sample Preparation	Other	Conclusion	TEM Image
1) Original Method	30 min at 80 watts	15,000 G for 15 minutes	-Resuspend pellet into 20 mL of water -20 μ L pipetted on to TEM grid	-0.15 grams in 40 ml of water	Presence of Nano needle-like HA	
2) Original without sonication	No sonication	15,000 G for 15 minutes	-Resuspend pellet into 20 mL of water -20 μ L pipetted on to TEM grid	-0.15 grams in 40 ml of water	Presence of Nano needle-like HA	
3) Original without sonication or centrifugation	No sonication	No centrifugation	-20 μ L pipetted directly on to TEM grid	-0.15 grams in 40 ml of water	Presence of Nano needle-like HA	
4) EAWAG Method	No sonication	4050 G for 4 hours	-TEM at bottom of vial - liquid is pipetted out of vial and TEM grid is removed for analysis	-6 grams in 40 mL of water (instructions on box) -100X dilution	Presence of Nano needle-like HA	
5) Ca/P additive to HA extracted sample 3	30 min at 80 watts	15,000 G for 15 minutes	-Resuspend pellet into 20 mL of water -20 μ L pipetted on to TEM grid	-0.15 grams of infant formula into 40 mL of water -Supernatant from centrifugation step was removed and spiked with $\text{CaCl}_2\text{H}_2\text{O}$ and Na_2HPO_4	No Nano needle-like HA	
6) Ca/P additive to sample 6 (sample absent of nano needle-like HA)	30 min at 80 watts	15,000 G for 15 minutes	-Resuspend pellet into 20 mL of water -20 μ L pipetted on to TEM grid	-0.15 grams in 40 mL of water and spiked with $\text{CaCl}_2\text{H}_2\text{O}$ and Na_2HPO_4	No Nano needle-like HA	
7) SEM analysis of dry powder	No addition to liquid. No sonication. No centrifugation. Sample S3 applied as dry powder to carbon tape on SEM stub				No nano needle-like HA observed	

Scanning Electron Microscopy Imaging of Infant Formula and Hydroxyapatite Reference Material

Two samples, Infant formula (sample 3) and HA reference material 1, were analyzed by scanning electron microscopy paired with energy dispersive X-ray spectroscopy (EDS) as dry powders with minimal sample preparation. To prepare the samples, the infant formula and HA reference material were poured into weigh boats. Double sided tape was placed onto an aluminum SEM stub and lightly pushed by hand into the powder samples to adhere the samples to the carbon tape. The samples were sputter coated with Au for 120 seconds (~10nm thick coating) to prevent charging by the electron SEM beam and placed within the SEM (FEI/Philips XL-30 Field Emission ESEM). Needle-like HA materials were characterized in the HA reference material 1 by SEM as shown in Figure SI.12-14 (average length: 156 ± 43 , width: 35 ± 7 nm). Sample 3 was analyzed for the presence of needle-like HA as shown in Figure SI.15-17 (average diameter: 33 ± 28 μ m). The abundance of carbon substances in sample 3 prevented meaningful analysis of the sample by SEM. Carbon particulate (figure SI.16) was observed in the dry infant formula (diameter: 187 – 499 nm); however, needle-like HA particles were not observed. The needle-like HA is suspected to be within the micron sized carbon compounds. We conclude that the salt and organic matrix that comprises the infant formula prevents detection of the needle-like HA in the powder, and that separation of the salts and organic matrix is required to detect the needle-like HA which other parts of this paper suggest represents < 1% of the total mass of the powder formula on a mass basis.

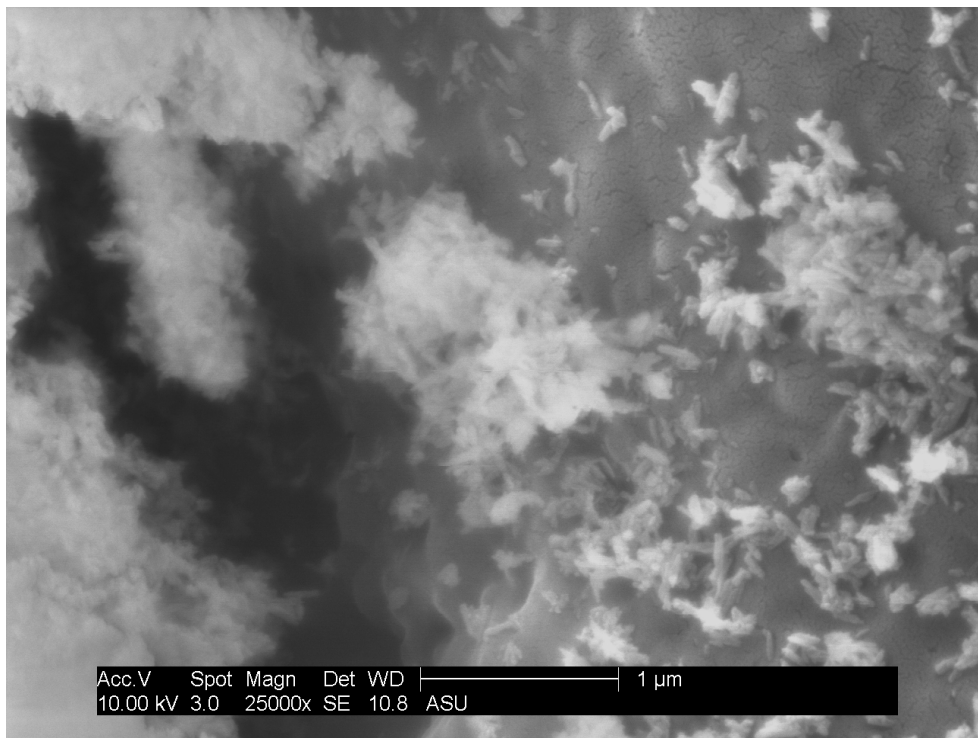


Figure SI.12: SEM image of HA reference material 1. Light substances are needle-like HA. The dark background is the carbon tape

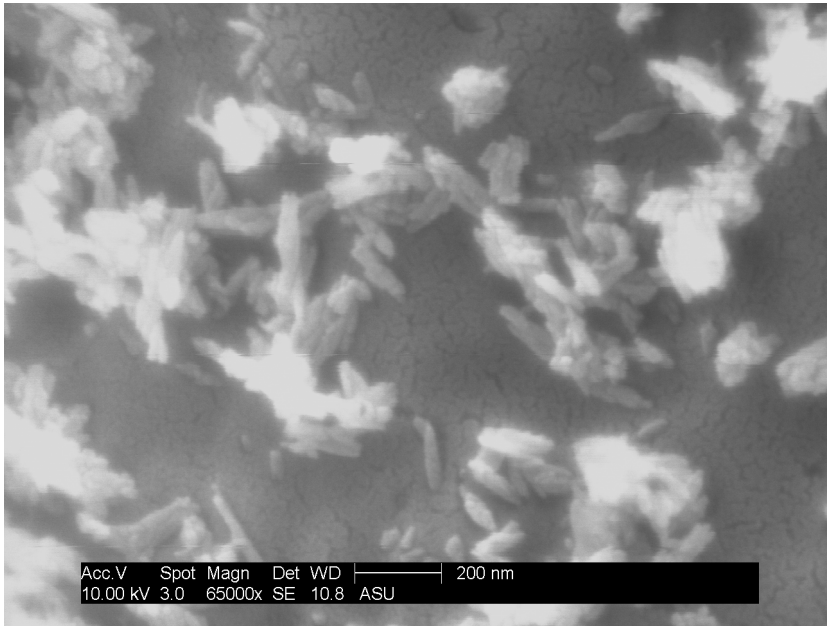
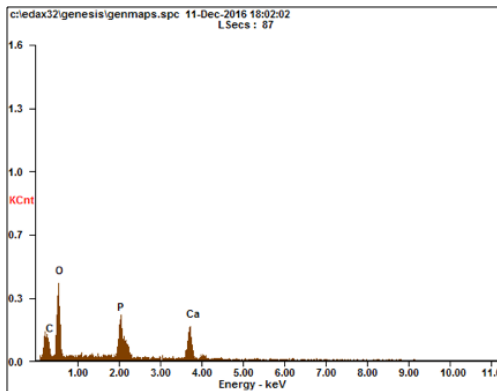


Figure SI.13: SEM of needle-like HA reference 1. Background is the carbon tape



<i>Element</i>	<i>Wt%</i>	<i>At%</i>
<i>CK</i>	15.32	25.79
<i>OK</i>	38.49	48.63
<i>PK</i>	15.39	10.04
<i>CaK</i>	30.80	15.54
<i>Matrix</i>	Correction	ZAF

Figure SI.14: EDS of needle-like HA (confirmed presence of calcium, oxygen, and phosphorous) found in image SI.13.

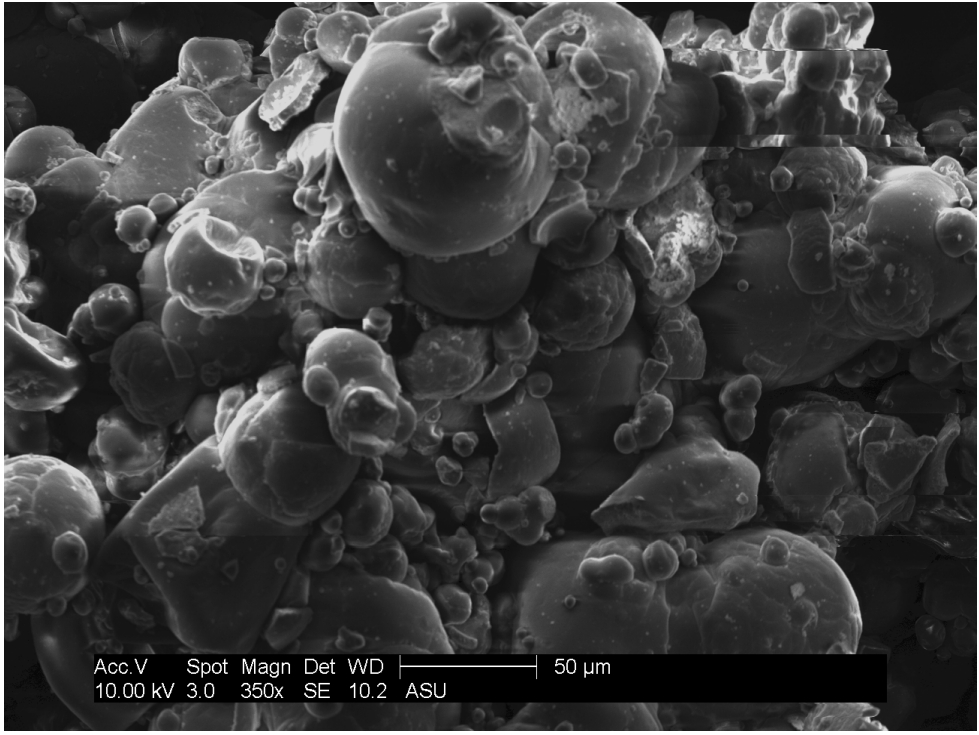


Figure SI.15: SEM of dry infant formula sample 3

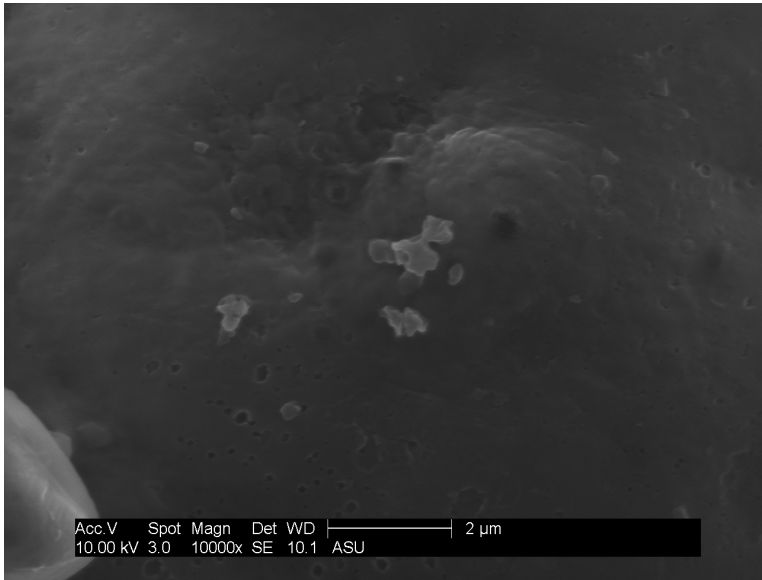
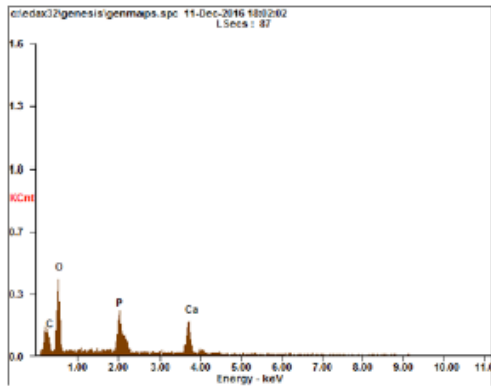


Figure SI.16: SEM of dry infant formula 3

Figure SI.17: EDS characterizing the presence of carbon, oxygen and gold in Figure SI.16. Gold peaks are from the goal sputtering.



<i>Element</i>	<i>Wt%</i>	<i>At%</i>
<i>CK</i>	15.32	25.79
<i>OK</i>	38.49	48.63
<i>PK</i>	15.39	10.04
<i>CaK</i>	30.80	15.54
<i>Matrix</i>	Correction	ZAF

Reference HA Dissolution Experiments: Phosphate Permeation through UF Plus Visual and Turbidity Changes

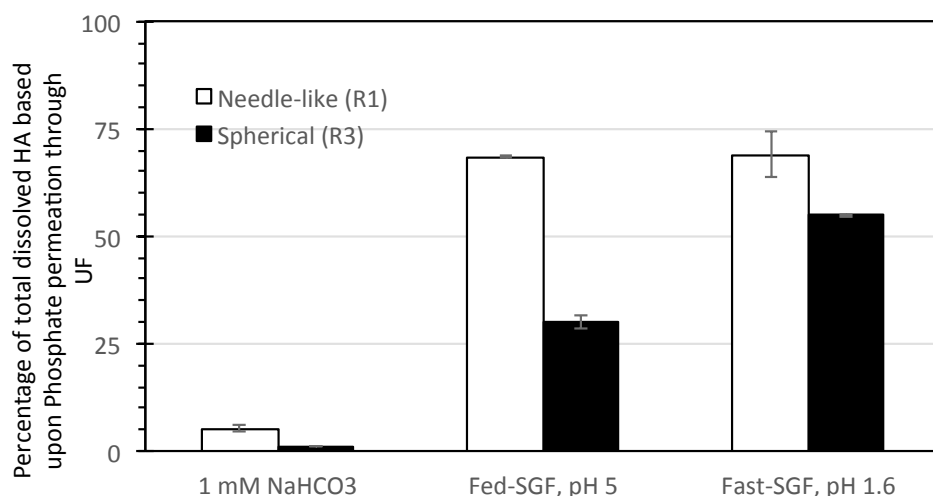


Figure SI.18 Percentage of total dissolved hydroxyapatite in the three simulated fluids based upon percentage of phosphate in the ultrafilter permeate relative to the added mass (100 mg HA/L and measured by ICP-MS) present as phosphate.

In addition to measuring calcium and phosphate during ultrafiltration experiments, other measurements with ultrafiltration were also conducted. Within 30 minutes of the end of mixing, the remaining unfiltered samples were analyzed for turbidity (DRT-15CE Turbidimeter), mean size, and polydispersity. A Primetime Turbidity Standard of 0.02NTU (Lot 21202) was used and triplicate turbidity measurements were performed in 4 second intervals. Hydrodynamic diameter was determined by Phase Analysis Light Scattering [PALS] (ZetaPALS, Brookhaven Instruments Corp., NY, USA).

Turbidity did not differ after four hours in the 1 mM bicarbonate solution (pH=8.3) with R1 or R3 suggesting the reference materials did not dissolve. Figure SI.19 shows the turbidity in this solution and is the baseline for comparison against HA exposure in other liquids. These results are consistent with the calcium and phosphate UF permeation results.

Turbidity with the spherical HA (R3) did not differ among the simulated biological fluids from the baseline sodium bicarbonate solution. This suggests that only a portion of the HA may readily dissolve, and TEM images suggest the presence of both crystalline and non-crystalline materials. In contrast to these results, turbidity decreased by >90% for the needle-like HA reference materials (R1 and R2) in the two gastric fluids and increased slightly in the shorter exposure period to simulated saliva. These turbidity measurements were consistent with visual assessment of relative “cloudiness”, which only decreased for R1 and R2 in the gastric fluids (see photos in Figure SI.21). There was no visual precipitation of sediment in any of the vials suggesting the materials dissolved rather than destabilized resulting in the decreased turbidity. Although the turbidity change were not quantified over reaction time, qualitative visual observations indicated near

complete dissolution of R1 and R2 within minutes, whereas the spherical HA reference (R3) remained cloudy throughout the experiment.

Mean particle size and polydispersity were also measured by phase-analysis light scattering (PALS) on the same samples as turbidity (Figure SI.19). Although PALS assumes spherical particles, they allow for the development of trends of particle hydrodynamic size and polydispersity. The results are consistent with turbidity: mean diameters decrease by >90% and polydispersities are lower for needle-like HA (R1 and R2) in the two gastric fluids whereas little change occurs for spherical HA (R3) material.

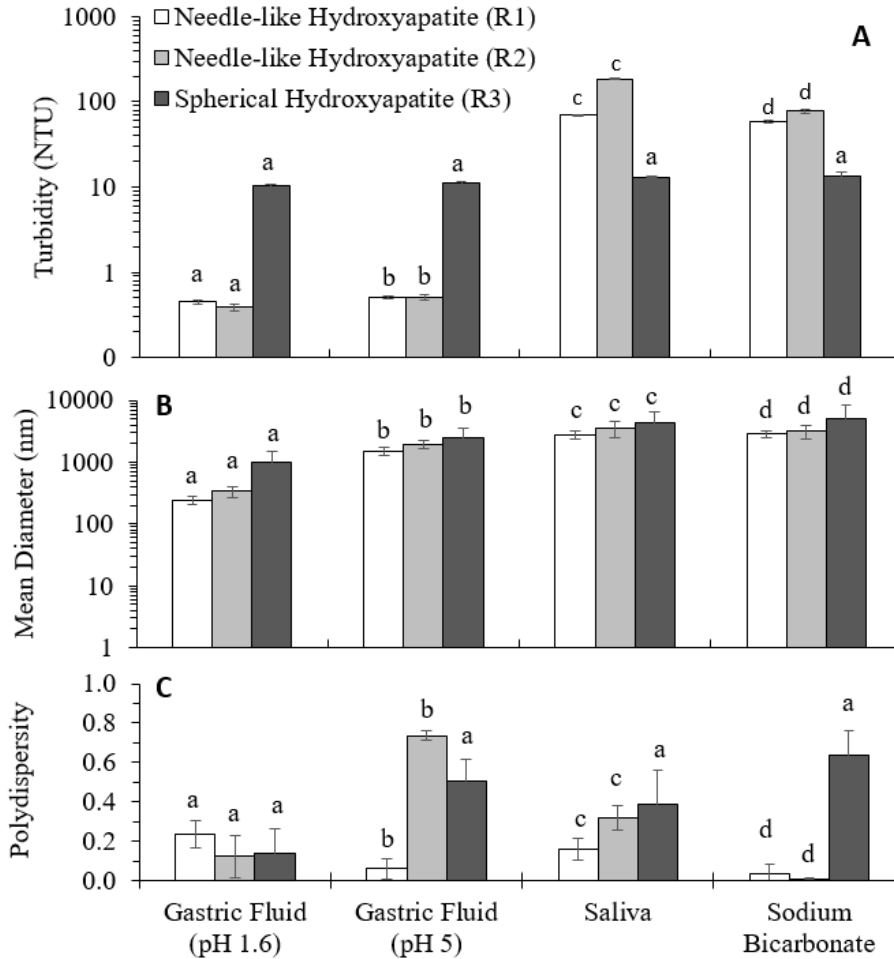


Figure SI.19 (A) Turbidity, (B) Mean Diameter, and (C) Polydispersity of the three different reference materials after mixing for two minutes (Saliva) and two hours (Gastric Fluids and Sodium Bicarbonate). One-way analysis of variance (ANOVA) tests were conducted at 95% confidence intervals to determine statistical significance (see Figure SI.20). The analysis was conducted to compare each individual reference material across the four simulated biological fluids for each nanomaterial physical property parameter. We did not compare each reference material to each other. We did not compare across the different nanomaterial properties. Turbidity controls containing no reference material

were as follows: 1mM sodium bicarbonate (0.29NTU), simulated saliva (2.20NTU), fed-state gastric fluid (0.23NTU), and fasted-state gastric fluid (0.20NTU).

Turbidity ANOVA Analysis														
NP	R1				NP	R2				NP	R3			
Assay	Gastric 1.6	Gastric 5	Saliva	SoBi	Assay	Gastric 1.6	Gastric 5	Saliva	SoBi	Assay	Gastric 1.6	Gastric 5	Saliva	SoBi
T1	0.29	0.28	66.80	56.72	T1	0.24	0.32	184.80	74.72	T1	10.81	11.28	11.20	11.72
T2	0.25	0.25	68.01	59.71	T2	0.18	0.24	178.81	82.71	T2	9.80	10.56	10.71	12.71
T3	0.22	0.31	67.70	58.70	T3	0.15	0.28	189.80	74.70	T3	9.60	10.97	10.90	14.70
Mean	0.25	0.28	67.50	58.38	Mean	0.19	0.28	184.47	77.38	Mean	10.07	10.94	10.94	13.04
95% Conf Interv	-2.35 to 2.86	-2.32 to 2.88	64.90 to 70.11	55.77 to 60.98	95% Conf Interv	-2.413 to 2.793	-2.32 to 2.88	181.9 to 187.1	74.77 to 79.98	95% Conf Interv	7.47 to 12.67	8.33 to 13.54	8.334 to 13.54	10.44 to 15.65
StDev	0.04	0.03	0.63	1.52	StDev	0.05	0.04	5.51	4.61	StDev	0.65	0.36	0.25	1.52
Hi	0.29	0.31	68.00	59.70	Hi	0.24	0.32	190.00	82.70	Hi	10.80	11.30	11.20	14.70
Low	0.22	0.25	66.80	56.70	Low	0.15	0.24	179.00	74.70	Low	9.60	10.60	10.70	11.70
Median	0.25	0.28	67.70	58.70	Median	0.18	0.28	185.00	74.70	Median	9.80	11.00	10.90	12.70
Dev From Med	0.02	0.02	0.40	1.00	Dev From Med	0.03	0.03	3.67	2.67	Dev From Med	0.40	0.24	0.16	0.99

Source of Variation	Sum of Squares	D.F.	Mean Squares	F-value	Source of Variation	Sum of Squares	D.F.	Mean Squares	F-value	Source of Variation	Sum of Squares	D.F.	Mean Squares	F-value
Between	1.19E+04	3	3970	5858	Between	6.84E+04	3	2.28E+04	1766	Between	1.44E+01	3	4.805	6.592
Error	5.421	8	0.677	-	Error	103.3	8	12.92	-	Error	5.831	8	0.7289	-
Total	1.19E+04	11	-	-	Total	6.85E+04	11	-	-	Total	2.03E+01	11	-	-
Result	P-Value = 0.000. Because P value is less than alpha (0.05), these results are significantly different				Result	P-Value = 0.000. Because P value is less than alpha (0.05), these results are significantly different				Result	P-Value = 0.015. Because P value is greater than alpha (0.05), these results are not significantly different			

Mean Diameter ANOVA Analysis														
NP	R1				NP	R2				NP	R3			
Assay	Gastric 1.6	Gastric 5	Saliva	SoBi	Assay	Gastric 1.6	Gastric 5	Saliva	SoBi	Assay	Gastric 1.6	Gastric 5	Saliva	SoBi
T1	1741.70	1702.30	8287.59	3262.20	T1	1803.20	2281.60	10289.43	3981.00	T1	1987.50	1702.30	7593.90	8300.70
T2	1793.10	1284.40	9011.80	2562.00	T2	1807.00	1635.80	8239.80	3205.90	T2	3011.80	2384.40	11563.60	2041.70
T3	1726.40	1518.10	8878.60	2629.80	T3	1920.20	1979.20	9683.45	2354.20	T3	2578.60	3518.10	11423.13	5194.40
Mean	1753.73	1501.60	8726.00	2818.00	Mean	1843.47	1965.53	9420.89	3180.37	Mean	2525.97	2534.93	10193.54	5178.93
95% Conf Interv	1364 to 2143	1112 to 1891	8336 to 9115	2428 to 3207	95% Conf Interv	944.6 to 2742	1066 to 2864	8522 to 10319	2281 to 4079	95% Conf Interv	-135.3 to 5186	-126 to 5195	7532 to 12854	2518 to 7839
StDev	35.20	209.00	385.47	386.18	StDev	66.40	324.00	1026.00	814.00	StDev	514.00	917.00	2250.00	3130.00
Hi	1790.00	1700.00	9010.00	3260.00	Hi	1920.00	2280.00	10290.00	3980.00	Hi	3000.00	3520.00	11560.00	8300.00
Low	1.73E+03	1280.00	8290.00	2560.00	Low	1800.00	1640.00	8289.00	2350.00	Low	1990.00	1700.00	7590.00	2040.00
Median	1.74E+03	1520.00	8880.00	2630.00	Median	1810.00	1980.00	9683.00	3205.00	Median	2.58E3	2380.00	11400.00	5190.00
Dev From Med	22.30	139.00	241.00	233.00	Dev From Med	38.90	216.00	667.00	542.00	Dev From Med	341.00	605.00	1323.00	2086.00

Source of Variation	Sum of Squares	D.F.	Mean Squares	F-value	Source of Variation	Sum of Squares	D.F.	Mean Squares	F-value	Source of Variation	Sum of Squares	D.F.	Mean Squares	F-value
Between	1.04E+08	3	3.46E+07	404.3	Between	1.16E+08	3	3.88E+07	85.14	Between	1.17E+08	3	3.90E+07	9.804
Error	6.85E+05	8	8.57E+04	-	Error	3.64E+06	8	4.56E+05	-	Error	3.19E+07	8	3.99E+06	-
Total	1.05E+08	11	-	-	Total	1.20E+08	11	-	-	Total	1.49E+08	11	-	-
Result	P-Value = 0.000. Because P value is less than alpha (0.05), these results are significantly different				Result	P-Value = 0.000. Because P value is less than alpha (0.05), these results are significantly different				Result	P-Value = 0.005. Because P value is less than alpha (0.05), these results are significantly different			

Polydispersity Statistics														
NP	R1				NP	R2				NP	R3			
Assay	Gastric 1.6	Gastric 5	Saliva	SoBi	Assay	Gastric 1.6	Gastric 5	Saliva	SoBi	Assay	Gastric 1.6	Gastric 5	Saliva	SoBi
T1	0.87	0.12	0.35	0.01	T1	0.74	0.74	0.50	0.01	T1	0.79	0.50	0.34	0.50
T2	0.66	0.04	0.26	0.01	T2	0.61	0.76	0.37	0.01	T2	0.53	0.62	0.50	0.64
T3	0.70	0.02	0.29	0.09	T3	0.40	0.71	0.50	0.01	T3	0.46	0.40	0.74	0.76
Mean	0.74	0.06	0.30	0.03	Mean	0.58	0.74	0.46	0.01	Mean	0.59	0.51	0.53	0.63
95% Conf Interv	0.63 to 0.84	-0.03 to 0.15	0.21 to 0.39	-0.06 to 0.13	95% Conf Interv	0.46 to 0.71	0.61 to 0.86	0.33 to 0.58	-0.12 to 0.14	95% Conf Interv	0.38 to 0.80	0.29 to 0.72	0.32 to 0.74	0.42 to 0.84
StDev	0.11	0.05	0.05	0.05	StDev	0.17	0.03	0.08	0.00	StDev	0.17	0.11	0.20	0.13
Hi	0.87	0.12	0.35	0.09	Hi	0.74	0.76	0.50	0.01	Hi	0.79	0.62	0.74	0.76
Low	0.66	0.02	0.26	0.01	Low	0.40	0.71	0.37	0.01	Low	0.46	0.40	0.34	0.50
Median	0.70	0.04	0.29	0.01	Median	0.61	0.74	0.50	0.01	Median	0.53	0.50	0.50	0.64
Dev From Med	0.07	0.03	0.03	0.03	Dev From Med	0.11	0.02	0.04	0.00	Dev From Med	0.11	0.07	0.13	0.09

Source of Variation	Sum of Squares	D.F.	Mean Squares	F-value	Source of Variation	Sum of Squares	D.F.	Mean Squares	F-value	Source of Variation	Sum of Squares	D.F.	Mean Squares	F-value
Between	9.60E-01	3	3.20E-01	66.29	Between	8.80E-01	3	2.90E-01	32.89	Between	3.00E-02	3	1.00E-02	0.41
Error	3.89E-02	8	4.86E-03	-	Error	7.14E-02	8	8.93E-03	-	Error	2.00E-01	8	2.00E-02	-
Total	1.01E+00	11	-	-	Total	9.50E-01	11	-	-	Total	2.30E-01	11	-	-
Result	P-Value = 0.000. Because P value is less than alpha (0.05), these results are significantly different				Result	P-Value = 0.000. Because P value is less than alpha (0.05), these results are significantly different				Result	P-Value = 0.747. Because P value is greater than alpha (0.05), these results are not significantly different			

Figure SI.20: ANOVA statistical analysis of (A) Turbidity, (B) Mean Diameter, and (C) Polydispersity

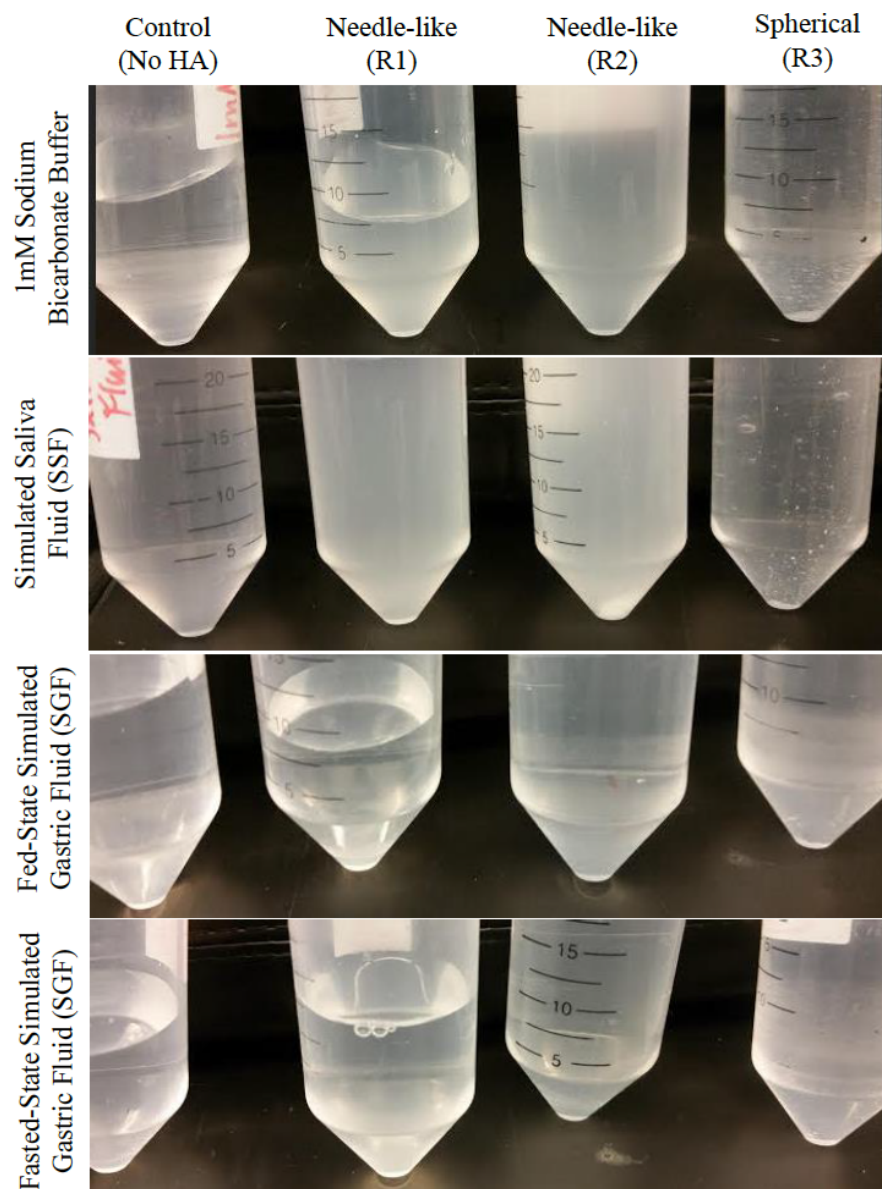


Figure SI.21 Photographs show vials containing hydroxyapatite (HA) reference materials (R1, R2, R3) or control (no HA added) in different fluids after the prescribed mixing times. The relative cloudiness of the samples differs among the vials.

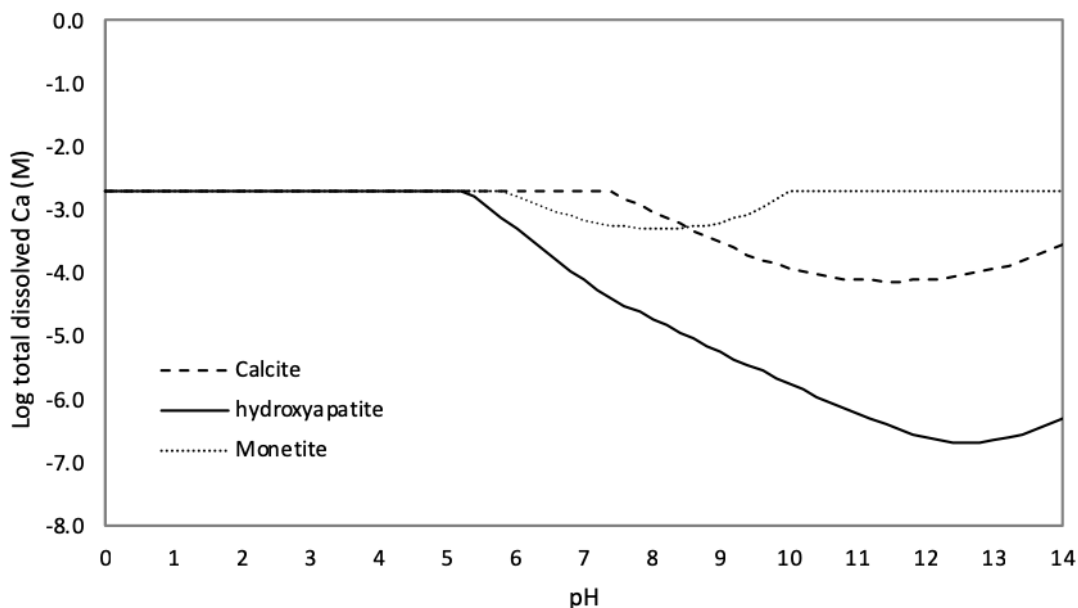


Figure SI.22 Calculated total dissolved Ca concentration ($\text{Log}[\text{Ca}]_T$) as a function of pH in simulated gastric fluid for the three calcium minerals found in infant formula, i.e., hydroxyapatite, calcite, and monetite. Calculations were performed using Visual MINTEQ software (ver. 3.1). Simulation conditions: sodium = 0.267 M, acetate = 0.0469 M, and chloride = 0.237 M. Calcium mineral concentrations: hydroxyapatite = 0.4 mM, calcite = 2 mM, and monetite = 2 mM, to achieve a total Ca concentration of 2 mM for all three minerals.

Estimated Usage of Needle-like Hydroxyapatite

The 2013 global market for infant formula was approximately \$41 Billion (US dollar), and growing rapidly in Asia and other markets [23]. The cost of powder formula is on the order of \$1 (US) per ounce (based upon market costs in US and web-based reports (e.g., <http://www.popsugar.com/moms/How-Much-Infant-Formula-Costs-8104334>)). Most of the infant formula is powder, as opposed to liquids [23]. We conservatively assume 75% of the market is infant formula. Based upon our estimate of 0.4 wt% HA in the formula from S3 sample, this results in a cost of \$8 per gram HA delivered in infant formula. Assuming \$41B (US) market at this cost results in production of up to 5125 metric tons of HA for infant formula alone. Nano-structured needle-like HA was not present in all samples. Assuming only 50% of infant formula uses needle-like HA, the global annual production may be on the order of 2500 metric tons. These estimates (2500-5000 metric ton/year) for needle-like HA in just this one product class (infant formula) is the same order of magnitude for the 2010 global production estimate for carbon nanotubes of 2916-3200 metric ton/year) (Table S4 in [24]). There are uses of needle-like HA in cosmetics [25] and probably many other applications, although data is not readily available.